Universidad
Carlos III de Madrid

TESIS DOCTORAL

A Neuroprosthesis for Tremor Management

Autor:

Juan Álvaro Gallego Abella

Directores:

José Luis Pons Rovira
Eduardo Rocon de Lima
Luis Moreno Lorente

Department of Systems Engineering and Automation

Leganés, June 2013

TESIS DOCTORAL

A Neuroprosthesis for Tremor Management

Autor: Juan Álvaro Gallego Abella

Directores: José Luis Pons Rovira, Eduardo Rocon de Lima y Luis Moreno Lorente

Firma del Tribunal Calificador:

Presidente:	Carlos Balaguer Bernaldo de Quirós	_____
Vocal:	Alicia Casals Gelpí	_____
Secretario:	Ramón Ceres Ruiz	_____

Calificación:

Leganés, 6 de Junio de 2013

A mis padres,
y a mi Carol

Acknowledgements

I would like to start by thanking all people affected by tremor who participated in the experiments performed in the framework of this dissertation. Without their friendly and patient collaboration, none of the results and findings here presented would have been possible.

Next, I would like to acknowledge my supervisors for guiding, challenging, and encouraging me while I performed this work. A very important role in this regard has also been played by my friends at the Bioengineering Group. Our mutual support, silly jokes and time together, both within and outside the lab, made surviving these years easier. Thank you guys! Also thanks to my friends at Aalborg University, who helped a lot during my research visit there. My gratitude also goes to those with whom I have collaborated in the different studies here included: I have learnt a lot working with you.

I would also like to thank my friends in Madrid, León (currently spread throughout the world), and everywhere else, for understanding the absences caused by these pages, and overall for all the great moments we have shared. My family has also shown a great ability for support and encouragement, thank you very much!

Finally, I would like to thank my parents, without whom this work would have been never performed (at least by me), and to Carol, for turning my whole world upside down.

Abstract

Tremor is the most common movement disorder, affecting ∼15 % of people over 50 years old according to some estimates. It appears due to a number of syndromes, being essential tremor and Parkinson's disease the most prevalent among them. None of these conditions is fully understood. Tremor is currently treated through drugs or neurosurgery, but unfortunately, it is not managed effectively in ∼25 % of the patients. Therefore, it constitutes a major cause of loss of independence and quality of life.

Various alternative approaches for tremor management are reported in the literature. Among them, those devices that rely on the application of forces to the tremulous segments show a considerable potential. A number of prototypes that exploit this principle are available, spanning fixed devices and orthoses. However, none of them has fulfilled user's expectation for continuous use during daily living.

This thesis presents the development and validation of a neuroprosthesis for tremor management. A neuroprosthesis is a system that restores or compensates for a neurological function that is lost. In this case, the neuroprosthesis aims at compensating the functional disability caused by the tremor. To this end, it applies forces to the tremulous limb through the control of muscle contraction, which is modulated according to the characteristics of the tremor. The concept design envisions the device as a textile that is worn on the affected limb, thus meeting the usability requirements defined by the patients. The development of the neuroprosthesis comprised the following tasks:

1. The development of a concept design of the neuroprosthesis, which incorporates state of the art knowledge on tremor, and user's needs.

2. The design and validation of a cognitive interface that parameterizes the tremor in functional contexts. This interface provides the information that the neuroprosthesis uses for tremor suppression. Two versions are developed: a multimodal interface that integrates the recordings of the whole neuromusculoskeletal system, and an interface incorporating only wearable movement sensors. The latter is intended for the functional validation of the neuroprosthesis, while the former is a proof of concept of an optimal interface for this type of applications.

3. The development of a novel approach for tremor suppression through transcutaneous neurostimulation. The approach relies on the modulation of muscle co-contraction as a means of attenuating the tremor without the need of conventional actuators. The experimental validation here provided demonstrates the feasibility and interest of the approach.

In parallel with the validation of the neuroprosthesis, I performed a detailed study on the physiology of motoneurons in tremor, given the lack of a complete description of its behavior. The outcome of this study contributes to the interpretation of the results obtained with the neuroprosthesis, and opens new research lines, both related to alternative interventions and basic neuroscience.

In summary, the results here presented demonstrate that tremor may be accurately parameterized while the patient performs functional activities, and that this information may be exploited to drive a neuroprosthesis for tremor management. Furthermore, the novel approach for tremor suppression presented in this dissertation constitutes a potential approach for treating upper limb tremor, either alone, or as a complement to pharmacotherapy. These results encourage the validation of the neuroprosthesis in a large cohort of patients, in order to enable its translation to the market.

Resumen

El temblor es el trastorno del movimiento más común, afectando, según algunas estimaciones, al ∼15 % de la población de más de 50 años. Existen diversos "síndromes" que causan temblor, siendo el temblor esencial y la enfermedad de Parkinson los que presentan mayor prevalencia. Además, cabe resaltar que no existe una descripción completa de ninguno de ellos. En la actualidad el temblor se trata mediante una serie de fármacos o neurocirugía. A pesar de ello, el ∼25 % de los pacientes sufren problemas funcionales debido a su condición. Por tanto, es evidente que el temblor constituye una de las principales causas de dependencia y pérdida de calidad de vida.

Realizando una revisión de las publicaciones científicas sobre el temblor, se observa que se ha propuesto un considerable número de tratamientos alternativos. Entre ellos destacan los dispositivos que se fundamentan en la aplicación de fuerzas sobre los segmentos afectados por el temblor, de los que ya se ha evaluado una serie de prototipos. Éstos abarcan desde dispositivos fijados a otras estructuras hasta ortesis. Sin embargo, ninguno de ellos satisface las expectativas de los usuarios para su uso durante el día a día.

Esta tesis presenta el diseño y validación de una neruoprótesis para el tratamiento del temblor. Una neuroprótesis es un sistema que reemplaza o compensa una función neurológica perdida. En este caso, la neuroprótesis tiene como objetivo compensar la discapacidad motora causada por el temblor. Para ello aplica fuerzas al miembro afectado a través del control del nivel de contracción muscular, que se modula según las características del temblor. El diseño conceptual contempla al dispositivo como un textil que se viste en el brazo afectado, satisfaciendo los requisitos de usabilidad definidos por los pacientes. El desarrollo de la neuroprótesis abarcó las siguientes tareas:

1. El desarrollo del diseño conceptual de la neuroprótesis, que incorpora el conocimiento actual sobre el temblor, y las necesidades de los usuarios.

2. El diseño y validación de una interfaz cognitiva que parametriza el temblor durante tareas funcionales. La información obtenida con esta interfaz es usada por la neuroprótesis para modular la corriente aplicada mediante técnicas de neuroestimulación. Se desarrollan dos versiones de la interfaz cognitiva: una interfaz

multimodal que integra información de todo el sistema neuromúsculoesqueletico, y una interfaz que implementa únicamente sensores vestibles de movimiento. La segunda interfaz fue la que se usó durante la validación funcional de la neuroprótesis, mientras que la primera es una prueba de concepto de una interfaz óptima para este tipo de aplicaciones.

3. El desarrollo de una nueva aproximación para la supresión del temblor mediante neuroestimulación transcutánea. Dicha aproximación se fundamenta en la modulación del grado de co-contracción de los músculos afectados como forma de atenuar el temblor, sin necesidad de usar actuadores convencionales. La evaluación experimental sirvió para demostrar la viabilidad e interés de la intervención.

En paralelo a la validación de la neuroprótesis, llevé a cabo un estudio detallado de la fisiología de las motoneuronas en el caso del temblor, dado que no existe una descripción del funcionamiento de las mismas en el caso de este trastorno. Este estudio sirve para ayudar a la interpretación de los resultados de la neuroprótesis, y para abrir una serie de líneas futuras de investigación, tanto sobre nuevas intervenciones para el temblor, como sobre neurociencia básica.

En resumen, los resultados que se presentan en esta tesis demuestran que es posible parametrizar de una forma precisa el temblor durante la realización de tareas funcionales, y que esta información sirve para controlar una neuroprótesis para el tratamiento del temblor. Además, la nueva aproximación para la compensación del temblor que se presenta tiene el potencial de convertirse en un tratamiento alternativo para el temblor de miembro superior, ya sea de forma independiente o como complemento a los fármacos. Estos resultados alientan la validación de la neuroprótesis en una cohorte grande pacientes, con el objetivo de facilitar su transferencia al mercado.

Contents

Abstract ix

Resumen xi

Nomenclature xxi

Objectives and Description of Work 1

1 Introduction 7
- 1.1 Introduction . . . 8
- 1.2 Tremor . . . 11
  - 1.2.1 Clinical Aspects and Diagnosis of Tremor . . . 11
  - 1.2.2 The Epidemiology of Tremor . . . 14
  - 1.2.3 The Neurophysiology of Tremor . . . 16
  - 1.2.4 Alternative Approaches for Tremor Management . . . 20
- 1.3 Concept design of the Neuroprosthesis . . . 27
  - 1.3.1 Concept Design of the Cognitive Human-Machine Interface . . . 27
  - 1.3.2 Concept Design of the Physical Human-Machine Interface . . . 30
  - 1.3.3 Neuroprosthesis Prototype . . . 33
- 1.4 Conclusions . . . 34

2 Online Estimation of Tremor Parameters 37
- 2.1 Introduction . . . 38
- 2.2 Preliminary considerations . . . 40
  - 2.2.1 Gyroscope Placement . . . 40
  - 2.2.2 Compensation of Gyroscope Drift . . . 42
  - 2.2.3 Analysis of Voluntary Movement and Tremor . . . 42
- 2.3 Two-Stage Algorithm for the Estimation of Tremor Parameters . . . 44
  - 2.3.1 Voluntary Motion Tracking . . . 45
    - 2.3.1.1 $g-h$ Filters . . . 46
    - 2.3.1.2 Kalman Filter . . . 47
  - 2.3.2 Estimation of Tremor Parameters . . . 48
    - 2.3.2.1 Weighted Frequency Fourier Linear Combiner . . . 49
    - 2.3.2.2 Bandlimited Multiple Fourier Linear Combiner . . . 50
    - 2.3.2.3 Kalman Filter . . . 50
- 2.4 Methods . . . 51
  - 2.4.1 Patients . . . 51
  - 2.4.2 Experimental protocol . . . 52

2.4.3 Recordings . . . 52
2.4.4 Data Processing and Analysis . . . 52
2.4.4.1 Evaluation Metrics . . . 53
2.5 Results . . . 54
2.6 Discussion . . . 57
2.7 Conclusions . . . 60

3 A Multimodal Human-Machine Interface for Tremor 63
3.1 Introduction . . . 64
3.2 Multimodal Human-Machine Interface to Parameterize Tremor during Volitional Movements . . . 66
3.2.1 Detection of Movement Intention . . . 69
3.2.2 Detection of Tremor Onset . . . 70
3.2.3 Estimation of Tremor Parameters . . . 71
3.3 Methods . . . 71
3.3.1 Patients . . . 71
3.3.2 Experimental protocol . . . 71
3.3.3 Recordings . . . 72
3.3.4 Data Processing and Analysis . . . 73
3.3.4.1 Evaluation Metrics . . . 73
3.4 Results . . . 75
3.5 Discussion . . . 78
3.6 Conclusions . . . 80

4 Tremor Attenuation through the Modulation of Muscle Co-contraction 83
4.1 Introduction . . . 84
4.2 Tremor Suppression Strategy . . . 85
4.2.1 Controller . . . 88
4.3 Methods . . . 89
4.3.1 Patients . . . 89
4.3.2 Experimental Protocol . . . 89
4.3.3 Recordings . . . 90
4.3.4 Data Processing and Analysis . . . 91
4.4 Results . . . 92
4.5 Discussion . . . 96
4.6 Conclusions . . . 101

5 Synaptic Inputs to the Motor Neuron Pool in Tremor 103
5.1 Introduction . . . 104
5.2 Methods . . . 106
5.2.1 Patients . . . 106
5.2.2 Experimental Protocol . . . 106
5.2.3 Recordings . . . 107
5.2.4 Surface EMG Decomposition . . . 107
5.2.5 Data Processing and Analysis . . . 109
5.3 Results . . . 111
5.3.1 Corticomuscular Coupling . . . 111

5.3.2 Common Input to Motor Neurons . . . 117
5.4 Discussion . . . 120
5.5 Conclusions . . . 123

6 Conclusions and Future Work **125**
6.1 Contributions . . . 126
6.2 Scientific Dissemination . . . 127
6.3 Future Work . . . 132

Bibliography **135**

List of Figures

1.1 An example of spiral drawing obtained from an ET patient, and of a patient implanted with a deep brain stimulator . . . 9
1.2 Tremor syndromes and clinical manifestation according to the consensus statement by the Movement Disorders Society . . . 13
1.3 Effect of added weight on the tremor in ET . . . 19
1.4 Examples of ambulatory orthoses for tremor management . . . 24
1.5 Concept design of the cHMI implemented in the NP . . . 30
1.6 Concept design of the NP, showing both the cHMI and the pHMI . . . 32
1.7 A control subject wearing the first prototype of the NP . . . 33

2.1 Placement of the gyroscopes to record wrist and elbow kinematics . . . 40
2.2 Relationship between gyroscope offset and temperature . . . 41
2.3 Amplitude spectrum showing the typical separation of the concomitant voluntary and tremulous movements in the frequency domain . . . 43
2.4 Example of EEMD of tremor oscillations . . . 44
2.5 Block diagram of the two-stage algorithm for the online estimation of tremor parameters . . . 45
2.6 An example of voluntary movement tracking with the three algorithms evaluated . . . 55
2.7 An example of tremor estimation with the three algorithms evaluated . . . 56
2.8 An example of the estimation of tremor frequency with the WFLC and the BMFLC . . . 57
2.9 Summary of the two-stage algorithm for the online estimation of tremor parameters . . . 58

3.1 Diagram that illustrates the mHMI to drive the NP . . . 67
3.2 A tremor patient instrumented for the validation of the mHMI . . . 72
3.3 Example of tremor characterization with the mHMI during a volitional task 75
3.4 Delay in the detection of voluntary movement and tremor from the sEMG, with and without movement intention detected from the EEG . . . 77

4.1 Bode diagram that illustrates the rationale for tremor attenuation through muscle co-contraction . . . 87
4.2 A patient equipped with the NP during the performance of a tremor suppression experiment . . . 90
4.3 Example of the controller that modulates muscle co-contraction to attenuate tremor . . . 92
4.4 Examples of reduction of tremor amplitude through NP-driven co-contraction, for six representative patients . . . 94

4.5 Comparison of the variation of tremor amplitude within a trial, in the pooled datasets of trials without and with NP-driven co-contraction . . . 95
4.6 Tremor attenuation as function of the initial severity of the tremor 96
4.7 Tremor attenuation as function of trial number 97
4.8 Effect of tremor attenuation through NP-driven muscle co-contraction on tremor frequency 98
4.9 Example of NP-driven modulation of muscle a co-contraction during a functional task 100

5.1 Example of the EEG, sEMG, and gyroscope signals, and of a few MNs identified through the decomposition of the sEMG 108
5.2 Cumulative ISI histograms for all the MNs identified 112
5.3 Example of the coherence between the EEG at the contralateral sensorimotor cortex, and all the possible CSTs 113
5.4 Estimation of corticomuscular coherence 114
5.5 Estimation of corticomuscular coherence at the tremor frequency and the beta band as function of the number of MNs 116
5.6 Strength and frequency content of the common synaptic inputs to the identified MNs 118
5.7 Examples of MN spike trains, and the result of applying a bandpass filter at the tremor frequency band 119

List of Tables

1.1 Alternative forms to manage tremor 22

2.1 Performance of the algorithms to track voluntary movement 55
2.2 Performance of the algorithms to estimate tremor parameters 56

3.1 Information about tremor and/or voluntary movement that can be extracted from each sensor modality within the mHMI 66
3.2 Performance of the mHMI 76
3.3 Performance of the EEG-based detection of intention to move 76
3.4 Estimation of tremor frequency from the sEMG 78
3.5 Tracking of tremor frequency with and without the input from the sEMG algorithm 78

4.1 Effect of NP-driven modulation of muscle co-contraction on tremor amplitude 93

5.1 Summary of corticomuscular coherence and motor unit synchronization . 115

Nomenclature

ADL	Activity of Daily Living
ANOVA	Analysis Of Variance
AO	Arms Outstretched
AU	Activation Unit
BBF	Benedict-Bordner Filter
BMFLC	Bandlimited Multiple Fourier Linear Combiner
CDF	Critically Dampened Filter
cHMI	Cognitive Human-Machine Interface
CIS	Strength of Common Input to motor neurons
CKC	Convolution Kernel Compensation
CNS	Central Nervous System
CO	Trial with Co-contraction
CV	Coefficient of Variation
CST	Composite Spike Train
CT	Cerebellar Tremor
DBS	Deep Brain Stimulation
DoF	Degree of Freedom
EEG	Electroencephalography
EEMD	Ensemble Empirical Mode Decomposition
EMD	Empirical Mode Decomposition
EMG	Electromyography
ERD	Event Related Desynchronization
ET	Essential Tremor
FES	Functional Electrical Stimulation
FLC	Fourier Linear Combiner
FF	Finger to Finger test
FN	Finger to Nose test
$FMSE_d$	Filtered Mean Square Error with Delay correction
KF	Kalman Filter
KTE	Kinematic Tracking Error
IHT	Iterated Hilbert Transform
IMF	Intrinsic Mode Function

IMU	Inertial Measurement Unit
ISI	Inter-Spike Interval
LINGO1	Leucine rich repeat and Ig domain containing Nogo receptor interacting protein-1
LMS	Least Mean Squares
MEMS	Microelectromechanical Systems
mHMI	Multimodal Human-Machine Interface
MPTP	1-methyl-4-phenyl-1,2,3,6-tetrahydropyridine
MN	Motor Neuron
MS	Multiple Sclerosis
NO	Trial without co-contraction
NP	Neuroprosthesis
PD	Parkinson's Disease
PET	Positron Emission Tomography
pHMI	Physical Human-Machine Interface
PNS	Peripheral Nervous System
RE	Rest
RMS	Root Mean Square
RMSE	Root Mean Square Error
SD	Standard Deviation
sEMG	Surface Electromyography
WFLC	Weighted frequency Fourier Linear Combiner
WG	Pouring Water from a bottle a into a Glass
WR	Wearable Robot

Objectives and Description of Work

Tremor is defined as a rhythmical, involuntary oscillatory movement of a body part. Although, under specific circumstances we all exhibit a certain degree of tremor, some suffer from severe forms that often lead to disability. These disabling tremors are grouped under the term pathological tremor and, as a whole, constitute the most prevalent movement disorder. Pathological tremor arises from a number of conditions, being Parkinson's disease and essential tremor the most prevalent causes.

None of the pathologies that cause tremor are fully understood, and epidemiological and neurophysiological studies are hampered by the lack of diagnostic methods other than purely clinical. Furthermore, the lack of knowledge on the mechanisms that cause the different types of tremor has obvious implications in the development of treatment forms. At the present time, tremors are treated through pharmacotherapy or neurosurgery, being the latter employed in patients refractory to drugs who satisfy a series of restringing criteria. However, both alternatives have significant drawbacks associated. Drugs often induce side effects, and exhibit decreased efficacy over time, while neurosurgical approaches have those risks intrinsic to the procedure, and are related to increased probability of intracranial hemorrhage, depression, and other psychiatric manifestations, such as suicidal tendencies.

As a consequence, tremor is not effectively managed in a large proportion of patients. Importantly, according to some estimates, 65 % of those suffering from upper limb tremor report difficulties when performing their activities of daily living, which makes tremor a major cause of dependence and loss of quality of life. Furthermore, tremor carries important social and psychological burden associated, which further affects the patents' and relatives' lives. This makes the development and validation of alternative forms to treat (upper limb) tremor a topic of great importance.

During the last decades, a number of novel interventions for tremor management have been explored. Among them, those relying on the alteration of tremor properties under mechanical loading emerge as a very promising path. By exploiting this concept, various table mounted, wheelchair-mounted, and—more recently—ambulatory devices have

been evaluated. In spite of their often promising results, these systems failed to meet user's expectations in terms of usability, wearability, and cosmetics.

Objectives

The main objective of this thesis is to develop and validate a neuroprosthesis for tremor management. The neuroprosthesis employs transcutaneous neurostimulation as a means to apply mechanical loads and suppress the tremor. In order to achieve an adequate control of the stimulation delivered, I developed a novel interface that robustly detects the onset of a voluntary movement and, in this context, delivers an accurate characterization of the tremor. This enables the use of the system for functional compensation in real scenarios.

As mentioned above, there are already a number of devices for tremor management based on mechanical loading. However, none of them is designed as an ambulatory, wearable system that fulfills user expectations in terms of usability and cosmetics. In this regard, the neuroprosthesis here presented takes the form of a textile that may be easily worn underneath the clothes, being therefore closer to a final product. This is enabled by the fact that the neuroprosthesis does not need external actuators, since it utilizes the patient's muscles to load the tremulous limb. Furthermore, most of the existing systems apply constant forces to the tremulous limb, while this neuroprosthesis adapts the force applied to the ongoing tremor characteristics, and has the ability to actuate only when needed, i.e. when tremor poses a functional problem. Obviously, this is an important improvement regarding user acceptance and the performance of the system itself.

By providing a novel interface to characterize tremor in functional contexts, I also allow for the future development of tremor suppression systems that are fully suitable for daily living use. At the same time, I show that the tremor does not provoke a major reorganization of motor pathways, and rather they function similarly to what is observed in healthy subjects. This, together with a series of findings about the mechanisms causing the tremor and how it manifests, also constitute important contributions to the field, and allow us to envision novel treatment alternatives to evaluate in the future.

In summary, this doctoral work has the following objectives:

- To provide a methodology for the ambulatory recording of joint kinematics in tremor patients.
- To gain insight into the properties of concomitant voluntary and tremulous movements.
- To develop and validate an algorithm that parameterizes tremor in the presence of concomitant voluntary movement.

- To define a multimodal interface for tremor patients that detects the intention to move and the onset of both voluntary motion and tremor, as a natural approach to drive the neuroprosthesis.
- To investigate the pathophysiological mechanisms that participate in tremorogenesis as a means to interpret the results obtained, and to envision future interventions.
- To develop a prototype of the neuroprosthesis in order to evaluate a novel approach for tremor management.
- To design a control algorithm that modulates muscle co-contraction, as the core of the tremor suppression strategy implemented in the neuroprosthesis.
- To provide a validation of the performance of the system in a representative group of patients, together with a detailed interpretation of the results.

Description of work

The methodology followed to achieve these objectives rests on a profound study of the different aspects of pathological tremor, namely its mechanical characteristics, the mechanisms that cause it, and the clinical and functional implications of the disorder. The work has been split in a series of studies, each presented as a chapter of this dissertation. Next, I proceed to detail each of these studies, relating them to the objectives presented above.

Chapter §1 starts by describing the rationale of the dissertation, and then it reviews different aspects of tremor. First, it explains how tremors are currently classified, and identifies the groups that are enrolled in the development and validation of the neuroprosthesis, according to the number of people affected and the characteristics of the tremor they exhibit. Next, it gives a brief background of the epidemiological and neurophysiological aspects of the two types of tremor considered in this work, which was performed to facilitate the realization of the different studies, and the interpretation of the results. The chapter also provides a detailed review of the alternative forms to treat tremor that are presented in the literature. Then, based on the analysis of the state of the art and the elicitation of user needs, I provide a concept design for the neuroprosthesis. In more detail, I give a series of requirements that an ideal system should meet, and that will be taken into consideration to develop the system components.

Chapter §2 is devoted to the kinematic analysis of tremor. First, it defines the sensors—solid-state gyroscopes—and the methodology employed to record upper limb kinematics throughout all the studies of the thesis. Next, it describes the characteristics of concomitant voluntary and tremulous movements, which are considered in the development

of the algorithm to parameterize the tremor. Among them, I present first evidences on the identification of multiple tremor oscillators in joint kinematics, a finding that will be employed in future neurophysiological studies. The core of the chapter is the development and validation of an algorithm for the online estimation of tremor parameters, which is carried out taking into consideration this knowledge and the design requirements defined in Chapter §1. The outcome of this chapter is a two-stage algorithm that provides an accurate estimation of instantaneous tremor amplitude and frequency, with almost zero phase, and short settling time.

Chapter §3 presents the development and validation of an optimal interface for the parameterization of tremor during functional tasks, which use is transparent to the user. To this end, the chapter starts by reviewing the design criteria partly met by the algorithm presented in Chapter §2, and how the current approach, a multimodal interface, aims at satisfying them. The multimodal interface relies on the concurrent recording of the whole neuromusculoskeletal system, and on the adequate selection of the features that each (sensor) modality needs to extract, to achieve optimal functionality. Furthermore, it exploits the inherent advantages of multimodality to implement a series of redundant mechanisms that enhance its reliability and robustness. Experimental results prove the feasibility of the approach, although the status of the neural interface technologies make the interface more suitable for future use.

Chapter §4 is devoted to the tremor suppression strategy implemented in the neuroprosthesis. First, it presents the rationale of modulation of muscle co-contraction as an approach for tremor management, and gives a detailed explanation of the controller implemented. Then, I review the experimental protocol employed for the validation of the tremor suppression approach, which design is of paramount importance to guarantee the significance of the evaluation. After presenting the results obtained in a group of 12 patients, which demonstrate that the strategy allows the NP to significantly attenuate the tremor, I provide a profound discussion of the data, highlighting that they encourage the realization of future clinical studies in a large cohort of patients.

The work on Chapter §5 was carried out in parallel to that on Chapter §4, and is a physiological study on the characteristics of the neural drive to muscle, and the behavior of its constituents motor units, in tremor patients. The motivation for this chapter is the lack of knowledge on how the central oscillations that cause tremor affect muscle behavior—ultimately causing the tremor oscillations—, which hampers both the interpretation of some of the results obtained, and the development of novel interventions. To this end, I employ recordings performed with the multimodal interface presented in Chapter §3 as a means to study how the central tremor oscillations are transmitted to a muscle, and gather evidences on the role of afferent feedback in tremorogenesis. These results give new insight about the pathophysiology of tremor, at the same time that inspire a novel intervention for tremor suppression, which is currently under development.

Chapter §6 summarizes the conclusions obtained during the realization of this doctoral work, at the same time that it identifies the major contributions to the fields related to this thesis, namely, biomedical and neural engineering, signal processing, rehabilitation robotics, and neurophysiology. Next, it presents the future work, which is planned based on the outcomes of this thesis. It must be mentioned that some of these studies are already under development in the framework of a project recently funded by the EU Commission (NeuroTREMOR[1], EU-2011-287739), which proposal was built on the results and opened questions presented in this dissertation.

This work has been carried out with the financial support of the Spanish Ministry of Education (through a FPU scholarship) in the framework of EU project TREMOR (ICT-2007-224051), and has also contributed to Spanish projects REHABOT (DPI-2008-06772-C03-01) and HYPER (CSD-2009-00067). My participation in TREMOR project enriched this research thanks to the collaboration with other groups included in the consortium, specially Instituto de Biomecánica de Valencia, the Center for Sensory-Motor Interaction (Aalborg University), and the Faculty of Electrical Engineering and Computer Science (University of Maribor).

[1] NeuroTREMOR project website: http://neurotremor.eu/

Chapter 1

Introduction

This chapter presents the background and rationale of this dissertation. It starts by explaining the reasons that encouraged the development of the neuroprosthesis for tremor management: the large number of people affected by tremor, and the significant proportion of them who do not benefit from any existing treatment. Next, the different aspects related to tremor—as a neurological condition, it is a multidisciplinary problem—are summarized, putting emphasis on its clinical heterogeneity, the current lack of understanding of all the syndromes causing it, the limitations in treatment, and the alternative therapies that have started appearing. This review focuses on essential tremor and Parkinson's disease, the two most common types of tremor, and the groups of patients enrolled for the development and validation of the neuroprosthesis. Afterwards, I present a series of design requirements defined by combining the expected functionality of the system with an analysis of user needs. These requirements are then translated into a concept design that will guide the development of the neuroprosthesis. The concept design is obtained for the cognitive and physical human-machine interfaces, being the former responsible for decoding user's commands and deriving a complete parameterization of the tremor, and the latter for modulating the current injected to compensate for it. The chapter thus sets the rationale and guidelines for the work presented in this dissertation.

1.1 Introduction

Tremor is defined as a rhythmical, involuntary oscillatory movement of a body part[1]. Under certain circumstances, like the performance of precise tasks or prolonged maintenance of a posture, we all exhibit a certain degree of tremor. This is called physiological tremor (Elble, 2009). When tremor arises from a neurological condition, becoming cause of disability, it is referred to as pathological tremor (McAuley and Marsden, 2000).

Pathological tremor is the most prevalent movement disorder (see, e.g., Wenning et al., 2005), and projection studies foresee that prevalence will double by 2050 (Bach et al., 2011). Importantly, pathological tremor—referred to as tremor in the remainder in the dissertation—does not constitute a monolithic entity, and appears caused by ten different so-called syndromes (Deuschl et al., 1998). Among them, Parkinson's disease (PD), and essential tremor (ET) are the most relevant in terms of prevalence (see Epigraph §1.2.2 for details).

None of the pathologies that cause tremor are fully understood, which hampers considerably their diagnosis and treatment. In addition, given that epidemiological, neurophysiological and therapeutical studies rely on experimental evidences gathered in groups of patients, diagnostic problems pose a risk to expanding what is known about the different aspects of tremor (Louis, 2008; Stefansson et al., 2009; Deuschl et al., 2011).

At the current time, tremor is mostly managed through pharmacotherapy, although refractory patients undergo neurosurgery if a series of inclusion criteria are met. Dopamine precursor levodopa constitutes the gold standard for treating PD, although the mechanisms that cause the amelioration of the symptoms are not fully understood (Fahn et al., 2004; Fahn and the Parkinson Study Group, 2005), and effectiveness is known to decrease over time (e.g., Rascol et al., 2000; Olanow and Obeso, 2000). All drugs for treating ET have been discovered by chance (Deuschl et al., 2011), and only two, propanolol and primidone, have established efficacy according to the American Academy of Neurology[2]. Furthermore, half of ET patients do not benefit from any known drug, and in those showing positive response, tremor is reduced in average to a ∼50 % of its original amplitude (Deuschl et al., 2011). Neurosurgery typically consists of the implantation of a deep brain stimulator (DBS), although gamma knife thalamotomy (or, less frequently, radiofrequency ablation, Niranjan et al., 1999) serves as alternative for those patents not eligible for DBS (Kondziolka et al., 2008). DBS of the ventral intermediate (Vim) nucleus of the thalamus has shown to ameliorate drastically the symptoms

[1] Consensus definition by the Movement Disorder Society, included in (Deuschl et al., 1998). An example of a typical test for tremor assessment is shown in Fig. 1.1A.

[2] These drugs are rated as level A. Level A means established as effective, ineffective, or harmful for the given condition in the specified population. Level A rating requires at least two consistent Class I studies (prospective, randomized, controlled clinical trial with masked outcome assessment, in a representative population). Details are given in (Zesiewicz et al., 2005), and its update (Zesiewicz et al., 2011)

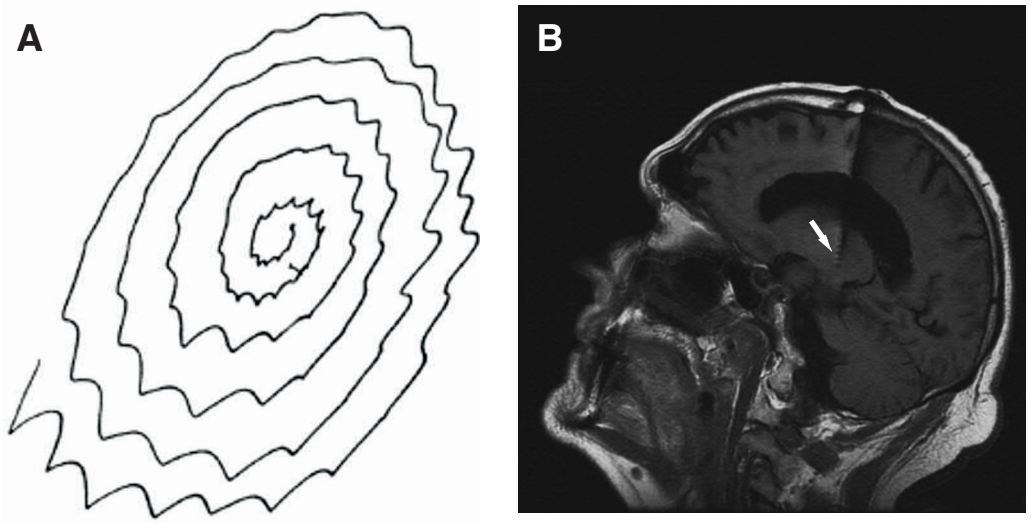

FIGURE 1.1: An example of spiral drawing obtained from an essential tremor patient (A), and of a patient implanted with a deep brain stimulator (B). Figure B corresponds to a cranial magnetic resonance showing the tip of the deep brain stimulation electrode in the ventral intermediate nucleus of the thalamus (signaled with an arrow). Reprinted from (Bain, 2002) and (Shneyder et al., 2012) with permission from the authors.

of PD and ET patients (see the review in Perlmutter and Mink, 2006), although the mechanism that mediates this remains to be elucidated (Fig. 1.1B shows a image of a patient implanted with a DBS). So does the optimal neurostimulation locus—or loci—, as other targets such as the internal segment of the globus pallidus appear as promising alternatives (Perlmutter and Mink, 2006).

Importantly, both drugs and neurosurgery carry significant drawbacks associated. Most drugs induce side effects (see Jankovic and Aguilar, 2008 and Deuschl et al., 2011 for a review on PD and ET respectively), and, as mentioned above, loose efficacy with time. DBS, the preferred neurosurgical treatment at the time of writing, is related to increased risk of intracraneal hemorrhage (Kleiner-Fisman et al., 2006), and psychiatric manifestations (Piasecki and Jefferson, 2004)—including elevated suicide rate (Voon et al., 2008).

In spite of the availability of these various alternatives, tremor is not effectively managed in a significant proportion of patients—up to 25 % according to some estimates (Rocon et al., 2004)—, and is a major cause of dependance and loss in quality of life (e.g., Hariz and Forsgren, 2011 and Louis et al., 2001a). In addition, tremor carries important social and psychological burden associated (see, e.g., Allain et al., 2000; Lorenz et al., 2011), which further affects both patients' and relatives' lives. This motivates that the development of novel therapies for tremor is matter of paramount importance (see Epigraph §1.2.4 for an exhaustive review on emerging alternatives).

Already in 1965, the pioneering work presented in (Chase et al., 1965) showed how the amplitude of cerebellar intention tremor could be reduced by applying weight loads to

the affected limb. This gave rise to subsequent efforts that exploited the alteration of the mechanical properties of the limb—and accompanying neurophysiological effects—to attenuate arm tremor. Most of these studies focused on viscous loading of the tremulous arm through different interfaces, ranging from damped manipulanda to orthoses (e.g., Adelstein, 1981; Arnold and Rosen, 1993), although alternatives other than mechanical loading have also been investigated. Overall, some of these works reported promising results when attenuating tremor of different etiologies (a more detailed review is presented in Epigraph §1.2.4), although systematic validation in representative groups of patients is lacking.

Wearable robots (WRs) and neuroprostheses (NPs) are emerging solutions for the rehabilitation or management of movement disorders. They are characterized by a close, frequently bidirectional, interaction with the user, both in terms of interchange of information (cognitive Human-Machine Interaction, cHMI) and force (physical Human-Machine Interaction, pHMI) (Pons, 2008). WRs consist of rigid structures that replicate to a certain extent the anatomy of the wearer, and apply forces through external actuators. NPs, on the contrary, use the residual—or intact—capability of the user to generate muscle force, through the application of percutaneous or transcutaneous neurostimulation[3]. WRs/NPs started as fixed systems or wheelchair mounted devices, although the development of novel technologies, overall in the field of sensors and actuators, enabled the production of ambulatory prototypes. Currently, a large number of applications for the rehabilitation and/or compensation of both upper and lower limb disorders are available, as well as in other fields such as human empowering (e.g., Zoss et al., 2006). A few examples of WRs/NPs for the rehabilitation of lower limb disorders are the Lokomat© (Jezernik et al., 2003), LOPES (Veneman et al., 2007), and GAIT exoskeletons (Moreno et al., 2008), and a series of interventions based on FES, like those presented in (Granat et al., 1993) and (Agarwal et al., 2003). Relevant upper limb WRs/NPs are the Bionic Glove© (Popovic et al., 1999)—a NP—, and the ARMEO Spring© (Gijbels et al., 2011), WOTAS (Rocon et al., 2007a) and WREX exoskeletons (Iwamuro et al., 2008). These devices cover a vast ensemble of neurological conditions such as post-polio syndrome, tremor, spinal cord injury (at different levels), multiple sclerosis (MS), hemiparesia and paraplegia.

As already mentioned, a few tremor management orthoses, WRs, and NPs are already available. All of them rely on the manipulation of the mechanical properties of the tremulous limb as the major mechanism to reduce tremor amplitude. The first of these systems implemented user interfaces with damped manipulanda, like a hand grasp (Adelstein, 1981) or a joystick (Sloan, 1981), although follow up works already consisted in

[3]In many contexts, transcutaneous neurostimulation is employed as synonym of Functional Electrical Stimulation (FES). Throughout this review, I will follow the nomenclature employed by the authors of the respective works, while in the remainder, I will refer to my application using the term transcutaneous neurostimulation.

table mounted (Aisen et al., 1992; Arnold and Rosen, 1993) or even ambulatory (Kotovsky and Rosen, 1998) orthoses, which integrated electric brakes and an *ad hoc* viscous damper respectively. At the same time, the pioneering work of Prochazka and collaborators showed how a non-ambulatory NP could alleviate PD, ET and cerebellar tremors (CT) by stimulating a pair of antagonist muscles in counterphase to the tremor bursts (Prochazka et al., 1992; Javidan et al., 1992). A few years later, these two approaches were successfully implemented and validated in the WR WOTAS (Rocon et al., 2007a). These latter two works constitute the departure point for the NP developed in this thesis.

This chapter presents both the motivation and context for the work presented in this dissertation, and the rationale and concept design of the NP for tremor management. In more detail, Section §1.2 reviews the major issues related to tremor, namely, its clinical manifestation, epidemiology, neurophysiology and emerging therapeutical approaches. Next, in Section §1.3 I present the rationale and concept design for the NP for tremor management here developed. The chapter ends, in Section §1.4, with some conclusions that summarize the major topics discussed.

1.2 Tremor

This section highlights how tremor arises from a variety of conditions—that are not straightforward to diagnose—, reviews the genetic and environmental factors that favor its appearance, and summarizes what is known about the neurophysiology of the different pathologies. I also discuss the emerging therapies for treating tremor that have been proposed so far. Importantly, the major points related to these topics that still need to be discovered are underscored. Throughout the different sections I mainly focus on PD and ET, because they are the most prevalent disorders that cause tremor and, as a consequence, they constitute the groups of patients recruited for the different studies included in this dissertation.

1.2.1 Clinical Aspects and Diagnosis of Tremor

Given the lack of a complete description of the disorders that cause tremor (Elble, 2009), tremors are currently classified according to phenomenological criteria (Deuschl et al., 1998). This way, tremor is designated as rest, postural or kinetic, depending on the circumstances under which it appears. In more detail:

- rest tremor occurs in a body part that is not voluntarily activated and is completely supported against gravity,

- postural tremor, on the contrary, appears when voluntarily maintaining a position against gravity, and
- kinetic tremor occurs during any voluntary movement, and may be further split into simple kinetic, intention, task-specific and isometric tremor (Deuschl et al., 1998).

Rest tremor is mostly encountered in PD patients, although it is required for the diagnosis of Holmes' and palatal tremors (Deuschl et al., 1998), which are much less prevalent disorders. Postural tremor is a hallmark of as many as four types of tremor, being ET the most relevant in terms of affected population. Action tremor is a typical manifestation of malfunction of the feedforward control loops, especially the cerebellum (Deuschl et al., 1998) and, as such, it appears in the criteria to diagnose CT, ET (see Section §1.2.3 for details on tremorogenesis), and Holmes' tremor. It is also a characteristic of dystonic tremor, the only syndrome causing action tremor that is unlikely to be mediated by cerebellar impairment (Deuschl et al., 2001).

Fig. 1.2 summarizes the syndromes that cause tremor as established by the Movement Disorder Society (Deuschl et al., 1998), together with its clinical manifestation, defined as activation condition and tremor frequency. This classification combines etiologically defined tremors, like PD and dystonic tremor, with other syndromes that are phenomenologically defined, such as CT or Holmes' tremor, which can arise from various etiologies (Deuschl et al., 2001). ET is separated into a number of entities, in agreement with the emerging view that ET is a heterogeneous clinical condition, probably a family of disorders whose central feature is action[4] tremor of the hands (Louis, 2009). Notice that the subtypes included in the classification presented in Fig. 1.2 are purely phenomenological, and do not take, for example, pathobiological evidences gathered by analyzing brain banks into account (see Epigraph §1.2.3).

Current neurological practice for tremor diagnosis consists of a clinical process that comprises the taking of a history, a physical examination, and, in some instances, laboratory tests (Benito-León and Louis, 2006). The clinical history details aspects such as the age at tremor onset, affected body areas, activating factors, relieving factors, or family history. During physical examination, the affected body areas are identified along with each activity state when the tremor occurs. Only in some cases, simple quantitative analyses such as the recording of arm motion are used, for example, to differentiate mild, early ET, from enhanced physiological tremor (Louis, 2001). Also in rare occasions, specific tests such as striatal dopamine transporter imaging might be used to distinguish patients with ET from those with PD (Benamer et al., 2000). Although some studies already encouraged the use of electrophysiological tests in the diagnosis of, for example, ET (Louis and Pullman, 2001), no step in this direction has been undertaken.

[4]The term action tremor encompasses both postural and kinetic tremor.

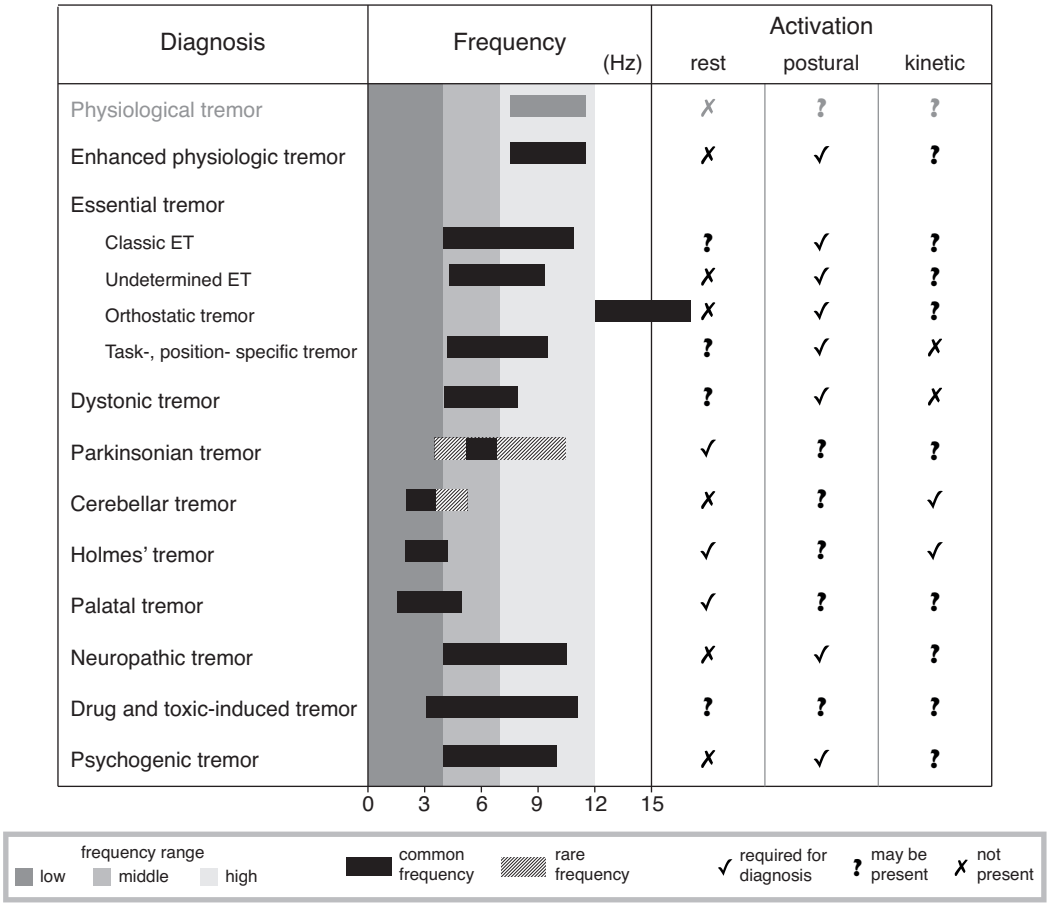

FIGURE 1.2: Tremor syndromes and clinical manifestation according to the consensus statement by the Movement Disorders Society. For each syndrome, the frequency range and the conditions under which it manifests are depicted (see the legend within the gray rectangle). Physiological tremor (in gray) is also included for the sake of comparison. Adapted from (Deuschl et al., 1998).

The most spread criteria for the diagnosis of PD are the London Brain Bank criteria (Daniel and Lees, 1993), while the diagnosis of ET commonly follows the clinical criteria given by the Movement Disorder Society (Deuschl et al., 1998), (later updated in Bain et al., 2000) or the Washington Heights-Inwood Genetic Study of ET criteria (Louis et al., 1997). However, the two criteria for the diagnosis of ET may contradict each other, which has obvious implications in terms of clinical practice and basic research. For example, a tremor diagnosed as mild ET according to the former may be excluded based on the latter. Independently from this, some estimates show that 30–50 % of the cases diagnosed as ET do not actually have ET (Benito-León and Louis, 2006), which highlights the need of developing objective metrics for tremor diagnosis relying on physiological evidences.

1.2.2 The Epidemiology of Tremor

In the prospective population-based study presented in (Wenning et al., 2005), the authors estimated that 14.5 % of people aged 50–89 years suffer from tremor. Although other studies report different figures (e.g. Moghal et al., 1994; Khatter et al., 1996), tremor is accepted to be the most prevalent movement disorder. Furthermore, as already mentioned, ET and PD are by far the most common types of tremor (e.g., Moghal et al., 1994). Indeed, a recent population study showed that ET might affect ∼5 % of those over 65 years (Benito-León et al., 2003) (a few similar estimates are reviewed in Louis, 2008), while PD is estimated to afflict tens of millions of people worldwide (Hammond et al., 2007). Due to the increase of life expectancy and accompanying decreased fertility, their prevalence is expected to approximately double by 2050 (Bach et al., 2011).

Genes and environment contribute to risk of age-related and neurological diseases. They do it in a complex manner, because the expression of genes, for example, can be—and typically is—influenced by environmental factors (Lobo, 2008). These interactions between genetic and environmental factors, together with the heterogeneity of patients with tremor arising from the same syndrome, motivates that much is yet to discover about the epidemiology of tremor.

Patients developing ET in early childhood have been documented (reviewed in Elble and Tremor Research Group, 2006), but the prevalence and incidence of ET increase with aging. Many cases are hereditary (Mendelian dominant fashion), and first-degree relatives are 5 times more prone to develop the condition than controls. This figure doubles if the proband's age of onset is below 50 years (Louis et al., 2001b). Reports on monozygotic twins depend drastically on the criteria chosen for patient recruitment (Elble and Tremor Research Group, 2006), which underscores what was previously said about misdiagnosis as a limiting factor to epidemiological studies of tremor. In addition, the proportion of hereditary versus sporadic ET cases is uncertain (ranging from 17 to 50 %, Louis, 2008). Despite the relative inconsistency of the figures reported, put together, these findings show that although ET has been widely regarded as a familial condition, environmental factors are likely to play a role (Louis, 2008).

In spite of the considerable efforts put on looking for genetic features of ET, it was not until recently that a genome wide association study signaled that two markers of the *LINGO1*[5] allele, rs9652490 and rs11856808, confer risk of ET (Stefansson et al., 2009). This finding, obtained in an icelandic population, was followed by a series of replication studies—11 and 7 respectively—in various ethnic groups. A meta-analysis of the outcomes of these studies showed that rs9652490 is related to risk of both hereditary and sporadic ET, while rs11856808 only confers risk of hereditary ET (Jiménez-Jiménez et al., 2012). Interestingly, *LINGO1* defects may cause impaired axonal function, which

[5] *LINGO1* stands for leucine rich repeat and Ig domain containing Nogo receptor interacting protein-1.

is in line with some of the evidences gathered in postmortem studies of ET brains (e.g., Louis and Vonsattel, 2008). Research on the environmental epidemiology of ET has not been that fruitful, and the accumulated evidence only serves to identify possible exposures that may facilitate the onset of ET (Louis, 2008). Among them, beta-carboline alkaloids such as harmine, harmane and harmaline seem the most reasonable choice, for, administrated to mice, rats, cats rabbits, sheep and primates, induces generalized action tremor resembling ET (Wilms et al., 1999). This tremor is likely to be mediated by a blocking of inhibitory GABA receptors at the inferior olive, which increases the natural tendency of olivary neurons for rhythmic oscillations (Llinás and Yarom, 1986). Elevated blood harmane concentration has been found in cohorts of ET patients, however, controversy still exists as to whether it is an indicator of abnormal brain concentration (Louis, 2008). In addition, beta-carboline alkaloids are produced endogenously, and although dietary sources are known to contribute 50 times more than these endogenous sources, it contributes to hampering the interpretation of these data (Louis, 2008). Lead, pesticides and ethanol have also been considered as potential exposures contributing to ET, but sufficient evidences are lacking (see Louis, 2008 for a review). Nevertheless, given that a significant proportion (∼2 %) of the population over 40 years is estimated to suffer from nonfamilial ET (Louis, 2008), research on environmental toxins as risk factors of ET becomes of paramount importance.

In 1817, the neurologist James Parkinson described the "Shaking Palsy" or "Paralysis Agitans" as an involuntary tremulous motion, which lessened muscular power, in parts not in action and even when supported; with a propensity to bend the trunk forward, and to pass from walking to running pace; the senses and intellects being uninjured (Parkinson, 1817). Today, it is known that PD is a neurodegenerative disease characterized by the loss of dopaminergic neurons in the substantia nigra (pars compacta), which results in a specific disorganization of the basal ganglia circuits (Bartels and Leenders, 2009), and that manifests with four cardinal symptoms: akinesia[6], bradykinesia[7], increased muscle tone (rigidity), and rest tremor. As to ET, the prevalence of PD increases with aging; 1 to 2 % of people over 50 years are estimated to suffer from it (Bartels and Leenders, 2009). Around 90 % of PD cases are sporadic (Archibald and Burn, 2008), which is known as idiopathic PD, although first-degree relatives have a two- to threefold increased relative risk to develop it (Gasser, 1998).

It is generally accepted that PD is the result of an interaction between genetic and environmental factors (Bartels and Leenders, 2009). According to this theory, genetic predisposition enabled by environmental factors induces mitochondrial respiratory failure and oxidative stress within the nigral neurons, leading to cell death (Schapira et al., 1992). The fact that exposure to 1-methyl-4-phenyl- 1,2,3,6-tetrahydropyridine (MPTP) can produce symptoms very similar to PD (Langston et al., 1999) proves that environmental factors may be causative factors in PD. In addition, the finding of increased risk

[6]The term akinesia denotes the inability to initiate movement.
[7]Bradykinesia describes a slowness in the execution of movement.

of developing PD in people who lived in an environment with pesticides structurally similar to MPTP gave further support to this finding (Bartels and Leenders, 2009). Administration of MPTP constitutes the most widely accepted model of PD; although in nonhuman primates tremor is not always reproduced, the other major symptoms of PD are consistently present. Further, in rhesus monkeys or common marmosets, tremor appears at posture, while clinical descriptions in macaque present large intra-animal variation (Wilms et al., 1999). It must be mentioned that other hypotheses (reviewed in Bartels and Leenders, 2009), such as the oxidation hypothesis, have been put forward to explain the dopamine depletion in PD.

Several genetic mutations can cause parkinsonian syndromes that are clinically close to idiopathic PD. As a matter of fact, 10 monogenic variants of PD have been found (reviewed in Klein and Schlossmacher, 2006). This encouraged the exploration of factors that motivate the onset of idiopathic PD, including interactions between various genes, modifying effects of susceptibility alleles, and epigenetic[8] factors.

Finally, debate exists as to whether PD and ET share a common link. At the present time, a wealth of clinical data is available (reviewed in Louis, 2008), overall showing a more common development of ET in PD patients, and a two- to fourfold increase in the probability of ET cases to develop PD. These observations were reinforced when *LINGO1* and *LINGO2* variants were signaled as a risk factor both for PD and ET, providing the first genetic evidence of linkage between both (Vilariño Güell et al., 2010). Future studies are expected to help expanding this emerging view.

1.2.3 The Neurophysiology of Tremor

It was explained before that due to the lack of knowledge on the etiology of tremors, a syndromic classification has been established (see Fig. 1.2). Each of these syndromes corresponds either to a well defined etiological entity or to a variety of conditions, although for both, much remains to be discovered. However, based on current evidences, it is accepted that all the tremors except for neuropathic tremor have a large central component (Deuschl et al., 2001), being peripheral and mechanical factors also present due to the intrinsic properties of the neuromusculoskeletal system, although in a lesser extent. Next, I review the structural changes and neural circuits involved in the pathogenesis of ET and PD, given that they represent the study groups of this thesis.

ET has been traditionally regarded as a "benign" condition, meaning that it appeared without any underlying pathological change and carried no burden associated except for the tremor (Louis and Okun, 2011). However, direct and indirect evidences gathered in the last decade suggest that this belief needs to be discarded. Direct evidences comprise

[8] Epigenetics is the study of heritable changes in gene expression or cellular phenotype caused by mechanisms other than changes in the underlying DNA sequence.

a series of abnormalities found in postmortem studies of ET brains. Louis and coworkers consistently found neuropathological changes consisting of either cerebellar degeneration, i.e. Purkinje cell loss and axonal dwellings—torpedoes—, or the presence of Lewy bodies in the locus coeruleus[9] (Louis et al., 2007; Louis and Vonsattel, 2008; Axelrad et al., 2008; Yu et al., 2012). However, these results are still controversial because replication studies failed to find these abnormalities in another sample of patients, and differences with age-matched controls were not significant (Rajput et al., 2011; Shill et al., 2008), although it has been claimed that insufficient statistical power might have biased the analysis and misled the conclusions in these latter studies (Louis et al., 2011). It is interesting to remark that Lewy bodies are also found in PD brains, although they are likely to be symptomatic and not causative of the condition (Bartels and Leenders, 2009). In addition to these findings from brain necropsies, indirect evidences are accumulating, suggesting that ET might be a slowly progressing degenerative condition, associated with mild deficits in attention, executive functions, memory, and possibly, other cognitive processes (see the review in Bermejo-Pareja, 2011). Other motor alterations, such as impaired tandem walking (Stolze et al., 2001), and loss of confidence in gait and balance (Louis et al., 2012) have been recently reported. All together, these bulk of knowledge suggests that the traditional view of ET needs to be replaced by that of a family of slowly progressing, probably neurodegenerative, disorders (Louis, 2009).

As to the structures involved in the pathogenesis of ET, the widely accepted view is that it originates at the cerebellar and thalamocortical loops (Benito-León and Louis, 2006; Elble, 2009), the pathways that regulate the realization of voluntary movements (Raethjen and Deuschl, 2012). This statement is supported by few complete observations, and abnormalities in all these structures have not been found in necropsies (e.g., Louis and Vonsattel, 2008). The involvement of the inferior olive has also been put forward due to its rhythmic properties, which, as mentioned above, mediate the production of tremor in harmaline models of ET (Wilms et al., 1999). Positron emission tomography (PET) has also revealed increased olivary glucose utilization (Boecker and Brooks, 1998), but differences were not found in other brain imagining studies (Wills et al., 1994; Bucher et al., 1997), and postmortem investigation has revealed no structural changes (Louis and Vonsattel, 2008; Louis et al., 2013). In the same study, (Boecker and Brooks, 1998), the authors reported increased blood flow in the cerebellum, thalamus and red nucleus[10] (data in Wills et al., 1994 also supported the involvement of the latter). Abnormal cerebellar activation has also been found during magnetic resonance imaging examination (bilaterally), and was accompanied by hyperactivation of the thalamus, globus pallidus[11] and primary sensorimotor cortex (Elble and Tremor Research Group, 2006). The involvement of the cerebellum in the etiology of ET is also supported by magnetic

[9]The locus coeruleus is a constituent of the pons, a part of the brainstem.

[10]The red nucleus is a structure in the rostral midbrain involved in motor coordination. It is located in the tegmentum of the midbrain next to the substantia nigra, and is a component of the extrapyramidal motor system.

[11]The globus pallidus is one of the four nuclei that constitute the basal ganglia.

resonance spectroscopy (Pagan et al., 2003) and brain necropsies (see above). Direct recordings of individual cells in the thalamus revealed the existence of activity coherent with the ongoing tremor (Hua et al., 1998), most frequently in the ventral intermediate among those nuclei analyzed (Hua and Lenz, 2005). Furthermore, this coupling only occurred intermittently, which cast further doubts about the traditional hypothesis to support the involvement of the inferior olive in the pathogenesis of ET (Hua and Lenz, 2005). The fact that ventrolateral thalamotomy and thalamic stimulation are effective treatments of ET (Herzog et al., 2007) also provides indirect cues of the involvement of the thalamus in tremorogenesis. Finally, the role of the somatosensory cortex in ET is supported by studies addressing cortico-muscular coupling (Hellwig et al., 2001, 2003; Raethjen et al., 2007; Muthuraman et al., 2012), although projection of the central tremor to muscles might occur by pathways other than corticospinal (e.g. rubrospinal) (Raethjen et al., 2007). Furthermore, although within a patient the tremulous muscles exhibit oscillations at a similar frequency, they are commonly uncoupled, suggesting that tremor in ET arises from the projection of different oscillators (Lauk et al., 1999; Raethjen et al., 2000), probably reflecting the somatotopic organization of the structures involved in tremorogenesis (Purves et al., 2004). Reflexes also seem to play a role in the manifestation of ET, in which they interact in a synergistic or competitive manner with the descending tremulous drive, altering the properties of the tremor (Elble, 1986; Héroux et al., 2009, see Fig. 1.3). Thus, the hypothesis that ET originates from the cerebellar and thalamocortical networks is supported by a number of studies in which involvement of one or some—but not all—these structures was observed. However, a detailed description of the oscillatory network of ET is lacking, and some evidences point that other loci such as the inferior olive, the red nucleus or the globus pallidus may participate in tremorgenesis. Furthermore, many of these studies find relevant inter-patient differences that are yet unexplained, or report inconsistent findings.

The loss of dopaminergic nigrostriatal neurons in PD patients is believed to cause abnormal oscillations in the loop linking the cortex, basal ganglia, and thalamus (Elble, 2000), which are the ultimate mechanism for the generation, maintenance and transmission of the tremor in PD. Although, the principal source remains unclear (Steigerwald et al., 2008; Elble, 2009), the basal ganglia appear to be the capital locus of the pathogenesis of PD (Obeso et al., 2000; Deuschl et al., 2000a; Archibald and Burn, 2008; Steigerwald et al., 2008; Bartels and Leenders, 2009). The basal ganglia are a group of functionally diverse subcortical nuclei that lie deep within the cerebral hemispheres. According to the most accepted view, the basal ganglia are four[12] nuclei, namely, the striatum, the globus pallidus, the substantia nigra and the subthalamic nucleus (Purves et al., 2004). According to the classic model, the basal ganglia form a complex network of parallel loops that integrate cerebral cortical areas (associative, oculomotor, limbic and motor),

[12]Some authors consider that the basal ganglia comprise three or five nuclei, depending on how constituents are grouped.

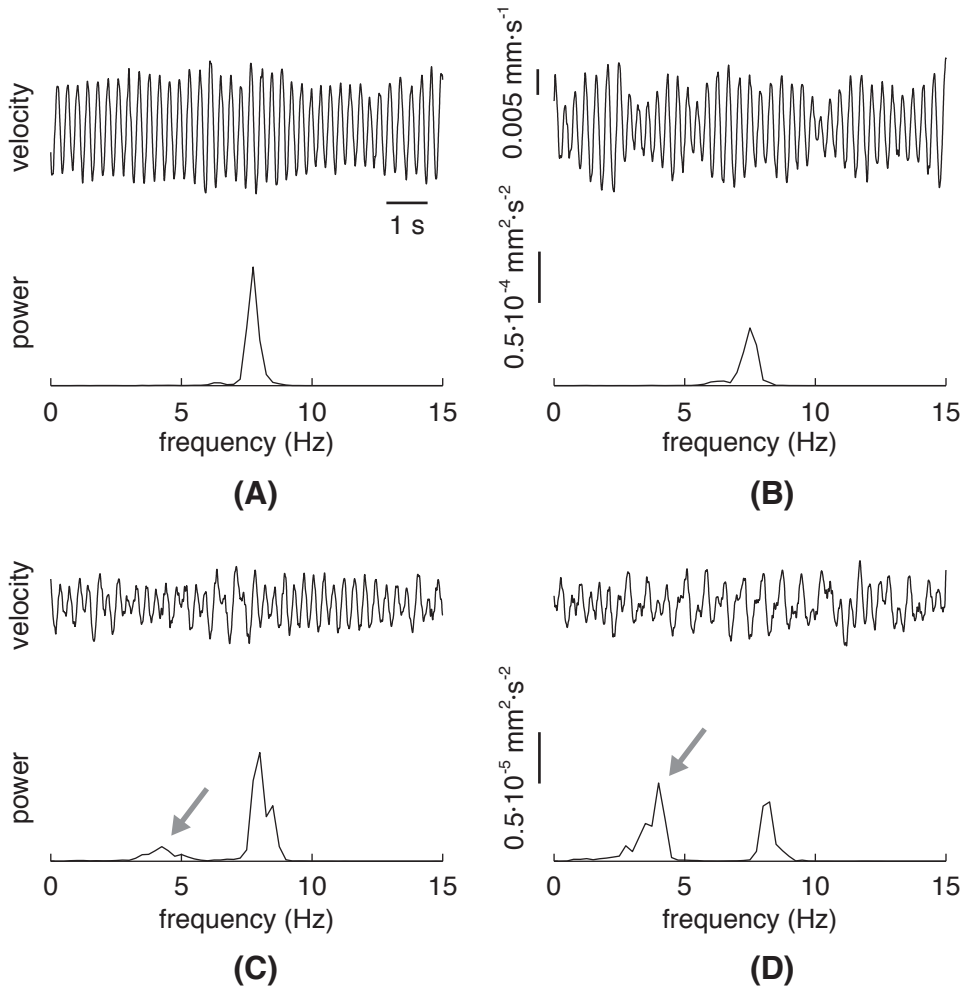

FIGURE 1.3: Effect of added weight on the tremor in ET. The plot illustrates how hand tremor varies as the inertial load is increased: A) corresponds to the unloaded limb, B) to the limb with a weight of 5 % of a normalized load attached to it, C) to a 15 % load, and D) to a 25 % load. In all the cases, the top panel represents the data in the time domain, and the bottom panel in the frequency domain. Panel (B) shows that the 5 % load reduces the amplitude of the tremor, while larger loads (C and D) also make a low frequency component, which corresponds to the mechanical reflex, appear (grey arrows). Notice the change in the scale of the power spectra in (C) and (D) when compared to (A) and (B). The data represented in this plot are from (Héroux et al., 2009), and have been reprinted with permission of the author.

the basal ganglia nuclei, and the thalamus (Alexander et al., 1986). Within this network, two major pathways exist: *i*) the "direct pathway," which "facilitates" movement by reducing the inhibitory effect of the basal ganglia nuclei on the thalamus, and *ii*) the "indirect pathway," which enhances the inhibitory effect on the thalamus, hereby "suppressing" movement (Bartels and Leenders, 2009). Dopamine depletion leads to inhibition of the thalamocortical and brainstem motor systems, causing the parkinsonian motor symptoms. Variations in the expression of PD may thus result from deficits in selective regions of the basal ganglia. Interestingly, studies at the peripheral (Hurtado et al., 2000; Raethjen et al., 2000) and central nervous system (Hurtado et al., 1999) indicate that multiple oscillators also cause PD, although they usually present the

same frequency, as in the case of ET. It is likely that this may be a consequence of the topographical organization of the basal ganglia themselves (Deuschl et al., 2000a).

A recent work showed abnormally large neural entrainment at low beta frequencies in basal ganglia circuits in PD (Hammond et al., 2007), opposed to their normal function during which subcircuits are uncorrelated (Bartels and Leenders, 2009). This finding is consistent with one of the most accepted theories to explain the pathophysiology of PD (Deuschl et al., 2000a). Notably, abnormal neural entrainment has also been observed in MPTP (Hammond et al., 2007) and DAT-KO[13] (Fuentes et al., 2009) rodent models of PD. Therefore, it has been hypothesized that dopaminergic drugs or high frequency DBS may disrupt this abnormal synchronization, and facilitate movement by removing the aberrant inhibition of the thalamus (Bartels and Leenders, 2009). As a matter of fact, the mechanism that mediates the alleviation of akinesia in PD mice through spinal cord stimulation replicates this: in (Fuentes et al., 2009), the authors observed that normal neural activity patterns, resembling the state preceding movement, appeared once spinal cord stimulation of the dorsal columns disrupted the abnormal, low frequency corticostriatal synchronization.

Apart from the four cardinal symptoms of PD, patients present freezing of gait (30–60 % of them, Giladi et al., 1997), and walk with shuffling, small steps and little arm swing. This is accompanied by loss of balance reflexes, which causes immobility and risk of falling (Bartels and Leenders, 2009). Motor symptoms in PD manifest together with by nonmotor complications, like a series of cognitive changes—that in 20–40 % of the cases develop into dementia—, fatigue, weight loss, scoliosis, alterations in sensory and autonomic functions, depression, anxiety, sleep disorders or sexual disfunction among others (Bartels and Leenders, 2009).

1.2.4 Alternative Approaches for Tremor Management

It was explained above that tremor is currently managed through pharmacotherapy or neurosurgery, and that in spite of the benefits provided by these therapies, a large proportion of patients do not benefit from either of them (see Section §1.1). Moreover, both approaches suffer from inherent drawbacks that may become troublesome in some cases. Therefore, considerable effort is being put into the improvement of existing therapies and the development of novel ones. In this section I review the alternative (emerging) forms to manage tremor, overall focusing on those envisioned as ambulatory devices.

Table 1.1 summarizes the most relevant works presenting alternative therapies for tremor management. The works there depicted present either a novel intervention, or the first evaluation of one of these interventions with a group of patients suffering from a different tremor syndrome. Notably, most therapies provide statistically significant positive

[13] DAT-KO mice are generated through genetic techniques, and lack the dopamine transporter DAT.

results, although patient groups are generally small (convenience samples), and most protocols do not account for a possible placebo effect, or are not randomized. Control subjects are in many cases not included, although in the author's opinion this does not constitute a mistake in the experimental proof of most of the interventions. Unfortunately, any of these alternatives has been validated for long term, and measures of health related quality of life are lacking (O'Connor and Kini, 2011). These interventions can be grouped into the following categories:

1. weight (inertial) loading,
2. orthoses (including WRs),
3. transcutaneous neurostimulation (FES),
4. physical therapy,
5. limb cooling,
6. vibration therapy,
7. bright light therapy,
8. transcranial magnetic stimulation, or
9. spinal cord stimulation.

Transcranial magnetic stimulation was the only alternative that did not ameliorate the patients' symptoms, although the authors acknowledge that selection of stimulation parameters may account for this (Filipovic et al., 2010). The improvement provided by bright light therapy was significant (Paus et al., 2007), although had little statistical power; however the simplicity of the approach (looking at a commercial light box for 30 min every morning), renders further evaluation of this intervention interesting. The results obtained with whole body- (Haas et al., 2006) or upper and lower limb vibration (King et al., 2009) in PD were also positive in terms of reduction of tremor amplitude, and, for the former, also of decreased rigidity. The authors of (Haas et al., 2006) speculated that this improvement was mediated by an increase in the activation level of the somatosensory area of the cortex, which is otherwise abnormally low in PD patients. Tendon vibration in patients with tremor arising from MS increased significantly its amplitude (Feys et al., 2006), although it decreased the amplitude of voluntary movements in healthy controls, and patients suffering from MS with and without tremor. Limb cooling succeeded in alleviating ET (Lakie et al., 1994; Cooper et al., 2000), PD (Cooper et al., 2000), and MS tremors (Feys et al., 2005), however, the nature of the approach hampers its exploitation for extended periods of time. All the authors argued that a reduction in conduction velocity may have facilitated the alleviation of tremor, and in (Feys et al., 2005) they also hypothesized that cooling may alter limb properties

TABLE 1.1: Alternative forms to manage tremor. Each row presents a relevant study, depicting the number of patients per tremor syndrome[‡] who participated, the outcome of the evaluation, and the main bibliographical reference(s).

Therapy	Tremor syndromes	Outcome	Bib. reference
Weight loading	ET (14), MS (10), FA (8), CS (5), CVA (4), PD (5), other(4)	Tremor reduction in 58 % of patients (objective); therap. benefit in 36 %	(Hewer et al., 1972)
Manipulandum: viscous damping/ isometric restraint	MS (3), ET (1), CS (1), CP (1), stroke (1)	Significant tremor reduction; vol. mov. not degraded	(Adelstein, 1981)
Energy dissipation orthosis (viscosity)	CS (10)	Statistical and functional improv.	(Aisen et al., 1993)
Limb cooling	ET (16)	Objective reduction of tremor severity.	(Lakie et al., 1994)
Limb cooling	ET (20), PD (20)	Tremor reduction	(Cooper et al., 2000)
Limb cooling	MS (18)	Tremor reduction, vol. mov. unaltered	(Feys et al., 2005)
FES	MS (6), PD (4), ET (3)	Significant tremor attenuation	(Javidan et al., 1992) (Prochazka et al., 1992)
Haptic interface	n.a. (5)	Objective reduction	(Pledgie et al., 2000)
Strength training	ET (13[†])	Objective but not functional improv.	(Bilodeau et al., 2000)
Weighted instruments and weight loading	PD (14)	No significant improvement	(Meshack and Norman, 2002)
Tendon vibration	MS (39[†])	Tremor amplitude increased	(Feys et al., 2006)
Whole body vibration	PD (68[†])	Reduction in tremor and rigidity	(Haas et al., 2006)
Neuromuscular therapy	PD (36[†])	Tremor reduction, motor improvement	(Craig et al., 2006)
Bright light therapy	PD (36[†])	Clinical improvem.	(Paus et al., 2007)
Transcranial magnetic stimulation	PD (10[†])	No signficant improvement	(Filipovic et al., 2010)
WR: viscosity/ notch filtering	ET (7), MS (1), PT (1), MT (1)	Significant tremor attenuation	(Rocon et al., 2007a) (Rocon et al., 2007b)
Spinal cord stimulation (thoracic level)	PD (1)	Tremor reduction, motor improvement in all 4 limbs	(Fénelon et al., 2012)

[‡] Additional abbreviations: CS: cerebellar syndrome, FA: Friedrich's ataxia, CVA: cerebrovascular accident, CP: cerebral palsy, PT: post traumatic tremor, MT: mixed tremor of unknown etiology.
[†] This figure includes a placebo group.

and the sensitivity of muscle spindles, which would contribute to tremor attenuation. The pioneering study of Fénelon and coworkers constitutes a very interesting approach since they showed how all motor symptoms of PD are drastically ameliorated by spinal cord stimulation at the thoracic (T9-T10) level of the spinal cord (Fénelon et al., 2012), on the contrary to what was reported for stimulation at the cervical level (Thevathasan et al., 2010). This single case report was inspired by a recent work that demonstrated that spinal cord stimulation of the dorsal columns in rodent models of PD alleviated

akinesia (Fuentes et al., 2009) (by disrupting abnormally large neuronal synchronization, as mentioned in Section §1.2.3). Importantly, the results in (Fénelon et al., 2012) were successfully replicated in a group of 15 PD patients (Agari and Date, 2012).

The remainder four categories of emerging interventions for tremor—weight loading, orthoses, transcutaneous neurostimulation and physical therapy—have in common that they primarily rely on the alteration of the mechanical properties of the affected limb to attenuate the tremor. This is performed either by directly changing the inertia of the tremulous limb by attaching a weight to it (in weight loading), or by exerting a force of a certain type (in the remainder three). Forces may be applied through external interfaces that typically apply a torque that is transmitted to the skeletal system, or by muscle contraction, voluntarily or artificially elicited. Notice, nonetheless, that by the intrinsic structure of the neuromuscular system, the "mechanical" manipulation of limb properties is always accompanied by an alteration of reflexes, and an afferent flow of information to the supraspinal centers. Stimulation may also add afferent stimuli transmitted to supraspinal centers.

The possibility of altering tremor properties through weight loading was already described in 1965, when Chase and coworkers observed that the amplitude of CT was reduced when the activity of antagonist muscles was increased by the effect of added weight (Chase et al., 1965). Since then, weight loading has received considerable attention, both as a tool to investigate the pathophysiology of tremors (see, e.g., Elble, 1986; Hömberg et al., 1987; Héroux et al., 2009, 2011; Caviness et al., 2006), and as the basis for novel interventions for tremor management (see, e.g., Hewer et al., 1972; Meshack and Norman, 2002).

The work presented in (Hewer et al., 1972) compared the response to weight loading of different tremor syndromes, and showed that tremor arising from various conditions such as MS, cerebral palsy or ET was significantly ameliorated in a number of patients. The symptoms of PD patients, however, were not significantly improved when compared to their basal condition. Also interestingly, the authors assumed for the first time that a pure mechanical effect could not account for tremor attenuation, in line with the current hypothesis that reduction of tremor amplitude could be mediated by some type of interaction between the reflex and central components at the motoneuron pool level (Elble et al., 1987; Héroux et al., 2009; Negro and Farina, 2011a). As a matter of fact, the authors of (Hewer et al., 1972) suggested that the different response of PD, when compared to other tremor syndromes, implied that there is a more significant contribution of peripheral components in essential or cerebellar tremors than in PD. It is still controversial whether the amplitude of PD tremor can be systematically attenuated with inertial loading, since subsequent works provided contradictory results (Hömberg et al., 1987; Meshack and Norman, 2002; Forssberg et al., 2000; Hwang et al., 2009); nonetheless, accumulated evidence points at tremor exacerbation when the limb is loaded. Results of

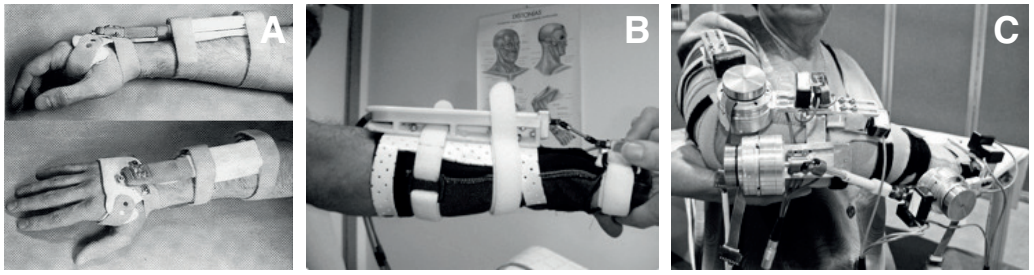

FIGURE 1.4: Ambulatory orthoses for tremor management: the viscous beam (A, Kotovsky and Rosen, 1998), the double viscous beam (B, Loureiro et al., 2005), and WOTAS (C, Rocon et al., 2007a).

weight loading in ET show that the response is weight dependent, meaning that above a certain mass tremor amplitude may be increased (Héroux et al., 2009).

The most typical example of the investigation of tremor mechanisms exploiting this approach is how the central and reflex components of ET are separated when an adequate weight is attached to the tremulous limb (Elble, 1986; Hömberg et al., 1987; Héroux et al., 2009, 2011). Given that this feature had not been initially observed in PD, some researchers underscored the potentiality of the method for differential diagnosis of both conditions. However, a recent work has shown how the postural tremor of PD exhibits a similar behavior during weight loading (Caviness et al., 2006). Other types of tremor such as that arising from MS (Feys et al., 2003), or psychogenic tremor (Piboolnurak et al., 2005) have also been investigated following this approach

The application of force on the tremulous limb constitutes another manner to manipulate its mechanical—and thus neurophysiological—properties, and alter the characteristics of the tremor. A number of studies that investigate this approach are available, and can be broadly classified as: *i*) those that deal with the application of external forces, and *ii*) those that focus on the influence of internal forces, i.e. through muscle contraction. The former category comprises works dealing with orthotic management of tremor, whereas studies falling in the latter category traditionally aim at investigating the pathophysiology of tremors. Notice that internal forces may also be driven by an external device, i.e. a NP, as done in FES-based interventions for tremor suppression (see below).

Most devices for tremor suppression through force loading rely on dissipative viscous elements (in a few cases combined with springs) to attenuate the tremor (Adelstein, 1981; Sloan, 1981; Broadhurst and Stammers, 1990; Aisen et al., 1993; Arnold and Rosen, 1993; Rosen et al., 1995; Kotovsky and Rosen, 1998; Pledgie et al., 2000; Loureiro et al., 2005). The rationale for this is that viscous elements exert a force that is proportional to velocity, and tremors are faster than volitional movements (see Epigraph §2.2.3 for details), therefore clinical and functional benefit should be, and in many cases is, obtained. The group of patients enrolled in the previous studies comprised people with intention tremor arising from MS, traumatic brain injury, cerebral palsy, cerebellar ataxia or ET

(Adelstein, 1981; Sloan, 1981; Broadhurst and Stammers, 1990; Aisen et al., 1993; Arnold and Rosen, 1993), and thus include the major disorders that cause tremor except for PD, likely because it is not always accompanied by intention tremor (Deuschl et al., 2012). Remarkably, a non-ambulatory solution based on viscous loading, the Neater Eater© (Michaelis, 1988), is available in the market[14]. A further classification of these systems is made by grouping them into orthoses (Aisen et al., 1993; Arnold and Rosen, 1993; Rosen et al., 1995; Kotovsky and Rosen, 1998; Loureiro et al., 2005) or manipulanda (Adelstein, 1981; Sloan, 1981; Broadhurst and Stammers, 1990; Michaelis, 1988; Pledgie et al., 2000). The former constitute the aim of this thesis, given that they have a higher potential to impact during the activities of daily living (ADLs). From an implementation perspective, orthoses (see the examples in Fig. 1.4) are grouped as table mounted (e.g., Adelstein, 1981; Sloan, 1981; Broadhurst and Stammers, 1990; Aisen et al., 1993; Michaelis, 1988; Pledgie et al., 2000), wheelchair mounted (e.g. Arnold and Rosen, 1993, or another version of Michaelis, 1988), or ambulatory-aimed (Kotovsky and Rosen, 1998; Loureiro et al., 2005; Rocon et al., 2007a), Finally, it must be noticed that works that compared different types of loads showed that viscous forces outperformed other approaches, e.g., added stiffness and inertia (Sanes et al., 1988). The most recent orthosis for tremor management is the WR WOTAS (Rocon et al., 2007a).

WOTAS consists of a mechanical structure—a robotic exoskeleton—that applies forces to upper limb joints through electric motors (see Fig. 1.4C), based on the kinematics and kinetics of concomitant voluntary and tremulous movements (Rocon et al., 2007a). Force is applied either in counterphase to the tremor, or as a constant damping as typically done in tremor suppression devices (see above), although in this case damping is not generated with passive elements, but with actuators. Experimental evaluation yielded that counterphase loading outperformed viscous loading, although the authors argued that given that a fixed viscosity was applied to all the patients, the results may be biased (Rocon et al., 2007a). The group of patients in which WOTAS was tested comprised patients with ET, tremor from MS, and post-traumatic tremor; therefore it thus included the most common syndromes that cause intention tremor. It must be mentioned that in spite of the successful results, the system had to major drawbacks that were inherent to its design (Rocon et al., 2007a; Belda-Lois et al., 2007a):

1. Soft tissues impede the efficient transmission of low forces to the musculoskeletal system, which caused that mild tremors were not successfully attenuated. The authors also concluded that inefficient transmission of low forces impede the implementation of solutions of this type for other applications.

2. Users reported that the exoskeleton did not fulfill their aesthetic, cosmetic and usability expectations. Despite the functional improvement often perceived by

[14]Neater Eater (Neater Solutions, Ltd.) website: http://www.neater.co.uk/main.htm

patients, they were reluctant to utilize such a bulky and anesthetic device as a robotic exoskeleton during daily living.

Therefore, in the design of a novel system, these limitations must be accounted for. As a matter of fact, the NP presented in this dissertation aims at circumventing these issues at the same time that providing a prototype for intensive clinical and functional testing. Details on the concept design of the NP are given in Section §1.3.

To the author's knowledge, only two studies dealt with the influence of voluntary muscle contraction on tremor amplitude. The first of them, (Dietz et al., 1974), addressed how different factors affected motor neuron (MN) behavior in PD. They observed that, during an isometric contraction, the amplitude of PD tremor decreased with added load. Although it must be reminded that works dealing with weight loading in PD (reviewed before) suggest that this cannot be extrapolated to all conditions. On the contrary, for ET it was found that tremor amplitude during isometric contractions was increased when muscle activation augmented (Héroux et al., 2010), and also did during movement (when compared to posture) (Héroux et al., 2011). This provides additional proof that the influence of peripheral changes in PD and ET is considerably different, as supported by many (e.g., Hewer et al., 1972; Cooper et al., 2000). In this line, the authors of (Bilodeau et al., 2000) reported that strength training enhanced limb steadiness in ET patients, but did not cause a functional improvement.

The last alternative intervention that has been evaluated as a means for treating tremor is transcutaneous neurostimulation. Transcutaneous neurostimulation constitutes a manner to directly activate MNs or reflex and afferent pathways artificially (Popovic and Sinkjaer, 2000), and therefore permits circumventing (at least partly) motor control mechanisms. Tremor attenuation with transcutaneous neurostimulation has been performed by activating the tremulous muscles out of phase with the tremor bursts (Prochazka et al., 1992; Gillard et al., 1999; Popovic-Maneski et al., 2011), normally using table mounted systems (Prochazka et al., 1992; Gillard et al., 1999). This approach resembles a selective notch filter at tremor frequency, and has proved to be an effective alternative for managing parkinsonian, essential and cerebellar tremors (Javidan et al., 1992; Gillard et al., 1999; Popovic-Maneski et al., 2011). Notice that this strategy was latter replicated in the WR WOTAS, also achieving significant tremor attenuation (Rocon et al., 2007a). However, transcutaneous neurostimulation has an important advantage compared to wearable orthoses/robots, which is that neurostimulation avoids the need of external actuators, for the patients' muscles are employed to generate joint torques. By implementing a NP, this aspect was already considered in the design of the tremor suppression system.

1.3 Concept design of the Neuroprosthesis

This section presents the concept design of the NP for tremor management whose development and validation is the aim of this thesis. It reviews the requirements defined to design the cHMI and pHMI (Pons, 2008) it implements, and finalizes by providing a concept of the final prototype of the NP. The concept design of all components was achieved by taking both the characteristics of the population that may benefit from the system (people suffering from disabling tremor, typically of advanced age) and the nature of the problem into account. The appearance of the prototype was defined after analyzing the work in a focus group held at Instituto de Biomecánica de Valencia[15] (Laparra-Hernández et al., 2010).

1.3.1 Concept Design of the Cognitive Human-Machine Interface

The goal of the NP is to provide a novel alternative for functional compensation of tremor during daily living. Hence, the NP is designed to actuate only when tremor may impede or hamper the performance of a voluntary movement. On the contrary, if tremor appears in a nonfunctional context, like, for example, rest tremor in PD, the NP should not actuate. Apart from this, the NP should ideally be triggered by the natural processes of the central nervous system (CNS), and not by "artificial" commands (or mental states as they are typically referred to), such as those employed in other solutions, and that consist in, e.g., imaging moving the left arm, or a square shape (Millan et al., 2004). These imply a learning process by the user, and thus are cognitively demanding. The use of natural commands will have a strong positive impact on usability, and would permit expanding the use of the NP to the elder, and to people with mild cognitive impairment, as it is the case of many patients with tremor (Bermejo-Pareja, 2011; Archibald and Burn, 2008).

These ideas can be put together as a series of functional requirements for the cHMI, which is in charge of decoding user commands, and generating information to the pHMI that controls the NP. These requirements are:

R_c1. The NP must actuate only when it is needed, i.e. when the user wants to perform a volitional movement during which tremor may be cause of disability.

R_c2. The interface must be natural, avoiding the performance of demanding cognitive processes.

R_c3. The response of the interface must be fast, because some ADLs typically have short duration; examples of this are signing a document, pouring water into a glass, or buttoning a shirt.

[15] The main authors of this work were J. Laparra-Hernández and J.M. Belda-Lois.

R_c4. Tremor, in the presence of concomitant voluntary movement, needs to be accurately parameterized, ideally with no delay, in order to drive the controller that modulates neurostimulation

The first two requirements impact on the selection of the neural processes to be recorded, and on the technologies employed for this. The third and fourth, on the other hand, are also related to the signal processing techniques employed, and constrain their response time and accuracy respectively.

Requirement R_c1 implies that the NP needs to record cortical activity at the motor area, for the motor cortex orchestrates the planning, initiation, and direction of voluntary movements (Purves et al., 2004). This can be performed using either noninvasive or invasive interfaces, which inherently have important differences in temporal and spatial resolution (see the review in Lebedev and Nicolelis, 2006). Invasive interfaces are capable of recording both the simultaneous activity of hundreds of individual cells at a single or multiple cortical areas, and the general behavior of a large ensemble of neurons (known as local field potentials). Electroencephalography (EEG), the most common technique for noninvasive recording of cortical activity, provides the general behavior of large groups of MNs, at the expense, however, of limited bandwidth and poor spatial selectivity. EEG is selected because there is a considerable bulk of knowledge dealing with the characterization and detection of different neural processes related to movement (e.g., movement related cortical potentials, Shibasaki and Hallett, 2006, or event related desynchronization, Pfurtscheller and Lopes da Silva, 1999), and because noninvasive technologies do not suffer from biocompatibility problems as invasive interfaces do (Lebedev and Nicolelis, 2006).

The existence of detectable cortical processes that underlie the preparation and control of movement imply that it is possible, *a priori*, to build an interface that requires no learning from the user, by being able to "naturally" trigger the NP when a volitional motion is about to be performed. Thus, requirement R_c2 is directly fulfilled by meeting requirement R_c1.

Requirement R_c3 imposes a constraint to the design of signal processing algorithms, at the same time it influences, among others, the selection of the cortical phenomenon to be detected (based on its ability to predict movement onset). Furthermore, it points at the interest of including recordings of the neural drive to muscle[16], because it could contribute to reducing the delay when detecting actual movements, for the onset of neural commands precedes the appearance of muscle contraction by some tens of milliseconds (see, e.g., Cavanagh and Komi, 1979). Given that the properties of the neuromuscular junction cause that muscle activation is a direct reflection of the axonal discharges of spinal MNs (Kandel et al., 2000), the response time of the cHMI should be improved

[16]The neural drive to muscle is the sum of the action potentials discharged by spinal MNs as a result of the integration of afferent and efferent information (Farina et al., 2010).

by the incorporation of electromyography (EMG) analysis. As for cortical recordings, noninvasive and invasive technologies are available, however multichannel intramuscular EMG is still under development (see Farina et al., 2008), which motivates my choice of surface EMG (sEMG). In more detail, the cHMI will implement high-density sEMG given its superior performance in terms of area of recording (spatial sampling), versatility, and robustness among others (e.g., Merletti et al., 2008), when compared to traditional electrodes.

The precise parameterization of tremor, requirement R_c4, needs for recording kinematic information given that *i*) EMG data does not suffice because of the complex, nonlinear, relationship between muscle activation and joint dynamics, and *ii*) wearable torque sensors are still unavailable. There are various technologies to measure joint kinematics, although only two of them are ambulatory: microelectromechanical systems (MEMS) sensors (see Section §2.1) and wearable sensors implemented within garments based, e.g., on conductive fibers (Gibbs and Asada, 2005), or on printed piezoresistive sensors (Pacelli et al., 2006), the so-called e-textiles. The latter are still under development whereas MEMS sensors are a mature technology, and allow for a more rapid prototyping than their e-textile counterparts. Therefore, the NP will implement MEMS sensors for the recording of joint kinematics. I provide details about sensor selection, placement and recording procedures in Chapter §2. Finally, given that tremor is a complex phenomenon, which may be present at a single or multiple joints and degrees of freedom (DoF), exhibiting nonstationary and uncoupled dynamics (see details on Epigraph §2.2.3), the cHMI needs to derive tremor parameters for each targeted DoF (targeted DoFs are described in Epigraph §1.3.2).

On the basis of this, Fig. 1.5 depicts the concept of the cHMI, showing the sensor modalities it will comprise, namely EEG, sEMG, and kinematic sensors based on MEMS technology. The information derived from these sources will be integrated or fused in order to meet the design requirements previously presented, and provide the pHMI with accurate information that allows for robust tremor management. A detailed explanation of the design of the cHMI, comprising the phenomena that are recorded and the technology with which it is performed, together with the rationale for their selection, is given in Section §3.2. In addition, the first sections in Chapter §2 review all the aspects dealing with kinematic recording of tremor.

This cHMI comprising multiple sensor modalities may result cumbersome for wearing it in all experimental studies, and thus a reduced version implementing only MEMS sensors will be developed, at the expense of degraded functionality (see Chapter §2). Furthermore, it is expected that the latter interface may enable a future large scale validation of the NP.

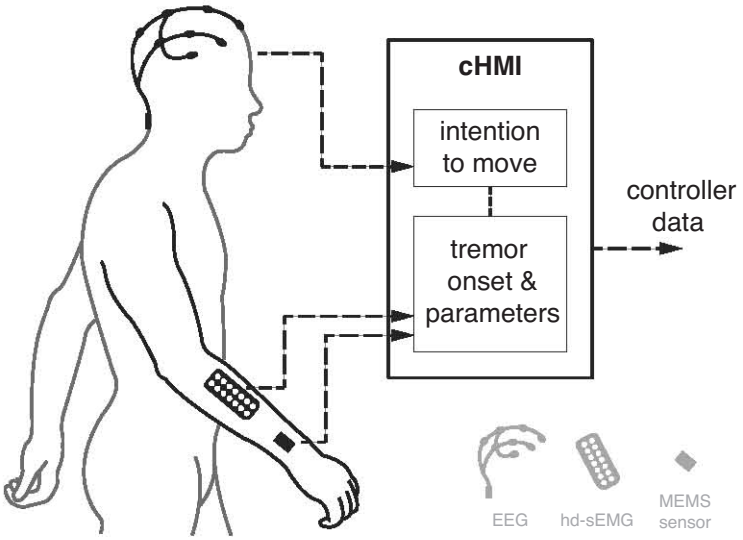

FIGURE 1.5: Concept design of the cHMI implemented in the NP. The concept shows how EEG, sEMG and kinematic recordings are integrated/fused in order to derive the intention to move, and the onset and parameters of the tremor in such context. A legend depicting the elements represented is shown in gray.

1.3.2 Concept Design of the Physical Human-Machine Interface

The NP here presented aims at the functional compensation of tremor during the performance of ADLs, and therefore needs to actuate at the DoF(s) that affect function the most, providing sufficient attenuation without impeding the performance of volitional motions. Next I review the considerations taken into account for the concept design of the pHMI.

Upper limb tremor typically appears at the distal segments, being more prominent at the hands and the forearm for ET (Deuschl et al., 1998), and at the hands, commonly expressed as a "pill rolling" pattern (pronation-supination), for PD (Deuschl et al., 2012). Functional analysis shows that wrist flexion-extension, forearm pronation-supination and elbow flexion-extension have the largest impact on disability (Belda-Lois et al., 2005), as expected from the segments exhibiting the most severe tremor. Given that the NP is envisioned as a functional compensation system, it has to compensate for tremor while not affecting the performance of voluntary movements. Furthermore, for the prototype to be usable, neurostimulation has to be delivered in such a way that discomfort and pain are avoided, and the appearance of muscle fatigue and accommodation is delayed to the maximum.

These ideas serve to establish a series of requirements for the pHMI:

R_p1. The NP needs to attenuate the tremor at the DoFs in which it impairs the performance of ADLs, namely wrist flexion-extension, forearm pronation-supination, and elbow flexion-extension.

R_p2. The NP has to reduce tremor amplitude without affecting concomitant voluntary movement.

R_p3. Drawbacks arising from neurostimulation, namely discomfort, appearance of muscle fatigue, and accommodation need to be avoided.

Requirement R_p1 is immediately met if the NP is capable of selectively activating the major pairs of antagonists that control wrist flexion-extension, forearm pronation-supination and elbow flexion-extension. Activation of the major muscles controlling elbow flexion-extension, the biceps brachii and the lateral head of the triceps, is straightforward, because of their anatomical properties (Delagi et al., 2005). It is also feasible to activate a pair of antagonists controlling wrist flexion-extension (extensor carpi radialis or carpi ulnaris, and flexor carpi radialis or carpi ulnaris), although the imbricated distribution of forearm muscles challenges the obtention of good selectivity (Popovic and Popovic, 2009). However, muscles producing pronation (pronator quadratus, pronator teres) and supination (supinator) are very deep, which together with the abovementioned imbricated distribution of forearm muscles (Delagi et al., 2005), renders accurate control of forearm pronation-supination with transcutaneous electrodes extremely complicated. Therefore, the NP will target wrist flexion-extension and elbow flexion-extension, but not forearm pronation-supination, which may be relevant mainly in the case of PD patients, who exhibit a classical pronation-supination ("pill rolling") pattern. However, this pattern is mostly prominent at rest (Deuschl et al., 2012), in which case the NP does not need to actuate, thus minimizing the expected impact of this limitation on the performance of the NP. On the basis of this, it can be assumed that the current design meets requirement R_p1.

I have already mentioned that tremor may appear at different joints/DoFs, and that in this case its characteristics (in terms of amplitude and frequency) are different, very likely due to the existence of multiple oscillators (e.g., Lauk et al., 1999; Hurtado et al., 2000; Raethjen et al., 2000.) Furthermore, tremors at different limbs are uncoupled, and so is their nonstationary behavior. Therefore, two independent controllers, one driving wrist flexion-extension, the other elbow flexion-extension, need to be implemented.

Achievement of requirement R_p2 needs for: *i*) the development of a control strategy that attenuates tremor but not voluntary movement, and *ii*) the selective activation of the targeted DoF(s), without affecting muscles that control other movements. The latter may be achieved by the combination of adequate electrode placement and minimization of the current injected, so that the electrical field does not "spill" and activate nerves innervating other muscles (e.g., Popovic and Popovic, 2009). As to the control strategy,

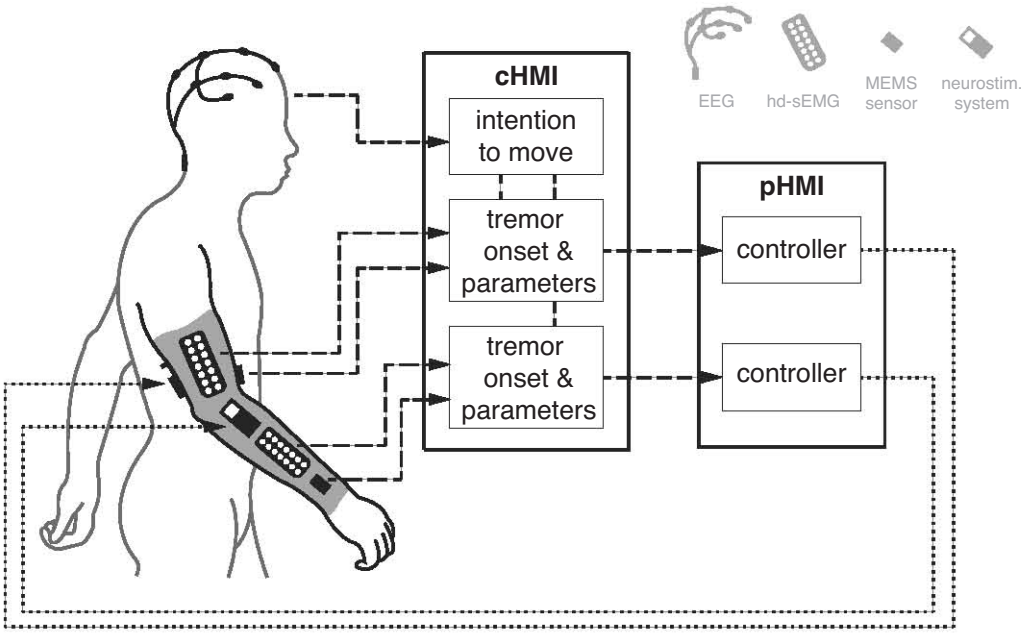

FIGURE 1.6: Concept design of the NP, showing both the cHMI and the pHMI. The concept shows the cHMI implementing algorithms to detect and parameterize tremor at each joint based on the integration/fusion of the recordings of hd-sEMG and MEMS sensors, and the EEG system in charge of predicting movement onset. Information on tremor and movement onset at each joint is fed into their respective joint controllers that modulate neurostimulation based on this information. High density sEMG electrodes, MEMS sensors and the neurostimulation system are integrated within a textile substrate (in gray). A legend depicting the components of the NP is also shown (in gray).

I believe that the key idea to reduce tremor amplitude without affecting concomitant volitional motion is their difference in frequency content. While tremor typically occurs in the 3–12 Hz band (see the table in Fig. 1.2), voluntary movements are performed at 0–2 Hz (Mann et al., 1989, see Epigraph §2.2.3). Therefore the controller may be defined in the frequency domain as either a notch filter at the tremor frequency (Prochazka et al., 1992; Rocon et al., 2007a), or a low pass filter with cut off frequency over 2 Hz. The latter may be assimilated to a viscous element with appropriate damping coefficient, the most common approach in tremor suppression devices (see, e.g., Adelstein, 1981; Aisen et al., 1993; Michaelis, 1988; Kotovsky and Rosen, 1998; Rocon et al., 2007b).

Finally, the issues included in requirement R_p3 are related to electrode placement, neurostimulation parameters, and their modulation. Electrode placement is constrained by the anatomy of the user, and therefore minimization of comfort, muscle fatigue and accommodation to neurostimulation needs to be carried out by controlling adequately the current injected. Given that the NP is a proof of concept, the controller will implement the classical strategy of modulation of a single neurostimulation parameter (typically amplitude or pulse width, see, e.g., Ferrarin et al., 2001; Lynch and Popovic, 2008), and more complex approaches will be left as matter of future research. So will be the use of multichannel electrode arrays, which, dynamically activated, delay the onset of

FIGURE 1.7: A control subject wearing the first prototype of the NP. The photograph shows the textile garment (left arm) implementing the neurostimulation and high-density sEMG electrodes, together with the MEMS sensors. The user also wears a commercial EEG system.

muscle fatigue and minimize discomfort (Popovic-Bijelic et al., 2005). Therefore, for the pHMI of the NP, the controller will have to select the values of those neurostimulation parameters that are constant so that they minimize muscle fatigue, discomfort and accommodation to neurostimulation. The parameter modulated by the controller will be regulated in such a way that the electrical charge injected will be the minimal that achieves effective tremor attenuation, which will delay the onset of muscle fatigue and accommodation to neurostimulation, at the same time that it minimizes discomfort. In addition, this criterion will also help to minimize the current injected and its possible spill to neighboring muscles, also helping to meet requirement R_p2.

Fig. 1.6 shows the concept design of the NP, comprising both the cHMI (based on Fig. 1.5) and the pHMI. It represents how the EMG and MEMS sensors, and the neurostimulation system are integrated within a textile substrate, an approach chosen to fulfill user expectations in terms of cosmetics, aesthetics, and wearability (see below).

1.3.3 Neuroprosthesis Prototype

The appearance of the NP prototype was defined after the analysis of the information gathered in a focus group with tremor patients. There, a representative group of users gave their opinion about a series of prototypes of the different components of the pHMI, cHMI, and the NP itself. Conjoint analysis was employed to elicit user preferences (Laparra-Hernández et al., 2010). The outcome of this usability analysis was as follows.

As expected, users did not want to show that they were using a NP, and therefore head and arm garments resembling regular clothes were the preferred options. Electronics should be ideally implemented in a control box as small as possible, and resembling an electronic gadget, e.g., a MP3 player. The preferred arm garment had the shape of a sleeve, and integrated the electrodes for neural recording and stimulation, and the MEMS sensors. Adjustable textile straps (using velcro©), one per targeted joint, were also positively regarded by patients. Users would wear either garment underneath their clothes.

Based on this, a functional prototype that comprised a sleeve with sewn electrodes for both neural recording and stimulation (Paradiso et al., 2010) was implemented. As to the EEG system, a commercial ambulatory amplifier was employed. Fig. 1.7 shows a control subject wearing the functional prototype. This prototype constitutes the basis for the experiments presented in this dissertation.

1.4 Conclusions

This chapter presented the motivation of this thesis: the development of a novel NP for functional compensation of tremor. Emphasis was put on the relevance of the problem given the large number of people affected by tremor, and the lack of effective treatment for a significant proportion of them. Furthermore, it was shown that given the heterogeneity of tremor syndromes, and the lack of knowledge on their pathophysiological mechanisms, alternative therapies are meant to play an important role as a complement or replacement to their traditional counterparts.

The clinical aspects and what is known about the mechanisms participating in tremorgenesis were also reviewed, given that their understanding is crucial for the development of effective neuroprosthetic or robotic interventions. Although tremor arises from 10 different syndromes, I focused on ET and PD, because they constitute the group of patients enrolled for the study. This choice was motivated by the considerably larger prevalence of both disorders when compared to other forms of tremor. Moreover, half of the patients with ET do not benefit from any existing therapy, and although PD tremor responds positively to dopamine antagonists, they provide a more significant improvement of symptoms other than tremor, and their efficacy is known to decrease with time.

Afterwards, I reviewed the concept design of the cHMI and pHMI of the NP, focusing on the requirements established after analyzing both user needs and the inherent properties of tremor, and what decisions were taken to fulfill them. This way, the cHMI was envisioned as a multimodal interface, in which different levels of the neuromuscular system are recorded, and their information integrated/fused to provide a detection of

movement intention, the actual onset of voluntary movement in the presence of concomitant tremor, and the instantaneous parameters of the latter. This information would serve to the pHMI to generate neurostimulation commands, based on the strategy defined after inspecting the optimal functionality of the system (i.e. design requirements). Furthermore, this strategy would also be aimed at minimizing the negative aspects of neurostimulation, at the same time that it provides systematic tremor attenuation. Finally, a prototype of the NP built based on user expectations was introduced.

In summary, this chapter presented the motivation of this dissertation after highlighting the problems related with its central topic, tremor management. It presented the rationale and concept design for the two major components of the proposed NP, namely its cHMI and pHMI. The major requirements for both were derived after analyzing user needs and the expected functionality of the NP, which in turn served to define a concept design. Such design set the basis for the development and validation of the different components the NP comprises (see Chapters §2, §3, and §4).

Chapter 2

Online Estimation of Tremor Parameters from Kinematic Recordings[1]

This chapter presents the development and validation of an algorithm for the online estimation of tremor parameters from kinematic data. The final objective was to track the instantaneous amplitude and frequency of the tremor with negligible delay, in order to exploit this information to drive the NP. To this end, I examined the properties of concomitant voluntary and tremulous movements, and evaluated a series of candidate algorithms on an experimental dataset by computing adequate metrics. This permitted defining an optimal architecture for the algorithm. The outcome was a two-stage filter that first estimated the voluntary component of movement, and afterwards tracked the amplitude and frequency of the tremor with two adaptive algorithms. By removing the volitional component of movement from the raw motion, I ensured the convergence of the adaptive filters that estimated tremor parameters, at the same time that enabled the identification of functional contexts. Experimental validation during clinical and functional tasks with a representative group of patients showed that the parameters derived were very accurate, and no phase distortion was introduced. This enabled the implementation of the two-stage algorithm in the cHMI of the NP, and the subsequent validation of the tremor suppression strategy proposed.

[1]This chapter is partly based on: J.A. Gallego, E. Rocon, J.O. Roa, J.C. Moreno, J.L. Pons. Real-time estimation of pathological tremor parameters from gyroscope data. Sensors 10(3):2129–49, 2010.

2.1 Introduction

Advances in MEMS permitted to develop miniaturized, low cost sensors that measure changes in displacement, velocity and acceleration (Pons, 2008). MEMS sensors rapidly became a widespread solution for motion analysis (Mayagoitia et al., 2002), and in all fields of robotics (Cheng and Oelmann, 2010; Sukkarieh et al., 1999; Kim and Sukkarieh, 2003). Importantly, their small size and low weight enabled the design of WRs—both robotic exoskeletons (Moreno et al., 2008) and NPs (Dosen and Popovic, 2008)—that relied on these sensors to record the status of the user and the system itself. Furthermore, MEMS sensors overcame the need of working in a restricted space that underlies the usage of traditional motion capture systems based on markers (Mayagoitia et al., 2002), setting the basis for ambulatory systems as the NP presented herein. Notice that, at the current time, e-textiles implementing different technologies start appearing as emerging alternatives (De Rossi and Veltink, 2010; Paradiso et al., 2010).

The most common types of MEMS sensors are accelerometers, gyroscopes, and magnetometers. Each of them has unique characteristics and drawbacks, which determines the selection of the type or types that suit each application the best. The combination of accelerometers and gyroscopes, typically referred to as an inertial measurement unit (IMU) (Luinge and Veltink, 2005), alone, or together with magnetometers (Harada et al., 2003; Zhu and Zhou, 2004), constitutes the optimal approach for the ambulatory recording of human kinematics. Given that the thesis aims at building a wearable NP (see Section §1.3), these solutions constitute my departure point because: *i*) they are state of the art techniques in terms of accuracy and robustness (Favre et al., 2008), *ii*) they have small size to guarantee minimum interference when performing a movement (Luinge et al., 2007), and *iii*) they have low weight, to avoid influencing limb mechanics (e.g., Hewer et al., 1972; Joyce and Rack, 1974).

Although techniques exist to minimize the impact of electromagnetic interferences in magnetic sensing of limb kinematics combined with inertial recordings (Roetenberg et al., 2005, 2007), the use of transcutaneous neurostimulation advices against the use of MEMS magnetometers in the NP. In addition, it must be taken into account that although tremor may be present at more than one joint within a limb, it arises from uncoupled oscillators (e.g., Hurtado et al., 2000; Raethjen et al., 2000, 2009). This motivates that tremor parameters are typically studied per joint, and thus the NP is conceived as a series of modules, one per each targeted DoF (see concept design in Section §1.3). Therefore, in the context of this work, joint rotation and not limb orientation is needed. Selection of the optimal MEMS technology must be performed taken this into consideration.

Traditionally, accelerometers have been the preferred alternative to measure tremor. However, they suffer from two inherent drawbacks that discourage their use in these applications when compared to gyroscopes. First, accelerometers measure sensor orientation with respect to gravity, and are thus influenced by the pose of the limb they are

attached to. Second, accelerometers are sensitive to linear changes, whereas articular movements are rotational. MEMS gyroscopes rely on vibrating mechanical elements to sense rotation through changes in Coriolis acceleration (Yazdi et al., 1998), and therefore they do not suffer from these two limitations. However, gyroscope recordings have an inherent drift (Luinge et al., 2007), which becomes increasingly important when integrated. This drift is thought to originate from the combined effects of mechanical wear and temperature (Luinge and Veltink, 2005), although for the specific chipset employed it is highly correlated with temperature (see Section §2.2.2). By exploiting this feature, I was able to perform accurate recordings of upper limb kinematics in tremor patients using solid state gyroscopes.

Other solutions for kinematic recording of tremors found in the literature are an instrumented glove (Vinjamuri et al., 2009), digitizing tablets (Elble et al., 1990) or laser displacement sensors (Héroux et al., 2009; Daneault et al., 2011). The latter two were discarded because they cannot be implemented within an ambulatory device, while the former resembles the NP to a certain extent, and might be considered in a future system that also targets finger tremor.

As to the existing signal processing methods employed to parameterize tremor, most have been developed for canceling physiological tremor in different Human-Machine Interfaces (HMIs). It was mentioned in Chapter §1 that physiological tremor is etiologically distinct to pathological tremors, and therefore it manifests differently: for example, its frequency lies within the 8–12 Hz band (Elble, 2009), thus being higher than that typically observed in ET and PD patients (see Epigraph §1.2.1), and its amplitude is considerably milder (Elble, 2009). According to this, algorithms built for physiological tremor tracking such as the Weighted Frequency Fourier Linear Combiner (WFLC) (Riviere et al., 1998), the Bandlimited Multiple Fourier Linear Combiner (BMFLC) (Veluvolu et al., 2007), and its posterior extensions (Veluvolu et al., 2010; Veluvolu and Ang, 2011), may not be optimal for tracking pathological tremor parameters. In fact, in (Rocon et al., 2007a) it was shown that a previous filtering stage that removed the volitional component of movement was needed to ensure the stability of the WFLC estimation of pathological tremor parameters. Similarly, in (Bo et al., 2011), the authors used a stochastic representation of voluntary movement to eliminate it from the raw recordings, in order to estimate pathological tremor parameters[2].

This chapter presents a novel algorithm for the real-time estimation of instantaneous tremor parameters—amplitude and frequency—from kinematic data. It is demonstrated that the two-stage architecture here proposed, which is built upon the characteristics of concomitant voluntary and tremulous movements, achieves accurate tracking of tremor amplitude and frequency with negligible delay and short settling time, outperforming

[2]From now on, I refer to pathological tremor simply as tremor, as in the rest of the dissertation.

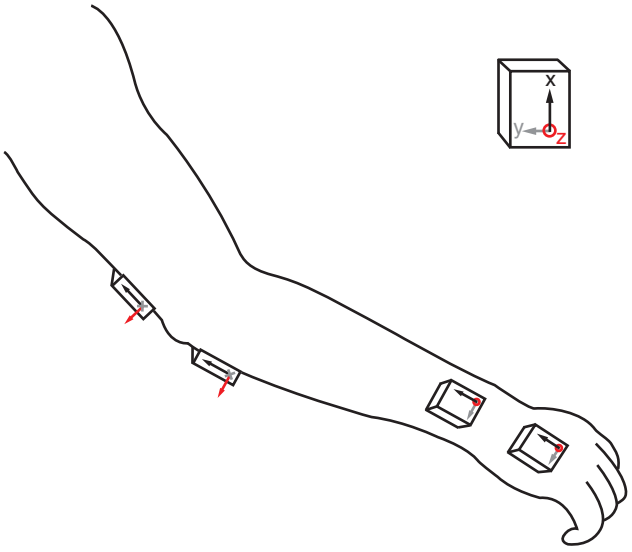

FIGURE 2.1: Placement of the gyroscopes to record wrist flexion-extension and elbow flexion-extension. The figure shows both where the gyroscopes are placed, and how they are oriented according to their axes of rotation (see the scheme displaying the legend for the axes at the top right of the figure).

state of the art approaches. This algorithm set the basis for the development of a multimodal interface to drive the NP during daily living (see Chapter §3), and constituted the cHMI upon which the tremor suppression strategy (see Chapter §4) was validated.

The organization of this chapter is as follows. Section §2.2 reviews a series of preliminary considerations regarding the use of solid state gyroscopes to record upper limb kinematics, and the properties of concomitant volitional and tremulous movements. Next, in Section §2.3, I present the development of the adaptive algorithm to track tremor parameters, including the architecture proposed and a series of candidate algorithms evaluated with patients data. Section §2.4 describes the methods employed for its validation, whereas Section §2.5 presents the results obtained. The chapter ends with a discussion of the results obtained, and conclusions emphasizing their relevance for the literature and the subsequent studies within this thesis.

2.2 Preliminary considerations

2.2.1 Gyroscope Placement

The concept design of the pHMI of the NP (see Epigraph §1.3.2) identified wrist flexion-extension and elbow flexion-extension as the targeted movements because they have the largest impact on disability together with forearm pronation-supination (Belda-Lois et al., 2005). However, the latter was disregarded because it is very complicated to control the muscles that produce it through transcutaneous neurostimulation, due to

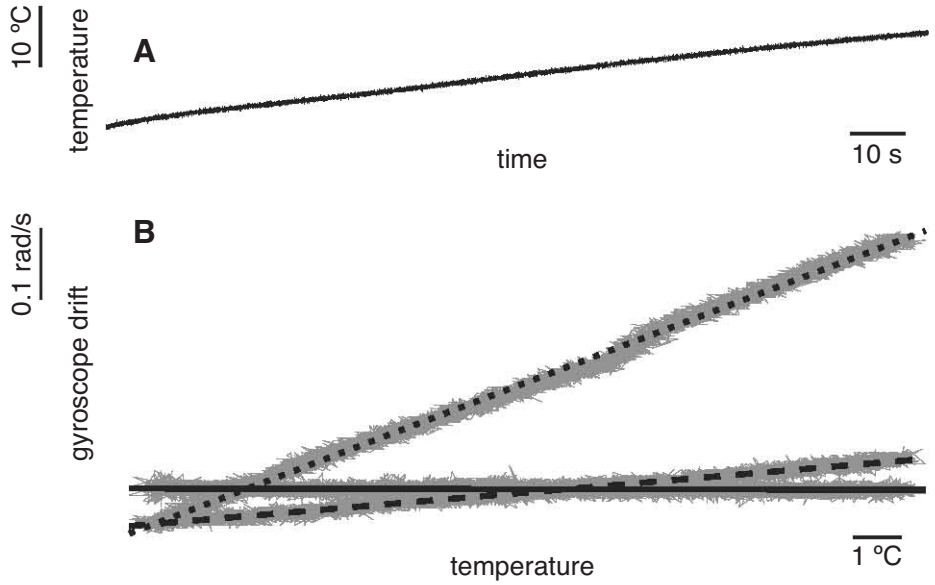

FIGURE 2.2: Relationship between gyroscope offset and temperature for one of the chipsets employed in the NP. Plot (A) represents the change in temperature measured by the chipset (the sensor was heated by a controlled source). Plot (B) represents the linear correlation between gyroscope drift and temperature for the x (solid line), y (dashed line) and z (dotted line) axes. The gray traces below each regression line show the data recorded by the respective gyroscopes.

their depth and imbricate distribution (Delagi et al., 2005, further details are given in Epigraph 1.3.2). Therefore, in the different studies performed during this thesis, wrist and elbow flexion-extension were measured with two pairs of solid state gyroscopes placed in the distal and proximal segments, similarly to what was proposed in (Rocon et al., 2006). In more detail, the sensors were placed as follows (see Fig. 2.1):

- Wrist flexion-extension: the distal gyroscope was placed on the hand dorsum; the proximal gyroscope was placed on the distal third of the forearm (dorsal side).
- Elbow flexion-extension: the distal gyroscope was placed on the proximal third of the forearm (dorsal side), near the olecranon process; the proximal gyroscope was located over the olecranon process, in the distal part of the arm.

Proper alignment between gyroscope axes and the anatomical joint was always ensured before the recordings, exploiting the design of the NP (modular garment). This setup allowed to compute joint rotation by simply subtracting the measurement of the proximal gyroscope from the distal one, what I refer to as differential recording. Fixation on soft tissues was avoided in order to eliminate the undesired oscillations they create, and their intrinsic low pass filtering behavior (Tong and Granat, 1999).

2.2.2 Compensation of Gyroscope Drift

As mentioned above, gyroscopes suffer from a drift commonly accepted to originate from the combined effects of mechanical wear and temperature (Luinge and Veltink, 2005). Given that the chipset employed incorporates a temperature sensor, I investigated the relationship between gyroscope drift and temperature. Fig. 2.2 shows a typical example for the three gyroscopes within a chipset. Visual inspection suggested that both variables were linearly related; calculation of the regression equations for this example yielded:

$$b_x = -0.000154 \cdot T + 0.00562 \tag{2.1}$$

$$b_y = 0.008506 \cdot T - 0.35245 \tag{2.2}$$

$$b_z = 0.038312 \cdot T - 0.13358 \tag{2.3}$$

where b_x, b_y and b_z represent the bias of the gyroscopes in the x, y and z axes, and T the temperature measured by the sensor.

Gyroscope drift and temperature were strongly correlated: for this specific chipset the RMSE between the recorded data and their linear fit was 0.0089, 0.0080 and 0.0127 rad/s for the x, y and z axes respectively. Goodness of fit was similar for all gyroscopes. Given the accurate representation of gyroscope drift by a linear model, I implemented an immediate method for online drift compensation. This ensured robust recording of wrist and elbow kinematics using the simple approach here presented.

2.2.3 Analysis of Voluntary Movement and Tremor

Tremor has been traditionally accepted to affect voluntary movement in an additive manner (Riley and Rosen, 1987), in spite of its nonlinear (Rocon et al., 2006) or chaotic nature (Timmer et al., 2000). Furthermore, tremor, irrespectively from its etiology, appears in a higher frequency band (3–12 Hz, see Epigraph §1.2.1) than that employed during the performance of ADLs (0–2 Hz, Mann et al., 1989, see the example in Fig. 2.3). According to this, separation of volitional and tremulous components of movement has been typically performed with zero-phase filters, and more recently with Empirical Mode Decomposition (EMD) (Rocon et al., 2006).

EMD is a technique for the analysis of nonlinear and non-stationary time series, which makes no a *a priori* assumption about the nature of the data, and thus overcomes the limitations arising from the hypothesis of stationarity and linearity that underlies Fourier analysis (Huang et al., 1998). EMD separates—sifts—the signal under study into a series of Intrinsic Mode Functions (IMFs), which satisfy two criteria derived from the notion of instantaneous frequency as defined in (Huang et al., 1998): *i*) in the whole

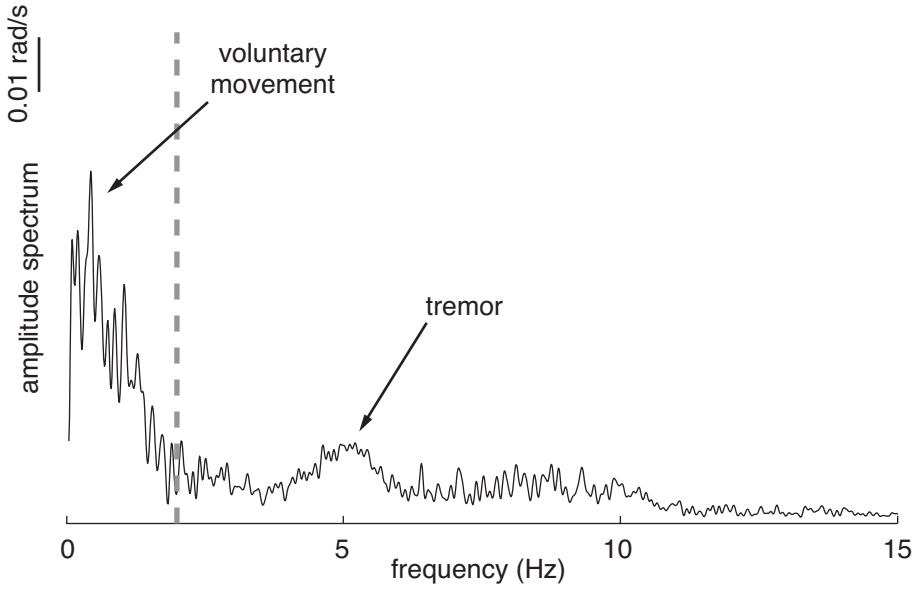

FIGURE 2.3: Amplitude spectrum showing the typical separation of the concomitant voluntary and tremulous movements in the frequency domain. The example corresponds to a patient suffering from moderate tremor arising from PD buttoning a shirt. The dashed gray line represents the frequency commonly employed to separate the volitional movement and the tremor (2 Hz).

dataset the number of extrema and zero crossings must be the same or differ by one, and *ii*) at every point, the mean value of the envelop defined by the local maxima and the local minima is zero. This sifting process is iterative: once the first IMF is extracted, the residual is sifted to generate the second IMF, and so it continues until a certain stop criterion is fulfilled. EMD of kinematic recordings of tremor showed that a single IMF represents the tremor (Rocon et al., 2006). Therefore, in spite of tremor being amplitude and frequency modulated, it appeared as a well defined oscillation embedded within the movement recordings, superimposed to the volitional motion.

Nevertheless, EMD suffers from mode mixing understood as: *i*) having IMFs that consist of signals of widely disparate scales, or *ii*) having a signal of a similar scale residing in different IMFs (Wu and Huang, 2009). In order to circumvent these limitations, Huang and coworkers recently proposed exploiting the inherent properties of white noise—generation of a uniform reference—to facilitate the EMD of a signal. This technique, called Ensemble Empirical Mode Decomposition (EEMD), improves EMD by avoiding mode mixing while preserving the uniqueness of the decomposition, because the ensemble mean obtained after applying EMD to the white noise contaminated signal (typically a few hundreds of times) cancels out the white noise. My first evaluation of EEMD with the dataset described in Section §2.4 showed that it outperforms EMD in terms of automatic extraction of the tremor (see Gallego et al., 2011b) and, interestingly suggests that the tremor may reside in more than one component (3 in most of the trials, see components C4 to C6 in Fig. 2.4). This indicates that the tremulous movement may be the manifestation of multiple oscillators that interact in a complex manner, as

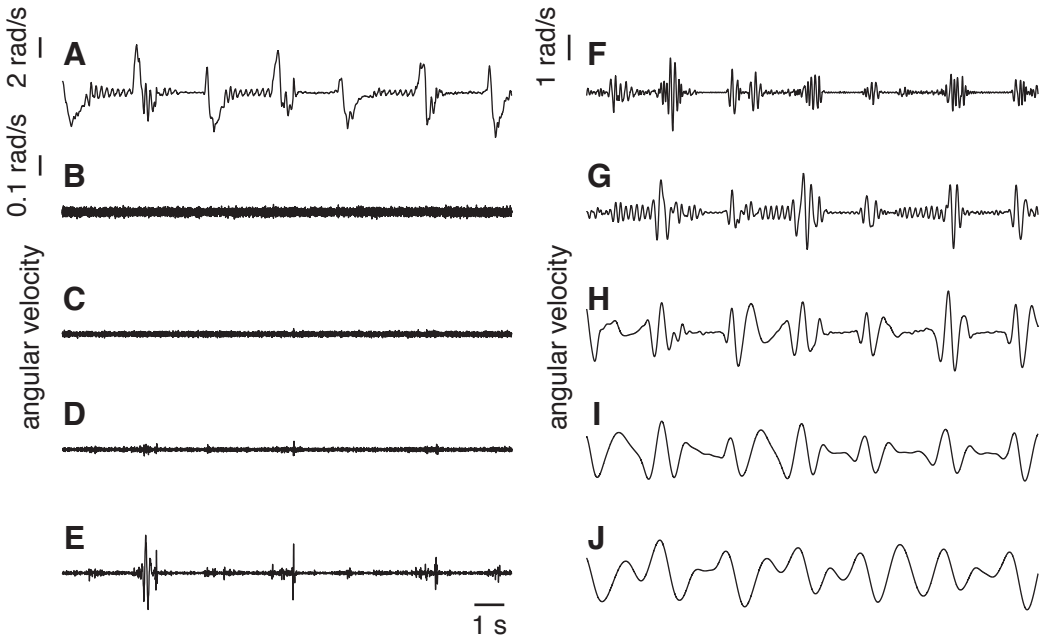

FIGURE 2.4: Example of EEMD of tremor oscillations. The data correspond to wrist rotation while an ET patient performed a FN test. Plot A corresponds to the raw wrist flexion-extension, and plots B to J to the first 9 components obtained with EEMD. It is shown that components C1 to C3 (plots B to D) correspond to noise of various sources, C4 to C6 (plots E to G) to tremor, and the sum of the remainder to voluntary movement (Gallego et al., 2011b). The first vertical scale (2 rad/s) corresponds only to plot A, the second (0.1 rad/s) to plots B to E, and the third (1 rad/s) to plots F to J.

could be expected from simultaneous recordings of the activity of various brain nuclei (Hurtado et al., 1999) or cortical areas (Raethjen et al., 2009) (see Epigraph §1.2.3). Interestingly, analysis of firing patterns of different compartments within a muscle group (e.g., wrist extensors) also revealed the existence of multiple oscillations that are close in the frequency domain (see Chapter §5 and Holobar et al., 2012). Detailed investigation of this finding is one of my topics of ongoing research (see Section §6.3).

2.3 Two-Stage Algorithm for the Estimation of Tremor Parameters

This section reviews a series of candidate algorithms evaluated (in Section §2.5) to build the adaptive algorithm for the online estimation of tremor parameters. The algorithm was designed to provide accurate tracking of instantaneous tremor amplitude and frequency with minimum delay. It relied on two assumptions derived from the kinematic analysis of concomitant voluntary movement and tremor (see Epigraph §2.2.3), and from the state of the art on signal processing algorithms. They are:

1. Concomitant voluntary movement and tremor are additive, and therefore:

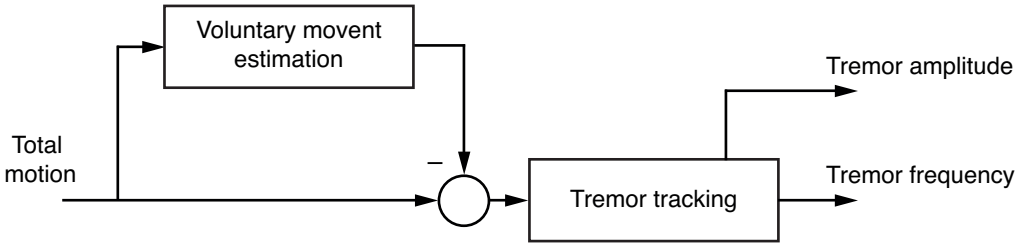

FIGURE 2.5: Block diagram of the two-stage algorithm for the online estimation of tremor parameters. The total motion is fed into an algorithm to estimate its voluntary component. This component is subsequently subtracted from the total movement, obtaining an estimation of tremor, which is employed by the tracking algorithm to estimate its instantaneous amplitude and frequency.

$$y(k) = y_{vm}(k) + y_{tr}(k) \tag{2.4}$$

where $y(k)$ represents the raw joint movement, and $y_{vm}(k)$ and $y_{tr}(k)$ its voluntary and tremulous components.

2. Concomitant voluntary movement and tremor are separated in the frequency domain, independently from the type of activity, and the etiology of the latter.

On the basis of this, a two-stage architecture (Gallego et al., 2010b, see Fig. 2.5), in which the algorithm first estimated the voluntary component of movement, and then computed the tremor based on the fact that they are additive, was proposed. Afterwards, the estimation of tremor was fed into a second algorithm that tracked the instantaneous amplitude and frequency of the tremor. By removing the low frequency, high energy, voluntary movement, I ensured the stability and convergence of the algorithms to track tremor parameters. The next two epigraphs summarize the algorithms evaluated for each stage.

2.3.1 Voluntary Motion Tracking

Given that voluntary movements occur at a lower frequency than tremor (see Epigraph §2.2.3), a straightforward solution would be to employ a low pass filter (typically < 2 Hz) to estimate the former. However, digital low pass filters introduce a time lag in the signal (Oppenheim et al., 1998), which would degrade the estimation of tremor, and thus the tracking of its parameters. In addition, the fact that voluntary movements occur in a relatively wide frequency band impedes the implementation of cascade architectures (e.g., comprising low pass and high pass elliptic filters, Ang et al., 2006) for phase equalization. Therefore, I evaluated a series of adaptive algorithms that adequately tuned neglect (most of) the component of movement over 2 Hz, i.e. the tremor.

The algorithms for voluntary movement tracking were built by assuming that it could be modeled as a first order process. This assumption would hold if, considering a Taylor series that represents voluntary movement (see Eq. (2.5)), the second derivative, $\ddot{x}$, could be neglected because either the sampling period, T_s, or the acceleration itself are small. In this case both assumptions were satisfied: the sampling period was 1 ms (see Epigraph §2.4.3), and the maximum value of $\ddot{x}$ for the dataset employed (see Section §2.4 for details on the patients and protocol) was $2.54{\cdot}10^{-4}$ rad·s^{-3}, 4 orders of magnitude smaller than the average angular velocity[3]. Voluntary movement was formulated as a Taylor series as follows:

$$\hat{y}_{vm}(t) = \hat{y}_{vm}(t_n) + T_s\dot{\hat{y}}_{vm}(t_n) + \frac{T_s^2}{2}\ddot{\hat{y}}_{vm}(t_n) + ... \tag{2.5}$$

where $\hat{y}_{vm}$ is the estimation of voluntary movement at a given instant.

Next, I review the two algorithms for voluntary movement tracking that were considered for its implementation within the two stage algorithm

2.3.1.1 $g-h$ Filters

$g-h$ filters are simple recursive filters that estimate the future position and velocity of a variable based on first order model of the process (see Eq. (2.5)). Measurements are used to correct these predictions, minimizing the estimation error. Traditional applications of $g-h$ filters are radar tracking and aeronautics (Brookner, 1998). The general form of a $g-h$ filter is:

$$x_{k,k} = x_{k,k-1} + g_k(y_k - x_{k,k-1}) \tag{2.6}$$

$$\dot{x}_{k,k} = \dot{x}_{k,k-1} + \frac{h_k}{T_s}(y_k - x_{k,k-1}) \tag{2.7}$$

$$x_{k+1,k} = x_{k,k} + T_s\dot{x}_{k,k} \tag{2.8}$$

$$\dot{x}_{k+1,k} = \dot{x}_{k,k} \tag{2.9}$$

where Eq. (2.6) and (2.7) are designated as update, tracking, or filtering equations, because they estimate the current position and velocity of the variable, $x_{k,k}$, $\dot{x}_{k,k}$, based on the previous predictions of position and velocity, $x_{k,k-1}$, $\dot{x}_{k,k-1}$, and taking current measurement y_k (i.e. the raw movement) into account. Confidence on the measures is weighted by gains g_k and h_k. Eq. (2.8) and (2.9) are called prediction equations because they provide a prediction of future position and velocity, $x_{k+1,k}$, $\dot{x}_{k+1,k}$, based on the

[3] This value was obtained after removing the tremor component offline with a low pass filter (< 2 Hz, zero phase)

first order dynamic model of the variable. As $g-h$ trackers consider a constant velocity model, the predicted velocity $\dot{x}_{k+1,k}$ is equal to the current one, $\dot{x}_{k,k}$. The estimated voluntary movement is $\hat{y}_{vm,k} = x_{k+1,k}$.

$g-h$ filters are affected by two error sources, (Brookner, 1998): *i*) the lag, dynamic, bias or systematic error, which is related to the constant velocity assumption, and *ii*) the measurement error, which is inherent to the sensor and measurement process. Typically, the smaller g_k and h_k are, the larger is the dynamic error and the smaller are the measurement errors, (Brookner, 1998). Therefore, in designing a $g-h$ tracking filter there is a degree of freedom in the choice of the relative magnitude of the measurement and dynamic errors. To simplify the selection of gains, I considered two filters that are optimal in some sense. These filters are the Benedict-Bordner Filter and the critically dampened filter, described next.

- Benedict-Bordner Filter (BBF): The BBF minimizes the total transient error, defined as the weighted sum of the total transient error and the variance of the prediction error due to measurement noise errors (Benedict and Bordner, 1962). The BBF is the constant $g-h$ filter that satisfies:

$$h = \frac{g^2}{2-g} \tag{2.10}$$

  The relationship defined in Eq. (2.10) implies that the BBF has one DoF. Because for the $g-h$ filters increasing the value of g diminishes the transient error, the larger g, the higher frequencies the BBF tracks.

- Critically dampened Filter (CDF): The CDF minimizes the least-squares fitting line of previous measurements (Brookner, 1998), giving old data lesser significance when forming the total error sum. This is achieved with weight factor θ. The parameters in the $g-h$ filter are related by:

$$\begin{aligned} g &= 1-\theta^2 \\ h &= (1-\theta)^2 \end{aligned} \tag{2.11}$$

  Selection of the filter gain, θ, is analogous to that of the BBF.

2.3.1.2 Kalman Filter

The Kalman filter (KF) is the most common estimation algorithm, and is employed in a large number of applications. In this context, I implemented a KF that tracked voluntary movement modelled as a first order process (see Eq. (2.5)). Therefore, the

state vector $\mathbf{x}(t)$ was composed by the variable to be estimated and its derivative, and the output vector was directly related to the former:

$$\begin{bmatrix} \hat{x}_{k,k-1} \\ \hat{\dot{x}}_{k,k-1} \end{bmatrix} = \begin{bmatrix} 1 & T_s \\ 0 & 1 \end{bmatrix} \begin{bmatrix} \hat{x}_{k-1,k-1} \\ \hat{\dot{x}}_{k-1,k-1} \end{bmatrix} \tag{2.12}$$

$$y_k = \begin{bmatrix} 1 & 0 \end{bmatrix} \begin{bmatrix} \hat{x}_{k-1,k-1} \\ \hat{\dot{x}}_{k-1,k-1} \end{bmatrix} \tag{2.13}$$

where $\hat{y}_{vm,k} = \hat{x}_{k,k-1}$ is the estimated voluntary movement.

Covariance matrices were defined by taking into account the following considerations. As voluntary motion was the variable to be tracked, tremor was assumed to be sensor noise; therefore $\mathbf{R}(k) = \sigma_\omega^2$, being σ_ω^2 the average variance of the tremor. As to the process noise covariance, $\mathbf{Q}(k)$, I hypothesized that it was related to fast changes in voluntary motion. To compensate for this effect, a piecewise constant acceleration model was considered, (Bar-Shalom and Li, 1998). This model assumed that voluntary movement underwent constant and uncorrelated acceleration changes between samples in the form of:

$$\mathbf{Q} = \sigma_\nu^2 \begin{bmatrix} \frac{T_s^4}{4} & \frac{T_s^3}{2} \\ \frac{T_s^3}{2} & T_s^2 \end{bmatrix} \tag{2.14}$$

where σ_ν^2 represents the variance of the random velocity component.

To select the value of σ_ν^2, I followed the recommendation in (Bar-Shalom and Li, 1998): $0.5 \cdot \max(\ddot{x}) \leq |\sigma_\nu| \leq \max(\ddot{x})$.

2.3.2 Estimation of Tremor Parameters

State of the art tremor modeling algorithms rely on a time-varying Fourier series, which parameters are estimated recursively. Adaptation to the input signal is typically performed with the Least Mean Squares (LMS) algorithm (Widrow et al., 1975), although KFs and other approaches have been recently recently proposed (Bo et al., 2011; Veluvolu and Ang, 2011). As the LMS recursion is a descend method that relies on a special estimate of the gradient (Widrow et al., 1975), high energy voluntary motion must be removed first to ensure proper convergence, i.e. tremor tracking. The first part of the two-stage algorithm accomplishes this task (see Fig. 2.5). Notice that the KF also benefits from an accurate measurement of the process to be estimated—the tremor, in this case—, which would be facilitated by removing the voluntary component of motion first.

In order to design the adaptive algorithm for the online estimation of tremor parameters, I evaluated the performance of two algorithms originally developed to track physiological tremor, and of a KF for the estimation of tremor amplitude, which I developed. It must be mentioned that tremor amplitude is the parameter most prone to change during the execution of a task, while tremor frequency keeps considerably constant (within a $\pm$ 1.5 Hz interval around tremor frequency according to some estimations, O'Suilleabhain and Matsumoto, 1998). Next, I review the algorithms considered for this stage.

2.3.2.1 Weighted Frequency Fourier Linear Combiner

The WFLC is the most widespread algorithm for the estimation of tremor parameters. It consists in an extension of the classical noise canceler (see the review in Widrow et al., 1975), the Fourier Linear Combiner (FLC) (Vaz et al., 1994), which also tracks the frequency of the input signal based on a LMS recursion. Therefore, the WFLC adapts in real-time its amplitude, frequency and phase (Riviere et al., 1998). The WFLC is formulated as follows:

$$x_{r_k} = \begin{cases} \sin\left(r \sum_{t=1}^{k} \omega_{0_t}\right), & 1 \leq r \leq M \\ \cos\left((r-M) \sum_{t=1}^{k} \omega_{0_t}\right), & M+1 \leq r \leq 2M \end{cases} \tag{2.15}$$

$$\varepsilon_k = s_k - \mathbf{W}_k^{\mathrm{T}} \mathbf{X}_k - \mu_b \tag{2.16}$$

$$\omega_{0_{k+1}} = \omega_{0_k} + 2\mu_0 \varepsilon_k \sum_{r=1}^{M} r \left(w_{r_k} x_{M+r_k} - w_{M+r_k} x_{r_k}\right) \tag{2.17}$$

$$\mathbf{W}_{k+1} = \mathbf{W}_k + 2\mu_1 \varepsilon_k \mathbf{X}_k \tag{2.18}$$

where Eq. (2.15) represents the time varying sinusoidal terms of the Fourier Series, x_{r_k}, being ω_{0_t} is the instantaneous frequency (pulsation). Eq. (2.16) defines the error ϵ_k to be minimized by the LMS recursion based on the adaptation of the amplitude weights $\mathbf{W}_k$, and Eq. (2.17) and (2.18) represent the frequency and amplitude adaptation, respectively. The estimated tremor is obtained as:

$$\hat{y}_{tr,k} = \mathbf{W}_k^T \mathbf{X}_k + \mu_b \tag{2.19}$$

The WFLC has four parameters: the number of harmonics of the model, M, the amplitude and frequency adaptation gains, μ_0, and μ_1, and a bias weight, μ_b, that is included to compensate for low frequency errors (Riviere et al., 1998; Rocon, 2006). The latter may also be adapted using a LMS recursion. The number of harmonics is typically fixed to 1, while the other parameters are chosen after tuning on experimental data.

2.3.2.2 Bandlimited Multiple Fourier Linear Combiner

The BMFLC is a more recent extension of the FLC. It emerged to compensate for the limitations of the WFLC to track physiological tremor when two constituent frequencies (Elble, 2009) are evident, or when frequency variations occur abruptly (Veluvolu et al., 2007). The BMFLC consists of a bank of FLCs that track the input signal based on different frequency components. Therefore, each FLC adapts its amplitude to the input signal, although by definition its frequency remains constant. An interval is thus defined with the lower and upper frequency of the FLC bank, ω_0, and ω_f. The number of FLCs in between these frequencies is defined by the parameter G. The BMFLC is formulated as follows (Veluvolu et al., 2007):

$$x_{r_k} = \begin{cases} \sin\left(r\left(\omega_0 + (\omega_f - \omega_0)\,\frac{g-1}{G+1}\right)k\right), & 1 \le r \le M \\ \cos\left((r-M)\left(\omega_0 + (\omega_f - \omega_0)\,\frac{g-1}{G+1}\right)k\right), & M+1 \le r \le 2M \end{cases} \tag{2.20}$$

$$\varepsilon_k = s_k - \mathbf{W}_k^{\mathrm{T}}\mathbf{X}_k - \mu_b \tag{2.21}$$

$$\mathbf{W}_{k+1} = \mathbf{W}_k + 2\mu\varepsilon_k\mathbf{X}_k \tag{2.22}$$

where Eq. (2.20) represents the sinusoidal terms of the Fourier Series x_{r_k} (being $1 \le g \le G+1$), Eq. (2.21) defines the error ϵ_k to be minimized by the LMS recursion, and Eq. (2.22) represents the amplitude adaptation. The estimated tremor is obtained using Eq. (2.19). The BMFLC has six parameters: the number of harmonics of each FLC, M, the amplitude adaptation gain, μ, the lower and upper frequency of the FLC bank, ω_0, and ω_f, and the number of filters in between, G. A bias weight μ_b was also included to compensate for low frequency errors (Riviere et al., 1998).

Although the BMFLC was not conceived as a frequency tracking algorithm, I developed a formula to estimate the current frequency of the input signal. Frequency estimation was performed by weighting the contribution of each FLC to amplitude adaptation (Gallego et al., 2010b). For a first order Fourier series, it is expressed as:

$$\omega_k = \sum_{r=0}^{L} \frac{\left(a_r^2 + b_r^2\right)\omega_r}{\sum_{r=0}^{L}\left(a_r^2 + b_r^2\right)} \tag{2.23}$$

2.3.2.3 Kalman Filter

The WFLC and BMFLC algorithms provide adaptation to the input signal based on special estimates of the gradient (Widrow and Stearns, 1985). On the contrary, the KF constitutes the optimal solution for estimation problems, in the sense that it minimizes the covariance of the *a posteriori* estimation error. Therefore, the performance of the

WFLC and the BMFLC, overall in terms of amplitude estimation—as mentioned above, the parameter that varies the most—, could be enhanced by implementing an adequate KF. To this aim, I proposed the following KF, which also implemented an harmonic model of the process:

$$\begin{bmatrix} A_{k,k-1} \\ B_{k,k-1} \\ tr_{k,k-1} \end{bmatrix} = \begin{bmatrix} 1 & 0 & 0 \\ 0 & 1 & 0 \\ \cos(\omega_{0,k,k-1}) & \sin(\omega_{0,k,k-1}) & 0 \end{bmatrix} \begin{bmatrix} A_{k-1,k-1} \\ B_{k-1,k-1} \\ tr_{k-1,k-1} \end{bmatrix} \tag{2.24}$$

$$\hat{y}_{tr,k} = \begin{bmatrix} 0 & 0 & 1 \end{bmatrix} \hat{\mathbf{x}}_{k-1,k-1} \tag{2.25}$$

where A and B represent the amplitude of the sinusoidal terms of a first order Fourier series, and $\hat{y}_{tr,k}$ the estimated tremor.

A WFLC was employed to estimate tremor frequency, $\omega_{0,k,k-1}$ (see Eq. (2.17)), because it has proven to be accurate also in the case of pathological tremor (Rocon et al., 2007a). Therefore, I defined a cascade filter that consisted of a WFLC that tracked tremor frequency and fed it into the KF that estimated tremor amplitude—I will refer to it as KF-WFLC in the remainder of the chapter—. A similar FLC-WFLC cascade architecture was proposed in (Riviere et al., 1998), and proved to simultaneously optimize amplitude and frequency tracking by adjusting the gains of each algorithm to estimate accurately one tremor parameter.

Covariance matrices were defined as follows. The measurement noise covariance was defined arbitrarily as $\mathbf{R}(k) = \sigma_\tau^2$. Analysis of the validation data set (see Section §2.4.1 and §2.4.2 for details on the patients and protocol respectively) showed that changes in the value of σ_τ^2 had only slight impact on transient duration. Process noise covariance was defined as $\mathbf{Q}(k) = \text{diag}(\sigma_A^2, \sigma_B^2, \sigma_T^2)$, because state variables were considered to be mutually independent. The value of σ_A^2 and σ_B^2 defined the adaptation rate of the amplitude terms in the Fourier series.

2.4 Methods

2.4.1 Patients

Five patients (4 male, 1 female) affected by tremor with different etiology participated in the study. Average age was 63.0 ± 9.6 years (ranging from 48 to 74). Patients 01 and 05 suffered from postural and kinetic tremor (grade 2 according to Fahn-Tolosa-Marin

rating scale[4] in both conditions) arising from ET. Patient 02 had postural (grade 2) and kinetic (grade 1) tremor originating from paraneoplastic syndrome. Patient 03 had idiopathic PD, which caused rest (grade 3) and postural (grade 1) tremor. Patient 04 had rest (grade 2) and postural (grade 1) tremor arising from extrapyramidal syndrome of vascular origin. Medication was not interrupted for the recordings. All patients signed a written informed consent to participate. The ethical committee of Hôpital Erasme (Brussels) gave approval to the experimental protocol.

2.4.2 Experimental protocol

Patients were seated in a comfortable chair during the whole experimental session. They were asked to perform 3 repetitions of 4 representative tasks, which were chosen due to their relevance from a clinical (first three tasks, Deuschl et al., 1998) or usability (fourth task, Belda-Lois et al., 2005) standpoint. The tasks were: holding both arms outstretched against gravity (AO), performing the finger to nose test (FN), resting the arm on the lap (RE), and pouring 20 cl of water from a standard bottle into a regular glass (WG). Patients were asked to start performing the task just after the recordings were initiated, and continued its execution until 30 s were elapsed, except for the WG test, in which case the recordings were stopped after completion (typically before 30 s).

2.4.3 Recordings

Tremor at the most affected side was recorded with two pairs of solid state gyroscopes (Technaid S.L., Madrid, Spain) in differential configuration (see Section §2.2.1 for details on sensor placement). Their raw signals were sampled by a 12 bit A/D converter at 50 Hz and low pass filtered ($<$ 20 Hz); afterwards the signals were upsampled offline to 1 kHz for validation of the different algorithms. The results presented throughout this chapter refer to wrist flexion-extension, because most patients did not exhibit significant elbow tremor. Trials with no visible wrist tremor were excluded from the analysis.

2.4.4 Data Processing and Analysis

The parameters for the different algorithms were set to the values given in the next paragraph, based on the minimization of the error metrics defined in the Epigraph §2.4.4.1. As for the algorithms to track voluntary movement, the goal was to find the filter parameter(s) that minimized the Kinematic Tracking Error (KTE, see Eq. (2.26))

[4]Tremor grades are defined as: 0: Absent, 1: Discrete and infrequent, not disturbing for the patient, 2: Mild: persistent tremor of discrete amplitude, or intermittent tremor of mild amplitude, 3: Intense: the tremor interferes in some ADLs, its amplitude is mild but appears all the time, and 4: Severe: the tremor interferes with most of the chores, its amplitude is high and appears most of the time (Fahn et al., 1998).

for the whole data set. Analogously, the parameters for the algorithms to estimate tremor amplitude and frequency were defined so that they minimized the Filtered Mean Square Error with delay correction (FMSE_d, see Eq. (2.28)). For their computation, the reference voluntary movement, $y_{vm,k}$, was obtained by low pass filtering (< 2 Hz, non causal) the input motion, while the remainder gave the reference tremor, $y_{tr,k}$ (see Eq. (2.4)).

The resultant parameters for the algorithms to track voluntary movement were: *i*) for the BBF: $g = 0.018$, *ii*) for the CDF: $\theta = 0.990$ and *iii*) for the KF: the measurement noise covariance was considered to be the average covariance of the separated tremor data, therefore: $\sigma_\omega^2 = 0.0643$ rad·s^{-3}, and the process noise covariance was defined based on the second derivative of the raw motion in the data set employed for validation (as explained in Epigraph §2.3.1.2), therefore: $\sigma_\nu^2 = 0.1042$ rad·s^{-3}. The parameters for the tremor estimation algorithms were set to: *i*) for the WFLC: $\mu_0 = 5 \cdot 10^{-4}$, $\mu_1 = 2 \cdot 10^{-2}$, $\mu_b = 1 \cdot 10^{-2}$, $M = 1$ and $f_0 = 6$ Hz, *ii*) for the BMFLC: $\mu = 2 \cdot 10^{-2}$, $\mu_b = 0$, $M = 1$, $f_0 = 6$ Hz, $f_n = 8$ Hz and $G = 4$ and *iii*) for the KF-WFLC: $\mu_0 = 5 \cdot 10^{-4}$, $\mu_1 = 1 \cdot 10^{-2}$, $\mu_b = 1 \cdot 10^{-2}$, $M = 1$, $f_0 = 6$ Hz, $\mathbf{R} = 1 \cdot 10^{-2}$ and $\mathbf{Q} = \text{diag}(1{\cdot}10^{-4}, 1{\cdot}10^{-4}, 1{\cdot}10^{-4})$.

2.4.4.1 Evaluation Metrics

The goodness of the estimation obtained with each algorithm to track voluntary movement was evaluated using the KTE. The KTE quantifies the smoothness, response time, and execution time of a tracking algorithm (Rocon, 2006), and is defined as:

$$\text{KTE} = \sqrt{\varphi_{|b^*|}^2 + \sigma_{|b^*|}^2} \tag{2.26}$$

where $\varphi_{|b^*|}$ and $\sigma_{|b^*|}^2$ represent the mean and the variance of the absolute estimation error (see Eq. (2.27)) respectively. The former quantifies how fast the algorithm is able to react when the velocity changes, whereas the latter measures the smoothness of the estimated variable (Rocon, 2006).

$$b^* = |y_{vm,k} - \hat{y}_{vm,k}| \tag{2.27}$$

The performance of the algorithms to estimate the tremor was quantified using the FMSE_d, a metric specifically designed to evaluate the accuracy of tremor tracking filters (Gonzalez et al., 2000, see Eq. (2.28)). The interest of using the FMSE_d lies in the fact that it considers the physical nature of the estimation error, and differentiates errors appearing due to phase distortion from those caused by undershoots or overshoots. The RMSE, which is the metric typically employed in estimation problems, suffers from two

drawbacks related to this: *i*) since errors due to undershoots or overshoots have great power, they overshadow the errors of interest in applications such as ours, and *ii*) the RMSE is severely affected by small delays, although this does not necessarily indicate poor performance (Gonzalez et al., 2000)—in some cases it can be compensated by phase advance algorithms, for example—. Both limitations are taken into consideration within the definition of $\mathrm{FMSE_d}$:

$$\mathrm{FMSE_d} = \mathrm{E}\left[y_{tr,k} - \hat{y}_{tr,k-\hat{d}_k}\right]^2 \tag{2.28}$$

where $\hat{y}_{tr,k-\hat{d}_k}$ stands for the delay compensated tremor estimation. The instantaneous delay, $\hat{d}_k$, was estimated by maximization of the cross-correlation function.

I also evaluated the total phase distortion introduced by the two-stage filter, because it has a critical influence on the response time of the control strategy implemented at the pHMI[5] (see Chapter §4). To this end, I computed the delay between the reference tremor and the estimation of tremor, through maximization of the cross-correlation function.

Throughout this chapter, results are reported as mean ± standard deviation (SD).

2.5 Results

Fig. 2.6 shows an example of voluntary movement tracking with the different algorithms. The figure is a representative example of the general results, and simple visual inspection suggests that the BBF and CDF outperformed the KF. As a matter of fact, in this trial the KF tended towards tracking the raw movement; this was observed in other repetitions, and caused a larger SD of the KTE for the KF (0.124 rad/s, compared to 0.083 and 0.073 rad/s for the BBF and CDF respectively, see results grouped according to type of trial in Table 2.1). This behavior could be avoided by trial- or patient-specific selection of filter parameters, but it was not done since the final goal was to define the optimal architecture and parameters for the algorithm, for all the patients and trials. As to the BBF and CDF, the latter proved to adapt slightly more rapidly during transient periods (e.g., see the arrow in Fig. 2.6), an observation that was repeated in all the trials. Furthermore, for the example in the figure, both algorithms provided a similar performance when no voluntary movement was present, although in other repetitions the estimation of the CDF was smoother (Gallego et al., 2010b). As a consequence, the CDF performed slightly better than the BBF (average KTE for all patients and trials 0.264 ± 0.073 rad/s, compared to 0.291 ± 0.083 rad/s for the BBF). Therefore, the results indicated that the CDF constitutes the optimal voluntary movement tracker for this application.

[5] Given its importance, I also evaluated in Chapter §3 whether the multimodal interface significantly reduced this latency (see Section §3.4).

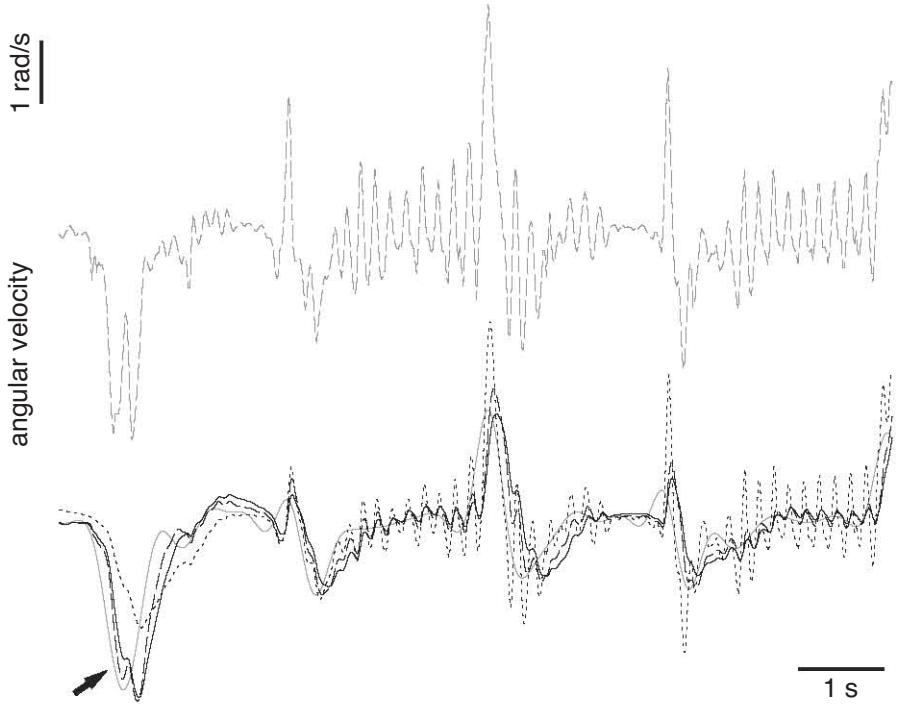

FIGURE 2.6: An example of voluntary movement tracking with the three algorithms evaluated. The data corresponds to an ET patient performing a FN test. The figure shows the raw flexion-extension (dashed gray line, on top), the reference voluntary movement (solid gray line), and the BBF, CDF and KF estimation of voluntary movement (solid, dashed and dotted black lines respectively).

TABLE 2.1: Performance of the algorithms to track voluntary movement depending on the type of task, as evaluated with the KTE (rad/s). The table shows the mean ± SD for all the trials of the same type performed by all the patients.

Algorithm	AO	FN	RE	WG
BBF	0.194 ± 0.058	0.400 ± 0.134	0.147 ± 0.091	0.291 ± 0.083
CDF	0.121 ± 0.053	0.372 ± 0.118	0.134 ± 0.081	0.264 ± 0.073
KF	0.169 ± 0.100	0.378 ± 0.143	0.174 ± 0.129	0.312 ± 0.129

The plot in Fig. 2.7 shows an example of tremor estimation with the three algorithms described in Section §2.3.2. In this case, the performance of the different algorithms was very similar. However, the overall results indicated that the WFLC provided a worse tremor estimation when compared to the BMFLC and the KF-WFLC, as measured with the FMSE_d (see Table 2.2), which originated from its worse transient response. This statement was supported by two observations: *i*) the difference in the FMSE_d became larger for the tasks that involved longer periods of voluntary movement (i.e. FN and WG), during which more tremor transients occurred, and *ii*) the KF-WFLC, which permitted independent optimization of the algorithm parameters, improved tremor tracking in more than one order of magnitude (for all the patients and trials, the average FMSE_d for the WFLC alone was 0.031 ± 0.025 rad/s while for the KF-WFLC it became 0.001 ±

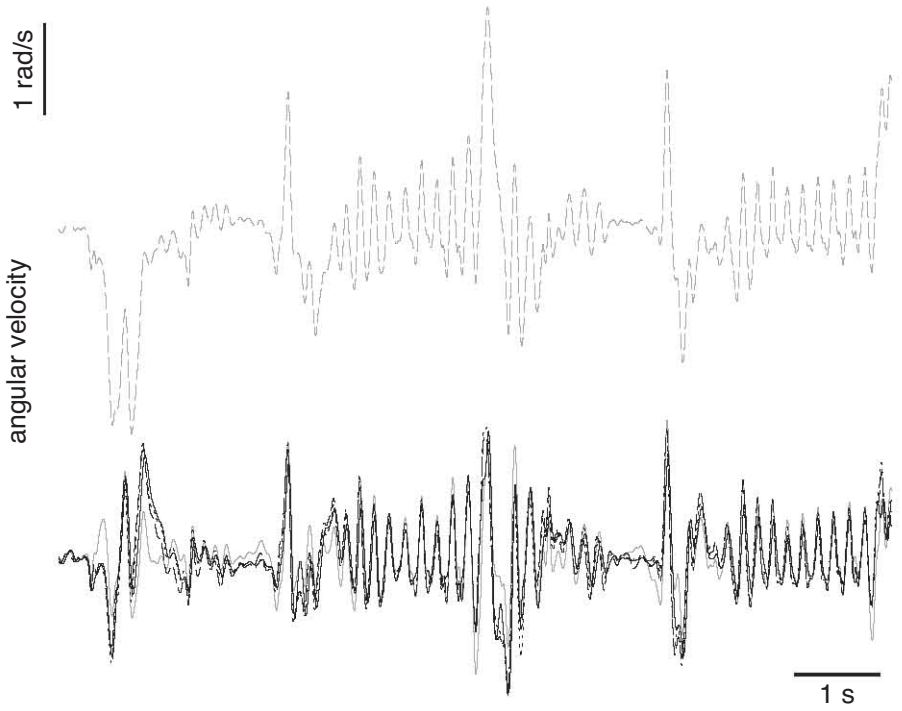

FIGURE 2.7: An example of tremor estimation with the three algorithms evaluated. The data corresponds to an ET patient performing a FN test (same example that in Fig. 2.6). The figure shows the raw flexion-extension (dashed gray line, on top), the reference tremor (solid gray line), and the WFLC, BMFLC and KF-WFLC estimation of tremor (solid, dashed and dotted black lines respectively).

TABLE 2.2: Performance of the algorithms to estimate tremor parameters depending on the type of task, as evaluated with the $FMSE_d$ (rad/s). The table shows the mean $\pm$ SD for all the trials of the same type performed by all the patients.

Algorithm	AO	FN	RE	WG
WFLC	0.017 $\pm$ 0.007	0.052 $\pm$ 0.023	0.014 $\pm$ 0.006	0.042 $\pm$ 0.020
BMFLC	0.007 $\pm$ 0.008	0.008 $\pm$ 0.019	0.005 $\pm$ 0.012	0.006 $\pm$ 0.013
KF-WFLC	0.001 $\pm$ 0.003	0.000 $\pm$ 0.002	0.001 $\pm$ 0.001	0.001 $\pm$ 0.003

0.003 rad/s, see Table 2.2 for results grouped per trial type). Furthermore, although the BMFLC also provided accurate tremor estimation, its performance was slightly worse than that of the KF-WFLC (for all patients and trials the $FMSE_d$ of the BMFLC was 0.007 $\pm$ 0.001 rad/s).

As to frequency tracking, both the KF-WFLC and the BMFLC provided accurate estimates, although it was less smooth for the latter (see Fig. 2.8). This was due to the fact that the BMFLC estimation was obtained as function of the instantaneous contribution of each FLC to tremor estimation (see Eq. (2.23)), and not as the time varying frequency of an adaptive harmonic model (Gallego et al., 2010a). On the basis of this, I concluded

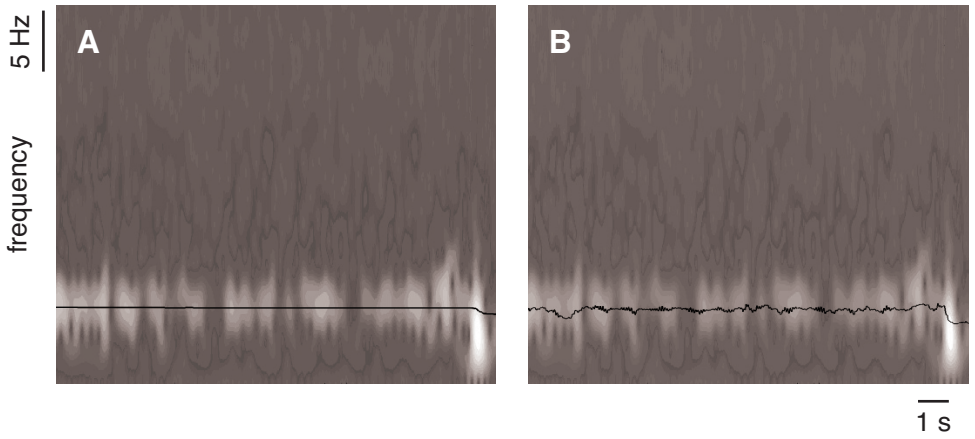

FIGURE 2.8: An example of the estimation of tremor frequency with the WFLC (A) and the BMFLC (B). The data corresponds to an ET patient performing a AO test. In each plot, the solid line represents the estimation of tremor frequency, and the surface is the spectrogram of the reference tremor (in the grayscale, high power is colored in white).

that the KF-WFLC constitutes the optimal algorithm to estimate instantaneous tremor amplitude and frequency.

I also evaluated the delay between the estimation of tremor (obtained with the KF-WFLC, see Eq. (2.24) and (2.25)) and the reference tremor, in order to characterize the overall delay of the two-stage filter. The average delay obtained for all the patients and trials was -0.015 $\pm$ 0.006 s. Interestingly, the final tremor estimate was slightly advanced with respect to the reference tremor because of the critically dampened estimation of voluntary movement, which resonates in a manner that makes it anticipate the tremor waveform. This behavior was also observed in datasets from posterior sessions. Regarding the settling time, the convergence of the tremor estimation algorithm was limited by the settling time of the stage that tracked voluntary movement, i.e. the CDF, and was in the range of $\sim$1–1.5 s for all the patients and trials.

2.6 Discussion

This chapter presented the rationale, development and validation of an adaptive algorithm for the online estimation of tremor parameters. The algorithm exploited the characteristics of the concomitant voluntary and tremulous movements to separate them, and then it tracked the amplitude and frequency of the tremor. This was achieved without significant phase distortion. In addition to this, in Section §2.2.3 I provided first evidence that decomposition of kinematic recordings of tremor with EEMD could separate the multiple oscillators that are likely to be embedded within the signal (Hurtado et al., 1999; Raethjen et al., 2000; Timmermann et al., 2003). Although this finding is

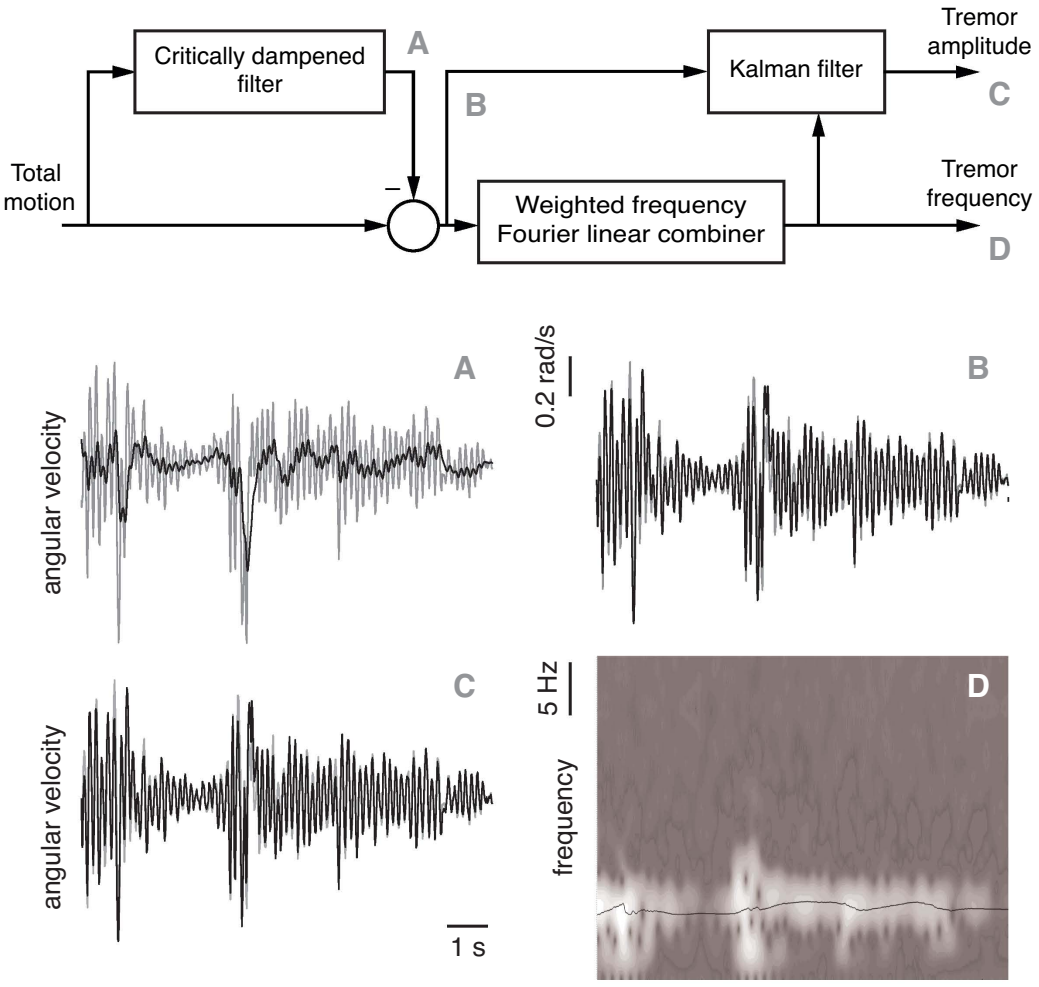

FIGURE 2.9: Summary of the two-stage algorithm for the online estimation of tremor parameters. The figure shows the final structure as defined after the evaluation of the different algorithms to track voluntary motion and estimate tremor parameters, and illustrates it with an example. The data corresponds to a trial during which an ET patient performed an AO test. The plot (A) shows the raw flexion-extension (gray line) and the voluntary movement estimated with the CDF (black line). The plot (B) represents the estimated tremor (as the difference between the raw and volitional movements, in black), and its reference obtained offline (in gray). The plot (C) displays the tremor estimated with the KF-WFLC (black line) and the reference tremor (gray line). The plot (D) compares the estimated tremor frequency (solid black line) with the spectrogram of the reference tremor (in the grayscale, high power is colored in white).

not translatable to the NP given that it uses a transcutaneous interface for neurostimulation, and therefore it has poor selectivity to activate the deep and imbricate muscles that control wrist movements (see Epigraph §1.3.2), it is an interesting topic of future research, and may be of great importance in invasive—i.e. highly selective—NPs for tremor management.

The two-stage adaptive algorithm here presented (summarized in Fig. 2.9) was the cHMI employed during the validation of the tremor suppression strategy implemented in the

NP (described in Chapter §4), despite the better performance of the multimodal interface described in the next chapter, mainly in terms of response time at (voluntary) movement onset. The reason for using the gyroscope algorithm alone was twofold: *i*) the performance of the two-stage algorithm alone during steady state was similar to that of the multimodal interface, and the tasks for clinical examination employed to validate the NP involve only limited transients, and *ii*) the multimodal interface described in Chapter §3 was a proof of concept of the approach, and due to the state of the art on the different neural interfaces it implements, it does not constitute a solution that may be incorporated into a functional prototype, because of their poor usability. Furthermore, the cHMI implementing only gyroscopes could allow for the development of a prototype available in the mid term for extensive clinical testing (see Future Work, Section §6.3), while a future commercial solution would require an interface that minimizes transient periods, which may be achieved by integrating concurrent EMG recordings (see Section §1.3.1) in order to increase its usability.

The fact that the architecture of the two-stage algorithm takes into consideration the inherent properties of voluntary movement and tremor (reviewed in Section §2.2.3), and that it has been defined after the evaluation of a series of adaptive algorithms with patients data, ensures optimality. Remarkably, the group of patients that participated in the validation was very heterogeneous, comprising users with different types of tremor, and the comparison of the algorithms was performed with metrics that took into consideration the various sources of error, for example, bad transient response, or lack of smoothness during steady state. Furthermore, the final architecture of the two-stage algorithm was implemented in the different studies of Chapters §3, and §4 (the results of the former are detailed in Section §3.4), providing always similar results. This constituted a further evidence of the performance of the algorithm in a larger group of patients.

As to the differences among algorithms, the reason that made the CDF outperform the BBF lied in its inherent oscillatory nature, which made it resonate almost in phase with the tremor. This occurs because the CDF has two equally spaced zeroes, which causes the critically dampened response (Brookner, 1998). In addition, this may—as observed—enable the CDF to adapt slightly faster when changes in voluntary movement occur, decreasing the error during transient periods. As a consequence, the CDF minimized the KTE both for rest (RE) and posture (AO), and more dynamically complex tasks (FN and WG), when compared to the BBF and the KF (see Table 2.1). Furthermore, the resonant behavior of the CDF was also the cause by which the two-stage algorithm did not introduce significant phase distortion on the final estimation of tremor. I found very hard to tune the first order KF with a unique set of covariance matrices to provide fast response during changes in voluntary movement without tracking the tremor; this manifested in its considerably worse performance. Regarding the algorithms to estimate tremor parameters, as expected the KF-WFLC outperformed the WFLC. This occurred

because: *i*) its cascade architecture permitted optimizing the gains of the WFLC for the optimal tracking of instantaneous tremor frequency, and the covariance matrices of the KF for optimal amplitude tracking, and *ii*) the KF minimizes the *a posteriori* error covariance (Bar-Shalom and Li, 1998), which has been shown to provide better adaptation during transient periods than methods built upon gradient estimates (Veluvolu and Ang, 2011). The KF-WFLC also provided a smaller estimation error when compared to the BMFLC, in my opinion, also due to the slightly slower adaptation rate of the latter. Again, this was expected from the fact that the BMFLC implements a bank of LMS—gradient descent like—algorithms that react less rapidly to transients. In addition, given that the frequency derived from the BMFLC was computed as the linear combination of the instantaneous contributions of its constituent band pass filters (Widrow et al., 1975), it was less smooth than that estimated with the KF-WFLC. A subsequent low pass filtering stage would overcome this, but it was not systematically tested since the KF-WFLC yielded up to five times more accurate tremor estimation (see Table 2.2) with no delay.

Settling time, both at start-up and during brisk voluntary movements, was minimized to the maximum (in the range of ∼1–1.5 s for all patients and tasks), but it constitutes the major drawback of the algorithm presented herein. Settling time at start-up may be cancelled with the integration of neural recordings at the CNS and the PNS, as demonstrated in Chapter §3. Furthermore, the settling time of the estimation of tremor frequency with the WFLC is largely dependent on its initial frequency, because the adaptation gain is limited by the sampling rate of the NP. By feeding a first guess of tremor frequency computed with simple spectral analysis (see Section §4.2) or derived from sEMG analysis (see Section §3.4), this period would be significantly shortened, more in the latter case.

2.7 Conclusions

The development of a NP for tremor management requires accurate techniques to record and parameterize the involuntary movement that has to be compensated for. To this end, gyroscopes were selected as the optimal means to perform ambulatory tremor recordings with the NP given their intrinsic characteristics, and because I found an approach to minimize online their inherent drift. Next, this chapter presented the development and validation of an adaptive algorithm to estimate the instantaneous tremor parameters from gyroscope recordings. The algorithm takes into consideration the properties of the concomitant voluntary and tremulous movements, and was defined after the evaluation of a series of tracking filters according to specific metrics. Furthermore, it constitutes one of the first efforts towards accurate online estimation of tremor parameters. The methodology I followed ensured optimality in the terms here defined: accurate tracking of tremor amplitude and frequency, with negligible phase distortion and short settling

time, at the same time that it avoided patient specific tuning of the algorithms. To my knowledge, this is a pioneering effort on the subject, and has been partly transferred to other problems and technologies in the field (Frizera Neto et al., 2010; Raya et al., 2012).

The two-stage algorithm was the cHMI employed for the validation of the tremor suppression strategies with the NP, during which it provided an accurate parameterization of the tremor that served to drive the neurostimulation delivered at the pHMI. In addition, in the next chapter I show how the settling time at start up, which is—together with the slight delay during brisk voluntary movements—its main drawback, can be minimized by integrating recordings of the neural system.

In summary, this chapter presented the methodology employed to perform ambulatory measurements of upper limb movements with the NP, and an adaptive algorithm for the online estimation of tremor parameters in the presence of voluntary movement (Gallego et al., 2010b). Experimental evaluation with a group of patients ensured that the two-stage algorithm here presented was optimal for the application, which enabled the development of the control strategy for tremor suppression based on the information derived with this cHMI.

Chapter 3

A Multimodal Human-Machine Interface to Parameterize Tremor in the Presence of Volitional Movement[1]

This chapter presents the design and proof of concept of a multimodal interface to drive the neuroprosthesis for tremor management. The interface has the objective of providing an accurate characterization of the tremor during functional tasks, at the same time that guaranteeing a transparent control by the user. To this end, the interface triggered the neuroprosthesis when movement intention was derived from the analysis of EEG, which provided a natural interface with the wearer. When this information was delivered, surface EMG served to detect the actual onset of the tremor in the presence of volitional activity. This would in turn trigger the tremor suppression strategy, which would modulate neurostimulation based on tremor parameters—amplitude and frequency—derived from a pair of gyroscopes that recorded the kinematics of the affected joint. The surface EMG also yielded a first characterization of the tremor, together with precise information on the preferred stimulation site. Apart from allowing for an optimized performance of the system, the multimodal interface permitted implementing redundant methods to both enhance the reliability of the system, and adapt to the specific needs of different users. Results with a representative group of patients served to illustrate the performance of the multimodal interface here presented, demonstrating its feasibility, and enabling its integration in future neuroprostheses once neural interface technologies become more mature.

[1]This Chapter is partly based on: J.A. Gallego, J. Ibáñez, J.L. Dideriksen, J.I. Serrano, M.D. del Castillo, D. Farina, E. Rocon. A multimodal Human-Robot Interface to drive a tremor management neuroprosthesis. IEEE Transactions on Systems, Man and Cybernetics, Part C: Applications and Reviews 42(6):1159–68, 2012.

3.1 Introduction

In Epigraph §1.3.1 I defined a series of design requirements that an optimal cHMI for a tremor management NP/WR should fulfill. Briefly, these were: R_c1) the NP only has to actuate if tremor appears when the user wants to perform a voluntary movement, R_c2) the interface must be natural, R_c3) it has to provide a fast response, and R_c4) it has to deliver an accurate estimation of concomitant voluntary and tremulous movements.

The algorithm based on gyroscope information presented in Chapter §2 met requirement R_c4 succesfully, and requirements R_c1 and R_c2 partly, because it detected both movement and tremor when they appeared and not when the user intended to perform the task. Nevertheless, it had a settling time (∼1–1.5 s) that could cause malfunctions during short duration ADLs, thus failing to fulfill requirement R_c3.

Here I present a novel multimodal human-machine interface (mHMI) designed to meet these 4 criteria, in order to provide with an optimal cHMI to drive a NP/WR for tremor management during daily living. The mHMI simultaneously assesses the preparation and execution of the movement based on concurrent recordings from the CNS, the peripheral nervous system (PNS), and the biomechanics of the affected limb. This is performed by concurrent EEG, EMG, and gyroscope recordings, and provides the patient with a natural interface that both requires no learning from her/his part, and reacts with a minimum latency when compared to the performance of volitional movements (thus also satisfying design requirement R_c3). These features maximize the ease of use, and make the interface suitable for a larger population, e.g., for those suffering cognitive impairment (see Epigraph §1.3.1). Therefore, this approach to mHMI guarantees that the system will only "assist when needed" based on the detection of intention to move from EEG, which also has positive implications in terms of energy efficiency, and of discomfort and accommodation to stimulation.

The other major benefit derived from this concept is that multimodality allows for redundant extraction of the same features, which enhances the overall reliability and performance of the system. The idea here is that at the same time that the interface exploits the sensor modality that provides the best characterization of a given phenomenon, it implements redundant methods that compensate for misdetections or false positives.

Apart from these considerations that could be contemplated as general to most mHMI-driven NPs and WRs, I had to incorporate additional features for the specific case of tremor management. The most important among them were the accurate parameterization of the tremulous movement, and having the capacity to adapt to slow and fast signal non-stationarities. Accurate estimation of tremor amplitude and frequency is necessary for precise modulation of the different control strategies that can be exploited to

suppress the tremor (Rocon et al., 2007a; Gallego et al., 2010b). As to the latter, examples of non-stationarity are the changes in EMG due to muscle fatigue (Gandevia, 2001; Dideriksen et al., 2010), or the inherent alterations in the basal rhythms of EEG (Shenoy et al., 2006). In addition, fast response is specially important in tremor, because most tremors tend to exhibit a transient stage during which their amplitude increases, and thus they can be compensated with less actuation effort if its done during this phase.

The practical implementation of the mHMI faced a number of scientific and technological challenges. Among the major scientific challenges were the online detection of movement intention in tremor patients and the real-time characterization of tremor from EMG, which had not been investigated before. Notice that most tremors are originated within brain nuclei that have strong direct and indirect cortical projections (e.g., Elble, 2000; Steigerwald et al., 2008; Bartels and Leenders, 2009, see also Epigraph §1.2.3), which may alter the properties of the EEG signals when compared to those recorded in healthy subjects (Tamás et al., 2006; Lu et al., 2010; Kinoshita et al., 2010). As for the online parameterization of tremor with inertial sensors, a number of works are available, as reviewed in Section §2.1. The major technological challenges were those intrinsic to the recording of EEG and EMG, being the most important obtaining a good interface that permitted acquiring signals with high signal to noise ratio. Since this chapter aims at providing a proof of concept of the mHMI, non-invasive technologies based on wet electrodes were used for both, although the mHMI might be implemented in systems that comprise other types of interfaces.

The state of the art techniques to model tremor in real-time normally exploit a single sensor modality, typically inertial sensors, either accelerometers (Veluvolu and Ang, 2011) or gyroscopes (Gallego et al., 2010b; Bo et al., 2011, for a detailed review see Section §2.1), or EMG recordings (Journée, 1983), although research works on fusion of both technologies have started appearing (Widjaja et al., 2011). On the other hand, to the author's knowledge there is no system in the literature similar to what I propose here, in the sense of employing a mHMI that exploits movement anticipation to drive, based on neural and kinematic information, a NP that compensates for a certain movement disorder, or that is aimed at rehabilitating patients after neurological injury.

Therefore, this chapter presents a novel mHMI to drive the tremor management NP—or any robot for functional compensation of tremor—during the performance of ADLs. I show that by integrating a prediction of motor commands derived from cortical recordings with neural and kinematic information from the tremulous limb, the mHMI is capable of detecting and parameterizing tremor during voluntary tasks, ignoring the tremor that appears in non-functional contexts. The experimental validation demonstrates the feasibility of the approach and encourages its implementation in future systems.

TABLE 3.1: Information about tremor and/or voluntary movement that can be extracted from each sensor modality within the mHMI, together with their respective positive characteristics and drawbacks

	Positive characteristics	Drawbacks
EEG	- Anticipation to movement onset. - Distinction of voluntary movement and tremor.	- Low reliability (false positive and false negative rates). - Uncertain anticipation time in a single trial analysis (∼2–0 s) - Some subjects do not present recognizable patterns to be classified. - Challenging to use concurrently with neurostimulation (physiological artifacts).
EMG	- Robust detection of voluntary and tremulous activity. - Fast, accurate detection of tremor. - Direct identification of muscles with tremor (preferred stimulation sites).	- Challenging to use concurrently with neurostimulation (physiological artifacts). - Nonlinear and complex relationship between muscle activation and kinematics. - Maximum movement anticipation limited by the electromechanical delay.
Inertial sensors	- Usable with FES (no EMI). - Reliable and accurate parameterization of tremor.	- Delay in the detection of voluntary motion and tremor onset (algorithms). - Impossibility to identify the muscle that causes the tremor because it is measured as joint movement and not as muscle activity. - Convergence time of tracking algorithms.

The organization of this chapter is as follows. Section §3.2 presents the rationale and implementation of the mHMI for the parameterization of tremor in the presence of voluntary movement, describing the algorithms employed by the different sensor modalities that constitute the interface. Section §3.3 describes the experimental protocol, materials and methods employed for its validation, together with the methodology for data analysis, focusing on the metrics for evaluation of the system as a whole. Section §3.4 summarizes the results of the evaluation of the system with a representative group of users. Next, I provide a critical discussion about the performance of the system, putting special emphasis on the integration of sensor modalities and the implications that the results have when driving the NP. The chapter ends with conclusions that summarize the major achievements of this study.

3.2 Multimodal Human-Machine Interface to Parameterize Tremor during Volitional Movements

The selection of the specific architecture for the mHMI was based on a detailed analysis of the information that can be extracted from each sensor modality available, paying

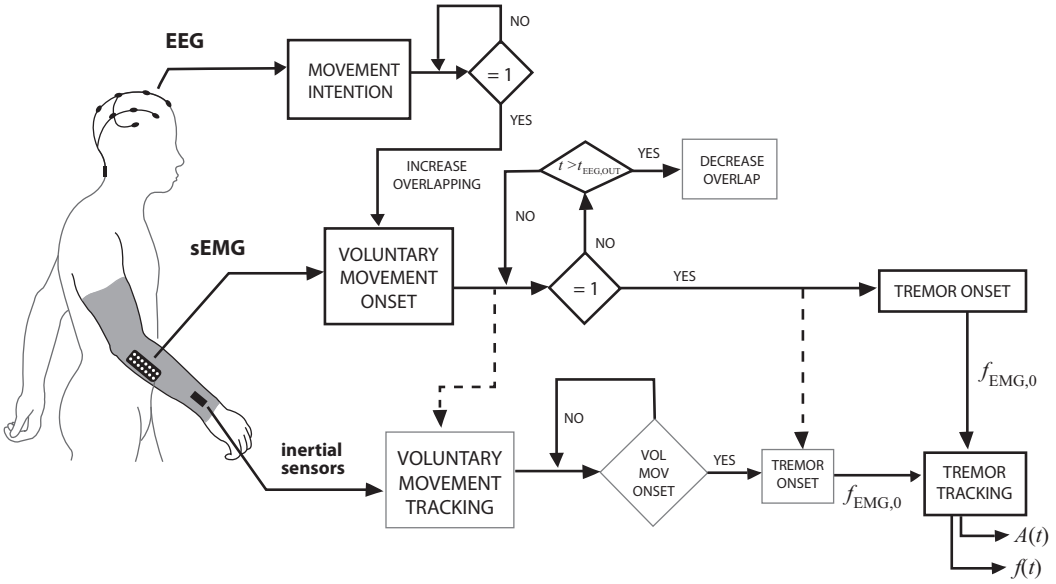

FIGURE 3.1: Diagram that illustrates the mHMI to drive the NP. The figure shows the normal performance of the system (thick black boxes), and the redundant and compensatory mechanisms (thin gray boxes). Redundant (dashed lines) and normal (solid lines) flows of information are also differentiated. The diagram shows the implementation of the mHMI assessing only the wrist.

special attention to the benefits and drawbacks for each choice, especially in the presence of transcutaneous neurostimulation (see Table 3.1).

On the basis of this, EEG was employed to detect the preparation of movement as a transparent way to trigger the NP, sEMG to monitor the onset of tremor in the presence of voluntary muscle activation, and gyroscopes to drive the NP during neurostimulation.

In more detail, the implementation of the mHMI was as follows (see Fig. 3.1). An EEG algorithm exploited the direct measurement of movement planning in order to trigger naturally the system. However, since the anticipation with which movement can be predicted from the technique employed varies both between and within subjects (Blankertz et al., 2006), a positive detection of movement intention was maintained for a period $t_{\mathrm{EEG,OUT}}$, to guarantee that the sEMG had time to detect the onset of both the voluntary muscle activity and the concomitant tremor. This in turn would trigger the pHMI, which would modulate neurostimulation based on the instantaneous tremor amplitude and frequency derived from the gyroscopes (see Chapter §4), because the sEMG is contaminated by physiological artifacts (the so-called M-wave) that appear due to neurostimulation (Mandrile et al., 2003). In addition, sEMG indicated the specific locus (loci) of the tremor, a piece of information that could be used by the controller to select the optimal stimulation site, and yielded an estimate of tremor frequency at the muscles recorded, which was employed by the gyroscope algorithm in the mHMI for its initialization.

The EEG algorithm run in overlapping (ov_{EEG}) windows of duration T_{EEG}. At the same time, the sEMG algorithm was executed in windows of duration T_{EMG} and overlapping ov_{EMG}. The latter was increased to $ov_{\mathrm{EMG,ho}}$ during the period $t_{\mathrm{EEG,OUT}}$ after a positive detection of the EEG classifier, to accelerate the identification of the concomitant voluntary and tremulous muscle activity. Simultaneously, the EEG algorithm went idle, and the voluntary movement filter of the gyroscopes started running, to minimize its settling time (see Section §2.6). In the presence of tremor, the sEMG algorithm provided the gyroscopes with an estimation of tremor frequency, $f_{\mathrm{EMG},0}$, and started the tremor suppression strategy.

The integration of different sensor modalities also allowed for the implementation of a set of redundant mechanisms that let the mHMI cope with unexpected conditions, such as misdetections, false positives, *et cetera*. Three mechanisms, described next, were considered (also see Table 3.1). First, state of the art algorithms for single trial detection of movement intention (from the EEG) are not completely accurate (Bai et al., 2011; Niazi et al., 2011), which originates a certain ratio of false negatives that would cause the no actuation of the NP in a situation in which it would be expected to. This was circumvented by using sEMG to detect the onset of both voluntary motion and tremor, at the expense, however, of loosing the capability to anticipate with the EEG. Moreover, the sEMG compensated for possible false positives of the EEG system, avoiding unnecessary periods of stimulation (see Fig. 3.1). Second, the appearance of muscle fatigue, a phenomenon that is intrinsic to the execution of relatively long tasks (Gandevia, 2001), has an important influence on the sEMG signals (Dideriksen et al., 2010), which would alter the thresholds for the detection of tremor and voluntary movement onset. This could be corrected based on the detection of volitional and/or tremulous motion from gyroscopes. Third, the adaptive filters employed to track tremor parameters from gyroscope information have an inherent settling time (see Section §2.6, and, e.g., (Vaz et al., 1994)) that is almost eliminated by adequate selection of their initial conditions. In this regard, the sEMG algorithm provided the gyroscopes with an accurate estimation of tremor frequency that considerably minimized such convergence time.

Given the intrinsic variability of EEG patterns because of factors such as age (Derambure et al., 1993) or pathology (Tamás et al., 2006), the performance of the classifier here proposed depended on the detection, in each patient, of recognizable patterns associated with the preparation of movement. Patients who did not exhibit these patterns relied entirely on the sEMG to detect voluntary movement onset, although the performance of the NP would be degraded. The benefit, on the contrary, is to extend the possible user group to a much larger population.

3.2.1 Detection of Movement Intention

This algorithm[2] was built to detect movement intention asynchronously, i.e. without any external cue (Mason and Birch, 2000), and it thus estimated the probability of identifying a pre-movement condition every period of duration t_{EEG}, at the same time that it avoided the generation of long periods with false activations.

The core of the approach was a single trial identification of the event-related desynchronization (ERD), a neurophysiological phenomenon that consists in the decay of the EEG signal power in the mu (8–12 Hz) and lower beta (12–15 Hz) bands over the sensorimotor area, which accompanies the performance of motor tasks (Pfurtscheller and Lopes da Silva, 1999). The ERD appears ∼2 s before the actual onset of the volitional movement, and typically begins over the contralateral hemisphere when movements are performed with the dominant limb (Bai et al., 2011). The ERD presents high inter- and intra-subject variability in its spatial and frequency distribution, and therefore an online methodology to choose the best features that describe the pre-movement state in each subject, by training a classifier with the set of most recent movements, was developed.

Such features were automatically selected based on the power decrease in the movement state with respect to the basal state, computed in all the channel-frequency pairs available after derivation with a spatial filter. This way the algorithm identified the 3 most significant channel-frequency pairs in terms of movement anticipation, which were used to generate a descriptive model of the pre-movement state by computation of their logarithmic power values.

During execution, a Bayesian classifier was used to decide, based on this model, whether each new data window corresponded to a pre-movement state. The classifier computed independently the probability of the 3 selected features, and combined them to generate the final output. This final output was then compared to a threshold in order to provide the sEMG algorithm with a binary signal that indicated the intention or not intention to move. If the classifier output was positive, it was maintained for the subsequent $T_{\mathrm{EEG,OUT}}$ s, in order to give a stable prediction to the sEMG system, and guarantee the possibility of acknowledging this detection. The threshold was also automatically generated from the training data set, following the optimization criterion of maximization of movement anticipation while minimizing the number of false positives during intervals of inactivity.

Finally, the EEG classifier used the detection of the voluntary movement to update both its descriptive model and the threshold during execution. This way the classifier always considered the set of most recent movement intervals, reducing the negative influence of the intrinsic non-stationarity of the EEG signal (Shenoy et al., 2006) on its performance.

[2]The main author of the work described within this epigraph was J. Ibáñez.

3.2.2 Detection of Tremor Onset

A method[3] based on a novel multicomponent AM-FM decomposition technique, the Iterated Hilbert Transform (IHT, Gianfelici et al., 2007), was employed to analyze the multichannel sEMG in overlapping windows of duration T_{EMG} (output updated every period t_{EMG}). The IHT consists in the iteration of the Hilbert transformation to a filtered version of the amplitude envelop of the signal. This approach considered the muscle activity to be a superimposition of the reflections of the voluntary activity (broadband component) and the narrowband oscillations causing the tremor (Dideriksen et al., 2011). On the basis of this, the sEMG signal was modeled as the sum of K locally narrowband modulated components according to:

$$Y(n) = \sum_{k=1}^{K} A_k(n) \cos[W_k(n) + P_k(n)] + R_k(n) \tag{3.1}$$

where n is the sample number, and A, W, P and R the amplitude envelope, the center frequency, the instantaneous phase and the residual respectively.

By applying this method on the tremor sEMG signals, it was shown that the first IHT component consistently reflects the tremor, and that the peak-to-peak amplitude of such component is correlated to the tremor amplitude (Dideriksen et al., 2011). Moreover, the level of concomitant voluntary muscle activity can be estimated by subtracting the SD of the tremor component from the offset of this component (low pass filtered, < 2 Hz).

This method was applied to the multichannel, high-density, sEMG, which implies that the information about muscle activity from all parts of the muscle was analyzed, but with the inherent risk of poor signal-to-noise ratio in a number of the channels. In order to minimize the influence of the latter, the IHT method was applied to each channel individually, and the final estimates of voluntary activation and tremor were obtained as the median value of each parameter from every single channel. These estimates were compared in a final stage to two thresholds defined as follows. The threshold for a significant change in the level of voluntary activity, $th_{\mathrm{EMG,vm}}$, was set to 3·SD above the baseline of the first 5 s of the recording. The tremor amplitude was calculated as the ratio between the root mean square (RMS) of the tremor component and the RMS of the raw, rectified sEMG signal. Significant tremor was defined as being present if this ratio exceeded a threshold, $th_{\mathrm{EMG,tr}}$.

The final output was thus a pair of binary signals (for each muscle recorded) that indicated the presence or not of voluntary movement and tremor in the analysis window. When tremor onset was detected, the algorithm triggered the actuation of the NP, and

[3] The main author of the work described within this epigraph was J.L. Dideriksen.

provided the gyroscope algorithm with an initial estimation of tremor frequency at the targeted joint, $f_{EMG,0}$. Muscle frequency was translated into joint frequency by simply taking the mean of frequencies of the antagonist muscle pair, in case both exhibited tremor.

3.2.3 Estimation of Tremor Parameters

Tremor parameters—instantaneous amplitude and frequency—were continuously estimated with the two-stage adaptive algorithm described in Chapter §2. This algorithm first removed the no-tremor component of the movement, which was considered to be the voluntary movement given that both are additive (see Section §2.2.3), and next, it estimated the instantaneous frequency and amplitude of the tremor.

The parameterization of tremor derived from this algorithm would serve to modulate the tremor suppression strategy implemented in the NP (see Chapter §4).

3.3 Methods

3.3.1 Patients

Five ET patients (3 male and 2 female) were included in the study. Age ranged from 47 to 79 years (mean 63.6 ± 11.9). All patients presented postural and kinetic tremor of mild or moderate severity. Medications were continued at the time of the recordings. All patients signed an informed consent to participate in the study; the Ethical Committee at Universidad Politécnica de Valencia gave approval to the experimental protocol, which was in accordance with the Declaration of Helsinki.

3.3.2 Experimental protocol

Patients were seated in a comfortable chair during the whole recording session. As in all studies carried out in this thesis, the experiments consisted in performing a series of exercises that are commonly employed in the clinic to assess tremor. These exercises comprised the so-called finger to finger (FF) and finger to nose tests (FN), and elevating both arms and keeping them outstretched against gravity (AO). In total, each patient performed 6 repetitions of each exercise. The execution of all the trials followed the same scheme: patients were asked to stay relaxed and keeping the gaze fixed on a wall about 2 m away, and self-initiate the exercise after allowing for a sufficient repose time after the trial started. Total trial duration was 50 s.

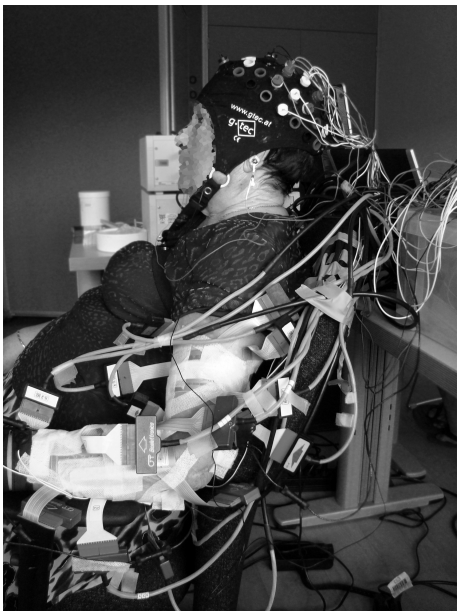

FIGURE 3.2: A tremor patient instrumented for the validation of the mHMI.

3.3.3 Recordings

Tremor was recorded from the most affected side with both high-density sEMG and gyroscopes. Surface EMG signals were recorded over the wrist extensors and flexors with a 128-channel amplifier (OT Bioelettronica, Torino, Italy) in differential configuration. The 64-channel array electrode was placed on the muscle belly, and a humidified wrist bracelet served as common reference. Their signal was amplified, band-pass filtered (10-500 Hz), and sampled at 2048 Hz by a 12 bit A/D converter. Wrist flexion-extension was measured with two solid-state gyroscopes (Technaid S.L., Madrid, Spain) in differential configuration (see Section §2.2.1 for details about placement). Their raw data were sampled by a 12 bit A/D converter at 50 Hz, and low pass filtered ($<$ 20 Hz). EEG signals were recorded from 13 positions over the sensorimotor area (FC3, FCz, FC4, C5, C3, C1, Cz, C2, C4, C6, CP3, CPz and CP4 according to the International 10-20 system, Niedermeyer and Lopes Da Silva, 2005) with passive Au electrodes. The reference was set to the common potential of the two earlobes, and AFz was used as ground. The signal was amplified (g.Tec gmbh, Graz, Austria), band-pass (0.1-60 Hz) and notch filtered (50 Hz), and sampled at 256 Hz by a 16 bit A/D converter. Synchronization of the different systems was controlled by a digital clock signal that was generated by the computer that recorded gyroscope signals. The data were stored for posterior offline analysis. Only results from those trials with visible tremor are presented here. A photograph of an instrumented patient is shown in Fig. 3.2.

3.3.4 Data Processing and Analysis

EEG signals were spatially filtered with a Laplacian filter (Hjorth, 1975) (5 electrodes: C3, C1, Cz, C2 and C4) or a common average reference (boundary electrodes); no additional pre-processing was done in the sEMG or gyroscope recordings. Notice that due to the lack of a larger number of trials per patient, a leave-one-out methodology was employed to train the EEG classifier.

The parameters for the different algorithms were defined as follows. The output of the EEG algorithm was updated each $t_{\mathrm{EEG}} = 125$ ms based on data from $T_{\mathrm{EEG}} = 1.5$ s windows ($ov_{\mathrm{EEG}} = 87.5$ %), in which the Welch's method with Hanning windows (128 samples, 50 % overlap) was employed to calculate the power spectral density of the signal; positive outputs were maintained for $T_{\mathrm{EEG,OUT}} = 2.5$ s. The length of the analysis window, T_{EEG}, was selected to be close to the average anticipation of the ERD (Pfurtscheller and Lopes da Silva, 1999); the duration of the windows in which it was split (128 samples, 50 % overlap) optimized the trade off between frequency resolution and variance of the estimation. The sEMG algorithm run in $t_{\mathrm{EMG}} = 1$ s windows with overlapping $ov_{\mathrm{EMG}} = 50$ %, and was therefore updated each $t_{\mathrm{EMG}} = 0.5$ s; when the EEG detected the intention to move this value was increased to $ov_{\mathrm{EMG,HO}} = 75$ %. The threshold for the detection of tremor onset was defined as $th_{\mathrm{EMG,tr}} = 0.25$. The length of the window, t_{EMG}, was selected to ensure that at least two complete oscillations were included within the data to be analyzed with the IHT, and double checked with a previous dataset (Dideriksen et al., 2011). The overlappings were chosen to keep the computational cost low, allowing for real-time implementation. The gyroscope algorithm, updated every sample, used the following parameters, which were conjointly defined for all subjects after examination of a previously recorded data set (from experiments carried out in the studies described in Chapters §2 and §4): i) for the critically dampened filter: $\theta = 0.9985$, ii) for the WFLC: $\mu_0 = 2{\cdot}10^{-5}$, $\mu_1 = 1{\cdot}10^{-3}$ and $M = 1$; f_0 was provided by the sEMG algorithm ($f_{\mathrm{EMG},0}$), and iii) for the Kalman filter: $\sigma_A^2 = 1{\cdot}10^{-7}$, $\sigma_B^2 = 1{\cdot}10^{-7}$ and $\sigma_T^2 = 1{\cdot}10^{-3}$.

3.3.4.1 Evaluation Metrics

The performance of the mHMI as a whole was assessed by computing movement anticipation, the delay in the detection of both voluntary movement and tremor onset, and the error in the estimation of tremor amplitude and frequency. These metrics were computed after decomposing the total movement into the reference voluntary and tremor components. As in the whole thesis, the reference voluntary component was obtained by low pass filtering (< 2 Hz, noncausal) the input motion, while the remainder gave the reference tremor. Visual inspection in combination with a threshold yielded the onset of both the volitional and tremulous movements, which served to compute the first three

metrics. The error in the estimation of tremor amplitude was directly computed as the RMSE between the reference tremor and the output of the gyroscope algorithm, whereas the error in tremor frequency was calculated as the RMSE between the real frequency (computed from the amplitude spectrum, calculated in 1 s, zero-padded, overlapping windows on the reference tremor) and the output of the gyroscope algorithm. Notice that the RMSE, and not the FMSE_d (see Epigraph §2.4.4.1), was employed to measure the goodness of tremor amplitude estimation because the delay introduced by the two-stage algorithm was negligible (see Results in this chapter and the previous, Sections §3.4 and §2.5 respectively) once the permanent period was reached.

In addition, specific metrics were employed to evaluate certain features of the EEG and sEMG algorithms. The performance of the detector of movement intention was evaluated according to the ratio of actual movements anticipated (Recall), and the ratio of false activations during rest periods (Specificity). These metrics used an event-based evaluation due to the fact that the classifier worked asynchronously, and because of the slower dynamics of EEG when compared to the classification rate (Mason and Birch, 2000; Ibáñez et al., 2010; Townsend et al., 2004). This way, an event (activation unit, AU) referred to a set of consecutive classifier outputs that are above the decision threshold. An AU was considered an event-based true positive (eTP) when it intersected the interval $[-0.5, 0]$ s (being movement onset at $t = 0$); otherwise it was treated as an event-based false positive (eFP). The Recall and Specificity were defined as:

$$\text{Recall} = \frac{eTP}{NT} \tag{3.2}$$

$$\text{Specificity} = \frac{\text{length}(\sum eFP)}{\text{length}(\sum \text{rest})} \tag{3.3}$$

where NT is the number of total movements, and $\text{length}(\sum eFP)$ and $\text{length}(\sum \text{rest})$ stand for the length of all the eFP and rest periods respectively.

The precision of the initial estimation of tremor frequency derived from the sEMG was evaluated by comparing the RMSE between it and that obtained from the amplitude spectrum of the reference tremor (also computed from the reference tremor in a 1 s window with zero-padding). The improvement of initializing the gyroscope algorithm at tremor frequency derived from sEMG ($f_{\text{EMG},0}$) was assessed by comparing its estimation with that obtained assuming $f_0 = 5$ Hz (as done, e.g., in Chapter §2 and Riviere et al., 1998).

Statistical differences were evaluated using a Wilcoxon rank test, given that the datasets analyzed did not conform normality (one sample Kolmogorov-Smirnov, $P < 0.05$ to reject). Throughout the chapter, results are displayed as mean ± SD.

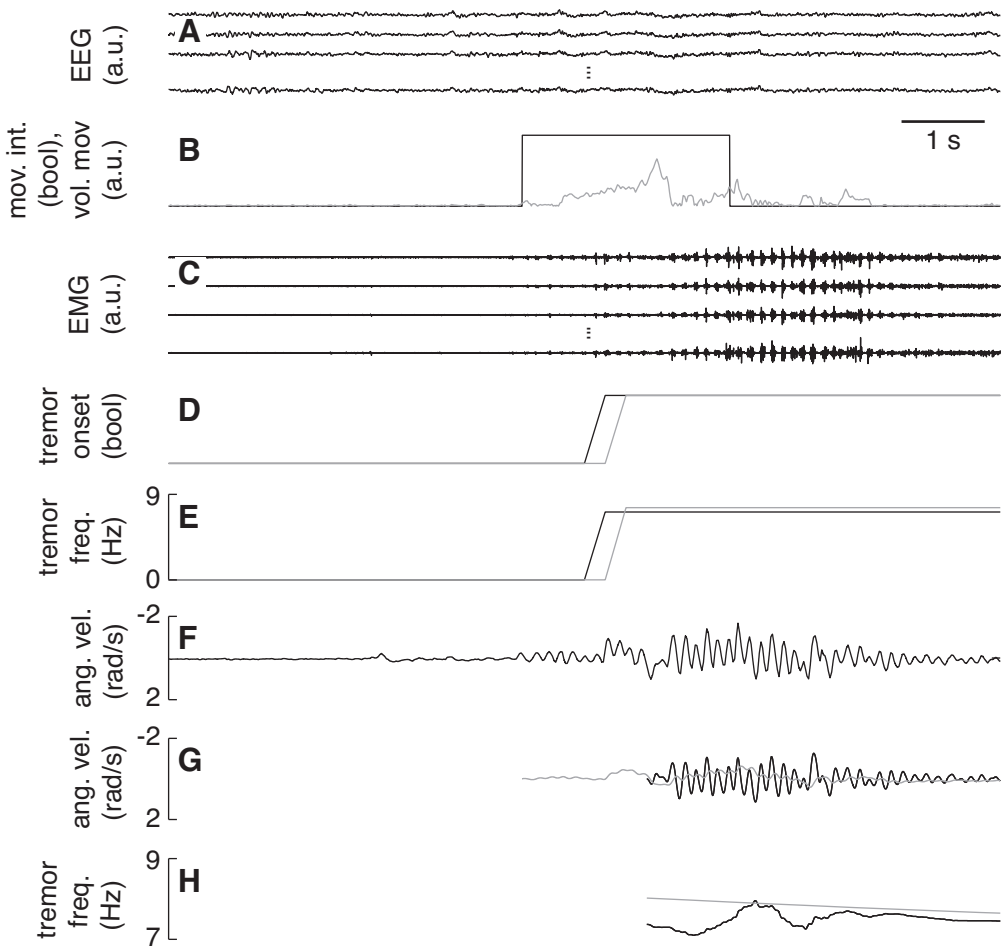

FIGURE 3.3: Example of tremor characterization with the mHMI during a volitional task. The example corresponds to an ET patient with moderate tremor performing an AO test. The plots show: A) a few EEG channels, B) the output of the EEG classifier (black) and the normalized and rectified reference voluntary movement (gray), C) a few sEMG channels from wrist extensors, D) tremor onset as detected by sEMG analysis of wrist extensors (black) and flexors (gray), E) tremor frequency as estimated from sEMG analysis at the time of detection, for wrist extensors (black) and flexors (gray), F) the raw wrist flexion/extension recorded with gyroscopes, G) the estimation of tremor (black) and voluntary movement (gray) derived from gyroscope data, and H) the tremor frequency estimated from the gyroscopes (black), and the offline reference (gray).

3.4 Results

Fig. 3.3 shows a representative example of the mHMI. The plot depicts both, the raw signals acquired by the different sensor modalities that constitute it (plots A, C, and F), and how the different algorithms were triggered and executed. First, the EEG classifier (plot B) predicted the intention to move (anticipation time 0.44 s). This triggered two events: *i*) the EEG classifier went idle for 2.5 s, and *ii*) the overlapping of the analysis windows of the sEMG algorithm was increased. During this interval, the sEMG algorithm detected the onset of tremor in the presence of concomitant voluntary activity (plot D), and yielded an estimation of tremor frequency (plot E). At this moment, the

TABLE 3.2: Performance of the mHMI. Results for all the trials of a patient are grouped together.

Patient	Movement anticip. (s)	Delay in vol. mov. detect. (s)	Delay in tremor detection (s)	RMSE tremor amplit. (rad/s)	RMSE tremor freq. (Hz)
01	0.75 ± 0.98	1.40 ± 0.40	0.75 ± 0.43	0.20 ± 0.08	1.20 ± 1.10
02	-	1.83 ± 1.77	1.79 ± 1.91	0.07 ± 0.08	1.36 ± 1.77
03	1.84 ± 1.52	0.78 ± 0.34	0.48 ± 0.61	0.10 ± 0.09	2.92 ± 3.44
04	0.41 ± 0.37	1.17 ± 0.14	1.17 ± 1.14	0.26 ± 0.22	3.22 ± 2.45
05	1.43 ± 1.39	1.03 ± 0.47	1.03 ± 0.98	0.28 ± 0.19	1.41 ± 0.86

TABLE 3.3: Performance of the EEG-based detection of intention to move.

Patient	Recall (eTP/NT)	Specifity (%)
01	15/17	96.34
02	–	–
03	11/12	95.35
04	4/6	96.16
05	4/5	85.81

NP would begin to actuate, relying entirely on the tremor parameters derived from the gyroscopes—instantaneous amplitude (the estimated tremor is shown in plot G) and frequency (plot H)—to modulate its control action. Notice that the gyroscope algorithm was initialized to the tremor frequency provided by the sEMG.

Table 3.2 summarizes the performance of the mHMI for all the patients and trials. No movement anticipation is given for Patient 02, since he did not exhibit visible ERD, and was thus not suited for using the EEG to trigger the system. Therefore, in this case the mHMI relied entirely on the sEMG to detect the onset of voluntary movement and tremor, without the prediction derived from the EEG classifier. Overall, the results indicate that the mHMI was capable of consistently anticipating the intention to move (in those patients that exhibited ERD), and that the onset of tremor in the presence of concomitant voluntary movement was rapidly detected (the average delay for all patients was 1.11 ± 1.39 s for voluntary movement detection, and 0.76 ± 0.45 s for tremor detection), and hence the NP would start assisting with short delay. Moreover, the delay in the detection of both voluntary movement and tremor was considerably increased in the patient without EEG-based movement anticipation (average delay 1.83 ± 1.77 s and 1.79 ± 0.91 s for the voluntary activity and the tremor respectively) when compared to the other patients (average delay in all trials 0.88 ± 0.45 s and 0.77 ± 0.45 s for the voluntary activity and the tremor respectively). Accurate tracking of tremor amplitude (average RMSE 0.18 ± 0.17 rad/s) and frequency (average RMSE 2.32 ±

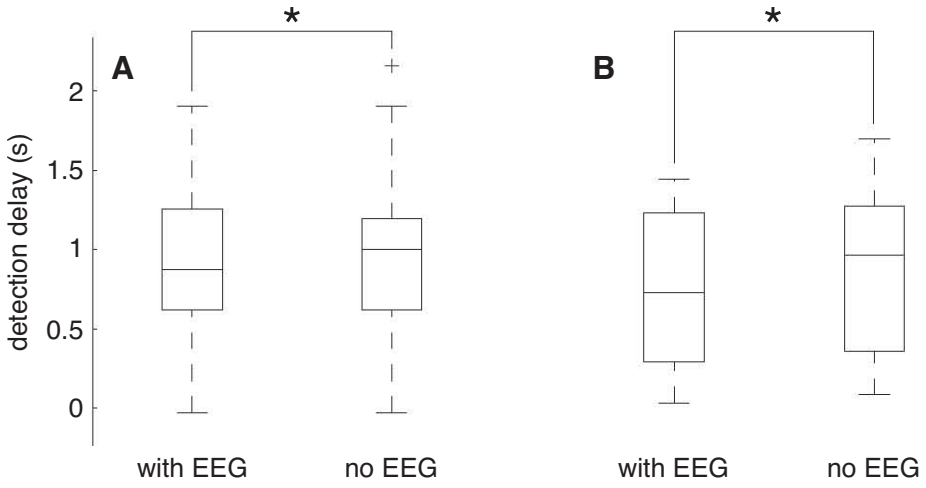

FIGURE 3.4: Boxplot that summarizes the delay in the detection of voluntary movement (A) and tremor (B) from the sEMG, with and without the information provided by the algorithm to detect movement intention from the EEG. The results correspond to all the patients and trials, and show the median as the central mark in the box, the 25^{th} and 75^{th} percentiles as the edges of the box, 1.5 times the interquartile range of the 25^{th} and 75^{th} percentiles as the length of the whiskers, and samples considered outliers as $+$. Asterisks denote the existence of statistical differences ($P < 0.05$, details are given in the text).

2.64 Hz) was achieved, and importantly for the controller, with almost zero phase (the average delay of the tremor estimation with respect to the offline reference was $3{\cdot}10^{-4} \pm 6{\cdot}10^{-4}$ s, calculated from the maximization of the cross-correlation function).

Regarding movement anticipation, as expected, notable inter and intra-subject differences were observed (see Table 3.2). However, the EEG classifier provided, for all of them, a good performance in terms of movement anticipated (Recall), and robustness to false activations (Specificity, see Table 3.3).

I also evaluated what was the outcome of increasing the overlapping of the windows that the sEMG algorithm used (from the 50 % to the 75 %) when movement intention was detected with EEG. Fig. 3.4 compares the average delay in the detection of voluntary movement and tremor onset with and without that feature. In both cases the improvement was statistically significant (Wilcoxon signed rank test, $P < 0.05$), which highlights the benefit that was extracted from using the prediction of movement onset derived from the EEG to drive the system.

The other major interaction between modalities in the mHMI was that between sEMG and gyroscopes. Table 3.4 shows the average RMSE in tremor estimation from sEMG; this is the value that the gyroscope algorithm used for initialization ($f_{\text{EMG},0}$). These results demonstrate that an accurate estimation of tremor frequency was derived with short delay after its onset (see Table 3.2). The benefit derived from directly initializing the gyroscope algorithm to the estimation of tremor frequency derived from sEMG was,

TABLE 3.4: Estimation of tremor frequency from the sEMG.

Patient	RMSE (Hz)
01	1.29 ± 1.26
02	0.54 ± 0.75
03	0.92 ± 1.15
04	2.81 ± 0.72
05	0.86 ± 0.48

TABLE 3.5: Tracking of tremor frequency with and without the input from the sEMG algorithm.

Patient	RMSE tremor freq. (Hz)—no sEMG	RMSE tremor freq. (Hz)—sEMG init.
01	6.50 ± 1.99	1.20 ± 1.10
02	4.36 ± 2.96	1.36 ± 1.77
03	1.85 ± 0.93	2.92 ± 3.44
04	3.79 ± 3.07	3.22 ± 2.45
05	4.20 ± 2.10	1.41 ± 0.86

as expected (see Section §2.6), clearly noticeable when comparing tremor frequency tracking (see Table 3.5), and also statistically significant (Wilcoxon signed ranked test, $P < 0.05$). Amplitude tracking, on the contrary, was not improved. It must be noticed that the patient that showed the worst performance (Patient 04) had a very mild tremor, and thus it was harder for the system to characterize its features. Also for this patient, the difference between initializing the gyroscope algorithm at the frequency indicated by the sEMG and not was smaller.

3.5 Discussion

The results presented in this chapter constitute a proof of concept of a novel approach to a mHMI that predicts the user's intention to move, and detects and parameterizes the concomitant tremor in order to drive a NP for tremor management through transcutaneous neurostimulation. This is achieved based on the integration of EEG, sEMG and gyroscope recordings.

The mHMI constitutes, mainly thanks to the movement anticipation provided by the EEG analysis, a natural interface that requires no learning from the user, because it triggers the NP based on the same mental process that he/she performs to execute a voluntary movement. This has also the additional benefit of encouraging user involvement (Gomez-Rodriguez et al., 2011). Apart from this, the integration of EEG within

the mHMI shortens the reaction time of the system (see Fig. 3.4), which has obvious implications during tremor compensation (see design requirements in Epigraph §1.3.1). There are, nevertheless, two scenarios in which the mHMI needs to overcome the absence of this information. The first of them is those patients that present not classifiable ERD, where the sEMG algorithm can assume its role at the expense of introducing a larger overall delay (as for Patient 02, see Table 3.2). This result implies that those patients that present, for example, a certain neurological condition that impedes the identification of such patterns, can also employ the NP to manage their tremor. The second scenario obviously is a misdetection of the EEG classifier, in which case the same sEMG mechanism is used. This scenario is the motivation for always running the sEMG classifier in parallel. However, it must be noticed that the number of false negatives of the EEG classifier is remarkably low (see Table 3.3). It is also worth mentioning that the overlapping of the sEMG windows could be increased more, which would yield a faster detection of both voluntary muscle activity and tremor.

As to the population who might benefit from the mHMI implementing the EEG, no general inclusion criteria can be defined a priori based on either the literature and/or the experimental results. Although one expects elderly people to exhibit altered spatiotemporal patterns of ERD when compared to their young counterparts (Derambure et al., 1993), the spatial distribution of ERD found in the patients enrolled was highly heterogeneous, and did not permit extracting any general conclusion; neither did any particular condition of Patient 02, who showed no classifiable ERD. Nevertheless, abnormalities in synchronization and desynchronization of the motor rhythms have been found both for PD (Defebvre et al., 1998) and ET (Tamás et al., 2006), which could hinder the implementation of accurate and reliable EEG classifiers for these patients. As a matter of fact, the performance of the classifier integrated within the mHMI with healthy subjects is in general better than for tremor patients (see Ibáñez et al., 2010 for comparison). This may originate from the fact that most tremors originate at deep brain nuclei, which oscillations are projected to a certain extent to the cerebral cortices, e.g., through the thalamocortical loop (Elble, 2000), and hence influence the EEG recordings. Notice however, that the false positives of the EEG classifier have no influence on the performance of the NP, given that it is triggered by the detection of volitional movement in the presence of tremor as detected by sEMG. Regarding the differences among patients and tasks, it was observed that the anticipation time during bimanual tasks (the finger-to-finger test, and outstretching the arms) was on average larger than in those movements that involve a single limb. Further research on this specific topic needs to be carried out.

Both the sEMG and gyroscope analysis performed better when the tremor was more severe. This result constitutes a positive finding, since these patients are the first potential user group of the NP. Frequency estimation from gyroscopes degrades the most, given that it is based on a gradient-descend like method (Widrow and Stearns, 1985). This

also occurred when the tremor appeared and reappeared, which happened in some patients during the FN test, probably due to the change of a postural to a kinetic condition (Deuschl et al., 1998).

As mentioned above, this mHMI constitutes an optimal cHMI to drive a tremor management WR or NP. Moreover, I think that this approach can be beneficial in other types of interventions, e.g., for stroke therapy (Gomez-Rodriguez et al., 2011), in order to maximize user involvement and provide the most natural interface to restore the neural pathways. Other technologies can be used to record the CNS, the PNS and limb biomechanics in order to construct similar architectures. This will be also required to take systems such as the current mHMI to the point of need (e.g., houses, work, see Section §1.3). Current advances on wearable EEG systems based on dry electrodes (Liao et al., 2012) and on ambulatory EMG amplifiers, together with the new implantable interfaces for decoding both brain activity at different scales (for a review see Lebedev and Nicolelis, 2006) and multichannel EMG (Farina et al., 2008) constitute a promising advance towards that goal.

3.6 Conclusions

The development of NPs and WRs for the management of movement disorders needs natural and reliable cHMIs to both extract user's intention and parameterize the involuntary movements that need to be compensated for. Although, in Chapter §2 I presented a method for the accurate estimation of tremor amplitude and frequency in the presence of voluntary movement with gyroscopes, the sole use of kinematic (or combined with recordings from the PNS) data does not capture user's intention, and thus it is not optimal for functional contexts. In this regard, this chapter presented the design and proof of concept of a mHMI that detects the intention to move in order to provide a fast compensatory action once the user initiates a voluntary movement and tremor appears.

By monitoring the whole neuromusculoskeletal system through EEG, sEMG and gyroscope information, the mHMI attains a natural and reliable interface with the NP. In this sense, this mHMI constitutes the first interface of its type, and may be replicated for other movement disorders. In addition, the use of multiple sensor modalities that work in a hierarchical fashion allows for the immediate implementation of redundant mechanisms to compensate for misdetections or false negatives, which increases the reliability of the system. This aspect is of paramount importance from the user's perspective, and will permit the future implementation of NPs and WRs as devices for functional compensation of movement disorders during daily living.

In summary, this chapter presented the first mHMI that characterizes the planning, transmission and execution of volitional movements in tremor patients, at the same time that provides with a precise parameterization of the tremulous movement (Gallego et al.,

2012). Experimental validation with a group of representative patients demonstrates the interest of the approach, and sets the basis for its integration in future systems, once the neural interfaces are improved in terms of usability.

Chapter 4

Tremor Attenuation through the Modulation of Muscle Co-contraction[1]

This chapter presents a novel approach for neuroprosthetic management of tremor. It relies on the alteration of the inherent low pass filter properties of muscles in order to attenuate the tremor, without affecting the voluntary movement. This was performed by modulating the level of co-contraction of a pair of antagonist muscles, resembling the motor control strategy naturally employed for limb stabilization during unstable tasks. The departure hypothesis was that provided that muscle stiffness and viscosity are monotonic functions of activation, a controller that increased the level of co-contraction according to the tremor amplitude should be an effective solution to compensate for it. Therefore, I implemented at the pHMI the proposed control strategy together with the gyroscope cHMI for tremor characterization. Experimental validation in a group of representative patients showed that tremor amplitude was significantly and systematically reduced independently from its etiology, severity and frequency. Neither tremor frequency nor amplitude were found to be significant factors that affected the performance of the NP. Furthermore, no shift in the frequency of the tremor was observed, as expected from its pathophysiological characteristics. The results obtained encourage the posterior evaluation of the current approach as a potential solution for tremor management during daily living.

[1]This Chapter is partly based on: J.A. Gallego, E. Rocon, J.M. Belda-Lois, J.L. Pons. A neuroprosthesis for tremor management through the control of muscle co-contraction. Journal of Neuroengineering and Rehabilitation, 10: 36, 2013.

4.1 Introduction

The properties of the musculoskeletal system play a crucial role on human motor control (see, e.g., Hogan, 1984; Burdet et al., 2001). For example, concurrent modulation of muscle impedance, understood as the resistance to an imposed motion (Burdet et al., 2001), and joint torque is crucial for the performance of many tasks, such as postural stabilization, object manipulation, locomotion and balance (Hogan, 1984; Milner and Cloutier, 1993; Burdet et al., 2001; Tee et al., 2010).

The determination of the mechanical impedance of a muscle is not a straightforward problem, given that muscle activation depends on many factors, such as its histological properties, its elongation and elongation rate, the level of fatigue, *et cetera* (Hill, 1938). However, it has been shown that individual motor units[2] exhibit a low pass filter response (Milner-Brown et al., 1973), and so do the muscles they subserve (e.g., Jacks et al., 1988; Prochazka et al., 1992; Pledgie et al., 2000). Furthermore, since the cut off frequency of both is ∼2–3 Hz, it is not unexpected that most ADLs are performed at a slower pace (Mann et al., 1989).

It has been mentioned through this dissertation that tremors occur at a higher frequency (3–12 Hz, see Epigraph §1.2.1) than that employed to perform most functional movements (0–2 Hz). This separation in the frequency domain lets us propose a controller for the NP that filters out those movements outside the volitional motion band, i.e. the tremor. Since muscles inherently behave as low pass filter, I hypothesized that by decreasing its cut off frequency, tremor could be attenuated without affecting concomitant voluntary movement to a great extent. This can be attained by increasing muscle contraction level, because muscle stiffness and viscosity show a positive correlation with it (Hunter and Kearney, 1982; Hogan, 1984). However, the establishment of a precise theoretical relationship for this is extremely complex, according to the reasons mentioned above.

In epigraph §1.3.2 I defined, based on the expected functionality of the NP and user needs, a series of design requirements for the pHMI. Briefly, these were: R_p1) the NP needs to actuate at the DoFs in which tremor is cause of functional disability, R_p2) tremor has to be attenuated without hampering concomitant voluntary movement, and R_p3) it needs to minimize the impact of the major drawbacks of neurostimulation. As to requirement R_p1, it was met by being able of selectively controlling both wrist and elbow flexion-extension (see Epigraph §1.3.2 for details). Furthermore, given that muscle force and impedance can be modulated independently (Hogan, 1984; Tee et al., 2010), this strategy should not hamper voluntary movement, thus fulfilling design requirement R_p2. The controller proposed in this chapter will modulate continuously the co-contraction

[2] A motor unit is the smallest functional element the CNS can control, and comprises an α motor neuron and all the fibers it innervates. All the motor units that constitute a muscle are designated as a motor unit pool.

level in order to adapt it to tremor parameters, thus attaining an effective suppression (see Section §4.2 for details). This implies that the co-contraction level will be kept to the minimum that provides successful tremor attenuation, thus reducing the amount of current injected at the antagonist pair, delaying the onset of fatigue and accommodation to neurostimulation as much as the current design permits (see Epigraph §1.3.2 for extensive details on this). This contributes to meeting requirement R_p3, and could also help minimizing the impact of the pHMI on volitional activity (requirement R_p2).

Therefore, this chapter presents a new approach for tremor management that consists in the NP-driven modulation of muscle co-contraction as a means to manipulate joint impedance. I show how adequate control of the current injected to a pair of antagonists permits the NP to achieve systematic tremor attenuation irrespectively from its etiology and characteristics, hence setting the basis for the evaluation of this approach as a novel therapy tremor. Notably, this approach resembles to a certain extent those implemented in many devices and orthoses for tremor suppression, because it relies on the modification of muscle, and thus joint, impedance (see the review in Epigraph §1.2.4). However, in this case forces are applied directly to the skeletal system based on artificially elicited muscle co-contraction, and not by external devices whose effect is less direct. In addition, neurostimulation permits circumventing—at least, partly—the motor pathways of tremor patients, which exhibit abnormal, and undescribed behaviors. According to the proposed controller (see Section §4.2), this strategy should guarantee *a priori* that the pHMI meets the 3 requirements defined in Epigraph §1.3.2.

The organization of this chapter is as follows. First, in Section §4.2 I present the rationale and concept for tremor attenuation through NP-driven muscle co-contraction. Next, in Section §4.3, the experimental protocol, patients and methods for the evaluation of the approach are reviewed. Section §4.4 summarizes the experimental results, whereas Section §4.5 discusses the most relevant findings, compares the results obtained with current treatments for tremor, and gives an overview of future studies. The chapter ends, in Section §4.6, with conclusions highlighting the relevance of the results achieved.

4.2 Tremor Suppression Strategy

The frequency response of individual human motor units resembles that of a linear second order system with almost critically dampened response, and cut off frequency ∼2–3 Hz (Milner-Brown et al., 1973). As expected from muscle physiology, the same response has been identified for various upper limb muscles by applying intramuscular or transcutaneous neurostimulation (Aaron and Stein, 1976; Jacks et al., 1988; Prochazka et al., 1992). Therefore, it was hypothesized that effective tremor attenuation could be achieved by further reducing the pass band of muscles, exploiting the fact that tremor has higher frequency than voluntary movement (see Epigraph §2.2.3).

Theoretically, the natural cut off frequency of muscles may be decreased by augmenting muscle viscosity—alone, or concurrently with stiffness—. This could be simply implemented by increasing its contraction level, because muscle viscosity and stiffness are monotonic functions of activation (Hunter and Kearney, 1982; Genadry et al., 1988). According to this, a joint could be stabilized, i.e., the tremor reduced, by co-contracting a pair of antagonists. Indeed, as I already mentioned, muscle co-contraction is exploited by the intact central nervous system to stabilize the limbs during specific tasks (Milner and Cloutier, 1993; Burdet et al., 2001; Hogan, 1984).

A simplified explanation of this approach is given next. Eq. (4.1) represents a human joint with the NP attached to it. There, the joint was modeled as a second order linear time invariant system (as done in many works in the literature, e.g. Milner-Brown et al., 1973; Pledgie et al., 2000; Belda-Lois et al., 2007b), while the NP was represented as a variable stiffness and viscosity, according to what was explained before. Given that the NP behaves as a system acting in parallel to the limb, the resultant response could be modeled as (Belda-Lois et al., 2007b; Pledgie et al., 2000):

$$\frac{\theta(s)}{T(s)} = \frac{G}{Is^2 + (D + D_{\mathrm{NP}})s + (K + K_{\mathrm{NP}})} \tag{4.1}$$

where $\theta(s)$ is the tremulous component of movement (estimated as described in Chapter §2), $T(s)$ represents the torque that generates the tremor, I, D, and K stand for the inertia, viscosity and stiffness of the joint, and G is the magnitude of the response of the resultant system (that is function of the mechanical parameters of the same). The viscosity and stiffness added by the NP as a result of increased muscle contraction are denoted by D_{NP} and K_{NP}, and satisfy $D_{\mathrm{NP}}, K_{\mathrm{NP}} \geq 0$, being $D_{\mathrm{NP}}, K_{\mathrm{NP}} = 0$ if the NP were not activated.

Given that the analytical expression that relates the changes in D_{NP} and K_{NP} caused by the NP to the cut off frequency of the resultant system (represented in Eq. (4.1)) is very complex, in Fig. 4.1 it is shown how a concurrent increase D_{NP} and K_{NP} would affect the frequency response of the joint. There, it is displayed how the cut off frequency would be decreased in a nonlinear manner when the contraction level, and thus the resultant stiffness, $K + K_{\mathrm{NP}}$, and viscosity, $D + D_{\mathrm{NP}}$, of the joint (Hunter and Kearney, 1982), were increased. The change in the magnitude of the response observed in Fig. 4.1 illustrates how co-contraction stabilizes the limb, as reported in the literature (Burdet et al., 2001; Hogan, 1984).

On the basis of this, I designed a controller that regulated the level of artificially elicited co-contraction, adapting it to the characteristics—instantaneous amplitude and frequency—of the tremor. As foreseen in the concept design, an independent controller was implemented for each joint, because the characteristics of tremor differs among them, and show a nonstationary behavior that is normally uncoupled (see Epigraph

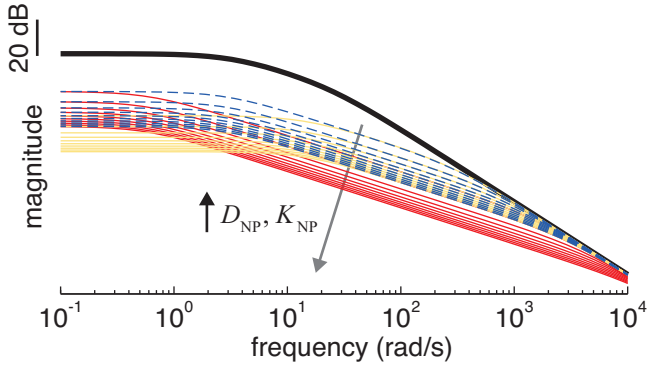

FIGURE 4.1: Bode diagram that illustrates the rationale for tremor attenuation through muscle co-contraction. The plot shows the frequency response of a human joint, showing how it is modified by the co-contraction of an antagonist muscle pair. The data for the human joint without the NP (black trace) corresponds to the model given in Eq. (4.1) fitted to the parameters identified for the wrist in (Belda-Lois et al., 2012). The remainder traces represent how the response of the joint is modified by a concurrent increase in viscosity and stiffness (defined as a multiple of the parameters D and K), and correspond to: i) equal increments of D_{NP} and K_{NP} (in multiples of 10, from 10 to 100, shown as blue traces), ii) larger increments of D_{NP} (in multiples of 50, from 50 to 500) than of K_{NP} (in multiples of 10, from 10 to 100, shown as red traces), and iii) larger increments of K_{NP} (in multiples of 50, from 50 to 500) than of DNP (in multiples of 10, from 10 to 100, shown as yellow traces). For all the cases, larger values of D_{NP} and K_{NP} cause the response of the joint to have smaller magnitude (as indicated by the arrow in gray).

§1.3.2). Furthermore, by continuously modulating the current injected at the pHMI, I aimed at decreasing the impact of the control strategy on voluntary movement, at the same time that the effect of muscle fatigue and accommodation to neurostimulation was minimized.

Neurostimulation was controlled as follows. Tremor frequency defined when the control output was to be updated, while tremor amplitude modulated the amount of current to be injected at each muscle. Both were derived from the raw gyroscope recordings employing the cHMI algorithm presented in Chapter §2. Tremor parameters estimated during a (tremor) period were employed to generate the control action in the subsequent one, analogously to repetitive control theory (Hara et al., 1988). This provided the controller with a certain predictive nature. Neurostimulation was modulated independently for each muscle in the antagonist pair because: *i*) they typically have different electrophysiological response to neurostimulation, and *ii*) this response varies with time in a heterogeneous manner. Neurostimulation was amplitude modulated; current frequency and pulse width were kept constant (see Epigraph §1.3.2 for further information). Details on the control algorithm are given next.

4.2.1 Controller

The controller that regulated neurostimulation amplitude was a rule-based proportional-integral law (see Eq. (4.2)), in which the integral gain was switched between two values depending on the amplitude of the residual tremor (see Eq. (4.3)). By switching the value of $K_i(tr_{k,k-1})$ to 0, the controller neglected the integral term when the amplitude of the tremor was small, i.e. below the threshold $th_{int\ gain}$, which avoided possible unnecessary periods of stimulation when the tremor was very mild and did not pose a functional problem. Furthermore, the integral was reset when tremor amplitude decreased below a certain threshold, $th_{int\ reset}$. This avoided adding the residual tremor to the integrator when tremor amplitude was very small, which prevented brisk transients if the tremor developed again. The inclusion of an integral term was very important to compensate for the time-varying response to neurostimulation that characterizes this type of applications, which manifests overall in terms of muscle fatigue and accommodation to neurostimulation (Alon and Smith, 2005). The controller was defined as:

$$u_k = K_p tr_{k,k-1} + K_i(tr_{k,k-1}) \sum_{j=1}^{k} tr_j \Delta t \tag{4.2}$$

$$K_i(tr_{k,k-1}) = \begin{cases} K_i & \text{if } tr_{k,k-1} \geq th_{int\ gain} \\ 0 & \text{if } tr_{k,k-1} < th_{int\ gain} \end{cases} \tag{4.3}$$

where K_p and $K_i(tr_{k,k-1})$, are the controller gains (the value of the latter depends on tremor amplitude, as defined in Eq. (4.3)), $tr_{k,k-1}$ the estimation of tremor derived from Eq. (2.24), and $u(k)$ the control action. Importantly, a saturation was applied to $u(k)$ in order to limit the electrical charge injected to the muscle. This value was defined for each muscle during a calibration phase.

The NP was triggered when the onset of tremor and its initial frequency were detected from the solid state gyroscopes. Tremor onset was directly obtained by comparing the estimated tremor amplitude $tr_{k,k-1}$ to a threshold tr_{th}. A gross estimation of tremor frequency was computed as the maximum of the amplitude spectrum in the 3–12 Hz band (Deuschl et al., 1998). This estimation was used to initialize the WFLC (see Section §3.4 for a discussion on the relevance of this). In order to double-check tremor detection, the following criterion that relied on the spectral characteristics of the total movement was used: if the ratio of tremor to voluntary movement (TVR, see Eq. (4.4)) was larger than a certain value defined manually (TVR_{th}), I considered that the spectrum reflected the presence of tremor. In case this condition was not fulfilled, the next window of equal length was employed for the calculation; 50 % overlapping was allowed. The TVR was defined as:

$$TVR = \frac{\sum_{f=3}^{f=12} X_f}{\sum_{f=0}^{f=3} X_f} \tag{4.4}$$

where $\sum_{f=0}^{f=3} X_f$ and $\sum_{f=3}^{f=12} X_f$ represent the integral of the amplitude spectrum in the 0-3 Hz and 3-12 Hz bands. Similar ratios have been employed in other works about tremor, e.g. for EMG analysis (Hurtado et al., 2000; Hellwig et al., 2003).

4.3 Methods

4.3.1 Patients

Twelve patients (2 female) suffering from parkinsonian ($n = 3$) or essential tremor ($n = 9$) participated in the study. Mean age was 54.1 $\pm$ 17.5 years (ranging from 22 to 70). Tremor amplitude, according to neurological rating, ranged from very mild to severe (from 2 to 30 according to Fahn-Tolosa-Marin score[3], Fahn et al., 1998). Medication intake was not interrupted for the recordings. All patients signed a written informed consent to participate. The protocol was in accordance with the Declaration of Helsinki, and received the approval from the Ethical Committee at Universidad Politécnica de Valencia.

4.3.2 Experimental Protocol

Each patient performed a number of repetitions of two types of trials (referred to them as CO and NO); the duration of each was 30–35 s. The first type of trial consisted of two sub-periods, during the second of which the NP was activated (CO trial). In the second type of trial (NO) the NP was never activated. This type of trial was included in the protocol to avoid a possible distortion of the study due to, for example, a natural reduction of tremor amplitude over time. The order of CO and NO trials was randomized, and the experimental design was balanced with an optimal design algorithm (Fedorov, 1972). In total, each patient performed between 6 and 12 repetitions. Some patients were asked to count mentally backwards during the experiments to exacerbate their tremor (Hellwig et al., 2001; Raethjen et al., 2008), and the 3 with PD counted out loud at the beginning of the session as recommended in (Raethjen et al., 2008).

During each trial, patients were asked to perform the clinical task that made their tremor most evident. As in the previous protocols, typical exercises for neurological examination were considered: resting the arm on the lap (RE), keeping both arms outstretched (AO),

[3]Notice that the score was computed considering among items 1–10 those 3 related to the rest, postural and action tremor at the most affected limb. Therefore this rating ranged from 0 to 64.

FIGURE 4.2: A patient equipped with the NP during the performance of a tremor suppression experiment. The photograph shows the textile supports in which the gyroscopes were placed and, underneath them, the electrodes for transcutaneous neurostimulation.

and the finger to finger (FF) and finger to nose test (FN) (Deuschl et al., 1998). Each patient performed one or two exercises during the whole protocol.

4.3.3 Recordings

Patients wore the NP at the most affected side and were sitting in a comfortable armchair during the whole session. The NP took the shape of a textile substrate that integrated the neurostimulation electrodes and the gyroscopes that drove the system, as defined in the concept design (see Section §1.3 for details). Fig. 4.2 shows a patient wearing the final prototype, which had modular design (it was not a continuous garment as represented in the original concept, but a series of straps) in order to maximize its adaptability to user's anatomy.

Both wrist flexion-extension and elbow flexion-extension were recorded with two pairs of solid state gyroscopes (Technaid S.L., Madrid, Spain) implemented in the NP (see Epigraph §2.2.1), although results are only presented for the wrist, because it was where the tremor was visible for all patients. At the wrist, neurostimulation was delivered at the flexor carpi radialis and extensor carpi ulnaris with a multichannel monopolar neurostimulator that injected charge compensated pulses (UNA Systems, Belgrade, Serbia); the common electrode was located at either the dorsal or volar side of the wrist. Maximum neurostimulation amplitude for each muscle was personalized during an initial calibration phase; pulse width and frequency were set to either 300 μs and 40 pps or 250 μs and 30 pps respectively, depending on the patient: the first combination of values was used for patients that needed high current density to elicit visible muscle contraction. The controller was implemented in a stand alone computer (QNX Software

Systems, Ontario, Canada). Notice that only trials with visible tremor were considered in the analysis.

4.3.4 Data Processing and Analysis

To quantify the effect of NP-driven co-contraction on tremor amplitude, I computed the ratio R_{att} of the integral of the power spectral density of the tremor during the part of the trial with co-contraction, to the same variable without it (thus for the CO trials) (Rocon et al., 2007a). Before, data were split into 1 s non-overlapping windows to minimize the effects of eventual non stationarities, and zero padded; R_{att} was calculated with the median values for both conditions. I computed R_{att} also for the trials during which NP-driven co-contraction was not delivered (NO trials) as the basis to investigate whether the strategy proposed had a real effect on the tremor. To this end, equivalent periods were considered for its calculation.

I assessed whether NP-driven co-contraction had a real effect on tremor amplitude by comparing R_{att} in the pooled CO and NO trials. This way it was ensured that a change in R_{att} did not arise from a natural decay in tremor amplitude, but for the effect of the NP. To this end, both datasets were log-transformed to ensure normality (Lilliefors test, $P < 0.05$ to reject), and compared with a one-way analysis of variance (ANOVA). Trials with no visible tremor were excluded from the analysis. I also evaluated whether there was an effect on tremor frequency with a one-way ANOVA, given that the datasets conformed normality after log-transformation (Lilliefors test, $P < 0.05$ to reject). Trials with no visible tremor were excluded from the analysis. Throughout the chapter, values are reported as mean ± SD.

The parameters for the controller were set to the following values. For the two-stage algorithm to track tremor parameters (see Chapter §2): i) for the $g - h$ filter, $\theta = 0.900$, ii) for the Kalman filter, $\sigma_\tau^2 = 0.01$, $\mathbf{Q} = \text{diag}(1, 1, 0)$, and iii) for the WFLC, $\mu_0 = 0.001$, $\mu_1 = 0.01$, $\mu_b = 0.01$, $M = 1$, f_0 was initialized to the value computed from the amplitude spectrum at tremor onset (data epoch of 2 s with zero padding). These parameters were defined from previous datasets, after resampling the data to the frequency of the controller, and fine-tuned during experiments on control subjects mimicking tremor. Controller gains were selected manually based on the amplitude of the tremor that was observed during calibration and the required neurostimulation amplitude. During this phase, I also defined the maximum current amplitude (saturation level) the controller could deliver at each muscle. Thresholds for the detection of tremor onset, frequency estimation, integral reset, and integral gain switch were $tr_{th} = 0.1$ rad/s, $TVR_{th} = 3$, $th_{int\ reset} = 0.1$ rad/s, and $th_{int\ gain} = 0.1$ rad/s respectively.

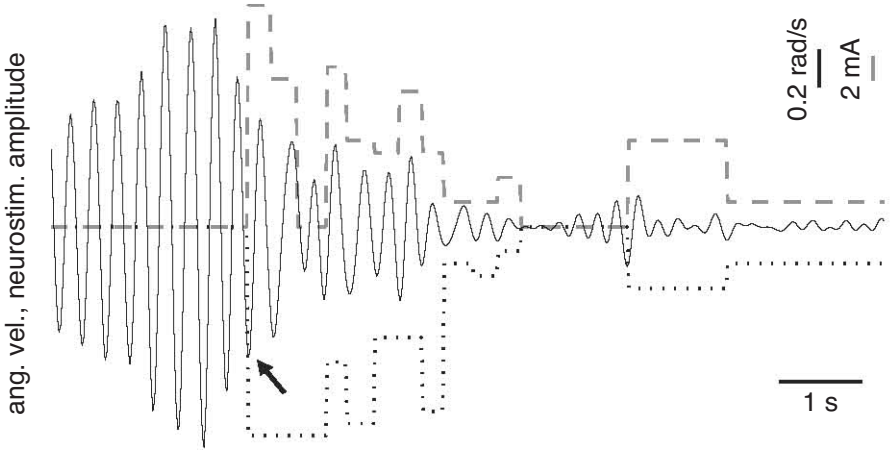

FIGURE 4.3: Example of the controller that modulates muscle co-contraction to attenuate tremor. The plot shows the estimation of tremor (solid line) and the amplitude of the current applied at the extensors (dashed line) and flexors (dotted line). The instant at which the NP was triggered is signaled with an arrow. Notice the different scales employed for the representation of neurostimulation amplitude and angular velocity. A positive value corresponds to wrist extension.

4.4 Results

Fig. 4.3 shows a typical example of the performance of the control strategy, representing the current amplitude delivered at each muscle together with the ongoing tremor (estimated with the two-stage algorithm, see Chapter §2). It was observed that ∼2.5 s after the system was triggered, the amplitude of the tremor was drastically reduced, and the control action diminished and became 0. In the case of this patient, low current kept the limb stabilized, i.e. prevented the tremor from reappearing with the severity typically observed in this patient. The contribution of the integral term is appreciated at time ∼0.5 s after neurostimulation onset at the flexors, because the controller maintained the maximum (saturation) current amplitude to compensate for the still severe tremor.

Remarkably, the NP achieved systematic reduction of tremor amplitude through muscle co-contraction, irrespectively from the characteristics it exhibited—etiology, severity and frequency. Table 4.1 summarizes the results per patient; large SDs in tremor amplitude corresponded to those with very fluctuating symptoms (e.g. patients 01, 05 and 07, who had a coefficient of variation (CV) of tremor amplitude close or greater than 100 %). This highlights the need of accounting for inter-trial tremor variations in the experimental protocol, as done by assessing the effect of co-contraction by comparing the evolution of tremor amplitude in trials without (NO) and with neurostimulation (CO). Fig. 4.4 shows representative examples of tremor attenuation for six different patients; results are depicted in the time and frequency domains (see Table 4.1 for details about the patients). In some cases very large attenuation was achieved (examples B and E), while in others reduction of tremor amplitude was milder (example C).

TABLE 4.1: Effect of NP-driven modulation of muscle co-contraction on tremor amplitude. The table compares, for all patients and CO trials performed by each of them, the mean ± SD of tremor amplitude in the ensemble of periods without (NP Off) and with (NP On) co-contraction. Amplitude was calculated as the integral of the power spectral density. Tremor frequency was computed as the mean position of the peak in the power spectral density in the absence of NP-driven co-contraction.

Patient	Etiology	Gen.	Task	Frequency (Hz)	Amplitude NP Off (rad^2s^{-3})	Amplitude NP On (rad^2s^{-3})
01	ET	M	PO	4.24	111.60 ± 185.03	34.06 ± 26.59
02	PD	M	PO, RE	3.51	65.42 ± 41.31	35.80 ± 55.27
03	ET	M	PO, FN	5.11	15.68 ± 8.01	10.51 ± 4.10
04	PD	M	RE	4.81	0.80 ± 0.52	0.51 ± 0.23
05	ET	F	PO, RE	4.50	24.34 ± 42.86	2.37 ± 2.74
06	ET	M	PO	8.08	0.62 ± 0.09	0.21 ± 0.06
07	ET	F	PO	6.25	3.05 ± 2.76	1.08 ± 0.74
08	ET	M	PO	8.38	0.22 ± 0.05	0.17 ± 0.15
09	ET	M	PO	8.37	0.11 ± 0.08	0.01 ± 0.01
10	ET	M	FN	5.60	0.19 ± 0.08	0.12 ± 0.03
11	PD	M	PO	5.46	0.15	0.13
12	ET	M	PO	9.27	0.03 ± 0.01	0.02 ± 0.01

By grouping all the trials with NP-driven tremor suppression (CO trials), I found that tremor amplitude was notably reduced (R_{att} = 52.33 ± 25.48 %) in 89.4 % of them (42 out of 47). This effect was found to be statistically significant (one-way ANOVA, $P < 0.001$, see Fig. 4.5 for a representation of both datasets). In addition, the experimental design of the study, in which the ratio R_{att} between the two periods that constitute a CO or NO trial were compared (see Epigraph §4.3.4 for details), guarantees that this attenuation was not a natural effect of the tremor *per se*, but caused by the NP.

Investigation of a possible relationship between tremor attenuation and the original amplitude of the tremor suggested that more severe tremors were attenuated to a greater extent (see Fig. 4.6). For example, tremor attenuation for severe tremors (defined, e.g., as those in which the integral of the power spectral density was > 50 rad^2s^{-3}) was R_{att} = 22.8 ± 21.3 % (compared to an overall attenuation of R_{att} = 48.1 ± 26.3 %). However, the difference did not turn out to be statistically significant ($P = 0.083$, Mann-Whitney test after raking the pooled CO trials according to tremor severity).

The NP exacerbated the tremor ($R_{att} > 100$ %) in 5 trials performed by 4 different patients (see Fig. 4.6 and 4.7). Interestingly, 3 of them corresponded to those during which 2 different patients (patients 04 and 05, who had PD and ET respectively) showed a much milder tremor than in the rest of the trials. This suggests that given that controller gains were chosen manually based on the tremor amplitude observed during calibration, the controller may have applied a current intensity (i.e. degree of co-contraction) that was not large enough to elicit a sufficient alteration of the frequency response of the

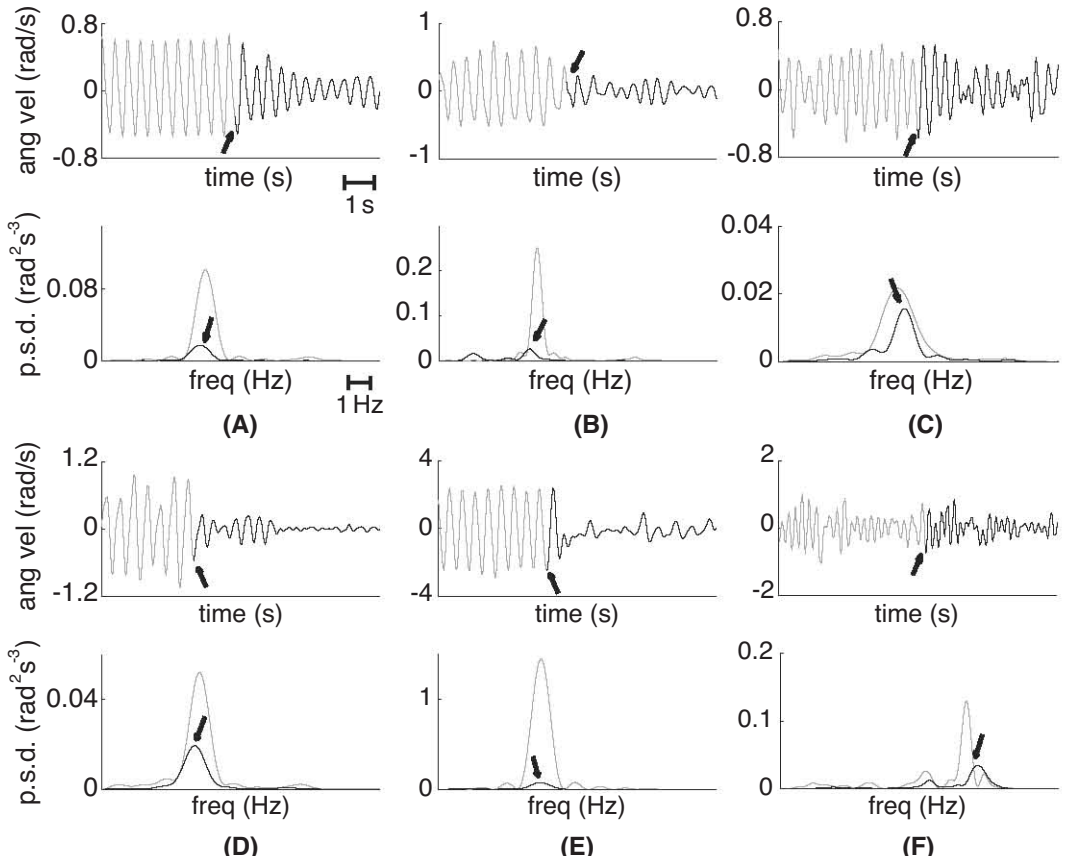

FIGURE 4.4: Examples of reduction of tremor amplitude through NP-driven co-contraction, for six representative patients. Each subplot (A to F) in this graphic shows a typical trial for patients 01 to 06 respectively, and compares the amplitude of the tremor before (gray) and after (black) the NP was activated. Top plots represent the data in the time domain, whereas bottom plots represent the same data in the frequency domain (mean power spectral density for the neurostimulation and non-neurostimulation periods). In the time domain, the moment at which the NP was triggered is signaled with an arrow; in the frequency domain, the arrow points at the tremor peak while the NP was activated. In the bottom panel of (F), the arrow points at a spectral peak that likely corresponds to the mechanical reflex.

forearm. In the case of the trial with tremor exacerbation for patient 08, the opposite occurred: in all the other the trials recorded in this patient tremor amplitude was smaller, which suggests that the maximum stimulation amplitude may have been underestimated during calibration. As a matter of fact, during a large part of this trial the NP was applying a co-contraction level (i.e. injecting a current with amplitude) close or equal to the maximum defined for each muscle. The remainder trial with tremor exacerbation was the last performed by a subject (patient 02) who showed an otherwise excellent response (R_{att} excluding this trial was 26.79 ± 13.13 %, see Fig. 4.6 and 4.7 for details on the trials). I hypothesize that exacerbation occurred due to the well known effects of accommodation to neurostimulation (Alon and Smith, 2005) that appear in interventions of this type. This observation was supported by the next two facts: *i*) this was the last trial of the session and, as mentioned above, the patient showed a very

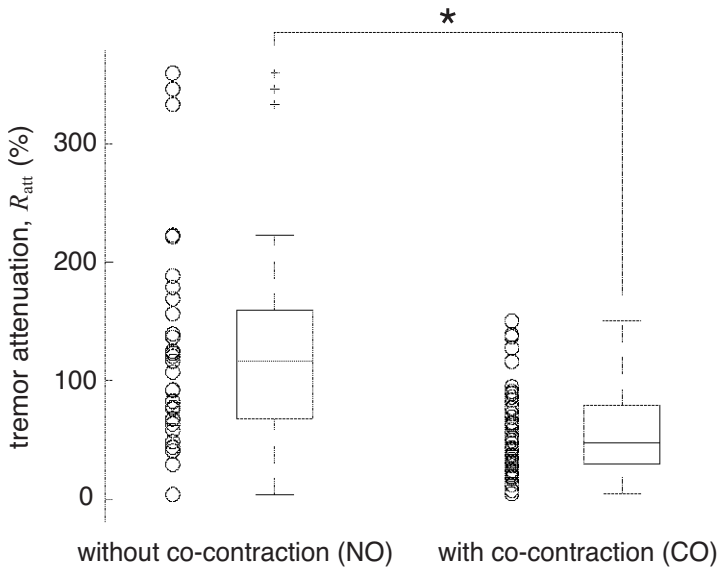

FIGURE 4.5: Comparison of the variation of tremor amplitude within a trial, as measured by R_{att}, in the pooled datasets of trials without co-contraction (NO) and with co-contraction (CO). Each circle (∘) represents a single trial in either condition. The box plots show the median as the central mark, and the first and third quartiles as the upper and lower edge of the box; whiskers extend to 1.5 times the interquartile range, and values outside this range are plotted individually (+). The asterisk denotes that both samples are statistically different ($P < 0.001$, see the text for details).

significant tremor reduction in the other trials (see Fig. 4.7), and *ii*) the controller applied the maximum current amplitude and did not alleviate the tremor, on the contrary to previous repetitions. Furthermore, the patient self-reported that he felt that current intensity "had decreased" at the end of the session, i.e. for this trial. Notice that, as shown in Fig. 4.7, trial order did not seem to influence the performance of the NP.

Observation of the power spectral densities in Fig. 4.4 suggests that tremor attenuation through NP-driven co-contraction did not shift significantly the frequency of the same. Fig. 4.8 compares tremor frequency without and with co-contraction for each patient, showing no visible differences. A pooled analysis comparing the two datasets supported this observation (Mann-Whitney test, $P = 0.801$). Interestingly, Fig. 4.8 shows how one of the patients exhibited a large variation in tremor frequency (patient 10, who had a CV of tremor frequency of 59.57 %, while for patient 04 it was 15.80 %, and for the rest of them always < 10 %), which appeared due to the very different characteristics of the tremor he exhibited in movement and posture—he was performing a FN test and was asked to maintain the fingertip pointing at his nose for a few seconds. This happened both without and with co-contraction, which further supports the finding that NP-driven muscle co-contraction does not modify the tremor frequency.

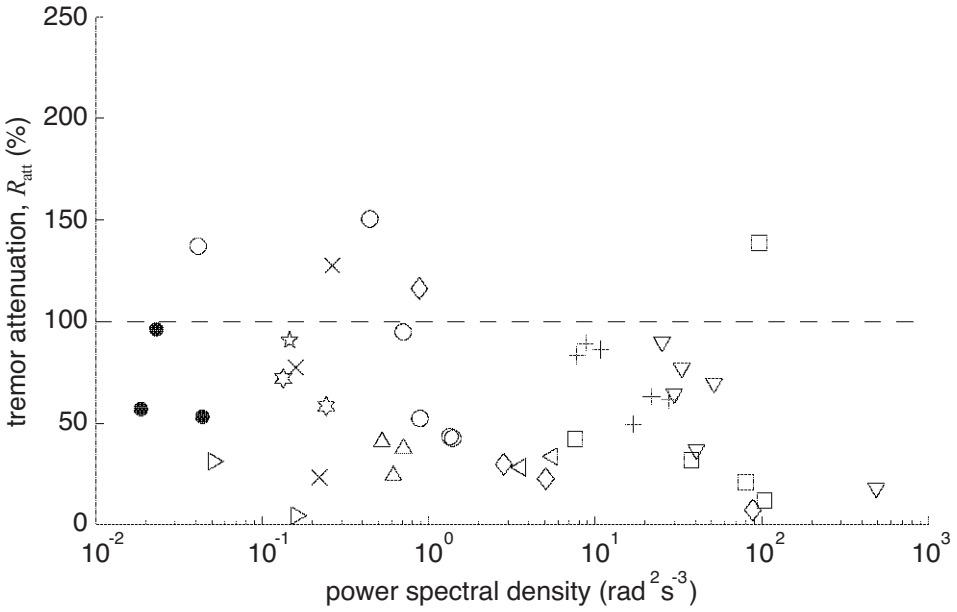

FIGURE 4.6: Tremor attenuation through NP-driven muscle co-contraction (in terms of R_{att}) as function of the initial severity of the tremor (defined by the median of the power spectral density in the period without neurostimulation). The plot shows all patients and CO trials, each marker being a single trial. The geometrical locus of null tremor attenuation is also displayed (dashed line). The plot is interpreted as the further below this locus, the larger tremor reduction is. Patients are coded as follows: ▽ corresponds to patient 01, □ to patient 02, + to patient 03, ○ to patient 04, ◇ to patient 05, △ to patient 06, ◁ to patient 07, × to patient 08, ▷ to patient 09, ✡ to patient 10, ☆ to patient 11, and • to patient 12.

4.5 Discussion

This chapter presented the development and validation of a controller for tremor attenuation through NP-driven muscle co-contraction. The results here described demonstrate the feasibility of the approach, and prove that manipulation of the intrinsic low pass filter properties of muscles effectively reduces tremor amplitude (Gallego et al., 2013). Interestingly, all the patients reported that the sensation elicited by the neurostimulation strategy was not unpleasant, and the overall impression was that they could habituate to it. Furthermore, a few patients spontaneously declared that when the NP was activated they could control better their limb. In addition, user's perception of the prototype was generally good, and remarkably better than for previous robotic devices (Rocon et al., 2007a).

The NP attained a systematic reduction of tremor amplitude in patients suffering from both PD and ET, in spite of their inherent differences in underlying pathophysiologic mechanisms (see, e.g., (Elble, 2009)) and symptomatology. My initial concern was that joint rigidity arising from PD (Bergman and Deuschl, 2002) could hinder NP-driven tremor reduction for these patients, given that their joints already show increased stiffness and viscosity (Park et al., 2011). The physiological reason for this would be a

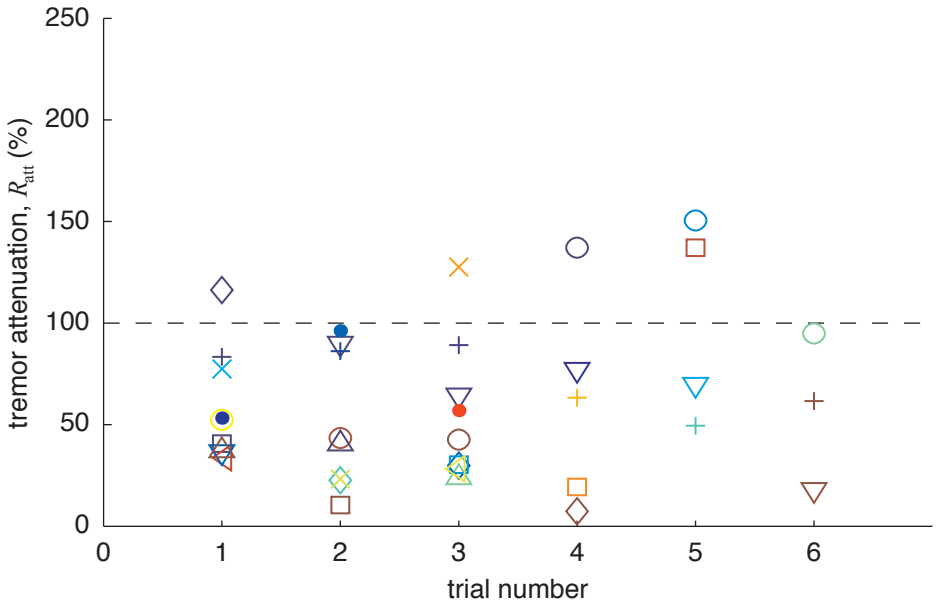

FIGURE 4.7: Tremor attenuation as function of trial number. The plot shows how tremor attenuation computed with R_{att} varies as more trials are performed, for all the patients with three or more trials exhibiting tremor. Each marker represents a single trial, and the color of the marker corresponds to the severity of the tremor during this trial (before the NP was activated). The color scale is adjusted to the amplitude of each patient's tremor, and represents trials with mild tremor as cold colors, and with severe tremor as hot colors. Patients are codified as follows: $\triangledown$ corresponds to patient 01, $\square$ to patient 02, $+$ to patient 03, $\circ$ to patient 04, $\diamondsuit$ to patient 05, $\triangle$ to patient 06, $\triangleleft$ to patient 07, $\times$ to patient 08, and $\bullet$ to patient 12.

displacement of the natural cut off frequency of their muscles towards lower values (for healthy individuals it is ∼2–3 Hz, Milner-Brown et al., 1973; Prochazka et al., 1992; Aaron and Stein, 1976), which could in turn impede attaining the level of co-contraction necessary to attenuate the tremor. However, the results deemed this hypothesis untrue, even in a patient with severe parkinsonian tremor of low frequency (patient 02, who had a tremor frequency of ∼3.5 Hz and experienced a tremor reduction with the NP of $R_{att} = 26.79 \pm 13.13\%$). I believe that the effects of levodopa intake might have facilitated this by decreasing limb rigidity (PD patients did not interrupt their medication for the experiments). The fact that the NP successfully alleviated low frequency tremors is of great interest, as the frequency of both ET and PD experience a decline with time (Hellwig et al., 2009), and thus broadens the group of potential users of the system.

Tremor frequency was not a factor that influenced the performance of the NP (Pearson's correlation between tremor frequency and R_{att} was 0.022, $P = 0.946$). Large tremor attenuation ($R_{att} < 50$ %) was obtained for patients with low (patients 01 and 05, which mean tremor frequencies were < 5 Hz), medium (patient 07, mean tremor frequency $=$ 6.25 Hz) and high frequency (patients 06 and 09, tremor frequency ∼8 Hz) tremors. It must be noticed that there exists a certain dependence between tremor amplitude and frequency, and therefore a comparison entirely based on these variables is not possible.

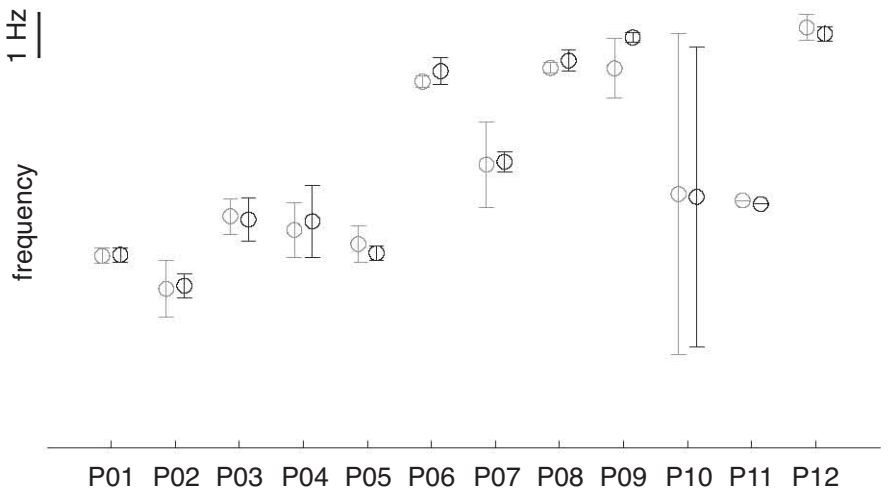

FIGURE 4.8: Effect of tremor attenuation through NP-driven muscle co-contraction on tremor frequency. The plot compares tremor frequency in the part of the CO trials without (gray) and with (black) the NP activated. Results are shown as mean (∘) ± SD (whiskers) of the mean frequency for the pooled trials.

Such dependence arises from two facts: *i*) the frequency of PD tremor is typically below 6 Hz (Deuschl et al., 1998), and *ii*) the severity of the tremor in ET is inversely correlated with its frequency (the slope between the log displacement and the log amplitude is ~ -4, Elble et al., 1992). Interestingly, there was a trend for tremor amplitude to decay naturally within a trial in those with tremor frequency greater than 8 Hz (patients 06, 08, 09 and 12), opposite to patients with low or medium frequency tremors, in which variations in tremor amplitude were largely unpredictable. Notice that this finding did not influence the evaluation of the strategy, because the protocol foresaw intra-trial variations. The result that tremor frequency did not influence tremor attenuation with the proposed approach is relevant because it was not clear *a priori* whether NP-driven co-contraction would attenuate low frequency tremors, due to the fact that they manifest close to the natural cut off frequency of muscles, and thus would need a larger alteration of their physiologic response. Given that average attenuation for patient 02 (tremor frequency ∼3.5 Hz) was $R_{att} = 26.79 \pm 13.13\%$, and for patient 01 (tremor frequency ∼4.2 Hz) it was $R_{att} = 58.99 \pm 26.81\%$, I conclude that low frequency tremors can be successfully managed through NP-driven co-contraction. In addition, these results suggest that tremor frequency is not a criterion that restricts the applicability of the system.

As shown in Fig. 4.8, the NP did not alter tremor frequency in spite of the obvious proprioceptive feedback, and the more than plausible activation of afferent pathways. This was motivated by the central origin of PD (Bergman and Deuschl, 2002) and ET (Elble, 2009), which predominates over the other mechanisms that contribute to their genesis,

mainly short and long latency reflexes and mechanical oscillations (see Section §1.2.3). Therefore, the results presented here are in line with the traditional view that sensory feedback plays a limited role in the generation, maintenance and modulation of tremor in PD (Bergman and Deuschl, 2002; notice however that the findings presented in Chapter §5 show that spinal afferents contribute notably to the amplitude of the tremor in PD). ET patients however, exhibit a more evident interaction between the stretch reflex and the tremor itself (see, e.g., Elble et al., 1987, or the review in Epigraph §1.2.3), being the most noticeable example the separation of both components, otherwise entrained, under inertial loading (Héroux et al., 2009, see Fig. 1.3). In this line, visual inspection of Fig. 4.4F suggests that the central and reflex tremor components were separated in patient 06 (as indicated in the power spectral density with a grey arrow), both when the NP was activated and not. A more profound investigation of this phenomenon is needed, and would require the integration of EMG recordings and advanced signal processing techniques—to remove the artifacts generated by the NP in the EMG signal—in a novel protocol.

Furthermore, given that the controller implements a proportional integral algorithm, these results suggest that an increase in tremor amplitude was compensated by an increase in the level of muscle co-contraction. As a consequence, I hypothesize that both ET and PD are reduced when muscle activation is large enough, i.e. when the stiffness and viscosity of the joint are adequately increased. By comparing this with previous works that assessed the influence of voluntary muscle contraction on the amplitude of tremor (reviewed in Epigraph §1.2.4), these results are in line with what has been reported for PD (Dietz et al., 1974), but contradict a recent study that showed how high contraction intensities caused larger amplitude fluctuations in ET (Héroux et al., 2010). Remarkably, these studies assessed the effect of volitional muscle activation on tremor, while ours dealt with NP-driven activation, and thus motor control mechanisms are involved in a lesser extent. Therefore, I believe that the pathophysiologic landmarks of PD and ET may account for this difference. Although the cerebellothalamic pathways play a role in the generation of parkinsonian symptoms (Liu et al., 1999), no evidence of cerebellar involvement apart from a compensative hyperactivation (Yu et al., 2007)—increased as the disease progresses (Sen et al., 2010)—, has been found. In ET, on the contrary, all three cerebellar areas are impaired to a certain extent (Deuschl and Elble, 2009). Thus I believe that cerebellar disfunction could explain the exacerbation of essential tremor during voluntary contractions.

When compared with current treatments for ET, the reduction of tremor provided by NP-driven muscle co-contraction ($R_{att} = 48.1 \pm 26.3$ %) was similar to that of drugs with proved efficacy (tremor attenuation ∼50 %, Deuschl et al., 2011), but worse than the results attained with DBS (tremor attenuation ∼50–80 %, Collins et al., 2010). Nevertheless, the latter implies a surgical procedure, while the NP is conceived as a mock up system that the user may wear underneath his clothes. Furthermore, when

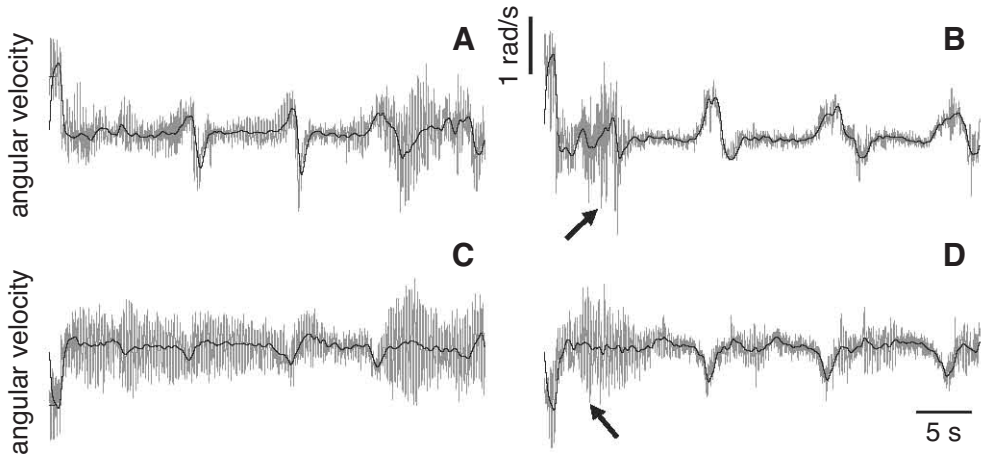

FIGURE 4.9: Example of NP-driven modulation of muscle a co-contraction during a functional task. The task consists in a simulation of eating soup with a spoon (soup was simulated with polymer pellets, and a regular soup plate and spoon were employed). The trial compares two realizations of the task without (left plots) and with NP-driven co-contraction (right plots), performed by patient 02. All plots show the raw movement (gray) and the estimation of voluntary movement derived from the cHMI. Plots correspond to: wrist flexion-extension (A) and elbow flexion-extension (C) without NP-driven co-contraction, and wrist flexion-extension (B) and elbow flexion-extension (D) during NP-driven muscle co-contraction. The arrows point at the instants at which the pHMI was triggered for each DoF. Considerable improvement in terms of tremor attenuation and smoothness of voluntary movement was observed.

compared to pharmacotherapy, the NP reduced tremor amplitude in all 9 ET patients in the current sample, while drugs are effective in ∼50 % of patients (Elble and Tremor Research Group, 2006). No conclusive results can be drawn given the size of the group of patients, although this finding is encouraging. The 3 patients with PD continued their intake of levodopa during the experiments and experienced a reduction of their tremor ($R_{att} = 47.96 \pm 28.38$ %). This suggests that for these patients the NP is an interesting approach to complement pharmacotherapy.

In a few trials, it was observed that the tremor migrated towards proximal joints when it was suppressed at the more distal ones; i.e. when it was suppressed at the wrist it appeared or increased at the elbow or at the shoulder. This occurred in patients with both PD and ET, and has been previously reported in two studies dealing with inertial or force loading in tremor. The first was a study on coordination during postural holding in PD, where the authors reported that mass loading of the index finger enhanced the tremor at the proximal segments while posture was maintained (Hwang et al., 2009). The second focused on the attenuation of ET with a WR that applied a constant viscosity to the affected joints (Rocon et al., 2007a). None of them found a plausible physiological explanation for tremor migration. Therefore, further research on this topic is needed, given that it constitutes a major aspect when developing NPs or WRs for functional compensation of tremor during daily living. Future studies will need to address both the coordination mechanisms *per se*, and the influence that inertial

loads and muscle activation have on them. In this regard, a preliminary experiment to assess the functional benefit that may be drawn when using the NP to perform ADLs has been conducted. The protocol consisted in asking the patient to perform (or simulate) activities that were normally perceived as difficult. Fig. 4.9 shows an example of tremor management while eating soup with a spoon. The data corresponds to patient 02, and illustrates how an important functional benefit was experienced by applying NP-driven co-contraction (compare plots (B) and (D) to plots (A) and (C)). Furthermore, it highlights how voluntary movement is not hampered when concomitantly suppressing tremor. However, as mentioned, these results are still preliminary, and future studies will be designed to evaluate the performance of patients with different types of tremor when performing ADLs wearing the NP.

Finally, the limitations of this study need to be acknowledged. First, although the results demonstrated that NP-driven muscle co-contraction constitutes a feasible alternative for tremor management, I believe they may be improved by developing an automatic method to select the gains of the controller. This would require the identification of a model of muscle response to stimulation. Indeed, as it was mentioned in Section §4.4, most trials (4 out of 5) in which tremor amplitude was exacerbated during NP-driven co-contraction would be immediately avoided by adequately selecting controller gains. Second, for extended use of NP-driven muscle co-contraction as a therapy for tremor, it will be necessary to adapt the parameters of the controller when the muscle exhibits accommodation to the ongoing level of neurostimulation (as it happened in the remainder trial with tremor exacerbation). Manual tuning of the parameters by a practitioner, together with adaptive control techniques may provide a solution for this.

4.6 Conclusions

Tremor is a major cause of functional disability and dependence, and given its high prevalence, constitutes a significant problem for today's society. This motivates that notable efforts are being devoted to the development of novel therapies for tremor. In this regard, in this chapter I have presented the concept and validation of a strategy to alleviate upper limb tremor through the modulation of muscle co-contraction with the NP developed within the thesis (Gallego et al., 2013). The approach to pHMI here described consists in the continuous adaptation of the current injected to a pair of antagonists to the instantaneous tremor parameters. Tremor could be parameterized with either of the methods presented in Chapters §2 or §3, although the former was employed for the sake of usability (see comments in previous chapters).

Tremor was attenuated irrespectively from its etiology (mean reduction $R_{att} = 48.1 \pm 26.3$ %, $p < 0.001$), and, for the current sample, its amplitude and frequency did not have an effect on the performance of the NP. However, there could be a subtle trend towards

larger attenuation of more severe tremors, although it was not statistically significant. Remarkably, no patient found the sensation induced by NP-driven muscle co-contraction unbearable, and a number of them spontaneously reported that felt an improvement in their condition. All patients exhibited a positive—yet variable—response to the approach here presented, which is of great interest for ET patients, given that only 50 % of them benefit from the drugs that are currently prescribed to manage their disorder. Therefore, I conclude that the design requirements (Epigraph §1.3.2) were successfully met.

The results here presented also have a neurological implication. In spite of the complex interaction between central oscillations, spinal and supraspinal reflexes, and the mechanical properties of the tremulous limb, an increase in the contraction level of a pair of antagonist muscles is capable of significantly reducing tremor amplitude for both ET and PD. This is mediated by a concurrent increase of the stiffness and viscosity of the muscles, which have a monotonic relationship with the activation level. Furthermore, this observation contradicts to a certain extent what has been reported for ET during voluntary contractions, although additional studies to unveil the underlying mechanisms are needed. A plausible hypothesis would be that the abnormal cerebellar motor control mechanisms are at least partly circumvented when using externally driven neurostimulation.

In summary, the results presented in this chapter demonstrate that irrespectively from its etiology, severity, and frequency, tremor is significantly attenuated by NP-driven muscle co-contraction. Furthermore, the positive outcome of these experiments encourages the large scale validation of the approach, either alone, or as a complement to pharmacotherapy.

Chapter 5

Neural Drive to Muscle and Common Synaptic Inputs to the Motor Neuron Pool in Tremor[1]

Tremor is ultimately generated by the projection of pathological oscillations originating at different parts of the CNS to the MN pool. However, it is still unknown how such projection occurs, what is its contribution to the neural drive to muscle, and how different pathways interact in the manifestation of tremor. It was hypothesized that pathological oscillations in ET and PD are a common cortical projection to the MN pool, which causes the abnormal MN firing patterns, and ultimately, the tremor. To test for this hypothesis I recorded the sEMG in 13 patients, concurrently with the EEG activity at the sensorimotor cortex. The sEMG was decomposed into constituent MN spike trains, which were employed to estimate corticomuscular coherence and to investigate the common inputs to the MN pool. The results showed that a few MNs (1.2 ± 0.6) were enough to transmit the tremor-related cortical activity to the output of the MNs. Further, the analysis of corticomuscular coherence indicated that the central oscillations that cause ET and PD constitute a common cortical projection to the MN pool, which occurs through a direct pathway, probably corticospinal. Estimates of coherence between groups of MNs suggested that the MN pool receives two strong common inputs, one that corresponds to the voluntary drive (< 2–3 Hz), and another related to the tremor. The latter was correlated ($r = 0.662$) to the abnormally large MN synchronization observed (common input strength index = 2.28 ± 2.71 pps). Given that the strength of common input at the tremor frequency was much greater than the amount of corticomuscular coupling observed, these results provide first proof that tremor in ET and PD is caused by a common cortical projection to the MN pool, which is selectively enhanced by spinal afferents.

[1]This Chapter is partly based on: J.A. Gallego, J.L. Dideriksen, A. Holobar, J. Ibáñez, J.L. Pons, E.D. Louis, E. Rocon, D. Farina. Neural drive to muscle and common synaptic inputs to the motor neuron pool in essential tremor. *To be submitted.*

5.1 Introduction

As explained in Epigraph §1.2.3, it is widely accepted that tremor appears due to the combination of central oscillations, reflex loops with different arc length, and the intrinsic mechanical properties of the limbs (McAuley and Marsden, 2000; Deuschl et al., 2001). However, how these mechanisms interact to generate the abnormal MN pool entrainment, and ultimately the tremulous movement, is yet elusive.

The analysis of MN behaviour provides a more precise characterization of the neural drive to muscle, i.e. of the number of action potentials discharged by the MN innervating a muscle, than traditional approaches based on the sEMG (e.g., Negro et al., 2009; Farina et al., 2010) and, therefore, may help in the elucidation of the mechanisms of tremor. However, to date, few studies have investigated the firing pattern of individual MNs in tremor, and all of these were constrained by the technological limitations involved in recording the discharge pattern of a sufficiently large number of motor units during the same trial (Merletti and Farina, 2009). Therefore, although these studies provided information about MN behavior in tremor patients, they lacked a complete characterization of the neural drive to the muscle, which normally requires a larger number of MNs (e.g., Negro et al., 2009; Negro and Farina, 2011b). A consistent finding of the existing works is the occurrence of paired (sometimes tripled) MN discharges with an inter-spike interval (ISI) in the range ∼20–80 ms in patients with different types of tremor performing isometric contractions (Das Gupta, 1963; Dietz et al., 1974; Elek et al., 1991; Christakos et al., 2009). Furthermore, it has been observed that small motor units fire a larger proportion of paired discharges when compared to large motor units (Dietz et al., 1974), and their ISI appears to be inversely correlated to the severity of the tremor (Elek et al., 1991). Given that paired discharges also occur when healthy subjects mimic tremor, they cannot be considered a phenomenon unique to tremor patients (Elek et al., 1991), and should rather be regarded as related to fast oscillatory movements.

It is commonly assumed that larger than normal MN synchronization contributes to the manifestation of tremor in PD and ET (Elek et al., 1991; Dietz et al., 1974; McAuley and Marsden, 2000; Christakos et al., 2009). However, the existing works, always dealing with PD, provide inconsistent conclusions: while a study reports that short-term synchronization is smaller in tremor patients compared to controls (Dengler et al., 1986), in another the authors did not find significant differences between these two groups (Baker et al., 1992); a third work reports abnormally MN synchronization in PD patients (Christakos et al., 2009) Very likely, disagreements occurred because of the different methods employed for data analysis, since it has been recently shown that the analysis technique employed to estimate common input strength influences significantly the results (Negro and Farina, 2012).

It has been shown that the central oscillatory networks that cause PD and ET (see Epigraph §1.2.3) are projected through the descending pathways to the MN pool that innervates a tremulous muscles (see, e.g., Volkmann et al., 1996; Timmermann et al., 2003; Raethjen et al., 2009; Florin et al., 2010; Reck et al., 2010; Muthuraman et al., 2012, and Hellwig et al., 2001, 2003; Hua et al., 1998; Hua and Lenz, 2005; Raethjen et al., 2007; Muthuraman et al., 2012, for studies on PD and ET respectively). Such coupling is derived from the existence of significant coherence at the frequency of the tremor between the cortical (e.g., Volkmann et al., 1996; Hellwig et al., 2001; Timmermann et al., 2003; Raethjen et al., 2007) or thalamic (e.g., Hua et al., 1998; Hua and Lenz, 2005) activity and the sEMG recorded over the contralateral muscles. This implies that the transmission is at least partly linear, due to the nature of the analysis technique itself (Halliday et al., 1995). However, given that in these works the neural drive to muscle was assessed as the overall sEMG, and not through the analysis of MN activities, information about the cause of such linearity, i.e. whether it occurred due to the common projection of the central oscillator that causes the tremor (see Epigraph §1.2.3) to the entire MN pool through corticospinal pathways (Negro and Farina, 2011b), or if it was mediated by other mechanisms, such as direct cortico-motoneuronal connections (Isa et al., 2007; Lemon, 2008), is still missing.

We have recently demonstrated that it is possible to identify the discharge pattern of a number of MNs contributing significantly to the expression of tremor in the sEMG by using a decomposition algorithm (Holobar et al., 2012). The technique, which consists in the application of an extended version of the convolution kernel compensation (CKC) algorithm to high density EMG recordings (Holobar and Zazula, 2007; Holobar et al., 2009), enabled the identification of the discharge pattern of up 21 MNs (average $\sim$ 8 MNs) during the performance of typical tasks employed for the neurological examination of patients with tremor (Holobar et al., 2012). Therefore, it constitutes a very powerful tool to investigate the behavior of the MN pool in tremor patients, with a higher potential than traditional approaches.

Therefore, in this chapter I investigate the characteristics of the MN discharge patterns (i.e. the neural drive to muscle) in patients with tremor arising from ET or PD, and how they relate to the cortical drive to muscle. To this end, I assess how tremor-related cortical oscillations are projected to the MN pool by computing the coherence between EEG signals and the discharges of individual or groups or MNs. Furthermore, I estimate the strength and frequency content of the common synaptic input(s) to the MN pool, and use this information to investigate the relative contribution of supraspinal and spinal pathways. The evidences presented here demonstrate that common input strength (and the accompanying high MN synchronization) is remarkably larger for both ET and PD than in nonpathological conditions, and indicate that tremor is generated by the existence of a common synaptic input to the MN pool. In addition, this chapter

provides, based on the results obtained, novel physiological evidence on the role of concurrent descending and afferent inputs in the manifestation of tremor.

This chapter is organized as follows. First, I describe the analysis techniques employed for the decomposition of sEMG, the estimation of cortical drive to muscle, and of strength of common input, after presenting the experimental protocol and patients enrolled for the study. Next, Section §5.3 summarizes the results obtained, which are discussed from technical and physiological points of view in Section §5.4. The chapter ends with conclusions summarizing the major findings obtained in this study.

5.2 Methods

5.2.1 Patients

This chapter presents results for thirteen patients (7 female) with tremor arising from PD ($n = 4$) or ET ($n = 9$). All patients had a definite diagnosis provided by her/his neurologist, and showed visible and persistent hand tremor (unilateral or bilateral) at rest, during posture or in both conditions. No patient exhibited head or trunk tremor during examination, or had a history of neurological diseases other than that causing the tremor. Mean age was 66.6 ± 7.8 years (ranging from 54 to 80 years). Tremor severity ranged from mild to severe, being the mean score 20.1 ± 10.3 (ranging from 3 to 32) according to the Fahn-Tolosa-Marin scale[2] (Fahn et al., 1998). ET patients were off medication for at least 12 h, while PD patients continued their medications normally. The ethical committees at Universidad Politécnica de Valencia and Hospital Doce de Octubre gave approval to the study, and warranted its accordance with the Declaration of Helsinki. All patients were informed beforehand, and signed a written informed consent to participate.

5.2.2 Experimental Protocol

Recordings were carried out while patients were seated in a comfortable armchair, in a dimly illuminated room. Postural or rest tremor was elicited by asking the patients to keep their hands outstretched, parallel to the ground, while the forearms were fully supported on an armrest, or by asking them to relax with the hands hanging freely, respectively. For each patient, the condition(s) in which tremor was (were) more evident was chosen. Patients were instructed to stay relaxed and keep their gaze fixed on a wall about 2 m distant. Those with PD counted out loud backwards during 3 min before the recordings to enhance their tremor, as recommended in (Raethjen et al., 2008).

[2]Notice that the score was computed considering among items 1–10 those 3 related to the rest, postural and action tremor at the most affected limb. Therefore the rating ranged from 0 to 64. The data for patient EP04 was not available.

Patients with mild tremor severity were asked to mentally count backwards during the experiments to obtain a similar effect (e.g., Hellwig et al., 2001).

Each patient performed a series of 4 min repetitions (between 1 and 3, depending on how she/he tolerated the setup, and the quality of the recordings) of the task(s) that elicited tremor. This ensured that at least one repetition with tremor being present during most of the trial was recorded; for each patient, I present results for the trial during which tremor was more persistent.

5.2.3 Recordings

Hand tremor at the most affected side was concurrently recorded with sEMG and solid-state gyroscopes. Surface EMG was recorded with 13 x 5 electrode grids (LISiN–OT Bioelettronica, Torino, Italy) with an inter-electrode distance of 8 mm. The electrode grids were placed over the extensors of the wrist, centered laterally above the extensor digitorum communis, and longitudinally above the muscle belly; a humidified wrist bracelet served as common reference. The signal was amplified (EMGUSB, OT Bioelettronica, Torino, Italy), band-pass filtered (10–750 Hz), and sampled at 2048 Hz by a 12-bit A/D converter. Hand movement was measured with a pair of solid-state gyroscopes (Technaid S.L., Madrid, Spain) placed at the hand dorsum and the distal third of the forearm, by simply computing their difference (see Epigraph §2.2.1 for details on placement). Their raw signals were low pass filtered (< 20 Hz), and sampled at 50 Hz by a 12-bit A/D converter. At the same time, EEG signals were recorded over 32 positions at the sensorimotor area (AFz, F3, F1, Fz, F2, F4, FC5, FC3, FC1, FCz, FC2, FC4, FC6, C5, C3, C1, Cz, C2, C4, C6, CP5, CP3, CP1, CPz, CP2, CP4, CP6, P3, P1, Pz, P2 and P4) with passive Au electrodes. The reference was set to the common potential of the two earlobes, and Az was used as ground. The signal was amplified (gUSBamp, g.Tec gmbh, Graz, Austria), band-pass (0.1–60 Hz) and notch (50 Hz) filtered, and sampled at 256 Hz by a 16 bit A/D converter. The recording systems were synchronized using a common clock signal generated by the computer acquiring gyroscope data. The data were stored, and analyzed offline. Fig. 5.1A to C show representative EEG, sEMG and gyroscope signals. Notice that the hardware setup corresponds to the mHMI described in Chapter §3.

5.2.4 Surface EMG Decomposition

MN spike trains were identified from the multichannel sEMG with the CKC technique (Holobar and Zazula, 2007; Holobar et al., 2009), and manually verified by an experienced operator. The CKC technique has been validated with the decomposition of MN activities in more than 15 muscles and 500 healthy subjects performing voluntary

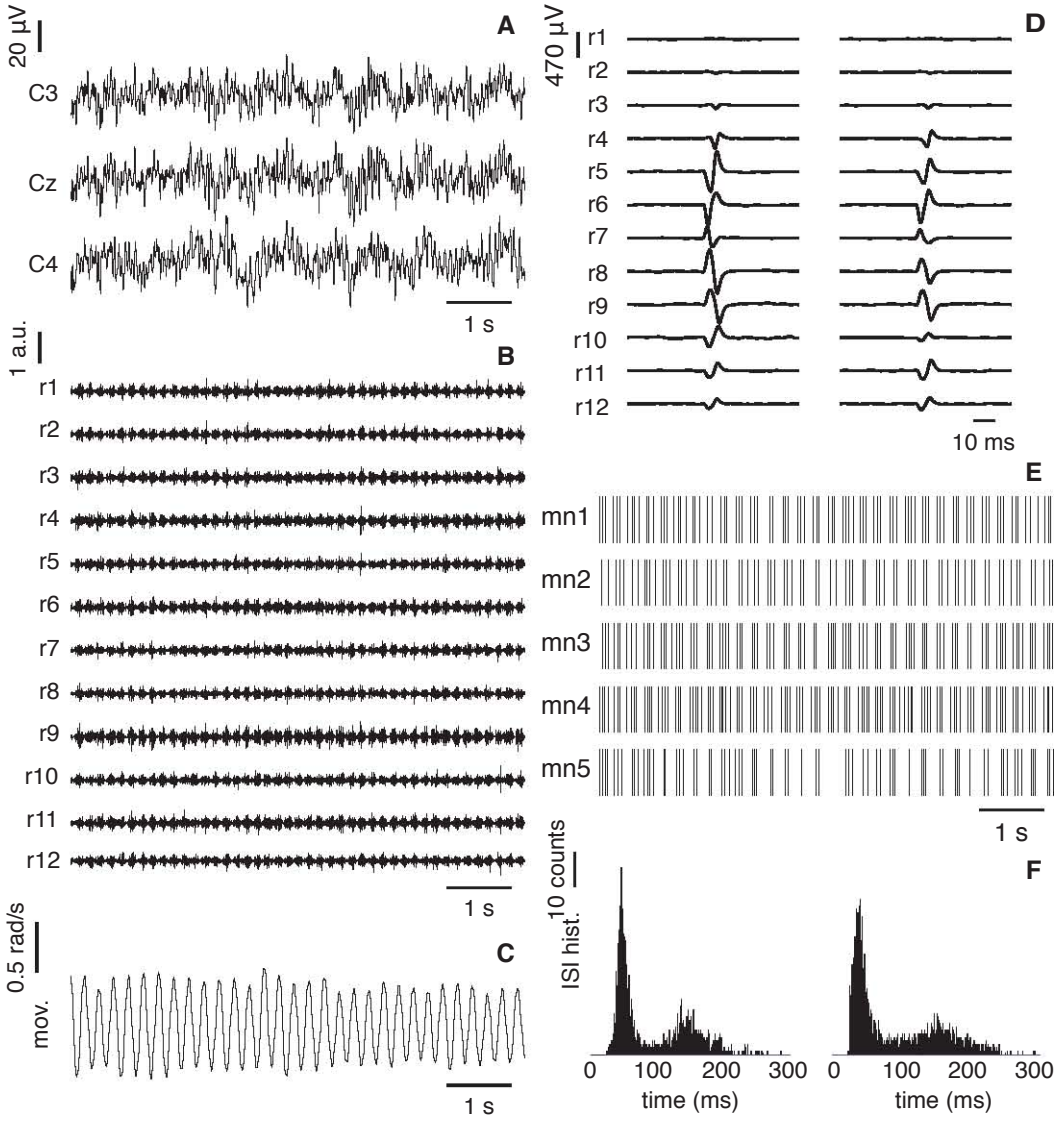

FIGURE 5.1: Example of EEG, sEMG, and gyroscope signals recorded, and of a few MNs identified through the decomposition of the sEMG. The data corresponds to ET patient 03. (A) shows data from 3 EEG channels (C3, Cz and C4), (B) displays signals from all the channels of the fourth column of the sEMG electrode array (rows 1 to 12), and (C) represents wrist tremor as recorded with a pair of gyroscopes. The rest of the plots are related to MN activities: (D) shows the shape of the motor unit action potential of one of the MNs identified, for all the channels of the fourth and fifth columns of the electrode array (rows 1 to 12), (E) displays the spike trains fired by 5 of the MNs identified, and (F) depicts the ISI histogram of two MNs, exhibiting a clear bimodal pattern caused by the occurrence of paired (or tripled) discharges, and the subsequent firings to complete a tremor burst.

contractions (e.g. Holobar et al., 2009, 2010), and has been recently shown to deal effectively with the special firing characteristics of MNs in tremor.

Since the accuracy of the decomposition was fundamental for assessing the properties of the neural drive to muscle in ET and PD patients, for the analysis I defined two inclusion cirteria for the identified single MN spike trains within each trial. First, given

that the calculation of corticomuscular coherence and common input typically require a sufficiently large number of epochs, I excluded those MNs that were not firing during more than the 65 % of the trial. In addition to ensure that only MNs whose spike trains were identified with great accuracy were considered in the analyses, I computed for each of them a modified version of the signal-to-interference metric (SIR) employed in (Holobar et al., 2010, 2012). This metric assessed the quality of the decomposition by comparing the height of the spike trains identified to the baseline jitter of the CKC algorithm and, by applying a threshold to it (26 dB), allowed the exclusion of MNs whose discharge pattern were not identified with high reliability. Fig. 5.1 shows an example of decomposition of the sEMG: Fig. 5.1D displays the shape of one of the motor unit action potentials (identified by spike triggered averaging), Fig. 5.1E shows the spike trains fired by 5 MNs (out of 11), and Fig. 5.1F represents the ISI histogram of 2 of these MNs.

5.2.5 Data Processing and Analysis

This section presents the methodology employed to investigate how the discharge pattern of individual and groups of MNs related to the cortical tremor contribution, and to assess the strength of common input to the MN pool.

EEG channels were spatially filtered using the Hjorth transform (Hjorth, 1975) (16 electrodes: Fz, FC3, FC1, FCz, FC2, FC4, C3, C1, Cz, C2, C4, CP3, CP1, CPz, CP2, and CP4), and artefacts were carefully removed. Manual inspection, in combination with a threshold (defined as the mean $\pm$ 3 SDs of a signal composed by 20 high-quality 1 s epochs chosen from different parts of the trial) served to ensure that the resultant EEG signal did not contain significant artefacts. This is of great importance given that for their inherent frequency content (Jung et al., 2000), artefacts may enhance coherence at the tremor frequency, without significantly influencing higher frequency bands. This implies that corticomuscular coherence at the beta band (13–35 Hz), which is accepted to mediate voluntary contractions in healthy subjects (e.g. Conway et al., 1995; Negro and Farina, 2011b), may be less influenced by the presence of artefacts.

Coherence was computed to investigate the cortical contribution to the neural drive to muscle, defined as the spike trains of individual or groups of MNs. MNs were grouped by adding their spike trains, building so-called composite spike trains (CSTs, Negro and Farina, 2011b, 2012). I calculated the corticomuscular coherence between all the processed EEG channels and all the possible combinations of CSTs comprising between 1 and the total number of MNs identified during the trial. Furthermore, given that coherence is interpreted as a measure of linear dependence (Halliday et al., 1995), I investigated whether the cortical input was common to the entire MN pool by assessing how corticomuscular coherence varied with the number of MNs considered. If the projection were common to all the MNs in the pool, coherence should increase exponentially as more

MNs are included in the CST, at the same time that it should be relatively invariant to which MNs are considered (Negro and Farina, 2011b).

I also investigated whether tremor was a common projection to the MN pool by calculating, for each trial, the coherence between all combinations of pairs of CSTs comprising the maximum possible number of MNs. This has been recently shown to be the most effective means of investigating the frequency content of the common synaptic inputs to MNs, circumventing the influence of the firing rate on traditional approaches (Negro and Farina, 2012).

In both cases the coherence was calculated following the method proposed in (Halliday et al., 1995). First EEG signals, and/or CSTs were divided in 1 s windows, from which the individual power spectra and cross-spectrum (Hann window of 1 s and 0.125 Hz resolution, achieved with zero-padding) were computed. Then, the coherence, $|R_{xy}(\lambda)|^2$, was calculated as the ratio of the magnitude squared cross-spectrum, $|C_{xy}(\lambda)|^2$, to the product of their individual power spectra, $C_{xx}(\lambda)$ and $C_{yy}(\lambda)$ (e.g., Halliday et al., 1995; Hellwig et al., 2001, 2003; Raethjen et al., 2007, 2009):

$$|R_{xy}(\lambda)|^2 = \frac{|C_{xy}(\lambda)|^2}{C_{xx}(\lambda)C_{yy}(\lambda)} \tag{5.1}$$

The confidence limit was obtained as:

$$1 - \left(1 - \frac{\alpha}{100}\right)^{\frac{1}{N-1}} \tag{5.2}$$

where N is the number of epochs employed in the calculations, and α the significance level (in %) (Rosenberg et al., 1989).

A standard metric for the estimation of short-term motor unit synchronization (Nordstrom et al., 1992) was calculated to directly compare the observed strength of common input to what is reported in the literature for healthy subjects. The rationale for this is that it is well established that motor unit synchronization arises from the existence of common synaptic inputs to the motor neuron pool (Sears and Stagg, 1976; Kirkwood and Sears, 1978). To this end, for each trial, I calculated the cross-correlation histogram and its correspondent cumulative sum ($\pm$ 100 ms relative to the reference MN discharge, in 1 ms bins) for all pairs of MN. The position and duration of the synchronous peak in the cross-correlation histogram considered to be significant was calculated from the cumulative sum (Ellaway, 1978), by finding the first relative minima moving backwards from the reference MN discharge, and the first relative maxima moving forward (Diderikssen et al., 2009). A peak in the cumulative sum function was defined as significant if it went over the mean of the baseline of the cross-correlogram more than three SDs of the first 50 bins (Davey et al., 1986). Finally, the strength of common input index (CIS)

was computed for all pairs of MNs exhibiting significant synchronization, as the number of counts within the synchronous peak in excess of that expected by chance, divided by the time during which the MNs were active (Nordstrom et al., 1992). The last 2 min of the trial were considered for these calculations to enable direct comparison with the literature (Dideriksen et al., 2009). We further investigated the relationship between motor unit synchronization as estimated with the CIS and the strength of coherence between pairs of CSTs by computing the CIS for the same data windows (Negro and Farina, 2012).

Throughout the chapter, results are given as mean ± SD. All coherence values were considered significant if $P < 0.05$. Relationships between pairs of variables were investigated either using Pearson's or Spearman's correlation; samples were checked for normality with a Lilliefor's test ($P < 0.05$). To calculate the minimum number of MNs that transmitted most accurately the cortical representation of tremor, I compared the coherence estimates for the pooled data of all the patients with a paired Student's t-test. Pairs of samples comprising n and $n+1$ MNs respectively were compared for increasing values of n until a non-significant difference was found.

5.3 Results

The total number of identified single motor unit spike trains was 79 (6.1 ± 2.1 MNs per trial). When examining their ISI histograms, three types of distributions were observed. Six patients (ET01–04 and PD01–02) exhibited a characteristic bimodal distribution consisting of one peak that corresponded to a paired discharge as described in the literature (with a mean ISI in the ∼20–80 ms range), and another peak that together with the former was related to the frequency of the tremor bursts (see Fig. 5.2A to D and Fig. 5.2J and K). One patient with PD (PD04) had an ISI histogram that followed a trimodal distribution, which corresponded to periods of paired discharges occurring synchronously with the tremor bursts (similarly to what was observed in patients with bimodal ISI histograms), and more tonic-like firing patterns during other parts of the trial (see Fig. 5.2M). The remaining 6 patients (ET05–09 and PD03) had a unimodal ISI histogram, with the peak located at ∼ 68.3 ± 23.6 ms, ranging from 50 to 113 ms (see Fig. 5.2E to I and Fig. 5.2L). The ISI at which this peak was found was not significantly related with tremor frequency ($P = 0.434$, Spearman's correlation). For all the patients, the relative proportion of both types of discharges varied considerably among MNs and patients, as previously reported for PD patients (Dietz et al., 1974).

5.3.1 Corticomuscular Coupling

The average number of 1 s segments not influenced by EEG artifacts, and with stable discharge of the identified MNs, was 93.5 ± 42.3, ranging from 36 to 182. These were

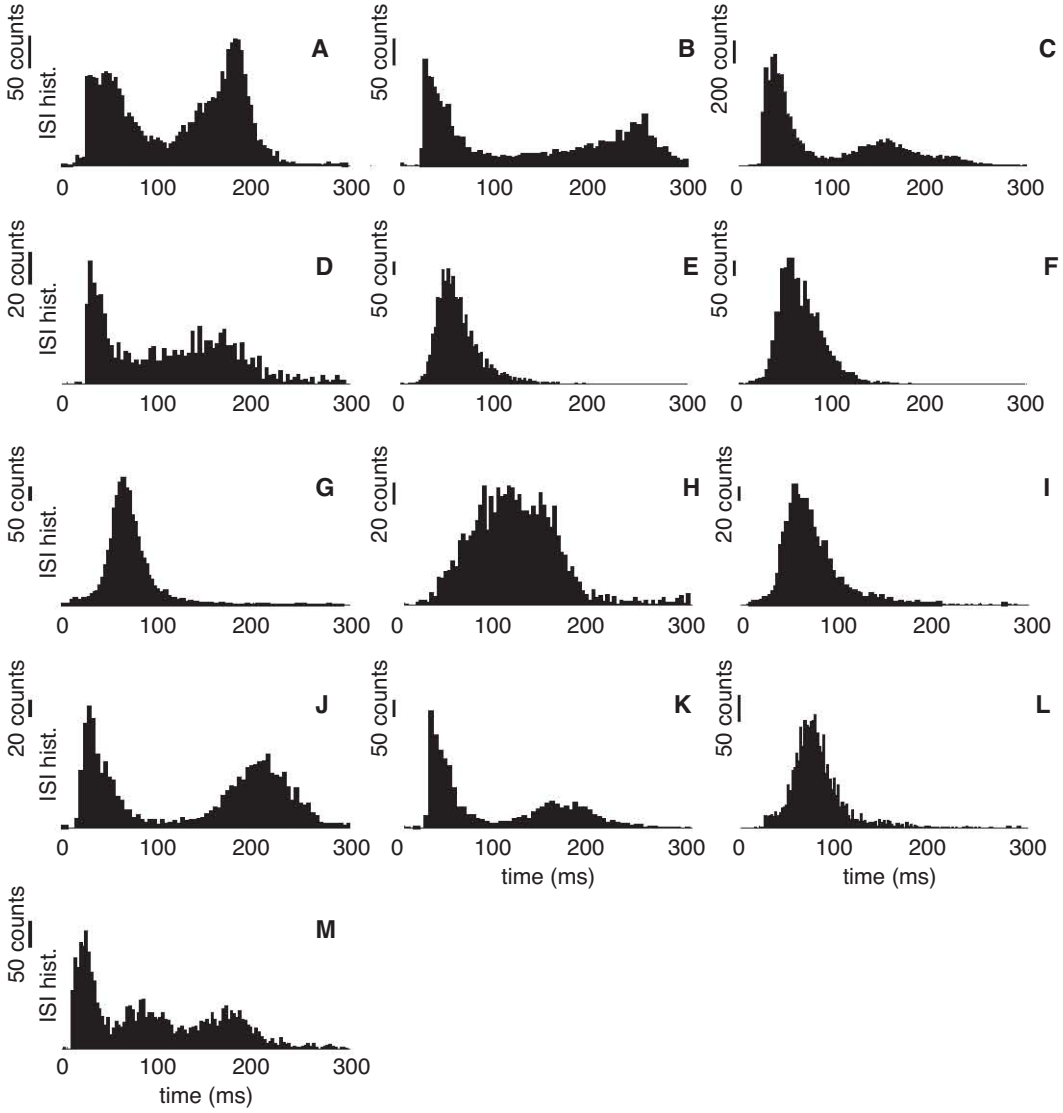

FIGURE 5.2: Cumulative ISI histograms for all the MNs identified, for each patient, showing the different types of distribution of MN discharges observed. Plots A to I correspond to ET patients 01 to 09, plots J to M to PD patients 01 to 04. Notice the different scales in the ordinate.

the data employed in the calculations of corticomuscular coupling, together with the motor unit spike trains described above.

Fig. 5.3 displays an example of corticomuscular coherence as estimated from the MN activities and the processed EEG signal recorded from the contralateral sensorimotor cortex. Each trace in Fig. 5.3A corresponds to the average coherence for the CSTs built with 1 to 11 MNs (all possible combinations). There, it is shown that the coherence peak at the tremor frequency (∼4.75 Hz, indicated with the black arrow in Fig. 5.3A) was always statistically significant, which indicates that, for this patient, the cortical-related tremor activity was projected to the output of the MN pool even when a single MN was sampled. In addition, as it is displayed in Fig. 5.3B, corticomuscular coherence

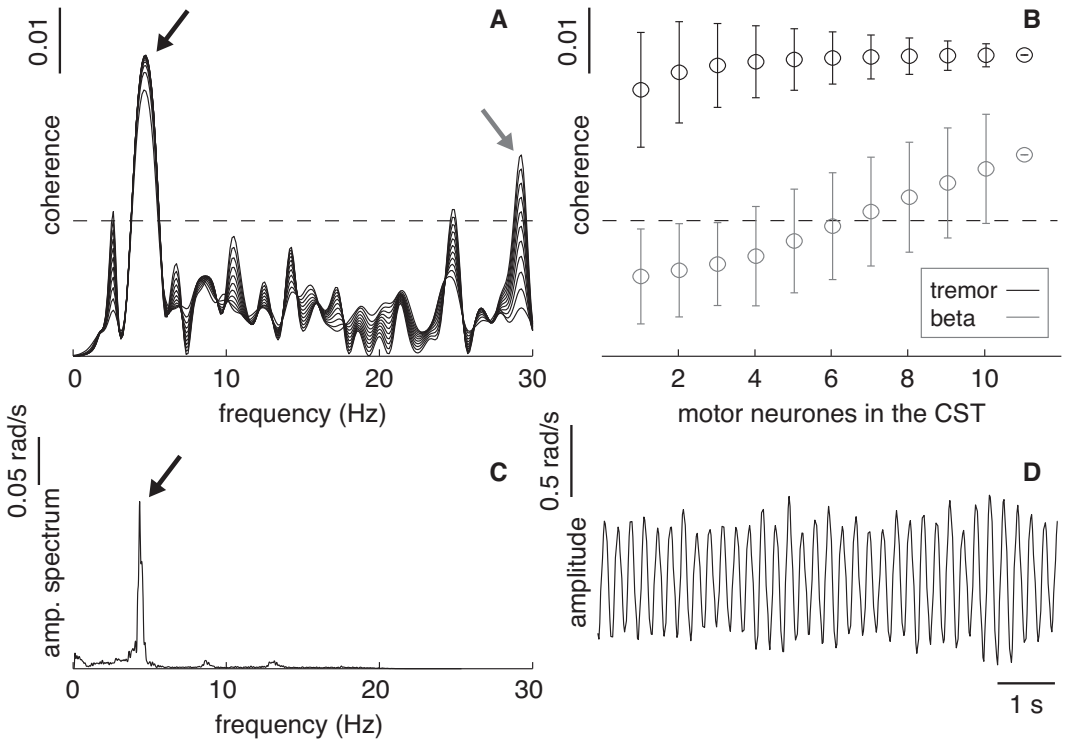

FIGURE 5.3: Example of the coherence between the EEG signals recorded from the contralateral motor cortex (C4, given that the left hand was recorded) and all the possible CSTs. The data are from ET patient 03. (A) Average coherence for all possible CSTs comprising from 1 to 11 MNs (black, solid lines). These coherence spectra always exhibited a significant peak at tremor frequency (black arrow), which height increased monotonically with the number of MNs considered. Coherence at the beta band (grey arrow), corresponding to the voluntary drive to muscle, became significant when 7 MNs were included in the CST. The confidence level ($P < 0.05$) is represented as a dashed black line. (B) Mean ± SD (the circle and the length of the whiskers, respectively) of the coherence at the tremor frequency (in black; it corresponds to the peak indicated with the black arrow in (A)) and the beta band (in grey; it corresponds to the peak indicated with the grey arrow in (A)) as function of the number of MNs in the CST. (C) Amplitude spectrum of the hand tremor as recorded with the gyroscopes, showing a clear peak at the tremor frequency (black arrow), which appeared very close to that observed in the corticomuscular coherence plots depicted in (A). (D) Hand oscillations during a portion of the trial.

at the tremor frequency increased monotonically with the number of MNs considered, until a plateau was reached when ∼5 MNs were included in the CST (visual inspection). Therefore, ∼5 MNs provided maximal corticomuscular coherence at tremor frequency, in the sense that considering more MNs increased negligibly the amount of coherence (the increase when considering 6 MNs was of 0.5 %, and when considering 11 MNs was of 1.5 %). Furthermore, the corticomuscular coherence was relatively invariant to which MNs were chosen to child a CST, as shown by the small SD of the data in Fig. 5.3B. This result, together with the fact that the variability of the estimation of corticomuscular coherence decreased as more MNs were considered, demonstrates that the descending cortical-related tremor activity was common to the entire MN pool (Negro and Farina,

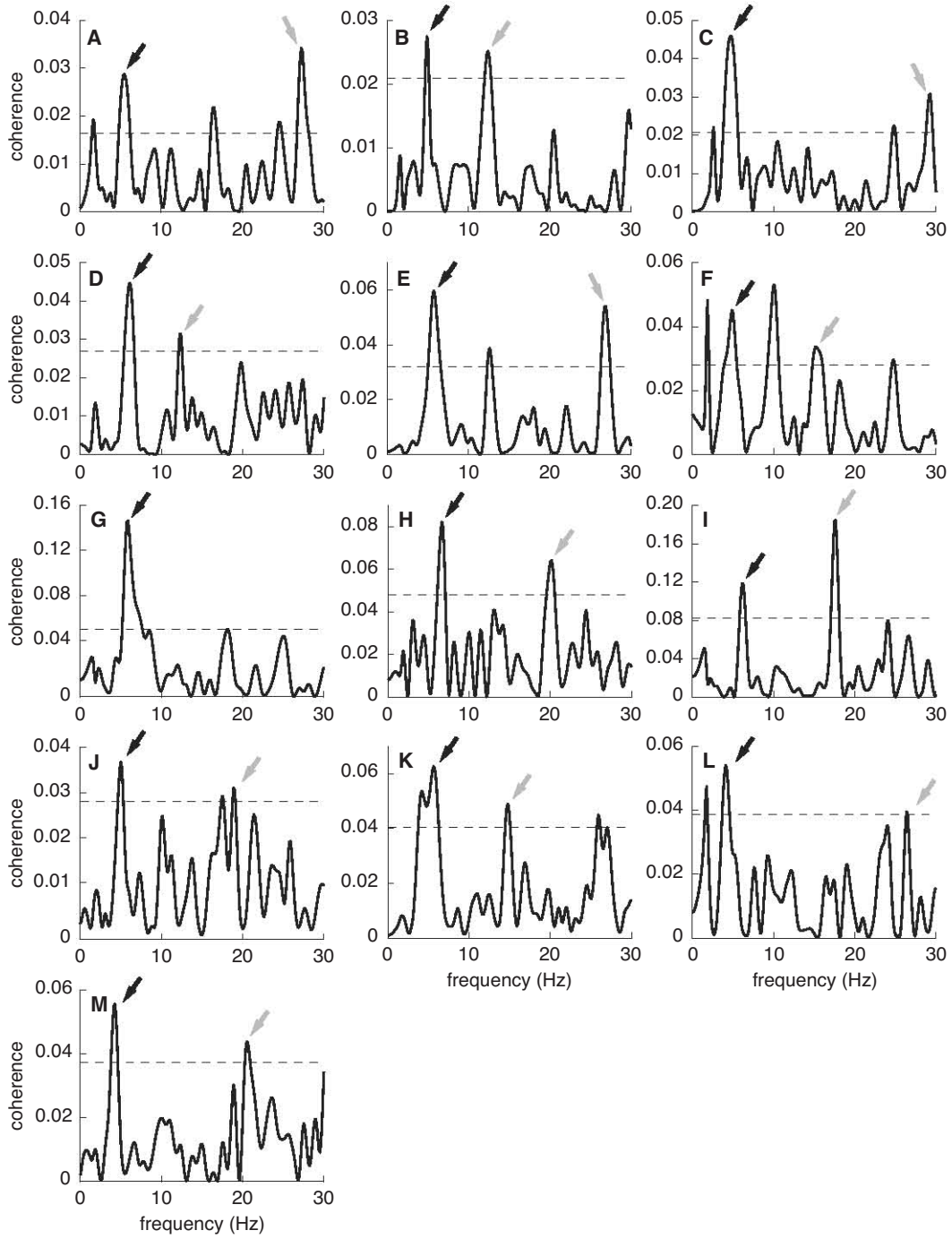

FIGURE 5.4: Estimation of corticomuscular coherence between the contralateral motor cortex and the CST comprising all the identified MNs, for all the patients. The EEG electrode shown is the one that exhibited the largest coherence at the tremor frequency (listed in Table 5.1). Plots A to I correspond to ET patients 01 to 09, and plots J to M to PD patients 01 to 04. In all the figures, the black arrow points at the coherence peak at tremor frequency, the grey arrow indicates the peak in the beta band, and the dashed black line shows the confidence level ($P < 0.05$).

2011b; Gallego et al., 2011a).

The coherence spectra also showed a significant peak at the beta band (indicated with a

TABLE 5.1: Summary of corticomuscular coherence and motor unit synchronization. The table shows, for each patient, the type of tremor elicited (postural, PO, at rest, RE, or while holding a weight during posture, WE), the number of MNs identified through decomposition, the height and frequency at which the peaks at the tremor frequency and the beta band were found for the CSTs comprising all the MNs identified, and the degree of motor unit synchronization according to the CIS (computed in 2 min windows). All coherence values were statistically significant ($P < 0.05$), except where stated otherwise (n.s.).

patient	tremor type	num. MNs	EEG ch.	Coh. tremor	freq. tremor	Coh. beta	freq. beta	CIS [2 min] (pps)
ET01	PO	5	C3	0.029	5.504	0.034	27.270	1.45 ± 0.22
ET02	RE	5	C1	0.027	4.878	0.025	12.380	0.98 ± 1.47
ET03	PO	11	FC4	0.046	4.753	0.031	29.270	2.32 ± 1.96
ET04	PO	4	FC3	0.090	6.130	0.063	12.390	0.95 ± 0.76
ET05	PO	5	CP3	0.060	5.754	0.054	26.890	1.61 ± 0.48
ET06	PO	4	CP4	0.045	4.878	0.034	15.260	1.63 ± 1.00
ET07	PO	9	FC2	0.156	5.879	n.s.	n.s.	1.46 ± 1.27
ET08	PO	7	CP3	0.083	6.629	0.064	20.140	0.36 ± 0.53
ET09	PO	6	CP2	0.119	6.254	0.185	17.640	0.96 ± 0.92
PD01	RE	5	C1	0.037	5.003	0.037	18.890	1.25 ± 1.39
PD02	RE	5	C3	0.063	5.629	0.058	25.890	1.65 ± 1.96
PD03	WE	5	C1	0.054	4.128	0.039	26.390	0.75 ± 0.61
PD04	RE	8	C2	0.047	4.753	0.056	19.890	7.67 ± 2.44

grey arrow in Fig. 5.3A), which is assumed to correspond to voluntary contractions (e.g. Conway et al., 1995; Negro and Farina, 2011b). The coherence in this band also increased monotonically as more MNs were considered, but the trend was not exponential, and neither did the variance in the estimation decrease notably when the CSTs included more MNs (see Fig. 5.3B). Therefore, in this patient differences existed in the manner in which both descending drives were projected to the output of the MN pool. As expected, the frequency of the hand tremor was close to that at which corticomuscular coherence was found (indicated with a black arrow in Fig. 5.3A and Fig. 5.3C).

Similar results were obtained for all the patients analysed. Fig. 5.4 shows the estimation of coherence between the CST comprising all the MNs identified and the processed EEG signal that provided the largest coherence at the tremor frequency (listed in Table 5.1), for all patients. Overall, I found significant corticomuscular coherence at the tremor frequency (indicated with black arrows in Fig. 5.4) for all the patients, which was accompanied, in thirteen out of fourteen patients, by another peak in the beta band (identified with grey arrows in Fig. 5.4), even in the four patients who performed the rest task (see Table 5.1). This implies that also in this case there was a certain amount of voluntary descending command. As to the patient with no significant coherence at the beta band (ET07), I hypothesize that the small number of windows employed for its calculation (49) may have impeded the observation of significant coupling, given that there were two peaks very close to the confident limit (at ∼18 and ∼25 Hz). Overall,

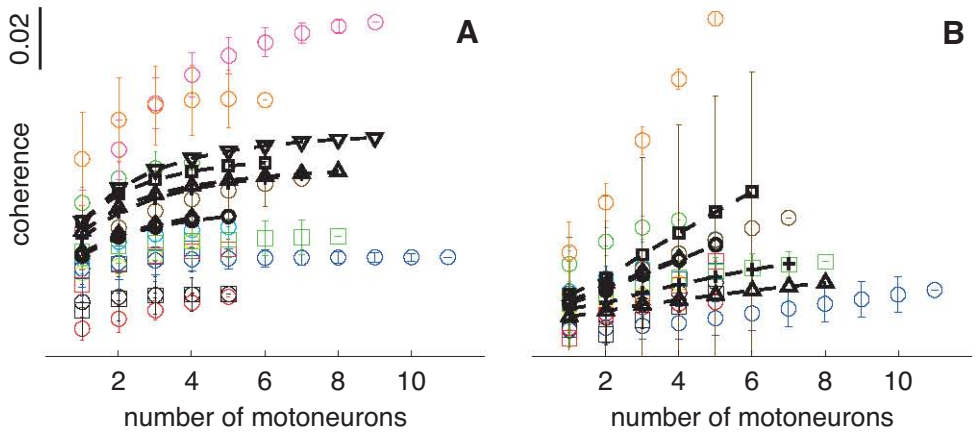

FIGURE 5.5: Estimation of corticomuscular coherence at the tremor frequency and the beta band as function of the number of MNs considered, for all patients. Panel (A): Mean ± SD (the circle and the length of the whiskers, respectively) of the coherence peak at the tremor frequency, obtained for all possible combinations of MNs to form a CST. Results are shown as function of the number of MNs included in the calculations, and each patient is represented in a different color, being the data from ET patients displayed as circles, and from PD patients as squares. Patients are color coded as follows: ET01 is displayed in black, ET02 in blue, ET03 in red, ET04 in green, ET05 in cyan, ET06 in yellow, ET07 in magenta, ET08 in brown, ET09 in orange, PD01 in black, PD02 in red, PD03 in blue, and PD04 in green. A series of grand means are also displayed, to represent the general trend of the data (in black): for all the patients (diamonds), for all the patients with 5 or more MNs detected (circles), for all the patients with 6 or more MNs detected (squares), for all patients with 7 or more MNs detected (crosses), and for all the patients with 9 or more MNs detected (triangles). Panel (B): Mean ± SD (the circle and the length of the whiskers, respectively) of the coherence peak at the beta band, obtained for all the possible combinations of MNs to form a CST. Results are shown as function of the number of MNs considered, and patients are color-coded as in (A); the same grand means are also displayed.

these results suggest that the MN pool received two descending cortical inputs simultaneously: one corresponding to the tremor oscillations, and the other to the voluntary drive. Remarkably, the corticomuscular coherence values found were small, although significant for both frequencies of interest ($P < 0.05$), in all the patients analyzed. As explained in the Methods (Section §5.2), I observed that artefact removal had a great influence in the magnitude of the coherence.

As observed for patient ET03 (Fig. 5.3B), in all the patients the corticomuscular coherence at tremor frequency increased monotonically as more MNs were included in the CST, at the same time that the variability of the estimation decreased (see Fig. 5.5A). Furthermore, the coherence at the tremor frequency reached a plateau after a few MNs were sampled for all the patients except for patient ET06, for whom only 4 MNs were identified, and therefore no conclusions could be drawn in this regard (see the yellow markers in Fig. 5.5A). Analysis of the pooled data of all the patients yielded that 5 MNs (paired Student's t-test, $P < 0.05$) were enough to sample most accurately the cortical tremor input, i.e. to obtain a negligible increase of coherence when more MNs were considered. As mentioned above, this indicates that tremor was a common cortical

projection to the MN pool (Negro and Farina, 2011b). Interestingly, for 11 patients (all except for patients ET02 and ET08) the estimation of corticomuscular coherence with only 1 MN showed a significant peak at the tremor frequency, being the average amount of MNs needed to observe significant coherence $n = 1.2 \pm 0.6$. This means that in most cases the descending tremor input was so strong that could be even observed in the output of a single MN. Regarding the corticomuscular coherence at the beta band, it also increased monotonically as more MNs were included in the CST employed for the analysis. However, an exponential trend was only observed in 3 patients (ET02, ET04, and EP04 represented as red circles, green circles, and green squares in Fig. 5.5B), while in the others the relative increase in corticomuscular coherence did not become smaller as MNs are considered, as expected from healthy subjects performing voluntary contractions (Negro and Farina, 2011b). Therefore, these results suggest that for the remaining 10 patients, the common tremor input disrupted the ability of the MN pool to sample accurately the voluntary deciding drive that was concurrently projected to the population of MNs. This finding is in line with the simulation results presented in (Negro and Farina, 2011a), which showed how a secondary common input projected to a MN pool may disrupt the transmission of an independent common input.

5.3.2 Common Input to Motor Neurons

I investigated the common input to MN population by a a means of extracting information about the frequency content of the neural drive to muscle. To this end, Fig. 5.6 represents, for each patient, the coherence between CSTs. There, it is shown that in all of them there were two large peaks in the spectrum, which indicate the presence of two strong common inputs to the MN pool: one at low frequency ($<$ 2–3 Hz), presumably related to the common drive to muscle (De Luca and Erim, 1994; Negro et al., 2009; Negro and Farina, 2012), and a second peak at the frequency of the tremor (mean frequency 5.192 ± 0.901 Hz, indicated in Fig. 5.6 with a black arrow). This suggests that the MN pool received a strong input at tremor frequency, apart from the common drive seen during normal function. Notice that these common inputs may not only reflect the descending drive to muscle, but also the contribution of afferent information (Farina et al., 2010). I found no significant relationship between the corticomuscular coherence at tremor frequency and its corresponding peak in the coherence between CSTs ($P = 0.345$, Pearson's correlation), which suggests that the relative contribution of the afferent and tremor-related cortical activity to the MN pool varied among subjects. The coherence spectra of patients ET01, ET02, ET08, PD01 and PD4 exhibited clear peaks at frequencies that were harmonics of that of the tremor (see Fig. 5.6A, 5.6B, 5.6F, 5.6J and 5.6M). However, this phenomenon was not related to the characteristics of MN firings, as indicated by the fact that three of these patients showed a bimodal ISI histogram, one a trimodal ISI histogram, and the remainder a unimodal distribution.

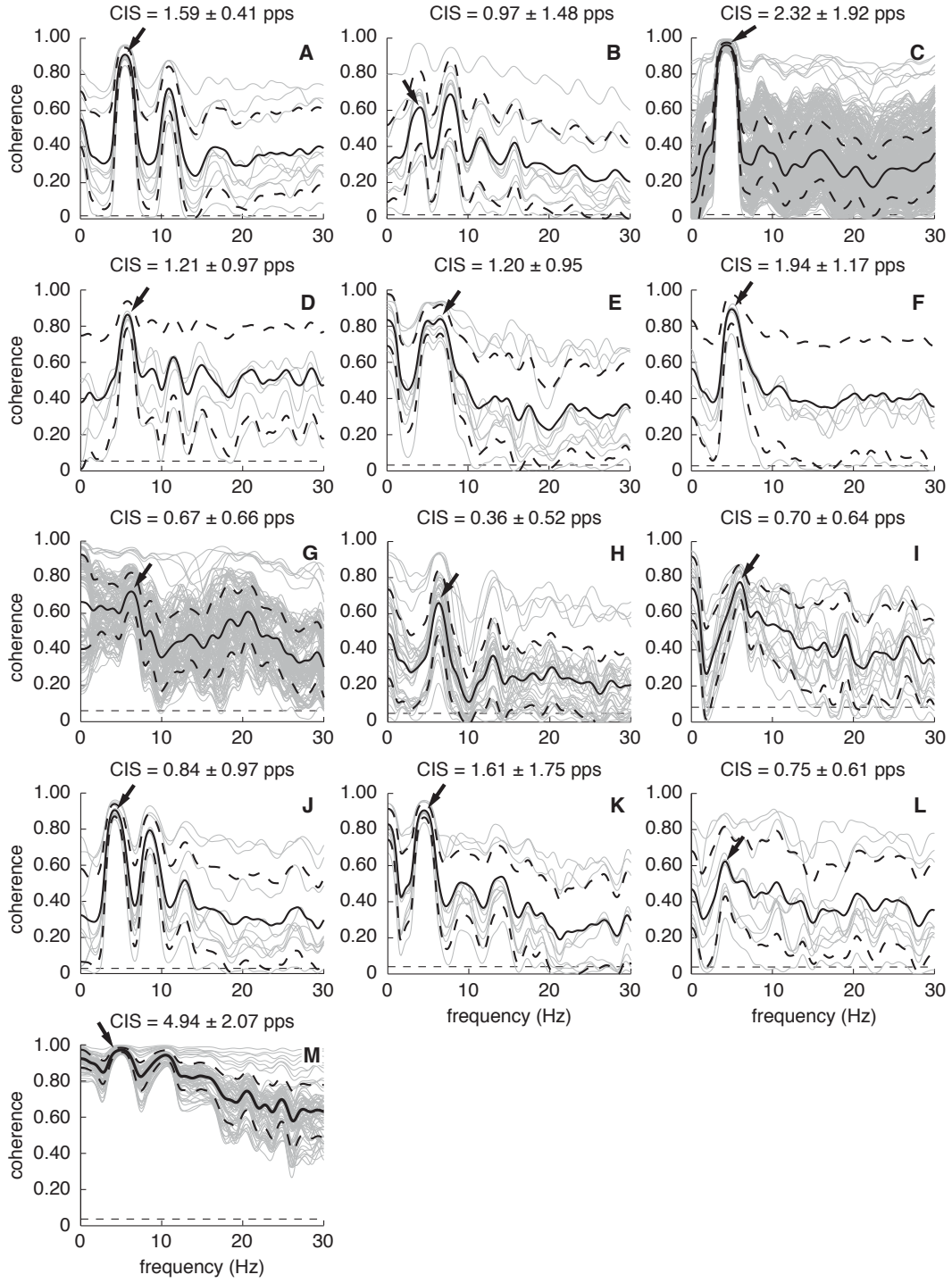

FIGURE 5.6: Strength and frequency content of the common synaptic inputs to the identified MNs, for all the patients. The plots show the coherence spectra for all possible pairs of CSTs comprising each the largest possible amount of MNs (in gray), and the mean (solid black line) ± SD coherence (dash and dot black line); the confidence limit ($P < 0.05$) is also displayed (dashed black line). The arrow points at the peak at the frequency of the tremor. Each panel represents a single patient, being A to I ET patients 01 to 09, and J to M PD patients 01 to 04. Common input strength estimated with the CIS during the same data windows is reported on top of each panel.

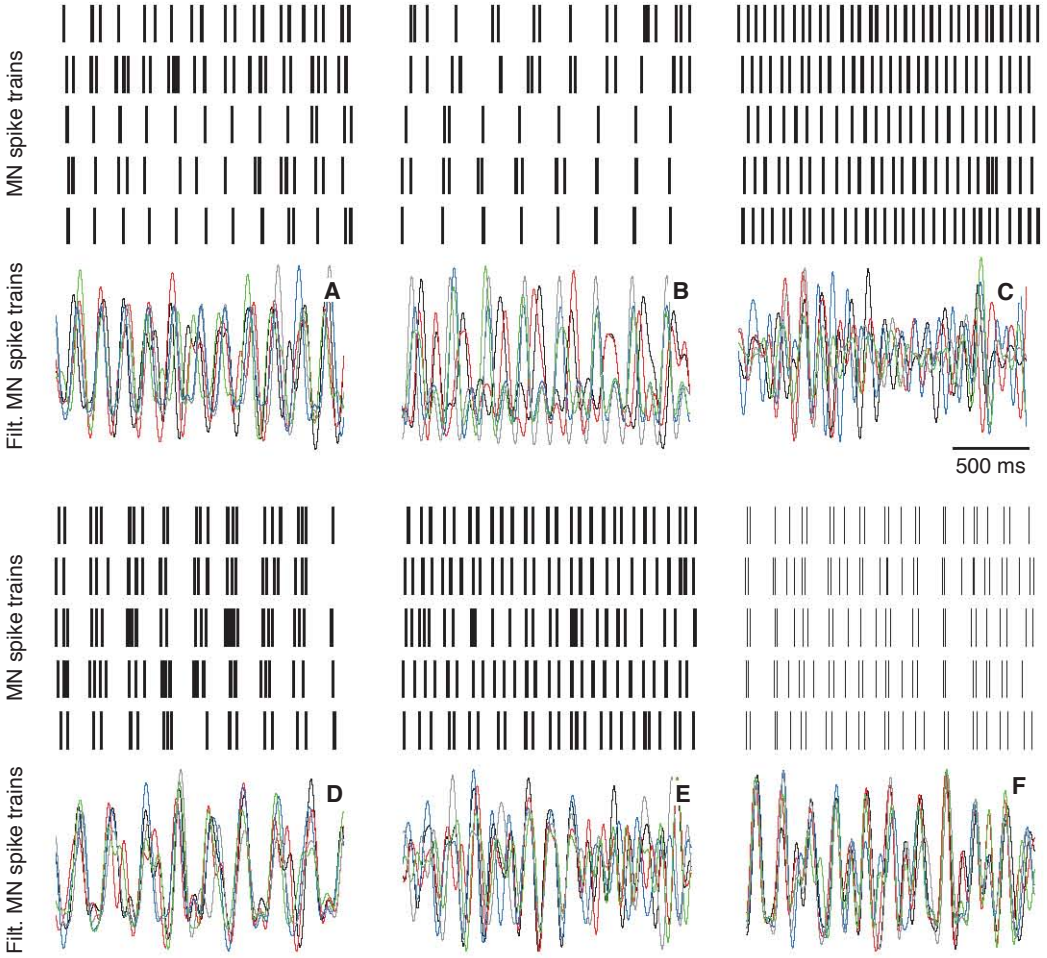

FIGURE 5.7: Examples of MN spike trains in ET and PD patients, and the result of applying a bandpass filter at the tremor frequency band. The figure shows, for each patient, the spike trains of 5 MNs (randomly chosen among those identified), and their filtered version (band-pass, 3–10 Hz, zero phase) at the top and the bottom of each panel, respectively. The filtered MNs are color-coded as follows: MN #1 (top) is shown in black, #2 in red, #3 in blue, #4 in green, and #5 (bottom) in grey. Each panel represents a single patient, corresponding (A), (B) and (C) to patients ET01, ET02 and ET07, and (D), (E) and (F) to patients PD02, PD03 and PD04. The plot illustrates MN synchronization, and how the spike trains identified are related to the tremor.

Notice that the very large coherence at the frequency of the tremor appeared because the MN spike trains were largely synchronized, as represented in the examples in Fig. 5.7. There, it is shown that the filtered MN spike trains (band-pass, 3–10 Hz) became oscillations that were locked up in phase in frequency, which illustrates directly the strong common input related to tremor.

In order to compare these results with existing studies, I analyzed the relationship between MN activities using the cross-correlogram, which constitutes the traditional approach for the estimation of short-term MN synchronization (common input strength; reviewed in Nordstrom et al., 1992; Negro and Farina, 2012). The application of this

method yielded that the activities of 185 out of 227 MN pairs were significantly synchronized. The average CIS for all the patients was 2.28 ± 2.71 pps, a value remarkably larger than that obtained in healthy subjects for the same muscle group during voluntary contractions (mean value ≤ 0.7 pps, Keen and Fuglevand, 2004; Schmied et al., 1993). Furthermore, the mean CIS for each patient was significantly correlated with the mean coherence between CSTs at the tremor frequency when the same data windows were for the calculations ($P = 0.014$, $r = 0.662$, Pearson's correlation). This suggests that the abnormally large MN synchronization, as derived with the CIS, was related to the presence of a strong common synaptic input at the frequency of the tremor (and probably caused by it, due to the well established relationship between common synaptic inputs and motor neuron synchronization, Sears and Stagg, 1976; Kirkwood and Sears, 1978). No significant relationship was found between the CIS and the frequency of the tremor ($P = 0.526$, Pearson's correlation), thus, for the current sample, the frequency of the tremor did not influence the estimation of MN synchronization.

5.4 Discussion

In this chapter, I investigated the properties of the neural drive to muscle and the synaptic inputs to motor neurons in patients with tremor arising from ET or PD, and what is their relationship with the tremor-related cortical activity. The results presented prove that the tremor in ET and PD is a common cortical projection to the MN pool, which is transmitted in a (partly) linear manner to its output. Moreover, the current data demonstrated, for the first time, that there exists a strong common synaptic at the frequency of the tremor, which causes abnormally large MN synchronization. This input appears concurrently to the descending voluntary drive. Finally, since there was no association between the strength of corticomuscular coupling and that of the common input to MNs, the current data constitutes the first strong evidence that suggests that spinal afferents enhance the cortically projected tremor oscillations.

This study relied on the assessment of the neural drive to muscle through the analysis of MN activities (Farina et al., 2010; Negro and Farina, 2011b, 2012), which were extracted by decomposing the surface EMG with a novel technique (Holobar et al., 2012). By using this technique, a sufficient number of concurrently active MNs were identified, which permitted to fully characterize the neural drive to muscle, circumventing the methodological limitations of traditional approaches (Merletti and Farina, 2009). The MNs identified often showed the characteristic paired and tripled discharges (see the examples in Fig. 5.1E) reported in previous studies with tremor patients (Das Gupta, 1963; Dietz et al., 1974; Elek et al., 1991; Baker et al., 1992; Christakos et al., 2009), which in many cases manifested as a clear multimodal distribution of the ISI histograms (see the examples in Fig. 5.11F). The MNs of those patients whose ISI histograms followed a unimodal distribution also exhibited periods with paired and tripled discharges,

but the firing pattern resembled more that observed during tonic MN firings. Overall, the relative proportion of paired discharges varied both within and among subjects, in good agreement with the literature (Dietz et al., 1974; Christakos et al., 2009).

For all patients, I found significant corticomuscular coherence at the frequency of the tremor over the contralateral cortex (see Fig. 5.4 and Table 5.1), as previously reported (e.g., Volkmann et al., 1996; Hellwig et al., 2001, 2003; Timmermann et al., 2003; Raethjen et al., 2007, 2009; Muthuraman et al., 2012). These coherence values were low, which suggests that ET and PD tremor does not appear due to a strong, direct, monosynaptic corticospinal connection (i.e., cortico-motoneuronal, see, e.g. Isa et al., 2007) that projects the central tremor oscillations (see Section §1.2.3), probably because of the small amount of monosynaptic connections from the motor cortex to MNs when compared to other descending pathways (Lemon, 2008). At the same time, I found significant coherence in the beta band, which is assumed to represent the voluntary drive to muscle (e.g. Conway et al., 1995; Negro and Farina, 2011b). This implies that the MN pool has the ability of sampling concurrently two common inputs that have different frequency content, which may facilitate that in many ET patients—and some PD patients—, tremor appears during the performance of voluntary movements (e.g. Deuschl et al., 2000b).

Although it has been previously demonstrated that the central oscillatory networks that cause ET and PD tremor are projected to the MN pool through descending pathways (e.g., Volkmann et al., 1996; Hua et al., 1998; Hua and Lenz, 2005; Hellwig et al., 2001, 2003; Raethjen et al., 2007, 2009, the manner by which the projection occurs has not been described yet. In this regard, the facts that *i*) corticomuscular coherence at the tremor frequency increased as more MNs were considered, reaching a plateau for 5 MNs, and *ii*) the variability of the coherence estimation decreased (see Fig. 5.5A), demonstrates that ET and PD are a common projection to the MN pool (Negro and Farina, 2011b; Gallego et al., 2011a). Furthermore, this observation implies that the tremor-related cortical activity is transmitted to the MNs in a partly linear manner (Negro and Farina, 2011b), because linearity is an assumption inherent to coherence analysis (Halliday et al., 1995). Since only a small number of MNs was sufficient for maximizing the linear transmission (coherence), and given that the presence of interneurons in the descending pathways introduces nonlinearities in the spiking process (Gerstner and Kistler, 2002), these data demonstrate that the transmission occurs (at least partly) through a direct pathway, likely the corticospinal tract, as it is hypothesized for the voluntary drive (Negro and Farina, 2011b). However, the involvement of other descending pathways, e.g. bulbospinal as it has been proposed for ET (Raethjen et al., 2007; Elble, 1996; Louis et al., 2007), cannot be asserted or disregarded based on the current data.

In some cases, the presence of the concurrent tremor altered slightly the manner in which the voluntary drive is transmitted to the output of the MN pool when compared to healthy subjects (Negro and Farina, 2011b). While, for all patients, coherence in the beta band also increased as more MNs were considered, only 3 subjects showed the

characteristic exponential profile with a plateau in coherence as function of the number of MNs were considered (see Fig. 5.5B). This may indicate that the presence of a common, strong, tremor input actually disrupts the sampling of the concurrent voluntary drive, as suggested by previous studies (Negro and Farina, 2011a).

The coherence between CSTs revealed that the MN pool received a very strong common input at the frequency of the tremor, apart from the common drive to muscle (De Luca and Erim, 1994; Negro et al., 2009; Negro and Farina, 2012). The existence of such a strong common input at the tremor frequency indicates that the afferent component (that is projected to the entire MN pool by Ia fibers, Mendell and Henneman, 1971) was large, because the tremor-related cortical contribution was relatively small as indicated by the values found when estimating corticomuscular coherence. This observation is also supported by the fact that I found no significant relationship between the amount of corticomuscular coherence and the strength of common input at the tremor frequency, and is in agreement with previous evidences showing that the modification of the mechanical properties of the tremulous limb alters the tremor based on the interaction between reflex pathways and descending tremor oscillations (e.g., Héroux et al., 2009; Elble et al., 1987). Further, the possible concurrent transmission of the central tremor oscillations through descending pathways other than corticospinal (see above) cannot explain by itself the very strong common input observed. Therefore, these current data suggest that afferent feedback facilitates the appearance of tremor in ET and PD.

The findings presented in this chapter also provide hypotheses to explain some undescribed phenomena observed during the validation of the NP, and set the basis for novel studies on the pathophysiology of tremors. In Section §4.4 I reported that in many cases when tremor amplitude was reduced significantly by means of neurostimulation, it started reappearing with a smaller amplitude than before and then the controller suppressed it again (see the example in Fig. 4.3). This phenomenon is also known from clinical practice, where it is observed that after the patient adopts the condition that triggers her/his tremor, the tremor develops until a (quasi) stationary state is reached (e.g., see the figures in Bilodeau et al., 2000; Rocon et al., 2006, and Fig. 1.1A). Such development of the tremor amplitude may be explained by the fact that the descending tremor drive is small to cause the very strong common input observed at tremor frequency (see Fig. 5.6) by itself, and thus afferent input may favor the expression of tremor in a close loop fashion (as suggested in a pioneering simulation study, Stein and Oguztöreli, 1976). Therefore, if the afferent input is limited by attenuating the amplitude of the tremor, it will not achieve the severity observed before. Another phenomenon observed in some patients during the validation of the NP was the migration of the tremor towards proximal segments when attenuated at the distal ones (see Section §4.5). I hypothesize that either the alteration of the tremor at the periphery favored its projection to other muscles, e.g. through afferent information delivered to supraspinal centers, or it triggered the manifestation of other central oscillator that otherwise did

not manifest. The somatotopic organization of the structures causing ET and PD may favor this (Purves et al., 2004).

5.5 Conclusions

Much is yet unknown about the mechanisms the cause tremor. ET and PD tremors originate at different brain structures that interact in a complex and dynamic manner (also not fully elucidated, see Epigraph §1.2.3), and then are projected to the affected muscles. However, the manner in which the transmission occurs still needs to be elucidated. In this chapter I examined the hypothesis that the pathological oscillations causing ET and PD are a common cortical projection to the MN pool, which causes abnormally high motor unit synchronization, thus favoring the manifestation of the tremor.

The results here presented show that, for both ET and PD, a few, randomly chosen, MNs are enough to transmit the central tremor oscillations to the output of the MN pool. Furthermore, the transmission improves exponentially until a plateau is reached, which suggests that the tremor is commonly projected to the entire population of MNs from the motor cortex. These data indicates that the descending pathway through which this occurs has few interneurons (given their nonlinear behavior), and thus it should be direct, i.e. corticospinal. Another finding of the study is that the MNs receive a very strong common synaptic input at the frequency of the tremor, which suggests that spinal afferents enhance the contribution of the descending tremor oscillations, given that the cortical input is not sufficiently strong to explain the observed common input strength *per se*. Finally, the results presented in this chapter also indicate that the MN pool has the ability of transmitting two common oscillations concurrently, because a similar behavior was observed for the concurrent voluntary drive. As expected from the fact that it is transmitted at higher frequencies than the tremor, more MNs are needed to sample the voluntary input than the descending tremor oscillations.

These findings help to explain some of the phenomena observed during the validation of the NP in Chapter §4, which have not been described in the literature. In addition, they serve to identify topics of future research such as the investigation of whether a single or multiple oscillators are projected to the tremulous muscles, and, in the latter case, how they are entrained. This analysis will further contribute to the elucidation of the mechanisms that mediate tremor in ET and PD.

In summary, this chapter demonstrates that central tremor oscillations are a common, (partly) linear projection to the MN pool, not so strong to justify the very large strength of common input to MNs. This suggests that tremor may be cortically triggered and enhanced by spinal factors, in such a manner that the interaction between supraspinal and spinal factors selectively enhances MN synchronization at the frequency of the tremor, causing the characteristic rhythmic entrainment of muscles.

Chapter 6

Conclusions and Future Work

This Chapter summarizes the most relevant contributions of the dissertation, and how they contributed to achieve the objectives defined. In addition, I summarize the publications that served to disseminate the different studies performed during the realization of this thesis. The chapter finishes with an outline of the future work, which spans through the investigation of the mechanisms of tremor, and the development of novel treatment forms.

6.1 Contributions

The work presented in this dissertation is aimed at the design and validation of a wearable NP for tremor suppression through mechanical loading. In order to reach this objective, I investigated a number of issues related to the recording and characterization of tremor, the pathophysiological mechanisms that cause it, and the application of biomechanical loads through transcutaneous neurostimulation. This work permits achieving the objective established at the beginning of the thesis, at the same time that they constitute important contributions to the field of biomedical and neural engineering, signal processing, rehabilitation robotics, and neurophysiology.

The major contributions of this dissertation are summarized next:

- The identification of a series of design criteria for the components of the NP (both the physical and cognitive interfaces), which were established after extracting user needs. These requirements are taken into consideration in the design of the cognitive and physical interfaces of the NP, in order to guarantee that the final solution is a functional prototype that meets user requirements.
- The definition of an adequate methodology for the ambulatory recording of upper limb kinematics in tremor patients with the NP.
- The first demonstration that the multiple tremor oscillators—that are likely to be projected to the tremulous muscles according to some evidences—may be identified from the decomposition of joint kinematics with EEMD.
- The definition and validation of an optimal algorithm for the estimation of instantaneous tremor parameters in the presence of concomitant voluntary movement. This algorithm provides the necessary information to drive any tremor suppression system, and is implemented in the NP.
- The demonstration that it is possible to build an optimal cognitive interface for a tremor suppression WR/NP based on concurrent recordings of the CNS, the PNS, and limb biomechanics. The interface is robust and reliable thanks to the redundant mechanisms implemented by exploiting the multimodal recordings, and requires no learning from the user.
- The development of a novel strategy for tremor suppression with the NP based on the modulation of muscle co-contraction. This strategy is implemented in the NP and afterwards evaluated.
- The proof that NP-driven modulation of muscle co-contraction constitutes a feasible alternative for tremor management. The results on a group formed by twelve patients encourage the evaluation of the device as an alternative treatment for tremor.

- The demonstration that tremor is a common descending projection to the pool of MNs that innervate a muscle. This result is obtained after employing, for the first time, the characterization of the neural drive to muscle in tremor patients as a means of investigating corticomuscular coupling.
- The extraction of indirect evidences that suggest that afferent information plays an important role in the manifestation of severe tremors. This is concluded after observing that the tremulous MN pool receives a very strong afferent input, which is not of descending origin.

6.2 Scientific Dissemination

The work described in this dissertation has produced a number of publications in scientific journals and conferences; partial results have also been included in two book chapters. In addition, the outcome of this work has been integrated in other research projects, which have also been properly disseminated. All the publications are depicted next.

Publications in scientific journals related with the investigation, characterization, or management of tremor:

- J.A. Gallego, J.L. Dideriksen, A. Holobar, J. Ibánez, E. Rocon, J.L. Pons, D. Farina. Neural drive to muscle and common synaptic inputs to the motor neuron pool in essential tremor. *To be submitted.*
- J. Ibánez, J.I. Serrano, M.D. del Castillo, J.A. Gallego, E. Rocon. Online validation of an asynchronous detector of the intention to move based on EEG - Application in tremor patients. *Biomedical Signal Processing and Control*, under review.
- J.A. Gallego, E. Rocon, J.M. Belda-Lois, J.L. Pons. A neuroprosthesis for tremor management through the modulation of muscle co-contraction. *Journal of Neuro-Engineering and Rehabilitation*, 10: 36, 2013.
- J.A. Gallego, J. Ibáñez, J.L. Dideriksen, J.I. Serrano, M.D. del Castillo, D. Farina, E. Rocon. A multimodal human-robot interface to drive a neuroprosthesis for tremor management. *IEEE Transactions on Systems, Man and Cybernetics, Part C: Applications and Reviews*, 42(6):1159–68, 2012.
- E. Rocon, J.A. Gallego, J.M. Belda-Lois, J. Benito-León, J.L. Pons. Biomechanical loading as an alternative treatment for tremor: a review of two approaches. *Tremor and Other Hyperkinetic Movements*, 2: 1–13, 2012.

- A. Holobar, V. Glaser, J.A. Gallego, J.L. Dideriksen, D. Farina. Non-invasive characterization of motor unit behaviour in pathological tremor. *Journal of Neural Engineering*, 9: 056011, 2012.
- J.A. Gallego, E. Rocon, J.O. Roa, J.C. Moreno, J.L. Pons. Real-time estimation of pathological tremor parameters from gyroscope data. *Sensors*, 10(3): 2129–39, 2010.

Other journal publications by the author, in topics related with the work in this thesis:

- R. Raya, E. Rocon, J.A. Gallego, R. Ceres, J.L. Pons. A robust Kalman algorithm to facilitate human-computer interaction for people with cerebral palsy, using a new interface based on inertial sensors. *Sensors*, 12(3): 3049–67, 2012.
- A. Abellanas, A. Frizera, R. Ceres, J.A. Gallego. Estimation of gait parameters by measuring upper limb. *Sensors and Actuators A: Physical*, 162(2): 276–83, 2010.
- A. Frizera-Neto, J.A. Gallego, E. Rocon, J.L. Pons, R. Ceres. Extraction of user's navigation commands from upper body force interaction in walker assisted gait. *BioMedical Engineering Online*, 9: 37, 2010.

Importantly, among the nine journal papers that are published, or undergoing revision, six are included in journals ranked in the first quartile of their respective fields according to the Journal Citation Report[1], them being: "Biomedical Engineering," "Rehabilitation," "Instruments and Instrumentation," "Engineering, Electrical and Electronic," "Computer Science, Artificial Intelligence," "Computer Science, Interdisciplinary Applications," and "Computer Science, Cybernetics." The manuscript to be submitted will be sent to a first quartile journal in the field of "Neurosciences." The remainder three journals are also indexed in the ISI Web of Knowledge and awarded an impact factor.

Two book chapters also include parts of the work presented in this dissertation:

- F. Barroso, D. Ruiz-Bueno, J.A. Gallego, P. Jaramillo, A. Kilicarsian. "Surface EMG in neurorehabilitation and ergonomics: state of the art and future perspectives" in *Emerging therapies in neurorehabilitation*, J.L. Pons and D. Torricelli (Eds.), Springer Verlag, in press.
- E. Rocon, J.C. Moreno, J.A. Gallego, J.L. Pons. "Wearable robots in rehabilitation engineering: Tremor suppression" in *Rehabilitation Engineering*, T.Y. Kheng (Ed.), In Tech Education and Publishing, 2009.

[1]Data retrieved from the ISI Web of Knowledge. Each publication was ranked according to the Journal Citation Report for the year in which it was published; those accepted in 2012 are compared with the 2011 ranking.

Contributions to scientific conferences directly related to the topics of the dissertation:

- J.A. Gallego, E. Rocon, J.M. Belda-Lois, J.L. Pons. Closed-loop modulation of a notch-filter stimulation strategy for tremor management with a neuroprosthesis. *XIII Mediterranean Conference on Medical and Biological Engineering and Computing*, submitted.

- J.A. Gallego, J.M. Belda-Lois, A. Castillo, J.P. Romero, J. Benito-León, J.L. Pons, E. Rocon. A novel treatment for essential tremor through transcutaneous neurostimulation. *17th International Congress of Parkinson's Disease and Movement Disorders*, accepted [Abstract].

- J.A. Gallego, E. Rocon, J.M. Belda-Lois, A.D. Koutsou, S. Mena, A. Castillo, J.L. Pons. Design and validation of a neuroprosthesis for the treatment of upper limb tremor. *2013 Annual International Conference of the IEEE Engineering in Medicine and Biology Society*, accepted.

- J.A. Gallego, E. Rocon, J.L. Pons. Advances in the assessment and suppression of pathological tremor in the framework of TREMOR project. *Converging Clinical and Engineering Research on Neurorehabilitation*, Part I, 61–66, 2012.

- P.P. Brzan, J.A. Gallego, D. Farina, A. Holobar. On repeatability of motor unit characterization in pathological tremor. *Converging Clinical and Engineering Research on Neurorehabilitation*, Part I, 553–556, 2012.

- J.L. Pons, E. Rocon, J.A. Gallego. A wearable neuroprosthesis for the suppression of pathological tremor. *34th Annual International Conference of the IEEE Engineering in Medicine and Biology Society (Unconference demo competition).*

- J.A. Gallego, E. Rocon, J.L. Pons. Alleviation of pathological tremor through neuroprosthetic approaches relying on biomechanical loading. *IFBME Proceedings of the World Congress on Medical Physics and Biomedical Engineering 2012* [Abstract].

- A. Holobar, R. Istenic, V. Glaser, J.A. Gallego, D. Farina. Novel approaches to electrophysiological quantification of pathological tremor. *IFBME Proceedings of the World Congress on Medical Physics and Biomedical Engineering 2012* [Abstract].

- J.A. Gallego, J. Ibáñez, J.L. Dideriksen, J.I. Serrano, M.D. del Castillo, D. Farina, E. Rocon, J.L. Pons. Simultaneous recordings of the central and peripheral nervous system together with joint biomechanics improve the characterization of tremor. *IFBME Proceedings of the World Congress on Medical Physics and Biomedical Engineering 2012* [Abstract].

- J.A. Gallego, E. Rocon, A.D. Koutsou, J.M. Belda-Lois, S. Mena, I. Busquets, A. Castillo, J.L. Pons. Atenuación del temblor patológico mediante estimulación eléctrica funcional. *Actas de las XXXII Jornadas de Automática*, 2011.

- A. Holobar, V. Glaser, J.A. Gallego, J.L. Dideriksen, D. Farina. Noninvasive analysis of motor unit behaviour in pathological tremor. *Proceedings of 2011 Annual International Conference of the IEEE Engineering in Medicine and Biology Society*, 2037–40, 2011.

- J.A. Gallego, J.L. Dideriksen, D. Farina, E. Rocon, A. Holobar, J.L. Pons. A modelling study on transmission of the central oscillator in tremor by a motor neuron pool. *Proceedings of 2011 Annual International Conference of the IEEE Engineering in Medicine and Biology Society*, 7512–15, 2011.

- J.L. Dideriksen, J.A. Gallego, D. Farina. Characterization of pathological tremor from motor unit spike trains. *IFBME Proceedings of the 15th Nordic-Baltic Conference on Biomedical Engineering and Medical Physics*, 34: 41–44, 2011.

- J. Ibáñez, J.I. Serrano, M.D. del Castillo, L. Barrios, J.A. Gallego, E. Rocon. An EEG-based design for the online detection of movement intention. *Lecture Notes on Computer Science*, 6691/2011: 370–377, 2011.

- J.A. Gallego, E. Rocon, J. Ibáñez, J.L. Dideriksen, A.D. Koutsou, R. Paradiso, M.B. Popovic, J.M. Belda-Lois, F. Gianfelici, D. Farina, M. Manto, T. DAlessio, J.L. Pons. A soft wearable robot for tremor assessment and suppression. *Proceedings of the 2011 IEEE International Conference on Robotics and Automation*, 2249–54, 2011.

- J.A. Gallego, E.Rocon, A.D. Koutsou, J.L. Pons. Analysis of kinematic data in pathological tremor with the Hilbert-Huang Transform. *Proceedings of 5th International IEEE/EMBS Conference on Neural Engineering*, 80–83, 2011.

- J.A. Gallego, E. Rocon, A.D. Koutsou, J. Ibáñez, L.J. Barrios, A.R. Victoria, J.I. Serrano, M.D. del Castillo, J.M. Belda-Lois, S. Mena, J.L. Pons. Monitorización y supresión del temblor mediante un neurorrobot blando. *Actas de las XXXI Jornadas de Automática*, 2010.

- E. Rocon, J.A. Gallego, L. Barrios, A.R. Victoria, J. Ibáñez, D. Farina, F. Negro, J.L. Dideriksen, S. Conforto, T. DAlessio, G. Severini, G. Grimaldi, M. Manto, J.L. Pons. Multimodal BCI-mediated FES suppression of tremor. *Proceedings of 2010 Annual International Conference of the IEEE Engineering in Medicine and Biology Society*, 3337–40, 2010.

- J.A. Gallego, E. Rocon, A.R. Victoria, J. Ibáñe, L. Barrios, D. Farina, F. Negro, S. Conforto, T. DAlessio, G. Severini, G. Grimaldi, M. Manto, J.L. Pons. Brain Neural Computer Interface for tremor identification, characterization and tracking.

Abstracts of the XVIII Congress of the International Society of Electrophysiology and Kinesiology, 2010 [Abstract].

- J.A. Gallego, E. Rocon, J.L. Pons. Estimation of instantaneous tremor parameters for FES-based tremor suppression. *Proceedings of the 2010 IEEE International Conference on Robotics and Automation*, 2922–27, 2010.
- A.D. Koutsou, J.A. Gallego, E. Rocon, J.C. Moreno. Aplicaciones neuroprotésicas en compensación y recuperación funcional. *Actas del VI Seminario Internacional Biomecńica e Ingeniería de Rehabilitación*, 2010.
- J.A. Gallego, E. Rocon, J.C. Moreno, A.D. Koutsou, J.L. Pons. On the use of inertial measurement units for real-time quantification of pathological tremor amplitude and frequency. *Procedia Chemistry - Proceedings of the Eurosensors XXIII Conference*, 1(1): 1219–22, 2009.
- J.A. Gallego, E. Rocon, A.D. Koutsou, A.R. Victoria, J.O. Roa, L.J. Barrios, J.L. Pons. Caracterización y compensación del temblor patológico mediante Brain Neural Computer Interface. *Actas de las XXX Jornadas de Automática*, 2009.
- A.D. Koutsou, J.C. Moreno, J.A. Gallego, E. Rocon, J.L. Pons. Estimulación Eléctrica Funcional en rehabilitación: introducción, aplicaciones, futuro. *Actas de las XXX Jornadas de Automática*, 2009.
- J.L. Pons, J.A. Gallego, E. Rocon, L.J. Barrios. A multimodal approach to BCI in TREMOR project. *Actas del Simposio CEA de Bioingeniera 2009.*

Conference publications in topics other than those included in this dissertation:

- A. Frizera, R. Ceres, J.L. Pons, E. Rocon, J.A. Gallego. Estimación continua de cadencia a través de la interacción de fuerzas en marcha asistida por andador. *Actas de las XXXI Jornadas de Automática*, 2010.
- A.D. Koutsou, J.C. Moreno J.L. Pons, J.A. Gallego, E. Rocon. Muscle selectivity algorithm for superficial matrix electrodes. *9^{th} International Symposium Computer Methods in Biomechanics and Biomedical Engineering*, 2010.
- J.C. Moreno, F. Brunetti, J.A. Gallego, J.L. Pons. Inertial sensing-based method for characterization of activities with walking assistive devices. *Proceedings of the XXII Eurosensors Conference*, 2009.

In summary, the work presented in this dissertation has produced nine journal publications (plus another that will be soon submitted), twenty two contributions to international conferences (plus another one has been recently submitted), five to national

conferences, and contributed to two book chapters. Moreover, the work on tremor suppression with the NP received the "Highest potential impact" award at the IEEE EMBS Unconference in Rehabilitation Robotics (held in the framework of the 34$^{\text{th}}$ Annual International Conference of the IEEE Engineering in Medicine and Biology Society, San Diego, USA, August, 2012). This award recognized the potential of the NP as a solution for the functional compensation of tremor during daily living.

6.3 Future Work

The methods developed in this thesis, and the results obtained, serve to define my future research lines. Some of the topics considered are related to questions that arose during the realization or the interpretation of the results presented herein, while others are studies planned as the continuation to those presented in this dissertation.

The first topic is the implementation of a new prototype of the NP that enables the realization of clinical trials involving a large cohort of patients. To this end, the Bioengineering Group is establishing, together with a leading company in the field of orthotics, and a team of neurologists with a strong background on tremor based at Hospital 12 de Octubre (Madrid), an adequate framework for these trials. The steps foreseen are:

1. The development and validation of a methodology to select adequately the gains of the controller, which will be later expanded to detect automatically the appearance of accommodation to neurostimulation. This methodology may rely on a simplified model of joint dynamics as the one utilized here.

2. The implementation of a pHMI that targets more muscles in the forearm, as a means to achieve a more robust suppression of the tremor. It is expected that this will enhance tremor suppression during the performance of ADLs. Notice that the incorporation of the controller here proposed is immediate.

3. The integration of high-density sEMG in the controller of the NP as a means to identify the tremorogenic muscles at the forearm, and thus define the optimal stimulation loci, minimizing the interference with the performance of ADLs.

4. To recruit a large cohort of patients, and perform the clinical and functional validation of the NP, assessing the long term outcome of the intervention.

The findings related to tremor physiology (presented in Chapter §5), the results obtained by applying EEMD to the kinematic tremor time series (see Chapter §2), and the knowledge gathered during the development and validation of the mHMI, also motivate research to elucidate the role of the different mechanisms that participate in tremorogenesis. Briefly, a few of the studies planned are:

1. The investigation of whether multiple tremor oscillators are projected to muscles in different limbs, synergistic and antagonist muscles, or even to different compartments in the same muscle. To this end, I will assess the common input strength using the same methodology employed in Chapter §5. The results will be also compared to the outcome of applying EEMD to the kinematic tremor data.

2. To assess the role of afferent inputs in the manifestation of tremor. This will be achieved by designing an adequate experimental protocol, probably involving controlled ischemia or limb cooling, in combination with a computational model of tremor the reproduces the main mechanisms causing it.

3. To develop a neuromusculoskeletal model that represents the mechanisms that mediate tremor attenuation through mechanical loading.

The observation of the apparent importance of afferent inputs in the manifestation of tremor also sets the basis for the development of a novel intervention for tremor suppression, which is currently under investigation. This intervention will be also implemented in a NP, but will rely on the application of sensory stimulation as a means to disrupt the afferent flow of information, and alleviate the tremor. The delivery of sensory and not mechanical stimulation will immediately meet the design requirements here defined. Another alternative, which will be also evaluated with the same NP, is the delivery of sensory stimulation with the intention of reaching the supraspinal centers, and desynchronizing the tremorogenic network that generates the tremor. The latter hypothesis originates from the results recently obtained with spinal cord stimulation in rodent models of PD, and is likely to be more challenging to implement.

The work on tremor physiology and the novel interventions for tremor suppression is being performed in the framework of project NeuroTREMOR[2], recently funded by the EU Commission (FP7-2011-287739).

[2]NeuroTREMOR project website: http://neurotremor.eu/.

Bibliography

S. L. Aaron and R. B. Stein. Comparison of an emg-controlled prosthesis and the normal human biceps brachii muscle. *Am J Phys Med*, 55(1):1–14, Feb 1976.

B. D. Adelstein. Peripheral mechanical loading and the mechanism of abnormal intention tremor. Master's thesis, Massachusetts Institute of Technology, 1981.

T. Agari and I. Date. Spinal cord stimulation for the treatment of abnormal posture and gait disorder in patients with parkinson's disease. *Neurol Med Chir (Tokyo)*, 52(7):470–474, 2012.

S. Agarwal, R. Kobetic, S. Nandurkar, and E. B. Marsolais. Functional electrical stimulation for walking in paraplegia: 17-year follow-up of 2 cases. *J Spinal Cord Med*, 26(1):86–91, 2003.

M. L. Aisen, B. D. Adelstein, J. Romero, A. Morris, and M. Rosen. Peripheral mechanical loading and the mechanism of the tremor of chronic alcoholism. *Arch Neurol*, 49(7):740–742, Jul 1992.

M. L. Aisen, A. Arnold, I. Baiges, S. Maxwell, and M. Rosen. The effect of mechanical damping loads on disabling action tremor. *Neurology*, 43(7):1346–1350, Jul 1993.

G. E. Alexander, M. R. DeLong, and P. L. Strick. Parallel organization of functionally segregated circuits linking basal ganglia and cortex. *Annu Rev Neurosci*, 9:357–381, 1986.

H. Allain, S. Schuck, and N. Mauduit. Depression in parkinson's disease. *BMJ*, 320(7245): 1287–1288, May 2000.

G Alon and G. V. Smith. Tolerance and conditioning to neuro–muscular electrical stimulation within and between sessions and gender. *Journal of Sports Science and Medicine*, 4:395–405, 2005.

W. T. Ang, M. Krichane, and T. Sim. Zero phase filtering for active compensation of periodic physiological motion. In *Biomedical Robotics and Biomechatronics, 2006. BioRob 2006. The First IEEE/RAS-EMBS International Conference on*, pages 182 –187, feb. 2006.

N. Archibald and D. Burn. Parkinson's disease. *Medicine*, 36(12):630–635, December 2008. ISSN 13573039.

A. Arnold and M. Rosen. Evaluation of a controlled-energy-dissipation orthosis for tremor suppression. *Journal of Electromyography and and Kinesiology*, 13(3):131–148, 1993.

J. E. Axelrad, E. D. Louis, L. S. Honig, I. Flores, G. W. Ross, et al. Reduced purkinje cell number in essential tremor: a postmortem study. *Arch Neurol*, 65(1):101–107, Jan 2008.

J.P. Bach, U. Ziegler, G. Deuschl, R. Dodel, and G. Doblhammer-Reiter. Projected numbers of people with movement disorders in the years 2030 and 2050. *Mov Disord*, 26(12):2286–2290, Oct 2011.

O. Bai, V. Rathi, P. Lin, D. Huang, H. Battapady, et al. Prediction of human voluntary movement before it occurs. *Clin Neurophysiol*, 122(2):364–372, 2011.

P. Bain, M. Brin, G. Deuschl, R. Elble, J. Jankovic, et al. Criteria for the diagnosis of essential tremor. *Neurology*, 54(11 Suppl 4):S7, 2000.

P. G. Bain. The management of tremor. *J Neurol Neurosurg Psychiatry*, 72 Suppl 1:I3–I9, Mar 2002.

J. R. Baker, N. J. Davey, P. H. Ellaway, and C. L. Friedland. Short-term synchrony of motor unit discharge during weak isometric contraction in parkinson's disease. *Brain*, 115 Pt 1:137–154, Feb 1992.

Y. Bar-Shalom and X. R. Li. *Estimation and tracking: Principles, techniques and software.* Artech House Publishers, 1998.

A. L. Bartels and K. L Leenders. Parkinson's disease: the syndrome, the pathogenesis and pathophysiology. *Cortex; a journal devoted to the study of the nervous system and behavior*, 45(8):915–21, September 2009. ISSN 0010-9452.

J. M. Belda-Lois, A. I. Martinez-Reyero, A. Castillo, E. Rocon, J. L. Pons, et al. Controllable mechanical tremor reduction. assessment of two orthoses. *Technology and Disability*, 19(4): 169–178, 2007a.

J. M. Belda-Lois, S. Mena-del Horno, I. Bermejo, A. Castillo, and J. Sancho. A biomechanical model for pathological tremor suppression. In *Proceedings of the International Conference on NeuroRehabilitation*, 2012.

J. M. Belda-Lois, A. Page, J. M. Baydal-Bertomeu, R. Poveda, and R. Barberà. *Rehabilitation robotics*, chapter Biomehcanical constraints in the design of robotic systems for tremor suppression. InTech Education and Publishing, 2007b.

J. M. Belda-Lois, E. Rocon, J. J. Sánchez-Lacuesta, A. F. Ruiz, and J. L. Pons. Functional assessment of tremor in the upper limb. In *Int J Rehabil Res*, volume 27, page 62, 2005.

T. S. Benamer, J. Patterson, D. G. Grosset, J. Booij, K. de Bruin, et al. Accurate differentiation of parkinsonism and essential tremor using visual assessment of [123I]-FP-CIT SPECT imaging: the [123I]-FP-CIT study group. *Mov Disord*, 15(3):503–510, May 2000.

T. R. Benedict and G. W. Bordner. Synthesis of an optimal track-while-scan smoothing equations. *IRE Trans Automat Control*, 7(4):27–32, 1962.

J. Benito-León, F. Bermejo-Pareja, J. M. Morales, S. Vega, and J. A. Molina. Prevalence of essential tremor in three elderly populations of central spain. *Mov Disord*, 18(4):389–394, Apr 2003.

J. Benito-León and E. D. Louis. Essential tremor: emerging views of a common disorder. *Nature clinical practice. Neurology*, 2(12):666–78;, 2006. ISSN 1745-834X.

H. Bergman and G. Deuschl. Pathophysiology of parkinson's disease: from clinical neurology to basic neuroscience and back. *Mov Disord*, 17 Suppl 3:S28–S40, 2002.

F. Bermejo-Pareja. Essential tremor–a neurodegenerative disorder associated with cognitive defects? *Nat Rev Neurol*, 7(5):273–282, May 2011.

M. Bilodeau, D. A. Keen, P. J. Sweeney, R. W. Shields, and R. M. Enoka. Strength training can improve steadiness in persons with essential tremor. *Muscle Nerve*, 23(5):771–778, May 2000.

B. Blankertz, G. Dornhege, S. Lemm, M. Krauledat, G. Curio, and K. R. Müller. The Berlin brain-computer interface: Machine learning based detection of user specific brain states. *Journal of Universal Computer Science*, 12:581–607, 2006.

A. P. L. Bo, P. Poignet, and C. Geny. Pathological tremor and voluntary motion modeling and online estimation for active compensation. *IEEE Trans Neural Syst Rehabil Eng*, 19(2): 177–185, Apr 2011.

H. Boecker and D. J. Brooks. Functional imaging of tremor. *Mov Disord*, 13 Suppl 3:64–72, 1998.

M. J. Broadhurst and C. W. Stammers. Mechanical feeding aids for patients with ataxia: design considerations. *J Biomed Eng*, 12(3):209–214, May 1990.

E. Brookner. *Tracking and Kalman Filtering made easy*. John Wiley & Sons, Ltd, 1998.

S. F. Bucher, K. C. Seelos, R. C. Dodel, M. Reiser, and W. H. Oertel. Activation mapping in essential tremor with functional magnetic resonance imaging. *Ann Neurol*, 41(1):32–40, Jan 1997.

E. Burdet, R. Osu, D. W. Franklin, T. E. Milner, and M. Kawato. The central nervous system stabilizes unstable dynamics by learning optimal impedance. *Nature*, 414(6862):446–449, Nov 2001.

P. R. Cavanagh and P. V. Komi. Electromechanical delay in human skeletal muscle under concentric and eccentric contractions. *Eur J Appl Physiol Occup Physiol*, 42(3):159–163, Nov 1979.

J. N. Caviness, H. A. Shill, M. N. Sabbagh, V. G. H. Evidente, J. L. Hernandez, and C. H. Adler. Corticomuscular coherence is increased in the small postural tremor of parkinson's disease. *Mov Disord*, 21(4):492–499, Apr 2006.

R. A. Chase, J. K. Cullen, Jr, S. A. Sullivan, and A. K. Ommaya. Modification of intention tremor in man. *Nature*, 206(983):485–487, May 1965.

P. Cheng and B. B. Oelmann. Joint-angle measurement using accelerometers and gyroscopes: A survey. *IEEE Transactions on Instrumentation and Measurement*, 59(2):404–414, 2010.

C. N. Christakos, S. Erimaki, E. Anagnostou, and D. Anastasopoulos. Tremor-related motor unit firing in parkinson's disease: implications for tremor genesis. *J Physiol*, 587(Pt 20):4811–4827, 2009.

K. L. Collins, E. M. Lehmann, and P. G. Patil. Deep brain stimulation for movement disorders. *Neurobiol Dis*, 38(3):338–345, 2010.

B. A. Conway, D. M. Halliday, S. F. Farmer, U. Shahani, P. Maas, et al. Synchronization between motor cortex and spinal motoneuronal pool during the performance of a maintained motor task in man. *J Physiol*, 489 (Pt 3):917–924, 1995.

C. Cooper, V. G. Evidente, J. G. Hentz, C. H. Adler, J. N. Caviness, and K. Gwinn-Hardy. The effect of temperature on hand function in patients with tremor. *J Hand Ther*, 13(4):276–288, 2000.

L. H. Craig, A. Svircev, M. Haber, and J. L. Juncos. Controlled pilot study of the effects of neuromuscular therapy in patients with parkinson's disease. *Mov Disord*, 21(12):2127–2133, Dec 2006.

J. F. Daneault, B. Carignan, and C. Duval. Finger tremor can be voluntarily reduced during a tracking task. *Brain Research*, 1370(0):164 – 174, 2011. ISSN 0006-8993.

S. E. Daniel and A. J. Lees. Parkinson's disease society brain bank, london: overview and research. *J Neural Transm Suppl*, 39:165–172, 1993.

A. Das Gupta. Paired response of motor units during voluntary contraction in parkinsonism. *J Neurol Neurosurg Psychiatry*, 26:265–268, 1963.

N. J. Davey, P. H. Ellaway, and R. B. Stein. Statistical limits for detecting change in the cumulative sum derivative of the peristimulus time histogram. *J Neurosci Methods*, 17(2-3): 153–166, 1986.

C. J. De Luca and Z. Erim. Common drive of motor units in regulation of muscle force. *Trends Neurosci*, 17(7):299–305, Jul 1994.

D. De Rossi and P. Veltink. Wearable technology for biomechanics: e-textile or micromechanical sensors? *IEEE Eng Med Biol Mag*, 29(3):37–43, 2010.

L. Defebvre, J. L. Bourriez, P. Derambure, A. Duhamel, J. D. Guieu, and A. Destee. Influence of chronic administration of l-dopa on event-related desynchronization of mu rhythm preceding voluntary movement in parkinson's disease. *Electroencephalogr Clin Neurophysiol*, 109(2): 161–167, 1998.

E. F. Delagi, A. O. Perotto, J. Iazzetti, and D. Morrison. *Anatomical guide for the electromyographer: the limbs and the trunk*. Charles C. Thomas Publisher, Ltd, 4th edition, 2005.

R. Dengler, W. Wolf, M. Schubert, and A. Struppler. Discharge pattern of single motor units in basal ganglia disorders. *Neurology*, 36(8):1061–1066, 1986.

P. Derambure, L. Defebvre, K. Dujardin, J. L. Bourriez, J. M. Jacquesson, et al. Effect of aging on the spatio-temporal pattern of event-related desynchronization during a voluntary movement. *Electroencephalogr Clin Neurophysiol*, 89(3):197–203, 1993.

G. Deuschl, P. Bain, and M. Brin. Consensus statement of the movement disorder society on tremor. ad hoc scientific committee. *Mov Disord*, 13 Suppl 3:2–23, 1998.

G. Deuschl and R. Elble. Essential tremor–neurodegenerative or nondegenerative disease towards a working definition of et. *Mov Disord*, 24(14):2033–2041, Oct 2009.

G. Deuschl, F. Papengut, and H. Hellriegel. The phenomenology of parkinsonian tremor. *Parkinsonism Relat Disord*, 18 Suppl 1:S87–S89, Jan 2012.

G. Deuschl, J. Raethjen, R. Baron, M. Lindemann, H. Wilms, and P. Krack. The pathophysiology of parkinsonian tremor: a review. *J Neurol*, 247 Suppl 5:V33–V48, Sep 2000a.

G. Deuschl, J. Raethjen, H. Hellriegel, and R. Elble. Treatment of patients with essential tremor. *Lancet Neurol*, 10(2):148–161, Feb 2011.

G. Deuschl, J. Raethjen, M. Lindemann, and P. Krack. The pathophysiology of tremor. *Muscle & Nerve*, 24:716–735, 2001.

G. Deuschl, R. Wenzelburger, K. Löffler, J. Raethjen, and H. Stolze. Essential tremor and cerebellar dysfunction clinical and kinematic analysis of intention tremor. *Brain*, 123 (Pt 8): 1568–1580, Aug 2000b.

J. L. Dideriksen, D. Falla, M. Baekgaard, M. L. Mogensen, K. L. Steimle, and D. Farina. Comparison between the degree of motor unit short-term synchronization and recurrence quantification analysis of the surface emg in two human muscles. *Clin Neurophysiol*, 120(12): 2086–2092, Dec 2009.

J. L. Dideriksen, D. Farina, and R. M. Enoka. Influence of fatigue on the simulated relation between the amplitude of the surface electromyogram and muscle force. *Philos Transact A Math Phys Eng Sci*, 368(1920):2765–2781, 2010.

J. L. Dideriksen, F. Gianfelici, L. Z. P. Maneski, and D. Farina. EMG-based characterization of pathological tremor using the iterated hilbert transform. *IEEE Trans Biomed Eng*, 58(10): 2911–2921, 2011.

V. Dietz, W. Hillesheimer, and H. J. Freund. Correlation between tremor, voluntary contraction, and firing pattern of motor units in parkinson's disease. *J Neurol Neurosurg Psychiatry*, 37 (8):927–937, 1974.

S. Dosen and D. B. Popovic. Accelerometers and force sensing resistors for optimal control of walking of a hemiplegic. *IEEE Trans Biomed Eng*, 55(8):1973–1984, Aug 2008.

R. J. Elble. Physiologic and essential tremor. *Neurology*, 36(2):225–231, Feb 1986.

R. J Elble. Central mechanisms of tremor. *Journal of Clinical Neurophysiology*, 13(2):133–44, 1996.

R. J. Elble. Origins of tremor. *Lancet*, 355(9210):1113–1114, 2000.

R. J. Elble. Tremor: clinical features, pathophysiology, and treatment. *Neurologic Clinics*, 27: 679–695, 2009.

R. J. Elble, C. Higgins, and L. Hughes. Longitudinal study of essential tremor. *Neurology*, 42 (2):441–443, Feb 1992.

R. J. Elble, C. Higgins, and C. J. Moody. Stretch reflex oscillations and essential tremor. *J Neurol Neurosurg Psychiatry*, 50(6):691–698, Jun 1987.

R. J. Elble, R. Sinha, and C. Higgins. Quantification of tremor with a digitizing tablet. *Journal of Neuroscience Methods*, 32:193–98, 1990.

R. J. Elble and Tremor Research Group. Report from a u.s. conference on essential tremor. *Mov Disord*, 21(12):2052–2061, Dec 2006.

J. M. Elek, R. Dengler, A. Konstanzer, S. Hesse, and W. Wolf. Mechanical implications of paired motor unit discharges in pathological and voluntary tremor. *Electroencephalogr Clin Neurophysiol*, 81(4):279–283, 1991.

P. H. Ellaway. Cumulative sum technique and its application to the analysis of peristimulus time histograms. *Electroencephalogr Clin Neurophysiol*, 45(2):302–304, 1978.

S. Fahn, D. Oakes, I. Shoulson, K. Kieburtz, A. Rudolph, et al. Levodopa and the progression of parkinson's disease. *N Engl J Med*, 351(24):2498–2508, Dec 2004.

S. Fahn and the Parkinson Study Group. Does levodopa slow or hasten the rate of progression of parkinson's disease? *J Neurol*, 252 Suppl 4:IV37–IV42, Oct 2005.

S. Fahn, E. Tolosa, and C. Marin. *Parkinson's Disease and Movement Disorders*, chapter Clinical rating scale for tremor, pages 225–234. Urban & Schwarzenberg, 1998.

D. Farina, A. Holobar, R. Merletti, and R. M. Enoka. Decoding the neural drive to muscles from the surface electromyogram. *Clin Neurophysiol*, 121(10):1616–1623, Oct 2010.

D. Farina, K. Yoshida, T. Stieglitz, and K. P. Koch. Multichannel thin-film electrode for intramuscular electromyographic recordings. *J Appl Physiol*, 104(3):821–827, 2008.

J. Favre, B. M. Jolles, R. Aissaoui, and K. Aminian. Ambulatory measurement of 3d knee joint angle. *J Biomech*, 41(5):1029–1035, 2008.

T. T. Fedorov. *Theory of optimal experiments*. Academic Press, 1972.

G Fénelon, C Goujon, J.M. Gurruchaga, P Cesaro, B Jarraya, et al. Spinal cord stimulation for chronic pain improved motor function in a patient with parkinson's disease. *Parkinsonism & Related Disorders*, 18(2):213–214, 2012. ISSN 1353-8020.

M. Ferrarin, F. Palazzo, R. Riener, and J. Quintern. Model-based control of fes-induced single joint movements. *Neural Systems and Rehabilitation Engineering, IEEE Transactions on*, 9 (3):245 –257, sept. 2001. ISSN 1534-4320.

P. Feys, W. Helsen, X. Liu, D. Mooren, H. Albrecht, et al. Effects of peripheral cooling on intention tremor in multiple sclerosis. *J Neurol Neurosurg Psychiatry*, 76(3):373–379, Mar 2005.

P. Feys, W. F. Helsen, A. Lavrysen, B. Nuttin, and P. Ketelaer. Intention tremor during manual aiming: a study of eye and hand movements. *Mult Scler*, 9(1):44–54, Feb 2003.

P. Feys, W. F. Helsen, S. Verschueren, S. P. Swinnen, I. Klok, et al. Online movement control in multiple sclerosis patients with tremor: effects of tendon vibration. *Mov Disord*, 21(8): 1148–1153, Aug 2006.

S. R. Filipovic, J. C. Rothwell, and K. Bhatia. Low-frequency repetitive transcranial magnetic stimulation and off-phase motor symptoms in parkinson's disease. *J Neurol Sci*, 291(1-2):1–4, Apr 2010.

E. Florin, J. Gross, C. Reck, M. Maarouf, A. Schnitzler, et al. Causality between local field potentials of the subthalamic nucleus and electromyograms of forearm muscles in parkinson's disease. *Eur J Neurosci*, 31(3):491–498, Feb 2010.

H. Forssberg, P. E. Ingvarsson, N. Iwasaki, R. S. Johansson, and A. M. Gordon. Action tremor during object manipulation in parkinson's disease. *Mov Disord*, 15(2):244–254, Mar 2000.

A. Frizera Neto, J. A. Gallego, E. Rocon, J. L. Pons, and R. Ceres. Extraction of user's navigation commands from upper body force interaction in walker assisted gait. *Biomed Eng Online*, 9: 37, 2010.

R. Fuentes, P. Petersson, W. B. Siesser, M. G. Caron, and M. A. L. Nicolelis. Spinal cord stimulation restores locomotion in animal models of parkinson's disease. *Science*, 323(5921): 1578–1582, Mar 2009.

J. A. Gallego, J. L. Dideriksen, D. Farina, E. Rocon, A. Holobar, and J. L. Pons. A modelling study on transmission of the central oscillator in tremor by a motor neuron pool. In *Proc. Annual Int Engineering in Medicine and Biology Society,EMBC Conf. of the IEEE*, pages 2037–2040, 2011a.

J. A. Gallego, E. Rocon, J. M. Belda-Lois, and J. L. Pons. A neuroprosthesis for tremor management through the control of muscle co-contraction. *J Neuroeng Rehabil*, 10(1):36, Apr 2013.

J. A. Gallego, E. Rocon, A. D. Koutsou, and J. L. Pons. Analysis of kinematic data in pathological tremor with the hilbert-huang transform. In *Proc. 5th Int Neural Engineering (NER) IEEE/EMBS Conf*, pages 80–83, 2011b.

J. A. Gallego, E. Rocon, and J. L. Pons. Estimation of instantaneous tremor parameters for fes-based tremor suppression. In *Proc. IEEE Int Robotics and Automation (ICRA) Conf*, pages 2922–2927, 2010a.

J. A. Gallego, E. Rocon, J. O. Roa, J. C. Moreno, and J. L. Pons. Real-time estimation of pathological tremor parameters from gyroscope data. *Sensors*, 10(3):2129–2149, 2010b.

J.A. Gallego, J. Ibanez, J.L. Dideriksen, J.I. Serrano, M.D. del Castillo, et al. A multimodal human-robot interface to drive a neuroprosthesis for tremor management. *Systems, Man, and Cybernetics, Part C: Applications and Reviews, IEEE Transactions on*, 42(6):1159–1168, 2012.

S. C. Gandevia. Spinal and supraspinal factors in human muscle fatigue. *Physiol Rev*, 81(4): 1725–1789, 2001.

T. Gasser. Genetics of parkinson's disease. *Ann Neurol*, 44(3 Suppl):S53–7, 1998.

W. F. Genadry, R. E. Kearney, and I. W. Hunter. Dynamic relationship between emg and torque at the human ankle: variation with contraction level and modulation. *Med Biol Eng Comput*, 26(5):489–496, Sep 1988.

W. Gerstner and W. M. Kistler. *Spiking neuron models. Single neurons, populations, plasticity.* Cambridge University Press, 2002.

F. Gianfelici, G. Biagetti, P. Crippa, and C. Turchetti. Multicomponent am–fm representations: An asymptotically exact approach. *IEEE Transactions on Audio, Speech, and Language Processing*, 15(3):823–837, 2007.

P. T. Gibbs and H. H. Asada. Wearable conductive fiber sensors for multi-axis human joint angle measurements. *J Neuroeng Rehabil*, 2(1):7, Mar 2005.

D. Gijbels, I. Lamers, L. Kerkhofs, G. Alders, E. Knippenberg, and P. Feys. The armeo spring as training tool to improve upper limb functionality in multiple sclerosis: a pilot study. *J Neuroeng Rehabil*, 8:5, 2011.

N. Giladi, R. Kao, and S. Fahn. Freezing phenomenon in patients with parkinsonian syndromes. *Mov Disord*, 12(3):302–305, May 1997.

D. M. Gillard, T. Cameron, A. Prochazka, and M. J. Gauthier. Tremor suppression using functional electrical stimulation: a comparison between digital and analog controllers. *IEEE Trans Rehabil Eng*, 7(3):385–388, Sep 1999.

M. Gomez-Rodriguez, M. Grosse-Wentrup, J. Hill, A. Gharabaghi, B. Scholkopf, and J. Peters. Towards brain-robot interfaces in stroke rehabilitation. In *Proc. IEEE Int Rehabilitation Robotics (ICORR) Conf*, pages 1–6, 2011.

J. G. Gonzalez, E. A. Heredia, T. Rahman, K. E. Barner, and G. R. Arce. Optimal digital filtering for tremor suppression. *IEEE Trans Biomed Eng*, 47(5):664–673, 2000.

M. H. Granat, A. C. Ferguson, B. J. Andrews, and M. Delargy. The role of functional electrical stimulation in the rehabilitation of patients with incomplete spinal cord injury–observed benefits during gait studies. *Paraplegia*, 31(4):207–215, Apr 1993.

C. T. Haas, S. Turbanski, K. Kessler, and D. Schmidtbleicher. The effects of random whole-body-vibration on motor symptoms in parkinson's disease. *NeuroRehabilitation*, 21(1):29–36, 2006.

D. M. Halliday, J. R. Rosenberg, A. M. Amjad, P. Breeze, B. A. Conway, and S. F. Farmer. A framework for the analysis of mixed time series/point process data–theory and application to the study of physiological tremor, single motor unit discharges and electromyograms. *Prog Biophys Mol Biol*, 64(2-3):237–278, 1995.

C. Hammond, H. Bergman, and P. Brown. Pathological synchronization in parkinson's disease: networks, models and treatments. *Trends Neurosci*, 30(7):357–364, Jul 2007.

S. Hara, Y. Yamamoto, T. Omata, and M. Nakano. Repetitive control system: a new type servo system for periodic exogenous signals. *Automatic Control, IEEE Transactions on*, 33(7):659 –668, jul 1988. ISSN 0018-9286.

T. Harada, H. Uchino, T. Mori, and T. Sato. Portable orientation estimation device based on accelerometers, magnetometers and gyroscope sensors for sensor network. In *Proc. IEEE International Conference on MFI2003 Multisensor Fusion and Integration for Intelligent Systems*, pages 191–196, 30 July–1 Aug. 2003.

G-M. Hariz and L. Forsgren. Activities of daily living and quality of life in persons with newly diagnosed parkinson's disease according to subtype of disease, and in comparison to healthy controls. *Acta Neurol Scand*, 123(1):20–27, Jan 2011.

B. Hellwig, S. Häussler, B. Schelter, M. Lauk, B. Guschlbauer, et al. Tremor-correlated cortical activity in essential tremor. *Lancet*, 357(9255):519–523, 2001.

B. Hellwig, P. Mund, B. Schelter, B. Guschlbauer, J. Timmer, and C. H. Lücking. A longitudinal study of tremor frequencies in parkinson's disease and essential tremor. *Clin Neurophysiol*, 120(2):431–435, Feb 2009.

B. Hellwig, B. Schelter, B. Guschlbauer, J. Timmer, and C. H. Lücking. Dynamic synchronisation of central oscillators in essential tremor. *Clin Neurophysiol*, 114(8):1462–1467, Aug 2003.

M. E. Héroux, G. Pari, and K. E. Norman. The effect of inertial loading on wrist postural tremor in essential tremor. *Clin Neurophysiol*, 120(5):1020–1029, May 2009.

M. E. Héroux, G. Pari, and K. E. Norman. The effect of contraction intensity on force fluctuations and motor unit entrainment in individuals with essential tremor. *Clin Neurophysiol*, 121(2): 233–239, Feb 2010.

M. E. Héroux, G. Pari, and K. E. Norman. The effect of inertial loading on wrist kinetic tremor and rhythmic muscle activity in individuals with essential tremor. *Clin Neurophysiol*, 122(9): 1794–1801, Sep 2011.

J. Herzog, W. Hamel, R. Wenzelburger, M. Pötter, M. O. Pinsker, et al. Kinematic analysis of thalamic versus subthalamic neurostimulation in postural and intention tremor. *Brain*, 130 (Pt 6):1608–1625, Jun 2007.

R. L. Hewer, R. Cooper, and M. H. Morgan. An investigation into the value of treating intention tremor by weighting the affected limb. *Brain*, 95(3):579–590, 1972.

A. V. Hill. The heat of shortening and the dynamic constants of muscle. *Proc R Soc Lond B*, 126:136–195, 1938.

B. Hjorth. An on-line transformation of eeg scalp potentials into orthogonal source derivations. *Electroencephalogr Clin Neurophysiol*, 39(5):526–530, 1975.

N. Hogan. Adaptive control of mechanical impedance by coactivation of antagonist muscles. *Automatic Control, IEEE Transactions on*, 29(8):681 – 690, aug 1984. ISSN 0018-9286.

A. Holobar, D. Farina, M. Gazzoni, R. Merletti, and D. Zazula. Estimating motor unit discharge patterns from high-density surface electromyogram. *Clin Neurophysiol*, 120(3):551–562, Mar 2009.

A. Holobar, V. Glaser, J. A. Gallego, J. L. Dideriksen, and D. Farina. Non-invasive characterization of motor unit behaviour in pathological tremor. *J Neural Eng*, 9(5):056011, Oct 2012.

A. Holobar, M. A. Minetto, A. Botter, F. Negro, and D. Farina. Experimental analysis of accuracy in the identification of motor unit spike trains from high-density surface emg. *IEEE Trans Neural Syst Rehabil Eng*, 18(3):221–229, Jun 2010.

A. Holobar and D. Zazula. Multichannel blind source separation using convolution kernel compensation. *Signal Processing, IEEE Transactions on*, 55(9):4487 –4496, sept. 2007. ISSN 1053-587X.

V. Hömberg, H. Hefter, K. Reiners, and H. J. Freund. Differential effects of changes in mechanical limb properties on physiological and pathological tremor. *J Neurol Neurosurg Psychiatry*, 50 (5):568–579, May 1987.

S. E. Hua and F. A. Lenz. Posture-related oscillations in human cerebellar thalamus in essential tremor are enabled by voluntary motor circuits. *J Neurophysiol*, 93(1):117–127, Jan 2005.

S. E. Hua, F. A. Lenz, T. A. Zirh, S. G. Reich, and P. M. Dougherty. Thalamic neuronal activity correlated with essential tremor. *J Neurol Neurosurg Psychiatry*, 64(2):273–276, Feb 1998.

N. E. Huang, Z. Shen, S. R. Long, M. C. Wu, H. H. Shih, et al. The empirical mode decomposition and the Hilbert spectrum for nonlinear and non-stationary time series analysis. *Proceedings of the Royal Society of London A*, 454:903–995, 1998.

I. W. Hunter and R. E. Kearney. Dynamics of human ankle stiffness: variation with mean ankle torque. *J Biomech*, 15(10):747–752, 1982.

J. M. Hurtado, C. M. Gray, L. B. Tamas, and K. A. Sigvardt. Dynamics of tremor-related oscillations in the human globus pallidus: a single case study. *Proc Natl Acad Sci U S A*, 96 (4):1674–1679, Feb 1999.

J. M. Hurtado, J. P. Lachaux, D. J. Beckley, C. M. Gray, and K. A. Sigvardt. Inter- and intralimb oscillator coupling in parkinsonian tremor. *Mov Disord*, 15(4):683–691, Jul 2000.

I-S. Hwang, C-C. K. Lin, and P-S. Wu. Tremor modulation in patients with parkinson?s disease compared to healthy counterparts during loaded postural holding. *Journal of Electromyography and Kinesiology*, 19(6):e520 – e528, 2009. ISSN 1050-6411.

J. Ibáñez, J. I. Serrano, M.D. del Castillo, and L. Barrios. An asynchronous bmi system for online single-trial detection of movement intention. In *Proceedings of the 32nd Annual International Conference of the IEEE Engineering in Medicine and Biology Society*, 2010.

T. Isa, Y. Ohki, B. Alstermark, L. G. Pettersson, and S. Sasaki. Direct and indirect cortico-motoneuronal pathways and control of hand/arm movements. *Physiology (Bethesda)*, 22: 145–152, Apr 2007.

B. T. Iwamuro, E. G. Cruz, Lauri L. L. Connelly, H. C. Fischer, and D. G. Kamper. Effect of a gravity-compensating orthosis on reaching after stroke: evaluation of the therapy assistant wrex. *Arch Phys Med Rehabil*, 89(11):2121–2128, Nov 2008.

A. Jacks, A. Prochazka, and P. S. Trend. Instability in human forearm movements studied with feed-back-controlled electrical stimulation of muscles. *J Physiol*, 402:443–461, Aug 1988.

J. Jankovic and L. G. Aguilar. Current approaches to the treatment of parkinson's disease. *Neuropsychiatr Dis Treat*, 4(4):743–757, Aug 2008.

M. Javidan, J. Elek, and A. Prochazka. Attenuation of pathological tremors by functional electrical stimulation. II: Clinical evaluation. *Ann Biomed Eng*, 20(2):225–236, 1992.

S. Jezernik, G. Colombo, T. Keller, H. Frueh, and M. Morari. Robotic orthosis lokomat: a rehabilitation and research tool. *Neuromodulation*, 6(2):108–115, Apr 2003.

F. J. Jiménez-Jiménez, E. García-Martín, O. Lorenzo-Betancor, P. Pastor, H. Alonso-Navarro, and J. A. G. Agúndez. Lingo1 and risk for essential tremor: results of a meta-analysis of rs9652490 and rs11856808. *J Neurol Sci*, 317(1-2):52–57, Jun 2012.

H. L. Journée. Demodulation of amplitude modulated noise: a mathematical evaluation of a demodulator for pathological tremor emg's. *IEEE Trans Biomed Eng*, 30(5):304–308, May 1983.

G. C. Joyce and P. M. H. Rack. The effects of load and force on tremor at the normal human elbow joint. *Journal of Physiology*, 240:375–396, 1974.

T. P. Jung, S. Makeig, C. Humphries, T. W. Lee, M. J. McKeown, et al. Removing electroencephalographic artifacts by blind source separation. *Psychophysiology*, 37(2):163–178, Mar 2000.

E. R. Kandel, J. H. Schwartz, and T. M. Jessell. *Principles of neural science*. McGraw-Hill Medical, 2000.

D. A. Keen and A. J. Fuglevand. Common input to motor neurons innervating the same and different compartments of the human extensor digitorum muscle. *J Neurophysiol*, 91(1):57–62, Jan 2004.

A. S. Khatter, M. C. Kurth, M. A. Brewer, C. T. Crinnian, J. F. Drazkowski, et al. Prevalence of tremor and parkinson's disease. *Parkinsonism Relat Disord*, 2(4):205–208, Oct 1996.

J-K. Kim and S. Sukkarieh. Airborne simultaneous localisation and map building. In *Robotics and Automation, 2003. Proceedings. ICRA '03. IEEE International Conference on*, volume 1, pages 406 – 411 vol.1, sept. 2003.

L. K. King, Q. J. Almeida, and H. Ahonen. Short-term effects of vibration therapy on motor impairments in parkinson's disease. *NeuroRehabilitation*, 25(4):297–306, 2009.

M. Kinoshita, T. Hitomi, M. Matsuhashi, T. Nakagawa, T. Nagamine, et al. How does voluntary movement stop resting tremor? *Clin Neurophysiol*, 121(6):983–985, 2010.

P. A. Kirkwood and T. A. Sears. The synaptic connexions to intercostal motoneurones as revealed by the average common excitation potential. *J Physiol*, 275:103–134, 1978.

C. Klein and M. G. Schlossmacher. The genetics of parkinson disease: Implications for neurological care. *Nat Clin Pract Neurol*, 2(3):136–146, Mar 2006.

G. Kleiner-Fisman, J. Herzog, D. N. Fisman, F. Tamma, K. E. Lyons, et al. Subthalamic nucleus deep brain stimulation: summary and meta-analysis of outcomes. *Mov Disord*, 21 Suppl 14: S290–S304, Jun 2006.

D. Kondziolka, J. G. Ong, J. Y. K. Lee, R. Y. Moore, J. C. Flickinger, and L. D. Lunsford. Gamma knife thalamotomy for essential tremor. *J Neurosurg*, 108(1):111–117, Jan 2008.

J. Kotovsky and M. J. Rosen. A wearable tremor-suppression orthosis. *J Rehabil Res Dev*, 35 (4):373–387, Oct 1998.

M. Lakie, E. G. Walsh, L. A. Arblaster, F. Villagra, and R. C. Roberts. Limb temperature and human tremors. *J Neurol Neurosurg Psychiatry*, 57(1):35–42, Jan 1994.

J. W. Langston, L. S. Forno, J. Tetrud, A. G. Reeves, J. A. Kaplan, and D. Karluk. Evidence of active nerve cell degeneration in the substantia nigra of humans years after 1-methyl-4-phenyl-1,2,3,6-tetrahydropyridine exposure. *Ann Neurol*, 46(4):598–605, 1999.

J. Laparra-Hernández, J. M. Belda-Lois, R. Paradiso, D. Popovic, and E. Rocon. Conceptual design of a fes system for tremor suppression. In *Abstracts of the XVIII Congress of the International Society of Electrophysiology and Kinesiology*, 2010.

M. Lauk, B. Köster, J. Timmer, B. Guschlbauer, G. Deuschl, and C. H. Lücking. Side-to-side correlation of muscle activity in physiological and pathological human tremors. *Clin Neurophysiol*, 110(10):1774–1783, Oct 1999.

M. A. Lebedev and M. A. L. Nicolelis. Brain-machine interfaces: past, present and future. *Trends Neurosci*, 29(9):536–546, Sep 2006.

R. N. Lemon. Descending pathways in motor control. *Annu Rev Neurosci*, 31:195–218, 2008.

L-D. Liao, C-Y. Chen, I-J. Wang, S-F. Chen, S-Y. Li, et al. Gaming control using a wearable and wireless eeg-based brain-computer interface device with novel dry foam-based sensors. *J Neuroeng Rehabil*, 9(1):5, 2012.

X. Liu, S. A. Tubbesing, T. Z. Aziz, R. C. Miall, and J. F. Stein. Effects of visual feedback on manual tracking and action tremor in parkinson's disease. *Exp Brain Res*, 129(3):477–481, Dec 1999.

R. Llinás and Y. Yarom. Oscillatory properties of guinea-pig inferior olivary neurones and their pharmacological modulation: an in vitro study. *J Physiol*, 376:163–182, Jul 1986.

I. Lobo. Environmental influences on gene expression. *Nature Education*, 1(1), 2008.

D. Lorenz, C. Poremba, F. Papengut, S. Schreiber, and G. Deuschl. The psychosocial burden of essential tremor in an outpatient- and a community-based cohort. *Eur J Neurol*, 18(7): 972–979, Jul 2011.

E. D. Louis. Clinical practice. essential tremor. *N Engl J Med*, 345(12):887–891, Sep 2001.

E. D. Louis. Environmental epidemiology of essential tremor. *Neuroepidemiology*, 31(3):139–149, 2008.

E. D. Louis. Essential tremors: a family of neurodegenerative disorders? *Arch Neurol*, 66(10): 1202–1208, Oct 2009.

E. D. Louis, L. Barnes, S. M. Albert, L. Cote, F. R. Schneier, et al. Correlates of functional disability in essential tremor. *Mov Disord*, 16(5):914–920, Sep 2001a.

E. D. Louis, P. L. Faust, and J-P. G. Vonsattel. Purkinje cell loss is a characteristic of essential tremor. *Parkinsonism Relat Disord*, 17(6):406–409, Jul 2011.

E. D. Louis, P. L. Faust, J-P. G. Vonsattel, L. S. Honig, A. Rajput, et al. Neuropathological changes in essential tremor: 33 cases compared with 21 controls. *Brain*, 130(Pt 12):3297–3307, Dec 2007.

E. D. Louis, B. Ford, S. Frucht, L. F. Barnes, M. X-Tang, and R. Ottman. Risk of tremor and impairment from tremor in relatives of patients with essential tremor: a community-based family study. *Ann Neurol*, 49(6):761–769, Jun 2001b.

E. D. Louis and M. Michael S. Okun. It is time to remove the 'benign' from the essential tremor label. *Parkinsonism Relat Disord*, 17(7):516–520, Aug 2011.

E. D. Louis, R. Ottman, B. Ford, S. Pullman, M. Martinez, et al. The washington heights-inwood genetic study of essential tremor: methodologic issues in essential-tremor research. *Neuroepidemiology*, 16(3):124–133, 1997.

E. D. Louis and S. L. Pullman. Comparison of clinical vs. electrophysiological methods of diagnosing of essential tremor. *Mov Disord*, 16(4):668–673, Jul 2001.

E. D. Louis, A. K. Rao, and M. Gerbin. Functional correlates of gait and balance difficulty in essential tremor: balance confidence, near misses and falls. *Gait Posture*, 35(1):43–47, Jan 2012.

E. D. Louis and J. P. Vonsattel. The emerging neuropathology of essential tremor. *Mov Disord*, 23(2):174–182, Jan 2008.

Elan D. Louis, Rachel Babij, Etty Corts, Jean-Paul G. Vonsattel, and Phyllis L. Faust. The inferior olivary nucleus: A postmortem study of essential tremor cases versus controls. *Mov Disord*, Mar 2013.

R.C.V. Loureiro, J.M. Belda-Lois, E.R. Lima, J.L. Pons, J.J. Sanchez-Lacuesta, and W.S. Harwin. Upper limb tremor suppression in adl via an orthosis incorporating a controllable double viscous beam actuator. In *Rehabilitation Robotics, 2005. ICORR 2005. 9th International Conference on*, pages 119 – 122, june-1 july 2005.

M-K. Lu, P. Jung, B. Bliem, H-T. Shih, Y-T. Hseu, et al. The bereitschaftspotential in essential tremor. *Clin Neurophysiol*, 121(4):622–630, 2010.

H. J. Luinge and P. H. Veltink. Measuring orientation of human body segments using miniature gyroscopes and accelerometers. *Med Biol Eng Comput*, 43(2):273–282, Mar 2005.

H. J. Luinge, P. H. Veltink, and C T M. Baten. Ambulatory measurement of arm orientation. *J Biomech*, 40(1):78–85, 2007.

C. L. Lynch and M. R. Popovic. Functional electrical stimulation. *Control Systems, IEEE*, 28 (2):40 –50, april 2008. ISSN 1066-033X.

F. Mandrile, D. Farina, M. Pozzo, and R. Merletti. Stimulation artifact in surface emg signal: effect of the stimulation waveform, detection system, and current amplitude using hybrid stimulation technique. *IEEE Trans Neural Syst Rehabil Eng*, 11(4):407–415, 2003.

K. A. Mann, F. W. Werner, and A. K. Palmer. Frequency spectrum analysis of wrist motion for activities of daily living. *Journal of Orthopedic Research*, 7(2):304–306, 1989.

S. G. Mason and G. E. Birch. A brain-controlled switch for asynchronous control applications. *IEEE Trans Biomed Eng*, 47(10):1297–1307, 2000.

R. E. Mayagoitia, A. V. Nene, and P. H. Veltink. Accelerometer and rate gyroscope measurement of kinematics: an inexpensive alternative to optical motion analysis systems. *J Biomech*, 35 (4):537–542, Apr 2002.

J. H. McAuley and C. D. Marsden. Physiological and pathological tremors and rhythmic central motor control. *Brain*, 123:1545–1567, 2000.

L. M. Mendell and E. Henneman. Terminals of single ia fibers: location, density, and distribution within a pool of 300 homonymous motoneurons. *J Neurophysiol*, 34(1):171–187, Jan 1971.

R. Merletti and D. Farina. Analysis of intramuscular electromyogram signals. *Philos Transact A Math Phys Eng Sci*, 367(1887):357–368, Jan 2009.

R. Merletti, A. Holobar, and D. Farina. Analysis of motor units with high-density surface electromyography. *J Electromyogr Kinesiol*, 18(6):879–890, Dec 2008.

R. P. Meshack and K. E. Norman. A randomized controlled trial of the effects of weights on amplitude and frequency of postural hand tremor in people with parkinson's disease. *Clin Rehabil*, 16(5):481–492, Aug 2002.

J. Michaelis. Introducing the neater eater. *Action Res*, 6:2–3, 1988.

Jd.R. Millan, F. Renkens, J. Mourino, and W. Gerstner. Noninvasive brain-actuated control of a mobile robot by human eeg. *Biomedical Engineering, IEEE Transactions on*, 51(6):1026 –1033, june 2004. ISSN 0018-9294.

T. E. Milner and C. Cloutier. Compensation for mechanically unstable loading in voluntary wrist movement. *Exp Brain Res*, 94(3):522–532, 1993.

H. S. Milner-Brown, R. B. Stein, and R. Yemm. The contractile properties of human motor units during voluntary isometric contractions. *J Physiol*, 228(2):285–306, Jan 1973.

S. Moghal, A. H. Rajput, C. D'Arcy, and R. Rajput. Prevalence of movement disorders in elderly community residents. *Neuroepidemiology*, 13(4):175–178, 1994.

J. C. Moreno, F. Brunetti, E. Rocon, and J. L. Pons. Immediate effects of a controllable knee ankle foot orthosis for functional compensation of gait in patients with proximal leg weakness. *Med Biol Eng Comput*, 46(1):43–53, Jan 2008.

M. Muthuraman, U. Heute, K. Arning, A. R. Anwar, R. Elble, et al. Oscillating central motor networks in pathological tremors and voluntary movements. what makes the difference? *Neuroimage*, 60(2):1331–1339, Apr 2012.

F. Negro and D. Farina. Decorrelation of cortical inputs and motoneuron output. *J Neurophysiol*, 106(5):2688–2697, Nov 2011a.

F. Negro and D. Farina. Linear transmission of cortical oscillations to the neural drive to muscles is mediated by common projections to populations of motoneurons in humans. *J Physiol*, 589 (Pt 3):629–637, 2011b.

F. Negro and D. Farina. Factors influencing the estimates of correlation between motor unit activities in humans. *PLoS One*, 7(9):e44894, 2012.

F. Negro, A. Holobar, and D. Farina. Fluctuations in isometric muscle force can be described by one linear projection of low-frequency components of motor unit discharge rates. *J Physiol*, 587(Pt 24):5925–5938, Dec 2009.

I. K. Niazi, N. Jiang, O. Tiberghien, J. F. Nielsen, K. Dremstrup, and D. Farina. Detection of movement intention from single-trial movement-related cortical potentials. *J Neural Eng*, 8 (6):066009, Dec 2011.

E. Niedermeyer and F. H. Lopes Da Silva. *Electroencephalography: Basic Principles, Clinical Applications, and Related Fields*. Lippincott Williams & Wilkins, 2005.

A. Niranjan, A. Jawahar, D. Kondziolka, and L. D. Lunsford. A comparison of surgical approaches for the management of tremor: radiofrequency thalamotomy, gamma knife thalamotomy and thalamic stimulation. *Stereotact Funct Neurosurg*, 72(2-4):178–184, 1999.

M. A. Nordstrom, A. J. Fuglevand, and R. M. Enoka. Estimating the strength of common input to human motoneurons from the cross-correlogram. *J Physiol*, 453:547–574, 1992.

J. A. Obeso, M. C. Rodríguez-Oroz, M. Rodríguez, J. L. Lanciego, J. Artieda, et al. Pathophysiology of the basal ganglia in parkinson's disease. *Trends Neurosci*, 23(10 Suppl):S8–19, Oct 2000.

R. J. O'Connor and M. U. Kini. Non-pharmacological and non-surgical interventions for tremor: a systematic review. *Parkinsonism Relat Disord*, 17(7):509–515, Aug 2011.

C. W. Olanow and J. A. Obeso. Preventing levodopa-induced dyskinesias. *Ann Neurol*, 47(4 Suppl 1):S167–76; discussion S176–8, Apr 2000.

A. V. Oppenheim, R. W. Schafer, and J. R. Buck. *Digital signal processing*. Prentice Hall, 1998.

P. E. O'Suilleabhain and J. Y. Matsumoto. Time-frequency analysis of tremors. *Brain*, 121 (Pt 11):2127–2134, 1998.

M. Pacelli, L. Caldani, and R. Paradiso. Textile piezoresistive sensors for biomechanical variables monitoring. *Conf Proc IEEE Eng Med Biol Soc*, 1:5358–5361, 2006.

F. L. Pagan, J. A. Butman, J. M. Dambrosia, and M. Hallett. Evaluation of essential tremor with multi-voxel magnetic resonance spectroscopy. *Neurology*, 60(8):1344–1347, Apr 2003.

R. Paradiso, L. Caldani, M. Pacelli, F. Negro, and D. Farina. E-textile platforms for rehabilitation. In *Proceedings of the 32ndAnnual International Conference of the IEEE Engineering in Medicine and Biology Society*, 2010.

B. K. Park, Y. Kwon, J-W. Kim, J-H. Lee, G-M. Eom, et al. Analysis of viscoelastic properties of wrist joint for quantification of parkinsonian rigidity. *IEEE Trans Neural Syst Rehabil Eng*, 19(2):167–176, Apr 2011.

J. Parkinson. *An essay on the Shaking Palsy*. 1817.

S. Paus, T. Schmitz-Hübsch, U. Wüllner, A. Vogel, T. Klockgether, and M. Abele. Bright light therapy in parkinson's disease: a pilot study. *Mov Disord*, 22(10):1495–1498, Jul 2007.

J. S. Perlmutter and J. W. Mink. Deep brain stimulation. *Annu Rev Neurosci*, 29:229–257, 2006.

G. Pfurtscheller and F. H. Lopes da Silva. Event-related eeg/meg synchronization and desynchronization: basic principles. *Clin Neurophysiol*, 110(11):1842–1857, 1999.

S. D. Piasecki and J. W. Jefferson. Psychiatric complications of deep brain stimulation for parkinson's disease. *J Clin Psychiatry*, 65(6):845–849, Jun 2004.

P. Piboolnurak, N. Rothey, A. Ahmed, B. Ford, Q. Yu, et al. Psychogenic tremor disorders identified using tree-based statistical algorithms and quantitative tremor analysis. *Mov Disord*, 20(12):1543–1549, Dec 2005.

S. Pledgie, K. E. Barner, S. K. Agrawal, and T. Rahman. Tremor suppression through impedance control. *IEEE Trans Rehabil Eng*, 8(1):53–59, Mar 2000.

J. L. Pons, editor. *Wearable Robots: Biomechatronic Exoskeletons*. John Wiley & Sons, Ltd, 2008.

D. Popovic, A. Stojanovic, A. Pjanovic, S. Radosavljevic, M. Popovic, et al. Clinical evaluation of the bionic glove. *Arch Phys Med Rehabil*, 80(3):299–304, Mar 1999.

D. B. Popovic and M. B. Popovic. Automatic determination of the optimal shape of a surface electrode: selective stimulation. *J Neurosci Methods*, 178(1):174–181, 2009.

D. B. Popovic and T Sinkjaer. *Control of movement for the physically disabled*. Springer, 2000.

A. Popovic-Bijelic, G. Bijelic, N. Jorgovanovic, D. Bojanic, M. B. Popovic, and D. B. Popovic. Multi-field surface electrode for selective electrical stimulation. *Artif Organs*, 29(6):448–452, Jun 2005.

L. Popovic-Maneski, N. Jorgovanovic, V. Ilic, S. Dosen, T. Keller, et al. Electrical stimulation for the suppression of pathological tremor. *Med Biol Eng Comput*, 49(10):1187–1193, Oct 2011.

A. Prochazka, J. Elek, and M. Javidan. Attenuation of pathological tremors by functional electrical stimulation. I: Method. *Ann Biomed Eng*, 20(2):205–224, 1992.

D. Purves, G. J. Augustine, D. Fitzpatrick, W. C. Hall, A.-S. Lamantia, et al., editors. *Neuroscience*. Sinauer Associates, Inc. Publishers, 3th edition, 2004.

J. Raethjen, K. Austermann, K. Witt, K. E. Zeuner, F. Papengut, and G. Deuschl. Provocation of parkinsonian tremor. *Mov Disord*, 23(7):1019–1023, May 2008.

J. Raethjen and G. Deuschl. The oscillating central network of essential tremor. *Clin Neurophysiol*, 123(1):61–64, Jan 2012.

J. Raethjen, R. B. Govindan, F. Kopper, M. Muthuraman, and G. Deuschl. Cortical involvement in the generation of essential tremor. *J Neurophysiol*, 97(5):3219–3228, May 2007.

J. Raethjen, R. B. Govindan, M. Muthuraman, F. Kopper, J. Volkmann, and G. Deuschl. Cortical correlates of the basic and first harmonic frequency of parkinsonian tremor. *Clin Neurophysiol*, 120(10):1866–1872, 2009.

J. Raethjen, M. Lindemann, H. Schmaljohann, R. Wenzelburger, G. Pfister, and G. Deuschl. Multiple oscillators are causing parkinsonian and essential tremor. *Mov Disord*, 15(1):84–94, Jan 2000.

A. H. Rajput, C. A. Robinson, M. L. Rajput, and A. Rajput. Cerebellar purkinje cell loss is not pathognomonic of essential tremor. *Parkinsonism Relat Disord*, 17(1):16–21, Jan 2011.

O. Rascol, D. J. Brooks, A. D. Korczyn, P. P. De Deyn, C. E. Clarke, and A. E. Lang. A five-year study of the incidence of dyskinesia in patients with early parkinson's disease who were treated with ropinirole or levodopa. 056 study group. *N Engl J Med*, 342(20):1484–1491, May 2000.

R. Raya, E. Rocon, J. A. Gallego, R. Ceres, and J. L. Pons. A robust kalman algorithm to facilitate human-computer interaction for people with cerebral palsy, using a new interface based on inertial sensors. *Sensors (Basel)*, 12(3):3049–3067, 2012.

C. Reck, M. Himmel, E. Florin, M. Maarouf, V. Sturm, et al. Coherence analysis of local field potentials in the subthalamic nucleus: differences in parkinsonian rest and postural tremor. *Eur J Neurosci*, 32(7):1202–1214, Oct 2010.

P. O. Riley and M. J. Rosen. Evaluating manual control devices for those with tremor disability. *Journal of Rehabilitation Research and Development*, 24(2):99–110, 1987.

C. N. Riviere, R. S. Rader, and N. V. Thakor. Adaptive canceling of physiological tremor for improved precision in microsurgery. *IEEE Transactions on Biomedical Engineering*, 45(7): 839–846, 1998.

E. Rocon. *Reducción activa de temblor patológico de miembro superior mediante exoesqueletos robóticos*. PhD thesis, Universidad Politécnica de Madrid, 2006.

E. Rocon, A. O. Andrade, J. L. Pons, P. Kyberd, and S. J. Nasuto. Empirical mode decomposition: a novel technique for the study of tremor time series. *Med Biol Eng Comput*, 44: 569–582, 2006.

E. Rocon, J. M. Belda-Lois, A. F. Ruiz, M. Manto, J. C. Moreno, and J. L. Pons. Design and validation of a rehabilitation robotic exoskeleton for tremor assessment and suppression. *IEEE Tans Neural Syst Rehab Eng*, 15(3):367–378, 2007a.

E. Rocon, J. M. Belda-Lois, J. M. Sanchez-Lacuesta, and J. L. Pons. Pathological tremor management: Modelling, compensatory technology and evaluation. *Technology and Disability*, 16:3–18, 2004.

E. Rocon, M. Manto, J. Pons, S. Camut, and J. M. Belda. Mechanical suppression of essential tremor. *Cerebellum*, 6(1):73–78, 2007b.

D. Roetenberg, C. T. M. Baten, and P. H. Veltink. Estimating body segment orientation by applying inertial and magnetic sensing near ferromagnetic materials. *IEEE Trans Neural Syst Rehabil Eng*, 15(3):469–471, Sep 2007.

D. Roetenberg, H. J. Luinge, C. T. M. Baten, and P. H. Veltink. Compensation of magnetic disturbances improves inertial and magnetic sensing of human body segment orientation. *IEEE Trans Neural Syst Rehabil Eng*, 13(3):395–405, Sep 2005.

M. J. Rosen, A. S. Arnold, I. J. Baiges, M. L. Aisen, and S. R. Eglowstein. Design of a controlled-energy-dissipation orthosis (cedo) for functional suppression of intention tremors. *J Rehabil Res Dev*, 32(1):1–16, Feb 1995.

J. R. Rosenberg, A. M. Amjad, P. Breeze, D. R. Brillinger, and D. M. Halliday. The fourier approach to the identification of functional coupling between neuronal spike trains. *Prog Biophys Mol Biol*, 53(1):1–31, 1989.

J. N. Sanes, P. A. LeWitt, and K. H. Mauritz. Visual and mechanical control of postural and kinetic tremor in cerebellar system disorders. *J Neurol Neurosurg Psychiatry*, 51(7):934–943, Jul 1988.

A. H. Schapira, V. M. Mann, J. M. Cooper, D. Krige, P. J. Jenner, and C. D. Marsden. Mitochondrial function in parkinson's disease. the royal kings and queens parkinson's disease research group. *Ann Neurol*, 32:S116–24, 1992.

A. Schmied, C. Ivarsson, and E. E. Fetz. Short-term synchronization of motor units in human extensor digitorum communis muscle: relation to contractile properties and voluntary control. *Exp Brain Res*, 97(1):159–172, 1993.

T. A. Sears and D. Stagg. Short-term synchronization of intercostal motoneurone activity. *J Physiol*, 263(3):357–381, Dec 1976.

S. Sen, A. Kawaguchi, Y. Truong, M. M. Lewis, and X. Huang. Dynamic changes in cerebello-thalamo-cortical motor circuitry during progression of parkinson's disease. *Neuroscience*, 166 (2):712–719, Mar 2010.

P. Shenoy, M. Krauledat, B. Blankertz, R. P. N. Rao, and K-R. Mller. Towards adaptive classification for bci. *J Neural Eng*, 3(1):R13–R23, Mar 2006.

H. Shibasaki and M. Hallett. What is the bereitschaftspotential? *Clin Neurophysiol*, 117(11): 2341–2356, Nov 2006.

H. A. Shill, C. H. Adler, M. N. Sabbagh, D. J. Connor, J. N. Caviness, et al. Pathologic findings in prospectively ascertained essential tremor subjects. *Neurology*, 70(16 Pt 2):1452–1455, Apr 2008.

N. Shneyder, M. K. Lyons, E. Driver-Dunckley, and V. G. H. Evidente. Cerebellar ataxia from multiple potential causes: hypothyroidism, hashimoto's thyroiditis, thalamic stimulation, and essential tremor. *Tremor and Other Hyperkinetic Movements*, 2, 2012.

M. H. Sloan. A damped joystick: Evaluation and testing using a two dimensional tracking task. Master's thesis, Massachusetts Institute of Technology, 1981.

H. Stefansson, S. Steinberg, H. Petursson, O. Gustafsson, I. H. Gudjonsdottir, et al. Variant in the sequence of the lingo1 gene confers risk of essential tremor. *Nat Genet*, 41(3):277–279, Mar 2009.

F. Steigerwald, M. Pötter, J. Herzog, M. Pinsker, F. Kopper, et al. Neuronal activity of the human subthalamic nucleus in the parkinsonian and nonparkinsonian state. *J Neurophysiol*, 100(5):2515–2524, Nov 2008.

R. B. Stein and M. N. Oguztöreli. Tremor and other oscillations in neuromuscular systems. *Biol Cybern*, 22(3):147–157, 1976.

H. Stolze, G. Petersen, J. Raethjen, R. Wenzelburger, and G. Deuschl. The gait disorder of advanced essential tremor. *Brain*, 124(Pt 11):2278–2286, Nov 2001.

S. Sukkarieh, E. M. Nebot, and H. F. Durrant-Whyte. A high integrity IMU/GPS navigation loop for autonomous land vehicle applications. *Robotics and Automation, IEEE Transactions on*, 15(3):572 –578, jun 1999. ISSN 1042-296X.

G. Tamás, L. Plvlgyi, A. Takts, I. Szirmai, and A. Kamondi. Delayed beta synchronization after movement of the more affected hand in essential tremor. *Neurosci Lett*, 405(3):246–251, 2006.

K. P. Tee, D. W. Franklin, T. Milner, M. Kawato, and E. Burdet. Concurrent adaptation of force and impedance in the redundant muscle system. *Biological Cybernetics*, 102:31–44, 2010.

W. Thevathasan, P. Mazzone, A. Jha, A. Djamshidian, M. Dileone, et al. Spinal cord stimulation failed to relieve akinesia or restore locomotion in parkinson disease. *Neurology*, 74(16):1325–1327, Apr 2010.

J. Timmer, S. Häussler, M. Lauk, and C. H. Lücking. Pathologic tremors: Deterministic chaos or nonlinear stochastic oscillators? *Chaos*, pages 278–288, 2000.

L. Timmermann, J. Gross, M. Dirks, Volkmann J., H. J. Freund, and A. Schnitzler. The cerebral oscillatory network of parkinsonian resting tremor. *Brain*, 126:199–212, 2003.

K. Tong and M. H. Granat. A practical gait analysis system using gyroscopes. *Med Eng Phys*, 21(2):87–94, Mar 1999.

G. Townsend, B. Graimann, and G. Pfurtscheller. Continuous eeg classification during motor imagery-simulation of an asynchronous bci. *IEEE Tans Neural Syst Rehab Eng*, 12(2):258–265, 2004.

C. Vaz, X. Kong, and N. Thakor. An adaptive estimation of periodic signals using a fourier linear combiner. *IEEE Trans Signal Proc*, 42(1):1–10, 1994.

K. C. Veluvolu and W. T. Ang. Estimation of physiological tremor from accelerometers for real-time applications. *Sensors*, 11(3):3020–3036, 2011. ISSN 1424-8220.

K. C. Veluvolu, W. T. Latt, and W. T. Ang. Double adaptive bandlimited multiple fourier linear combiner for real–time estimation/filtering of physiological tremor. *Biomedical Signal Processing and Control*, 5(1):37–4, 2010.

K. C. Veluvolu, U. X. Tan, W. T. Latt, C. Y. Shee, and W. T. Ang. Bandlimited multiple fourier linear combiner for real-time tremor compensation. In *Proc. International Conference of the IEEE Engineering in Medicine and Biology Societyr*, 2007.

J.F. Veneman, R. Kruidhof, E.E.G. Hekman, R. Ekkelenkamp, E.H.F. Van Asseldonk, and H. van der Kooij. Design and evaluation of the lopes exoskeleton robot for interactive gait rehabilitation. *Neural Systems and Rehabilitation Engineering, IEEE Transactions on*, 15(3): 379 –386, sept. 2007. ISSN 1534-4320.

C. Vilariño Güell, C. Wider, O. A. Ross, B. Jasinska-Myga, J. Kachergus, et al. LINGO1 and LINGO2 variants are associated with essential tremor and parkinson disease. *Neurogenetics*, 11(4):401–408, Oct 2010.

R. Vinjamuri, D. J. Crammond, D. Kondziolka, H-N. Lee, and Z-H. Mao. Extraction of sources of tremor in hand movements of patients with movement disorders. *IEEE Trans Inform Tech Biomed*, 13(1):49–56, Jan. 2009.

J. Volkmann, M. Joliot, A. Mogilner, A. A. Ioannides, F. Lado, et al. Central motor loop oscillations in parkinsonian resting tremor revealed by magnetoencephalography. *Neurology*, 46(5):1359–1370, May 1996.

V. Voon, P. Krack, A. E. Lang, A. M. Lozano, K. Dujardin, et al. A multicentre study on suicide outcomes following subthalamic stimulation for parkinson's disease. *Brain*, 131(Pt 10):2720–2728, Oct 2008.

G. K. Wenning, S. Kiechl, K. Seppi, J. Müller, B. Högl, et al. Prevalence of movement disorders in men and women aged 50-89 years (bruneck study cohort): A population-based study. *Lancet Neurology*, 4(12):815–820, 2005.

F. Widjaja, C. Y. Shee, W. L. Au, P. Poignet, and W. T. Ang. Using electromechanical delay for real-time anti-phase tremor attenuation system using functional electrical stimulation. In *Proc. IEEE Int Robotics and Automation (ICRA) Conf*, pages 3694–3699, 2011.

B. Widrow, J. R. Glover, J. M. McCool, J. Kaunitz, C. S. Williams, et al. Adaptive noise canceling: Principles and applications. *Proceeding of the IEEE*, 63(12):1692–1716, 1975.

B. Widrow and S. D. Stearns. *Adaptive signal processing*. Prentice Hall, 1985.

A. J. Wills, I. H. Jenkins, P. D. Thompson, L. J. Findley, and D. J. Brooks. Red nuclear and cerebellar but no olivary activation associated with essential tremor: a positron emission tomographic study. *Ann Neurol*, 36(4):636–642, Oct 1994.

H. Wilms, J. Sievers, and G. Deuschl. Animal models of tremor. *Mov Disord*, 14(4):557–571, Jul 1999.

Z. Wu and N. E. Huang. Ensemble empirical mode decomposition: A noise assisted data analysis method. *Advances in Adaptive Data Analysis*, 1(1):1–41, 2009.

N. Yazdi, F. Ayazi, and K. Najafi. Micromachined inertial sensors. *Proceedings of the IEEE*, 86 (8):1640 –1659, aug 1998. ISSN 0018-9219.

H. Yu, D. Sternad, D. M. Corcos, and D. E. Vaillancourt. Role of hyperactive cerebellum and motor cortex in parkinson's disease. *Neuroimage*, 35(1):222–233, Mar 2007.

M. Yu, K. Ma, P. L. Faust, L. S. Honig, E. Corts, J-P G. Vonsattel, and E. D. Louis. Increased number of purkinje cell dendritic swellings in essential tremor. *Eur J Neurol*, 19(4):625–630, Apr 2012.

T. A. Zesiewicz, R. Elble, E. D. Louis, R. A. Hauser, K. L. Sullivan, et al. Practice parameter: therapies for essential tremor: report of the quality standards subcommittee of the american academy of neurology. *Neurology*, 64(12):2008–2020, Jun 2005.

T. A. Zesiewicz, R. J. Elble, E. D. Louis, G. S. Gronseth, W. G. Ondo, et al. Evidence-based guideline update: treatment of essential tremor: report of the quality standards subcommittee of the american academy of neurology. *Neurology*, 77(19):1752–1755, Nov 2011.

R. Zhu and Z. Zhou. A real-time articulated human motion tracking using tri-axis inertial/magnetic sensors package. *IEEE Trans Neural Syst Rehabil Eng*, 12(2):295–302, Jun 2004.

A. B. Zoss, H. Kazerooni, and A. Chu. Biomechanical design of the berkeley lower extremity exoskeleton (BLEEX). *Mechatronics, IEEE/ASME Transactions on*, 11(2):128 –138, april 2006. ISSN 1083-4435.